

Quantifying entanglement of overlapping  
indistinguishable particles

A thesis submitted to  
University College London  
for the degree of  
Doctor of Philosophy  
in the Department of Physics  
by Joseph R. Gittings

February 2006

UMI Number: U592844

All rights reserved

INFORMATION TO ALL USERS

The quality of this reproduction is dependent upon the quality of the copy submitted.

In the unlikely event that the author did not send a complete manuscript and there are missing pages, these will be noted. Also, if material had to be removed, a note will indicate the deletion.



UMI U592844

Published by ProQuest LLC 2013. Copyright in the Dissertation held by the Author.  
Microform Edition © ProQuest LLC.

All rights reserved. This work is protected against  
unauthorized copying under Title 17, United States Code.



ProQuest LLC  
789 East Eisenhower Parkway  
P.O. Box 1346  
Ann Arbor, MI 48106-1346

I declare that the work presented in this thesis is my own.

**Joe Gittings**

## Abstract

This thesis develops the quantitative study of quantum entanglement in systems of identical particles. Understanding this topic is essential for the construction of quantum information processing devices involving identical particles.

A brief overview of necessary concepts and methods, such as the density matrix, the entanglement in pure and mixed states of distinguishable particles, and some common applications of entanglement is given in the introduction.

Some competing methods of calculating the entanglement in bipartite pure states of indistinguishable particles are examined. It is shown that only the 'site entropy' measure introduced by Zanardi satisfies all the criteria for a correct entanglement measure. A teleportation protocol which utilizes all the entanglement carried (in both the spin and space degrees of freedom) in a doubly-occupied molecular bonding orbital is presented.

The output from an interferometer in a thought experiment described by Omar et al. is studied as an example to see whether entanglement can be separated into space-only, spin-only, and space-spin components. A similar exercise is performed for a doubly-occupied molecular bonding orbital. The relationship between these results and the application of superselection rules (SSRs) to the quantification of useful entanglement is discussed.

A numerical method for estimating the entanglement of formation of a mixed state of arbitrary dimension by a conjugate gradient algorithm is described. The results of applying an implementation of the algorithm to both random and isotropic states of 2 qutrits (i.e. two three-dimensional systems) is described.

Existing work on calculating entanglement between two sites in various spin systems is outlined. New methods for calculating the entanglement between two sites in various types of degenerate quantum gas - a Fermi gas, a Bose condensate, and a BCS superconductor - are described. The results of numerical studies of the entanglement in a normal metal and a BCS superconductor are reported, both with and without the application of superselection rules for local particle number conservation.

# Contents

<b>1</b>	<b>Introduction</b>	<b>16</b>
1.1	The density matrix . . . . .	16
1.1.1	Pure and impure states and the density operator . . . . .	16
1.1.2	The density matrix . . . . .	18
1.1.3	The density matrix expresses measurement probabilities . . . . .	19
1.1.4	The density matrix gives correct measurement averages . . . . .	19
1.1.5	Distinguishing pure from mixed states . . . . .	20
1.1.6	Freedom in the representation of $\hat{\rho}$ . . . . .	20
1.1.7	The reduced density matrix . . . . .	21
	The partial trace . . . . .	21
	Justification for using the partial trace . . . . .	22
	Example of the reduced density operator . . . . .	22
1.2	An introduction to entanglement . . . . .	23
1.2.1	The qubit and the ebit . . . . .	24
1.2.2	The Bell states . . . . .	24
1.2.3	Von Neumann entropy . . . . .	25
1.2.4	Other properties of the von Neumann entropy . . . . .	25
1.2.5	Wootters tangle . . . . .	26
1.2.6	Pure state concurrence . . . . .	26
1.2.7	Entanglement monotones . . . . .	27
1.2.8	Quantum relative entropy . . . . .	28
1.2.9	Entanglement of formation . . . . .	28
	Entanglement of formation for a pure quantum state . . . . .	29
	Entanglement of formation for a mixed quantum state . . . . .	31

Wootters formula for entanglement of formation of two qubits . . . . .	32
Postulated additivity of entanglement of formation . . . . .	32
1.2.10 Entanglement of distillation . . . . .	34
1.3 What can entanglement do? . . . . .	34
1.3.1 Bell's theorem . . . . .	35
Preamble . . . . .	35
Nomenclature . . . . .	35
Introduce a hidden variable . . . . .	36
Hidden variables are consistent with the results of measurements on a single spin . . . . .	37
Hidden variables are not consistent with the results of separate measurements on two spins in a singlet state . . . . .	38
A choice of measurement axes which violates Bell's inequality . . . . .	40
Bell's theorem and entanglement . . . . .	40
1.3.2 Quantum teleportation . . . . .	41
Summary of the teleportation protocol . . . . .	41
Description of the teleportation protocol . . . . .	41
Significance of the teleportation protocol . . . . .	45
1.3.3 Quantum key distribution . . . . .	45
The BB84 QKD protocol . . . . .	46
The EPR QKD protocol . . . . .	48
1.3.4 Quantum computing . . . . .	52
Overview of quantum computing . . . . .	52
A universal set of quantum gates must have at least one entangling gate . . . . .	54
Quantum logic gate model of the teleportation protocol . . . . .	59
1.4 Conclusion . . . . .	59
<b>2 Entanglement of indistinguishable particles</b>	<b>61</b>
2.1 Introduction . . . . .	61
2.1.1 Why the focus on fermions? . . . . .	62
2.1.2 The Kane proposal . . . . .	62

2.1.3	Why is quantifying entanglement between indistinguishable particles a problem? . . . . .	63
2.2	There is no entanglement due to the overall symmetry of the wavefunction . . . . .	64
2.2.1	Definition of a 'remote' state for any measurement . . . . .	64
2.2.2	Entanglement and overall symmetry . . . . .	65
2.3	Methods of partitioning Hilbert space of two entangled spinful particles . . . . .	66
2.3.1	Requirements for partitioning . . . . .	66
	Tensor product structure . . . . .	66
	Delocalization . . . . .	67
	Indistinguishability . . . . .	67
2.3.2	Partitioning used by existing entanglement measures . . . . .	68
2.4	Desirable properties of any entanglement measure . . . . .	69
2.4.1	Invariance under local unitary transformations . . . . .	69
2.4.2	Non-invariance under some non-local unitary transformations is not an undesirable property . . . . .	69
2.4.3	Correct behaviour as distinguishability of subsystems A and B is lost . . . . .	69
	Behaviour of $ \Psi\rangle^\pm$ Bell states . . . . .	70
	Behaviour of $ \Phi\rangle^\pm$ Bell states . . . . .	71
2.5	Wootters measure for distinguishable particles (tangle) . . . . .	72
2.6	Schliemann measure for fermions . . . . .	72
2.6.1	Slater decomposition form . . . . .	73
2.6.2	Behaviour as overlap of single particle wavefunctions is increased . . . . .	74
2.6.3	Relation to Wootters measure . . . . .	75
2.6.4	Non-invariance under local unitary transformations . . . . .	76
2.6.5	Invariance under non-local unitary transformations . . . . .	77
2.6.6	Understanding the anomalous behaviour of the Schliemann measure in terms of the Slater decomposition . . . . .	78
2.7	Zanardi measure . . . . .	78
2.7.1	Behaviour as overlap of single particle wavefunctions is increased . . . . .	79
2.7.2	Application to an example state . . . . .	81

2.7.3	Behaviour under unitary transformations . . . . .	84
	One-site two-particle (local) unitary transformations . . .	84
	Two-site one-particle (non-local) unitary transformations	84
2.7.4	Site entropy measure applied to a completely general state	85
	Bosonic particles. . . . .	85
	Fermionic particles . . . . .	86
2.7.5	Relationship to Wootters tangle . . . . .	87
2.7.6	Relationship to ‘mode’ picture of entanglement . . . . .	87
2.8	Vaccaro’s accessible entanglement, $E_P$ . . . . .	88
2.9	Teleporting two qubits using an example delocalized state . . . .	89
	2.9.1 Protocol design. . . . .	89
	2.9.2 Protocol implementation. . . . .	91
	2.9.3 Applicability to fermionic systems . . . . .	93
	2.9.4 Phase considerations due to the use of a coherent state . .	93
2.10	Conclusion . . . . .	94
<b>3</b>	<b>Spin-only, space-only, spin-space entanglement</b>	<b>96</b>
3.1	Introduction . . . . .	96
3.2	The Omar thought-experiment . . . . .	97
3.3	Can space and spin degrees of freedom be ‘entangled’ with one another? . . . . .	100
	3.3.1 A density operator which gives correct measurement av- erages for spatial measurements is also parameterized by spin . . . . .	100
	Variable number of particles . . . . .	102
	Example: Side 1 of the Omar apparatus . . . . .	102
	3.3.2 Tracing out space and spin . . . . .	103
	3.3.3 Showing that the delocalized state $ \psi\rangle = \frac{1}{\sqrt{2}}(c_{A\uparrow}^\dagger + c_{B\uparrow}^\dagger) \frac{1}{\sqrt{2}}(c_{A\downarrow}^\dagger + c_{B\downarrow}^\dagger) 0\rangle$ is separable into space-only and spin-only pure states	103
	3.3.4 Space-spin entanglement of a parameterized version of the delocalized state $ \psi\rangle = \frac{1}{\sqrt{2}}(c_{A\uparrow}^\dagger + c_{B\uparrow}^\dagger) \frac{1}{\sqrt{2}}(c_{A\downarrow}^\dagger + c_{B\downarrow}^\dagger) 0\rangle$ . .	104
	3.3.5 Tracing out space and spin from the locally antisymmetrized Omar output state . . . . .	105
	3.3.6 Tracing out space and spin from the fully antisymmetrized Omar output state . . . . .	107



3.3.7	Fully antisymmetrizing the output state . . . . .	108
3.3.8	Obtaining the coefficients of the four-spin-half eigenfunc- tions . . . . .	109
3.3.9	Symmetry projections of the four-way antisymmetrized spatial states . . . . .	110
3.3.10	Calculating the space-spin entanglement from the fully antisymmetrized output state . . . . .	111
3.3.11	Calculating the space-spin entanglement in the fully anti- symmetrized <i>input</i> state . . . . .	112
3.3.12	Mutual information between measurements on $ \psi\rangle = \frac{1}{\sqrt{2}}(c_{A\uparrow}^\dagger +$ $c_{B\uparrow}^\dagger) \frac{1}{\sqrt{2}}(c_{A\downarrow}^\dagger + c_{B\downarrow}^\dagger) 0\rangle$ . . . . .	114
	One-site measurements . . . . .	114
	Two-site measurements . . . . .	116
3.3.13	Holevo bound on mutual information between measure- ments on $ \psi\rangle = \frac{1}{\sqrt{2}}(c_{A\uparrow}^\dagger + c_{B\uparrow}^\dagger) \frac{1}{\sqrt{2}}(c_{A\downarrow}^\dagger + c_{B\downarrow}^\dagger) 0\rangle$ . . . . .	117
	One-site measurements . . . . .	117
3.4	Can space and spin degrees of freedom carry entanglement be- tween two parts, and how do they contribute to the total entan- glement? . . . . .	120
3.4.1	Space-only and spin-only entanglement . . . . .	120
3.4.2	Available entanglement in the doubly-filled bonding MO under spin-only and charge-only measurement restrictions 122 Available entanglement in the doubly-filled bonding MO when Alice can only measure spin . . . . .	123
	Available entanglement in the doubly-filled bonding MO when Alice can only measure charge . . . . .	125
3.4.3	Available entanglement in the doubly-filled bonding MO under a charge-only measurement restriction, calculated from the reduced density matrix . . . . .	125
3.4.4	Spin-space entanglement transfer in the Omar thought experiment . . . . .	127
	Side 1 of the apparatus. . . . .	127
	Single-occupancy and double-occupancy entanglements are additive. . . . .	129

Left arm of side 1 of the apparatus. . . . .	131
Operator-sum representation for spin-space entanglement transfer. . . . .	131
3.4.5 Calculating space-only and spin-only entanglement between sides 1 and 2 of the Omar interferometer . . . . .	132
Spin-only entanglement between the two sides of the Omar apparatus . . . . .	132
Space-only entanglement between the two sides of the Omar apparatus . . . . .	133
An argument for the optimality of the space-only decomposition . . . . .	133
<b>4 Entanglement and super-selection rules</b>	<b>134</b>
4.1 Introduction to superselection rules . . . . .	134
4.1.1 Definition of a superselection rule (SSR) . . . . .	135
4.1.2 Showing that a superposition of eigenstates of $\hat{G}$ with different eigenvalues is not possible . . . . .	135
SSRs and the density matrix . . . . .	137
4.1.3 Example of an SSR: Wick's description of the SSR for parity	137
4.2 Superselection rules and entanglement . . . . .	139
4.3 Effect of superselection rules on entanglement of the doubly-filled bonding MO in the site entropy picture . . . . .	140
4.3.1 By explicit consideration of possible quantum operations .	141
4.3.2 By application of Bartlett and Wiseman's approach . . .	144
SSR for local particle number conservation . . . . .	144
SSR for local particle number conservation modulo 2 . . .	146
Applicability to fermionic and bosonic systems . . . . .	146
<b>5 Numerically estimating the entanglement of formation</b>	<b>148</b>
5.1 Introduction . . . . .	148
5.2 Introduction to the conjugate gradient algorithm. . . . .	149
5.2.1 What's wrong with steepest descent . . . . .	149
5.2.2 Conjugate gradient minimization . . . . .	150
Fletcher-Reeves conjugate gradient algorithm . . . . .	150
Fletcher-Reeves in full . . . . .	151
5.3 A gradient for the average entanglement. . . . .	153

5.4	Existence of local and global minima . . . . .	155
5.5	Using the gradient to minimize the average entanglement. . . . .	156
5.6	Performance against two-qubit mixed states . . . . .	156
5.7	Performance against two-qudit isotropic mixed states . . . . .	157
5.8	Performance against two-qudit random mixed states. . . . .	157
5.9	Modelling locally depolarized Bell states of two qudits. . . . .	158
5.9.1	Bit flip for qudits . . . . .	158
5.9.2	Depolarizing channel for qudits . . . . .	159
<b>6</b>	<b>Entanglement in degenerate quantum gases</b>	<b>162</b>
6.1	Introduction . . . . .	162
6.2	Natural entanglement in spin systems . . . . .	163
6.2.1	The Ising model . . . . .	163
	1D Ising model at $T = 0$ . . . . .	163
	1D Ising model at $T > 0$ . . . . .	164
6.2.2	The Heisenberg model . . . . .	164
6.2.3	The hybrid XY and Ising model . . . . .	165
	$\gamma = 1$ : the Ising model . . . . .	166
	$\gamma < 1$ : models which are intermediate between Ising and XY . . . . .	166
6.2.4	A star network of interacting spins . . . . .	166
6.2.5	A spin chain . . . . .	167
6.2.6	A chain of harmonic oscillators . . . . .	167
6.3	Entanglement in a BCS superconductor . . . . .	168
6.3.1	The BCS ground state . . . . .	168
6.3.2	The reduced Hamiltonian for the BCS ground state . . . . .	169
	The quasi-particle excitation energy and the energy gap . . . . .	173
	The equation for the energy gap and its solutions . . . . .	173
6.3.3	Constructing a two-site density matrix for a BCS super- conductor at $T=0$ . . . . .	175
	Expressing the matrix elements as strings of second-quantized operators . . . . .	175
	Evaluating the matrix elements using Wick's theorem . . . . .	177
	Evaluating the pairings using single-particle operators for Bogoliubov quasi-particles . . . . .	178

6.3.4	The full two-site density matrix for the BCS superconductor at $T = 0$ . . . . .	181
6.3.5	Calculating the two-site entanglement in the BCS ground state - results . . . . .	186
6.3.6	Martín-Delgado's work on entanglement in the BCS ground state . . . . .	186
6.4	Entanglement in a Fermi sea . . . . .	190
6.4.1	Fermi sea two-site density matrix for two spin directions .	190
6.4.2	Fermi sea two-site density matrix for a single spin direction	192
	Off-diagonal one-particle density matrix element in a Fermi sea . . . . .	193
	Infinite separations: $R \rightarrow \infty$ . . . . .	194
	Finite separations: $R < \infty$ . . . . .	194
6.4.3	Relationship between two spin direction and single spin direction Fermi sea density matrices . . . . .	194
	Entanglement of formation results . . . . .	196
	Graphing the entanglement of formation surfaces for a sea of fermions (with or without spin) . . . . .	196
6.4.4	Physicality of Fermi sea parameters . . . . .	196
	Relationship between single-spin and two-spin entanglements . . . . .	199
6.5	Entanglement in a Bose condensate . . . . .	202
6.5.1	Binomial probability form of the Bose condensate density matrix . . . . .	204
6.5.2	$\hat{\rho}_{n,j}(n_i, n_j; n'_i, n'_j)$ is the density matrix for $n$ particles in the bonding ground state . . . . .	205
6.5.3	Limit for large systems . . . . .	206
6.5.4	Bose condensate density matrix in the limit of small $f$ . . . . .	207
	To first order in $f$ . . . . .	207
	To second order in $f$ . . . . .	208
6.5.5	Work of Simon on entanglement in Bose-Einstein condensates . . . . .	210

**7 Conclusions** **211**

<b>A Omar 2 x 2 eigenfunctions</b>	<b>214</b>
A.1 Locally antisymmetrized spin and spatial eigenfunctions for the Omar apparatus . . . . .	214
A.1.1 Locally antisymmetrized spin eigenfunctions . . . . .	214
S=0 . . . . .	215
S=1 . . . . .	215
S=2 . . . . .	216
A.1.2 Locally antisymmetrized spatial states . . . . .	216
A.1.3 Rewriting the 50/50 ++ output state for fermions as a sum of products of space and spin eigenfns . . . . .	216

# List of Figures

1.1	Geometry for a spin-half particle in a pure spin state with polarization $\hat{\mathbf{p}}$ , and one or more hidden variable(s) represented by $\hat{\lambda}$ , which has a uniform probability distribution over the hemisphere $\hat{\lambda} \cdot \hat{\mathbf{p}} > 0$ . . . . .	38
1.2	Outline of the Bennett et al. teleportation protocol [1]. . . . .	42
2.1	Positioning of ‘A’- and ‘J’-gates relative to donor nuclei in the Kane quantum computer (reproduced from [2]). . . . .	62
2.2	Schliemann entanglement $\eta$ of all Bell states vs overlap $S =  \langle \phi_a   \phi_b \rangle $ of single particle states. . . . .	75
2.3	Zanardi entanglement $E$ of a $ \Psi-\rangle$ Bell state of two fermions vs overlap $S =  \langle \phi_a   \phi_b \rangle $ of single particle states. . . . .	81
2.4	Zanardi entanglement $E$ of the doubly-filled molecular orbital after the application of the non-local unitary transformation generated by equation (2.57). . . . .	85
3.1	The spin-space entanglement apparatus used in the Omar et al. thought experiment (reproduced from [3]). . . . .	98
3.2	Von Neumann entropy of $\rho_{\text{space}}$ , traced out from a parameterized version of the doubly-occupied molecular bonding orbital, versus parameter $\theta$ . . . . .	106
5.1	Introducing a new state $ \tilde{\psi}_i\rangle$ to the decomposition doesn’t make any difference when its amplitude is small, as the gradient of $E_{\text{av}}$ with respect to the amplitude of $ \tilde{\psi}_i\rangle$ is zero at that point. . . . .	155
5.2	Convergence of $\min(E_{\text{av}})$ for a random two-qutrit mixed state using conjugate gradient algorithm. . . . .	160

5.3	Entanglement of formation (ebits) of $ \Psi\rangle^+$ of two qubits vs probability of qubit $A$ depolarizing through various channels (calculated using Wootters formula). . . . .	161
5.4	Entanglement of formation (etrits) of $ \Psi\rangle^+$ of two qutrits vs probability of qutrit $A$ depolarizing through various channels (calculated using conjugate gradient algorithm). . . . .	161
6.1	Surfaces for the entanglement of formation in the BCS ground state plotted against $f, I$ , and calculated for all possible values of $g$ and $J$ . The maximum is $E_F = 2.0$ at $f = I = 0.5, g = J = 0$ . . . . .	187
6.2	The same exercise as in Figure 6.1, performed subject to an SSR for local particle number. The maximum is $E_F = 0.5$ at $f = I = 0.5, g = J = 0$ . . . . .	188
6.3	The same exercise as in Figure 6.1, performed subject to an SSR for local particle number modulo two. The reduction in entanglement is less than that caused by the SSR for local particle number in Figure 6.2. The maximum is $E_F = 1.0$ at $f = I = 0.5, g = J = 0$ . . . . .	189
6.4	Surface for the entanglement of formation in a sea of spinless fermions. The maximum entanglement is one ebit at $f = I = 0.5$ . . . . .	197
6.5	Surface for the entanglement of formation in a sea of spinful fermions. The maximum entanglement is two ebits at $f = I = 0.5$ . . . . .	197
6.6	Surface for the difference in entanglement of formation between a sea of spinless fermions and a sea of spinful fermions . . . . .	198
6.7	$I_{\max}(f)$ plotted versus $f$ at $g = J = 0$ . . . . .	199
6.8	Entanglement of formation in the Fermi sea plotted against $f, I_{\max}(f)$ . . . . .	200
6.9	Entanglement of formation in the Fermi sea plotted against $f, I_{\max}(f)$ , with the SSR for local particle number conservation in force. . . . .	200
6.10	Entanglement of formation in the Fermi sea plotted against $f, I_{\max}(f)$ , with the SSR for local particle number modulo 2 conservation in force. . . . .	201
6.11	Entanglement between two sites in a Bose condensate for small filling factors $f$ , calculated from the density matrix expressed to first order in $f$ , using the Wootters formula. . . . .	208

# List of Tables

1.1	Relationship between Alice’s Bell state measurement result, the state of Bob’s particle after her measurement, and the correction Bob needs to apply to it . . . . .	44
3.1	Character table for $\mathcal{S}_4$ . . . . .	111
3.2	One site measurements: joint probabilities . . . . .	116
3.3	Two site measurements: joint probabilities . . . . .	117
3.4	Projection outcomes corresponding to Alice’s measurement results	119
3.5	The states of Alice’s ‘virtual’ qubits in terms of the eigenvalues of Alice’s commuting observables that they correspond to . . . .	124
3.6	The states of Alice’s ‘virtual’ qubits in terms of Alice’s $m_s^{\text{total}}$ measurement results on site $A$ . . . . .	124
3.7	The states of Alice’s ‘virtual’ qubits vs Alice’s charge measurement results . . . . .	126
4.1	CNOT on virtual qubit $\alpha$ . . . . .	141
4.2	CNOT on virtual qubit $\beta$ . . . . .	142

I would like to thank my supervisor Professor Andrew Fisher for his expert help and support, my colleagues in CMMP for a stimulating and good natured working environment, Vlatko Vedral and Sougato Bose for helpful advice, Konrad Audenaert for supplying a copy of his conjugate gradient code, the EPSRC for providing financial support, and above all Tingting and my parents for their love and support.



# Chapter 1

## Introduction

This chapter outlines some of the tools needed in the rest of this thesis. First, the density matrix is discussed. This enables a probabilistic mixture of quantum states to be described using the quantum formalism. Then some basic concepts to do with entanglement are introduced, and finally some standard applications of entanglement are outlined.

### 1.1 The density matrix

#### 1.1.1 Pure and impure states and the density operator

A quantum state is described as *pure* if it can be written as a sum of one or more kets. Eg.

$$|\Psi-\rangle = \frac{1}{\sqrt{2}}(|\uparrow\downarrow\rangle - |\downarrow\uparrow\rangle) \quad (1.1)$$

is pure.

How do we describe a statistical mixture of pure states? For example, one could imagine a source producing a stream of spin-half particles, with a Stern-Gerlach experiment at the output of the source to measure the spin-z component and thus randomly project each particle into definitely spin-z-up or spin-z-down. An observer positioned beyond the Stern-Gerlach experiment receives particles whose spin-z component has a definite, but random, value. This is what we mean by a statistical mixture of pure states.

We seek a quantum mechanical way of describing such a statistical mixture. This may seem a perverse goal, given that it is a classical stream of probabilities we are describing. But there are good reasons for doing such a thing, as we'll see later.

In this example, say the probability of a given spin in the stream having the definite spin-z value  $|\uparrow\rangle$  is  $p_\uparrow$ , and the probability of it having the definite spin-z value  $|\downarrow\rangle$  is  $p_\downarrow$ . To be analogous to a pure state, a QM description of this statistical mixture should have the property that the inner product of it with any pure state yields the probability of that state occurring in a given measurement. Let's call such a description a mixed state, and denote it by  $\hat{\rho}$ . Then we require

$$\langle\sigma|\hat{\rho}|\sigma\rangle = p_\sigma \quad (1.2)$$

where  $|\sigma\rangle$  denotes a particular pure spin state in the mixture  $\hat{\rho}$ . There are two ways that, in practice, one obtains a mixed state: either by considering some small part of a larger system which is in a pure state, or by being in receipt of a stream of pure states emitted by a classical source. However, in principle one could have a mixed state even in an isolated system, by carefully preparing a statistical mixture of states of particles that are shielded from all external interactions.

We can satisfy such a requirement by representing the mixed state as a sum of projectors onto pure states:

$$\hat{\rho} = \sum_{\sigma} p_{\sigma} |\sigma\rangle\langle\sigma| \quad (1.3)$$

or more generally for any statistical mixture of pure states  $\{|\psi_i\rangle\}$  (ie. not necessarily spin states):

$$\hat{\rho} = \sum_i p_i |\psi_i\rangle\langle\psi_i|. \quad (1.4)$$

If the  $\{|\psi_i\rangle\}$  are orthonormal, then the  $p_i$  are probabilities, as required above, since for some specific  $|\psi_j\rangle$ ,

$$\begin{aligned} \langle\psi_j|\hat{\rho}|\psi_j\rangle &= \sum_i p_i \langle\psi_j|\psi_i\rangle\langle\psi_i|\psi_j\rangle \\ &= \sum_i p_i \delta_{ji} \delta_{ij} \\ &= p_j. \end{aligned} \quad (1.5)$$

$\hat{\rho}$  is a sum of projection operators, therefore it is itself an operator: it is called the **density operator**, and was independently developed by Landau and von Neumann [4, 5].

### 1.1.2 The density matrix

Like any other quantum mechanical operator, the density operator can be written as a matrix in some orthonormal basis of pure states. For a density operator constructed according to equation (1.4) written in some orthonormal basis of pure states  $\{|k\rangle\}$  where

$$|\psi_i\rangle = \sum_k c_{i,k} |k\rangle \quad (1.6)$$

the elements of this matrix are

$$\begin{aligned} \hat{\rho}_{kk'} &= \langle k | \hat{\rho} | k' \rangle \\ &= \sum_i \langle k | \psi_i \rangle p_i \langle \psi_i | k' \rangle \\ &= \sum_i p_i c_{i,k}^* c_{i,k}. \end{aligned} \quad (1.7)$$

If the ‘diagonal’ basis of the  $|\psi_i\rangle$  is used, ie. if  $\hat{\rho}$  is diagonalized, it is clear that this reduces to

$$\hat{\rho}_{kk'} = p_k \delta_{kk'} \quad (1.8)$$

where the  $\{p_k\}$  are the eigenvalues of  $\hat{\rho}$ . Thus one obtains a density matrix with the probabilities  $\{p_k\}$  on the diagonal and zeros everywhere else. Of course, this means that the eigenvalues must satisfy  $0 \leq p_i \leq 1$ .

For our example above, the diagonal basis is

$$|\uparrow\rangle, |\downarrow\rangle \quad (1.9)$$

yielding the density matrix

$$\hat{\rho} = \begin{pmatrix} p_\uparrow & 0 \\ 0 & p_\downarrow \end{pmatrix} \quad (1.10)$$

If, however, we choose to write this mixture in the spin-x basis

$$\begin{aligned} |\uparrow_x\rangle &= \frac{1}{\sqrt{2}}(|\uparrow\rangle + |\downarrow\rangle) \\ |\downarrow_x\rangle &= \frac{1}{\sqrt{2}}(|\uparrow\rangle - |\downarrow\rangle) \end{aligned} \quad (1.11)$$

then the elements of the density matrix  $\hat{\rho}_{\text{row,col}}$  are

$$\begin{aligned}
\hat{\rho}_{11} &= p_{\uparrow} \langle \uparrow_x | \uparrow \rangle \langle \uparrow | \uparrow_x \rangle + p_{\downarrow} \langle \uparrow_x | \downarrow \rangle \langle \downarrow | \uparrow_x \rangle \\
&= p_{\uparrow} \frac{1}{\sqrt{2}} \frac{1}{\sqrt{2}} + p_{\downarrow} \frac{1}{\sqrt{2}} \frac{1}{\sqrt{2}} = \frac{1}{2} (p_{\uparrow} + p_{\downarrow}) \\
\hat{\rho}_{12} &= p_{\uparrow} \langle \uparrow_x | \uparrow \rangle \langle \uparrow | \downarrow_x \rangle + p_{\downarrow} \langle \uparrow_x | \downarrow \rangle \langle \downarrow | \downarrow_x \rangle \\
&= p_{\uparrow} \frac{1}{\sqrt{2}} \frac{1}{\sqrt{2}} + p_{\downarrow} \frac{1}{\sqrt{2}} \left(-\frac{1}{\sqrt{2}}\right) = \frac{1}{2} (p_{\uparrow} - p_{\downarrow}) \\
\hat{\rho}_{21} &= p_{\uparrow} \langle \downarrow_x | \uparrow \rangle \langle \uparrow | \uparrow_x \rangle + p_{\downarrow} \langle \downarrow_x | \downarrow \rangle \langle \downarrow | \uparrow_x \rangle \\
&= p_{\uparrow} \frac{1}{\sqrt{2}} \frac{1}{\sqrt{2}} + p_{\downarrow} \left(-\frac{1}{\sqrt{2}}\right) \frac{1}{\sqrt{2}} = \frac{1}{2} (p_{\uparrow} - p_{\downarrow}) \\
\hat{\rho}_{22} &= p_{\uparrow} \langle \downarrow_x | \uparrow \rangle \langle \uparrow | \downarrow_x \rangle + p_{\downarrow} \langle \downarrow_x | \downarrow \rangle \langle \downarrow | \downarrow_x \rangle \\
&= p_{\uparrow} \frac{1}{\sqrt{2}} \frac{1}{\sqrt{2}} + p_{\downarrow} \left(-\frac{1}{\sqrt{2}}\right) \left(-\frac{1}{\sqrt{2}}\right) = \frac{1}{2} (p_{\uparrow} + p_{\downarrow}).
\end{aligned} \tag{1.12}$$

Thus the density matrix in the spin-x basis  $|\uparrow_x\rangle, |\downarrow_x\rangle$  is

$$\hat{\rho} = \frac{1}{2} \begin{pmatrix} p_{\uparrow} + p_{\downarrow} & p_{\uparrow} - p_{\downarrow} \\ p_{\uparrow} - p_{\downarrow} & p_{\uparrow} + p_{\downarrow} \end{pmatrix} \tag{1.13}$$

### 1.1.3 The density matrix expresses measurement probabilities

Regardless of the basis used, the diagonal elements  $\hat{\rho}_{kk}$  of the density matrix express the probability of a measurement of the mixed state yielding the pure state  $|k\rangle$ , ie.

$$p(|k\rangle) = \hat{\rho}_{kk} \tag{1.14}$$

In the language of the above example, this is the probability of the member of the stream of spins that one happens to measure being in the pure state  $|k\rangle$ . The density matrix also expresses the normalization of probability, since

$$\text{tr}(\hat{\rho}) = 1. \tag{1.15}$$

### 1.1.4 The density matrix gives correct measurement averages

A primary justification for the use of the density operator to describe a ‘mixed state’ is that it gives the correct measurement averages for an operator acting

on that state. Returning to our example, if the recipient of the spins measures them using  $\hat{\sigma}_z$ , which has eigenvalue  $+1$  for  $|\uparrow\rangle$  and  $-1$  for  $|\downarrow\rangle$ , it is obvious that he/she will obtain an average value of  $p_\uparrow - p_\downarrow$ .

More generally, for any operator  $\hat{A}$ ,

$$\begin{aligned}
\langle \hat{A} \rangle &= \sum_i p_i \langle \psi_i | \hat{A} | \psi_i \rangle \\
&= \sum_i p_i \sum_k \sum_{k'} c_{i,k'}^* c_{i,k} \langle k' | \hat{A} | k \rangle \\
&= \sum_k \sum_{k'} \langle k | \hat{\rho} | k' \rangle \langle k' | \hat{A} | k \rangle \quad \text{by using equation (1.7)} \\
&= \sum_k \langle k | \hat{\rho} \hat{A} | k \rangle \\
&= \text{tr}(\hat{\rho} \hat{A}).
\end{aligned} \tag{1.16}$$

It is easy to check this result against the above example:

$$\begin{aligned}
\langle \hat{\sigma}_z \rangle &= \text{tr} \left( \begin{pmatrix} p_\uparrow & 0 \\ 0 & p_\downarrow \end{pmatrix} \begin{pmatrix} +1 & 0 \\ 0 & -1 \end{pmatrix} \right) \\
&= \text{tr} \left( \begin{pmatrix} p_\uparrow & 0 \\ 0 & -p_\downarrow \end{pmatrix} \right) \\
&= p_\uparrow - p_\downarrow
\end{aligned} \tag{1.17}$$

as expected.

### 1.1.5 Distinguishing pure from mixed states

The density matrix provides a convenient way of distinguishing a pure state from a mixed one:

$$\begin{aligned}
\text{Pure state:} & \quad \hat{\rho}^2 = \hat{\rho} \therefore \text{tr}(\hat{\rho}^2) = 1 \\
\text{Mixed state:} & \quad \hat{\rho}^2 \neq \hat{\rho} \therefore \text{tr}(\hat{\rho}^2) < 1 \quad (\text{assuming the eigenvalues} \\
& \quad \text{are between 0 and 1})
\end{aligned} \tag{1.18}$$

For a pure state, one of the eigenvalues of the density matrix is equal to one, and the others are all zero.

### 1.1.6 Freedom in the representation of $\hat{\rho}$

There are an infinite number of ensembles of pure states which will generate a given  $\hat{\rho}$ . These are known as pure state decompositions of  $\hat{\rho}$ . One can use

a unitary transformation to move from one of these decompositions to another that generates the same  $\hat{\rho}$ :

$$|\tilde{\psi}_i\rangle = \sum_j U_{ij} |\tilde{\phi}_j\rangle \quad (1.19)$$

where  $\{U_{ij}\}$  are the elements of a unitary matrix, and the  $\{|\tilde{\psi}_i\rangle\}$  and  $\{|\tilde{\phi}_j\rangle\}$  are subnormalized states defined by

$$\begin{aligned} |\tilde{\psi}_i\rangle &:= \sqrt{p_{\psi_i}} |\psi_i\rangle, \\ |\tilde{\phi}_j\rangle &:= \sqrt{p_{\phi_j}} |\phi_j\rangle. \end{aligned} \quad (1.20)$$

Thus,  $\{|\tilde{\psi}_i\rangle\}$  and  $\{|\tilde{\phi}_j\rangle\}$  both generate  $\hat{\rho}$ :

$$\hat{\rho} = \sum_i |\tilde{\psi}_i\rangle \langle \tilde{\psi}_i| = \sum_j |\tilde{\phi}_j\rangle \langle \tilde{\phi}_j|. \quad (1.21)$$

$U_{ij}$  does not have to be a square matrix. The number of rows equals the number of pure states in the existing decomposition, and the number of columns equals the dimension of the Hilbert space.

### 1.1.7 The reduced density matrix

Suppose one is in possession of a density operator describing the joint state of several systems:  $A$ ,  $B$ , and  $C$ . What is the density operator that describes the state of just one of those systems, and how does one obtain it? The density operator describing the state of one subsystem of the entire system is known as the *reduced density operator*. It is obtained by a procedure known as the *partial trace*, or *tracing out*.

#### The partial trace

For a bi-partite system  $AB$  in the state

$$|\psi\rangle_{AB} = \sum_{i,\mu} a_{i\mu} |i\rangle_A \otimes |\mu\rangle_B \quad (1.22)$$

the reduced density operator for system  $A$  is obtained by ‘tracing out’ the states of system  $B$ :

$$\begin{aligned}
\hat{\rho}_A &= \text{tr}_B \hat{\rho} = \text{tr}_B (|\psi\rangle_{AB} \langle\psi|_{AB}) \\
&= \sum_{i,j,\mu} a_{i\mu} a_{j\mu}^* |i\rangle_A \langle j|_A \\
&= \sum_{\mu} \langle\mu|\psi\rangle_{AB} \langle\psi|\mu\rangle_B.
\end{aligned} \tag{1.23}$$

Thus, one sums over all inner products of the projector  $|\psi\rangle_{AB} \langle\psi|_{AB}$  with the basis states of system  $B$ . The symbol  $\text{tr}_B$  denotes ‘trace out states of system  $B$ ’.

### Justification for using the partial trace

We choose the partial trace because it gives the correct measurement statistics for any observable  $M_A$  acting only on system  $A$ . To achieve this, we require:

$$\begin{aligned}
\langle M_A \rangle &= \text{tr}(M_A \hat{\rho}_A) \\
&= \text{tr}(M_{AB} \hat{\rho}_{AB})
\end{aligned} \tag{1.24}$$

where

$$M_{AB} = M_A \otimes I_B \tag{1.25}$$

is the observable for the same measurement performed on system  $AB$ . The partial trace

$$\hat{\rho}_A = \text{tr}_B(\hat{\rho}_{AB}) \tag{1.26}$$

is the *only* function satisfying this condition [6].

### Example of the reduced density operator

Consider the following state. We shall see below that it is ‘entangled’, i.e. not factorizable into states of particles  $A$  and  $B$ :

$$|\psi\rangle_{AB} = a|0\rangle_A |0\rangle_B + b|1\rangle_A |1\rangle_B. \tag{1.27}$$

The density operator for it is

$$\begin{aligned}
\hat{\rho} &= |\psi\rangle_{AB} \langle\psi|_{AB} \\
&= |a|^2 |0\rangle_A |0\rangle_B \langle 0|_A \langle 0|_B + ab^* |0\rangle_A |0\rangle_B \langle 1|_A \langle 1|_B + \\
&\quad a^* b |1\rangle_A |1\rangle_B \langle 0|_A \langle 0|_B + |b|^2 |1\rangle_A |1\rangle_B \langle 1|_A \langle 1|_B.
\end{aligned} \tag{1.28}$$

Performing the partial trace yields the reduced density operator for particle  $A$ :

$$\begin{aligned}\hat{\rho}_A &= |a|^2|0\rangle_A \langle 0| + |b|^2|1\rangle_A \langle 1| \\ &= \begin{pmatrix} |a|^2 & 0 \\ 0 & |b|^2 \end{pmatrix}\end{aligned}\quad (1.29)$$

in the  $|0\rangle_A, |1\rangle_A$  basis. This  $\hat{\rho}_A$  is identical to the  $\hat{\rho}_A$  for a classical mixture of  $|0\rangle_A$  and  $|1\rangle_A$ : this equivalence is one way of looking at entanglement.

## 1.2 An introduction to entanglement

A pure quantum state of two systems is described as **entangled** if it cannot be factored into a product of pure states of those two systems. For example, if we have electrons  $A$  and  $B$ , the joint spin state

$$|\chi_{11}\rangle = |\uparrow_A\rangle|\uparrow_B\rangle \quad (1.30)$$

is not entangled as it is a product of the spin-up states of the two electrons. On the other hand,

$$|\chi_{00}\rangle = \frac{1}{\sqrt{2}}(|\uparrow_A\rangle|\downarrow_B\rangle - |\downarrow_A\rangle|\uparrow_B\rangle) \quad (1.31)$$

is entangled, as it is not possible to choose basis states of systems  $A$  and  $B$  such that

$$|\chi_{00}\rangle = |a_A\rangle|b_B\rangle. \quad (1.32)$$

This can be seen as follows. Suppose we could find  $|a_A\rangle$  and  $|b_B\rangle$  that satisfied this condition. Each would be a superposition of up and down states on their respective sites:

$$\begin{aligned}|a_A\rangle &:= p|\uparrow_A\rangle + q|\downarrow_A\rangle, & |p|^2 + |q|^2 &= 1, \\ |b_B\rangle &:= r|\uparrow_B\rangle + s|\downarrow_B\rangle, & |r|^2 + |s|^2 &= 1.\end{aligned}\quad (1.33)$$

Then the singlet state could be rewritten

$$\begin{aligned}|\chi_{00}\rangle &= (p|\uparrow_A\rangle + q|\downarrow_A\rangle)(r|\uparrow_B\rangle + s|\downarrow_B\rangle) \\ &= pr|\uparrow\uparrow\rangle + ps|\uparrow\downarrow\rangle + qr|\downarrow\uparrow\rangle + qs|\downarrow\downarrow\rangle.\end{aligned}\quad (1.34)$$



To achieve equality between the expressions for  $|\chi_{00}\rangle$  in equations (1.31) and (1.34) clearly requires

$$\begin{aligned} pr &= qs = 0 \quad \text{and} \\ ps &= -qr = \frac{1}{\sqrt{2}}, \end{aligned} \quad (1.35)$$

which is not evidently possible. Therefore it is impossible to choose basis states of system  $A$  and system  $B$  in which  $|\chi_{00}\rangle$  can be expressed as a product.

### 1.2.1 The qubit and the ebit

**The qubit** The qubit is a parallelised equivalent of a classical bit, and can in principle be implemented using any two-state quantum system. It makes use of the fact that a quantum system may be prepared in a superposition of its possible states. A qubit is defined thus:

$$|\Psi\rangle = a|0\rangle + b|1\rangle, \quad |a|^2 + |b|^2 = 1. \quad (1.36)$$

**The ebit** The ebit is a unit of entanglement. It is most naturally defined as the amount of entanglement required to transmit one qubit of quantum information from one two-state quantum system to another. This can be achieved with a protocol called quantum teleportation, described in section 1.3.2.

### 1.2.2 The Bell states

Bell-states are a complete orthonormal basis for the state of any pair of 2-state quantum systems. Any pair of 2-state quantum systems will either be in one of the Bell-states, or in some superposition of them. There are four Bell-states, and they are:

$$\begin{aligned} |\Psi_{12}^{\pm}\rangle &= \frac{1}{\sqrt{2}}(|\uparrow\rangle_1|\downarrow\rangle_2 \pm |\downarrow\rangle_1|\uparrow\rangle_2) \\ |\Phi_{12}^{\pm}\rangle &= \frac{1}{\sqrt{2}}(|\uparrow\rangle_1|\uparrow\rangle_2 \pm |\downarrow\rangle_1|\downarrow\rangle_2) \end{aligned} \quad (1.37)$$

They are useful in the context of entanglement because each Bell state contains exactly one ebit of entanglement between the two subsystems.

### 1.2.3 Von Neumann entropy

Suppose the possible values of a random variable  $X$  occur with probabilities  $p_1, \dots, p_n$ . The Shannon entropy of  $X$  is defined:

$$H(X) := H(p_1, \dots, p_n) \equiv - \sum_i p_i \log_2 p_i \quad (1.38)$$

The von Neumann entropy of a quantum state is defined as the Shannon entropy of the eigenvalues  $\{\lambda_i\}$  of that state's density matrix:

$$\begin{aligned} S(\hat{\rho}) &:= -\text{Tr}(\hat{\rho} \log_2 \hat{\rho}) \\ &= - \sum_i \lambda_i \log_2 \lambda_i \\ \text{with } 0 \log_2 0 &:= 0. \end{aligned} \quad (1.39)$$

If a state is pure, as defined previously, its density matrix has a von Neumann entropy of zero. If it is impure, the von Neumann entropy will be non-zero.

In section 1.2.9, we shall see that one of the most important applications of the von Neumann entropy is that it provides a way of quantifying the degree of entanglement in arbitrary (pure or mixed) quantum states. For example, the reduced density matrix for one system of a pair of systems that are in a Bell state has a von Neumann entropy equal to one, and thus the Bell states are said to each contain one ebit of entanglement.

The von Neumann entropy of  $\hat{\rho}_A$  is a maximum if  $\hat{\rho}_A$  is completely mixed, ie. if

$$\hat{\rho}_A = I/d \quad (1.40)$$

where  $d$  is the dimension of the Hilbert space. In that case,

$$S(\hat{\rho}) = d \times -(1/d) \log_2(1/d) = \log_2 d. \quad (1.41)$$

### 1.2.4 Other properties of the von Neumann entropy

Von Neumann entropy has some other interesting properties [7, 8]:

- If  $p_i$  are probabilities, and the states  $\hat{\rho}_i$  have support on orthogonal subspaces, then

$$S\left(\sum_i p_i \hat{\rho}_i\right) = H(p_i) + \sum_i p_i S(\hat{\rho}_i) \quad (1.42)$$

- **Joint entropy theorem** If  $p_i$  are probabilities,  $|i\rangle$  are orthogonal pure states for system  $A$ , and  $\hat{\rho}_i$  is any set of density operators for another system  $B$ , then

$$S\left(\sum_i p_i |i\rangle\langle i| \otimes \hat{\rho}_i\right) = H(p_i) + \sum_i p_i S(\hat{\rho}_i) \quad (1.43)$$

### 1.2.5 Wootters tangle

Wootters [9, 10, 11] considers a general spin-state of two distinguishable particles:

$$\begin{aligned} |\phi\rangle &= a|\uparrow\uparrow\rangle + b|\uparrow\downarrow\rangle + c|\downarrow\uparrow\rangle + d|\downarrow\downarrow\rangle, \\ |a|^2 + |b|^2 + |c|^2 + |d|^2 &= 1. \end{aligned} \quad (1.44)$$

The Wootters entanglement is simply a reexpression of the von Neumann entropy of  $\hat{\rho}_B$ , and is defined as

$$E = h\left[\frac{1}{2}(1 + \sqrt{1 - \tau})\right], \quad (1.45)$$

where

$$h(x) = -(x \log_2 x + (1 - x) \log_2 (1 - x)) \quad (1.46)$$

and the quantity  $\tau$  is known as the ‘tangle’ and is defined by

$$\tau = 4|ad - bc|^2. \quad (1.47)$$

### 1.2.6 Pure state concurrence

The tangle is an example of a more general entanglement measure called concurrence, defined by Hill and Wootters [10] for a pure state  $|\psi\rangle$  as

$$C(\psi) := |\langle\psi|\tilde{\psi}\rangle| \quad (1.48)$$

where  $\tilde{\psi}$  is the ‘spin-flipped’ state. For a pure state  $|\psi_A\rangle$  of a single qubit, this is defined as

$$|\tilde{\psi}_A\rangle := \sigma_y |\psi_A^*\rangle. \quad (1.49)$$

This is due to the fact that the time reversal operator  $\Theta$  for a spin-half system must be antiunitary [12]:

$$\Theta = -i\eta \left(\frac{2S_y}{\hbar}\right) K \quad (1.50)$$

where  $K$  is the complex conjugation operator and  $\eta$  is an arbitrary phase. A suitable choice of  $\eta$  therefore gives

$$\Theta = \sigma_y K \quad (1.51)$$

and hence the above definition of  $|\tilde{\psi}_A\rangle$ . For a general state  $|\psi_{AB}\rangle$  of two qubits, the spin-flipped state is

$$|\tilde{\psi}_{AB}\rangle := \sigma_y^A \otimes \sigma_y^B |\psi_{AB}^*\rangle. \quad (1.52)$$

For some pure state  $\psi_{AB}$  of two qubits, the entanglement between the two qubits is

$$E(\psi_{AB}) = \mathcal{E}(C(\psi_{AB})) \quad (1.53)$$

where

$$\mathcal{E}(C) := h\left(\frac{1 + \sqrt{1 - C^2}}{2}\right) \quad (1.54)$$

and  $h(x)$  is the binary entropy function:

$$h(x) := -x \log_2 x - (1 - x) \log_2 (1 - x). \quad (1.55)$$

### 1.2.7 Entanglement monotones

As first described by Vidal [13], an entanglement monotone is a function that satisfies:

$$\begin{aligned} &\text{For } \hat{\rho} \xrightarrow{\text{LOCC}} \{p_i \hat{\rho}_i\} \\ &\text{then } E(\hat{\rho}) \geq \sum_i p_i E(\hat{\rho}_i). \end{aligned} \quad (1.56)$$

Vidal put it this way: "monotonicity under local transformations is proposed as the only natural requirement for measures of entanglement". LOCC means 'local operations and classical communication', ie. the combination of operations performed locally on the two subsystems, and classical signals sent between those two subsystems. A non-entangled state can be prepared through LOCC, whereas an entangled state can't. If one defines a pure-state entanglement function

$$f(\text{tr}_B |\psi\rangle\langle\psi|) := E(|\psi\rangle) \quad (1.57)$$

with the properties:

- Local unitary transformations on subsystem  $A$  leave it invariant:

$$f(U_A \hat{\rho} U_A^\dagger) = f(\hat{\rho}) \text{ for all local unitary operations } \{U_A\}. \quad (1.58)$$

- It is concave:

$$\begin{aligned} f(\lambda \hat{\rho}_1 + (1 - \lambda) \hat{\rho}_2) &\geq \lambda f(\hat{\rho}_1) + (1 - \lambda) f(\hat{\rho}_2) \\ \text{for all } \hat{\rho}_1, \hat{\rho}_2, 0 \leq \lambda \leq 1. \end{aligned} \quad (1.59)$$

Then the convex-roof extension of  $E$  is an entanglement monotone:

$$E(\hat{\rho}) := \min_{\text{decomps}} \sum_j p_j E(|\psi\rangle_j). \quad (1.60)$$

There are many possible entanglement monotones. One example is the entanglement of formation, which is described in section 1.2.9. Another example is the quantum relative entropy. The monotonicity of relative entropy under completely positive mappings was proven by Uhlmann and is known as Uhlmann's theorem [14, 15].

### 1.2.8 Quantum relative entropy

The relative entropy of a quantum state  $\hat{\rho}$  with respect to the quantum state  $\hat{\sigma}$  is defined by

$$S(\hat{\rho}||\hat{\sigma}) = \text{tr } \hat{\rho} \log_2 \hat{\rho} - \text{tr } \hat{\rho} \log_2 \hat{\sigma}. \quad (1.61)$$

The quantum relative entropy is non-negative:

$$S(\hat{\rho}||\hat{\sigma}) \geq 0 \text{ with equality iff } \hat{\rho} = \hat{\sigma} \text{ (Klein's inequality)}. \quad (1.62)$$

The quantum relative entropy can be thought of as a 'distance' between density operators.

### 1.2.9 Entanglement of formation

A well-known example of an entanglement monotone is the entanglement of formation, which is the convex roof extension of the von Neumann entropy. The von Neumann entropy is a convenient measure of entanglement for bipartite pure states, but it cannot provide an answer for the entanglement between two

subsystems which are in a mixed state. Instead, it gives the entanglement between one of the subsystems and ‘everything else’ (the other subsystem plus the environment). However, the entanglement of formation turns out to be a particularly natural measure of entanglement between two systems which are jointly in a mixed state.

If  $m$  copies of a (pure or mixed) state  $\hat{\rho}$  are produced from  $n$  Bell states, then the entanglement of formation of  $\hat{\rho}$  is the number of Bell states  $n/m$  required to produce each copy of  $\hat{\rho}$  as the supply of Bell states  $n \rightarrow \infty$ . This process is known as entanglement dilution [16].

### Entanglement of formation for a pure quantum state

If  $\hat{\rho}$  is a pure quantum state, then the entanglement of formation equals the von Neumann entropy. This can be seen as follows. If an entangled state  $|\psi\rangle$  has a Schmidt decomposition

$$|\psi\rangle = \sum_x \sqrt{p(x)} |x_A\rangle |x_B\rangle \quad (1.63)$$

then

$$|\psi\rangle^{\otimes m} = \sum_{x_1, x_2, \dots, x_m} \sqrt{p(x_1)p(x_2)\dots p(x_m)} |x_{1A}x_{2A}\dots x_{mA}\rangle |x_{1B}x_{2B}\dots x_{mB}\rangle. \quad (1.64)$$

For the next step, it is necessary to define the concept of a ‘typical sequence’. This is a sequence of  $m$  symbols from an information source which has a fraction  $q$  of the symbols equal to 1, and a fraction  $1 - q$  equal to zero. The probability of such a sequence is

$$p(x_1 \dots x_m) \approx 2^{-mH(X)} \quad (1.65)$$

where  $H(X)$  is the Shannon entropy of the source. An  $\epsilon$ -typical sequence is one for which the Shannon entropy of the source satisfies this relationship to within a tolerance of  $\pm\epsilon$ , ie.

$$2^{-m(H(X)+\epsilon)} \leq p(x_1 \dots x_m) \leq 2^{-m(H(X)-\epsilon)}. \quad (1.66)$$

It can be shown that for any  $\epsilon \geq 0$ , the maximum number of  $\epsilon$ -typical sequences is [17]

$$\text{no. of sequences} \leq 2^{m(H(X)+\epsilon)}. \quad (1.67)$$

We now discard all the terms in the sum where the coefficients  $p(x_1)p(x_2)\dots p(x_m)$  are not  $\epsilon$ -typical, giving

$$|\psi_m\rangle := \sum_{x \in \epsilon\text{-typical}} \sqrt{p(x_1)p(x_2)\dots p(x_m)} |x_{1A}x_{2A}\dots x_{mA}\rangle |x_{1B}x_{2B}\dots x_{mB}\rangle \quad (1.68)$$

and renormalize it:

$$|\psi'_m\rangle := \frac{|\psi_m\rangle}{\sqrt{\langle \psi_m | \psi_m \rangle}}. \quad (1.69)$$

Now by the result in equation (1.67), the maximum number of terms in equation (1.68) is

$$2^{m(H(p(x)) + \epsilon)} = 2^{m(S(\hat{\rho}_A) + \epsilon)} \quad (1.70)$$

where  $\hat{\rho}_A = \text{tr}_B |\psi\rangle\langle\psi|$ . How close is  $|\psi'_m\rangle$  to  $|\psi\rangle^{\otimes m}$ ? As  $m \rightarrow \infty$  it becomes very close indeed as measured by the fidelity:

$$F(|\psi\rangle^{\otimes m}, |\psi'_m\rangle) \rightarrow 1. \quad (1.71)$$

Consider this entanglement dilution procedure:

- Alice and Bob have  $n = m(S(\hat{\rho}_A) + \epsilon)$  Bell pairs shared between them.
- Alice prepares the state  $|\psi'_m\rangle$ .
- Alice teleports Bob's half of  $|\psi'_m\rangle$  over to him using the Bell pairs, by following the protocol to be defined in section 1.3.2. Note that this protocol requires the use of classical communication.

The entanglement of formation of the state obtained through this procedure is

$$n/m = \frac{m(S(\hat{\rho}_A) + \epsilon)}{m} = S(\hat{\rho}_A) + \epsilon \quad (1.72)$$

One can make  $\epsilon$  as small as is required, so the entanglement of formation of  $|\psi'_m\rangle$  for  $\epsilon \rightarrow 0$  tends to

$$E_F(|\psi'_m\rangle) = n/m \rightarrow S(\hat{\rho}_A). \quad (1.73)$$

As  $m \rightarrow \infty$ ,  $|\psi'_m\rangle$  becomes equal to  $|\psi\rangle^{\otimes m}$ , and thus this result becomes true for  $|\psi\rangle^{\otimes m}$  as well.

If the joint state of two systems  $A$  and  $B$  is not pure, systems  $A$  and  $B$  are, in general, themselves entangled with another, unspecified system ('the environment'). In this case, applying the above procedure does not give the entanglement of system  $A$  with  $B$ , but instead the entanglement of system  $A$  with system  $B$  plus the environment. To calculate the entanglement of formation between  $A$  and  $B$  we need to use a different procedure, outlined in the next section.

### Entanglement of formation for a mixed quantum state

A particular pure state decomposition of a mixed state  $\hat{\rho}$  shared between subsystems  $A$  and  $B$  can be written

$$\hat{\rho} = \sum_i p_i \hat{\rho}_i = \sum_i p_i |\psi_i\rangle\langle\psi_i| = \sum_i |\tilde{\psi}_i\rangle\langle\tilde{\psi}_i| \quad (1.74)$$

where the  $\{|\tilde{\psi}_i\rangle\}$  are subnormalized states defined by [18]

$$|\tilde{\psi}_i\rangle := \sqrt{p_i} |\psi_i\rangle. \quad (1.75)$$

The average entanglement of the decomposition, in ebits, is

$$\begin{aligned} E_{av}(\{|\tilde{\psi}_i\rangle\}) &= \sum_i p_i E_i \\ &= - \sum_i p_i \text{Tr}_A[\hat{\rho}_i^A \log_2 \hat{\rho}_i^A] \end{aligned} \quad (1.76)$$

where  $E_i$  is the entanglement of  $|\psi_i\rangle$ . The entanglement of formation of  $\hat{\rho}$  is defined as the minimum of  $E_{av}$  over all possible decompositions of  $\hat{\rho}$ :

$$E_F(\hat{\rho}) := \min_{\{|\tilde{\psi}_i\rangle\}} E_{av} \quad (1.77)$$

The decomposition which gives the minimum is described as 'optimal'. It is possible to make unitary transformations between different decompositions of a given mixed state [18]:

$$|\tilde{\psi}_i\rangle \rightarrow \sum_j U_{ij} |\tilde{\phi}_j\rangle. \quad (1.78)$$

Although these decompositions all generate the same mixed state, they have different values of the average entanglement.



### Wootters formula for entanglement of formation of two qubits

Wootters [11] derives a formula for the entanglement of formation of a mixed state of two qubits, or any other pair of two-level quantum systems. It is analogous to the concurrence-based entanglement measure derived by Hill and Wootters for a pure state of two qubits (see section 1.2.6), and is given by

$$E(\rho) := \mathcal{E}(C(\rho)). \quad (1.79)$$

The convex function  $\mathcal{E}$  is the same one as defined in equation (1.54).

The mixed-state concurrence is defined by

$$C(\rho) := \max\{0, \lambda_1 - \lambda_2 - \lambda_3 - \lambda_4\} \quad (1.80)$$

The  $\lambda_i$ 's can be viewed as either:

- The eigenvalues in decreasing order of the Hermitian matrix

$$R := \sqrt{\sqrt{\rho}\tilde{\rho}\sqrt{\rho}}. \quad (1.81)$$

- The square roots of the eigenvalues of  $\rho\tilde{\rho}$  (which is non-Hermitian).

Here,  $\tilde{\rho}$  is the 'spin-flipped' mixed state, and is defined by

$$\tilde{\rho} = (\sigma_y \otimes \sigma_y)\rho^*(\sigma_y \otimes \sigma_y) \quad (1.82)$$

which follows from the expression for  $|\tilde{\psi}_{AB}\rangle$  given previously in equation (1.52).

### Postulated additivity of entanglement of formation

An open problem in quantum information theory is whether the entanglement of formation is additive [19]. For the tensor product  $\hat{\rho}$  of a pair of bipartite density operators  $\hat{\rho}_1, \hat{\rho}_2$ ,

$$\hat{\rho} := \hat{\rho}_1 \otimes \hat{\rho}_2, \quad (1.83)$$

where  $\hat{\rho}_1$  and  $\hat{\rho}_2$  are each shared between Alice and Bob, it is possible to show that  $E_F$  is subadditive [20]:

$$E_F(\hat{\rho}) \leq E_F(\hat{\rho}_1) + E_F(\hat{\rho}_2). \quad (1.84)$$

This can easily be seen as follows. Let

$$\begin{aligned}\hat{\rho}_1 &:= \sum_i |\tilde{\psi}_i\rangle_{11} \langle \tilde{\psi}_i| \text{ and} \\ \hat{\rho}_2 &:= \sum_j |\tilde{\psi}_j\rangle_{22} \langle \tilde{\psi}_j|\end{aligned}\quad (1.85)$$

be optimal decompositions of  $\hat{\rho}_1$  and  $\hat{\rho}_2$  respectively. Then

$$\hat{\rho} := \hat{\rho}_1 \otimes \hat{\rho}_2 = \sum_{ij} |\tilde{\psi}_i\rangle_1 |\tilde{\psi}_j\rangle_{22} \langle \tilde{\psi}_j|_1 \langle \tilde{\psi}_i| \quad (1.86)$$

is a decomposition of  $\hat{\rho}$  that is not necessarily optimal. It has an average entanglement

$$E_{av} = \sum_{ij} p_{ij} E(\hat{\rho}_{ij}) \quad (1.87)$$

where

$$\hat{\rho}_{ij} := |\psi_i\rangle_1 |\psi_j\rangle_{22} \langle \psi_j|_1 \langle \psi_i| \quad (1.88)$$

(note that these  $\psi$ 's are NOT subnormalized). Now

$$\begin{aligned}|\tilde{\psi}_i\rangle_1 &= \sqrt{p_i} |\psi_i\rangle_1 \\ \therefore p_{ij} &= p_i p_j\end{aligned}\quad (1.89)$$

And

$$E(\hat{\rho}_{ij}) = E(\hat{\rho}_i) + E(\hat{\rho}_j) \quad (1.90)$$

because the entanglement of pure states is additive. So from equation 1.87, one gets

$$\begin{aligned}E_{av} &= \sum_{ij} p_{ij} [E(\hat{\rho}_i) + E(\hat{\rho}_j)] \\ &= \sum_i p_i E(\hat{\rho}_i) + \sum_j p_j E(\hat{\rho}_j) \\ &= E(\hat{\rho}_1) + E(\hat{\rho}_2).\end{aligned}\quad (1.91)$$

So you can at least get the average entanglement as low as the sum of  $E_F(\hat{\rho}_1)$  and  $E_F(\hat{\rho}_2)$ , and therefore

$$E_F(\hat{\rho}) \leq E_F(\hat{\rho}_1) + E_F(\hat{\rho}_2). \quad (1.92)$$

But it is not known whether ‘ $\leq$ ’ can be replaced by ‘ $=$ ’, ie. whether equality applies for all mixed states. However, Vidal et al have proven additivity for several families of bipartite mixed states [20].

The open question of the additivity of the entanglement of formation matters because, in the words of K. Vollbrecht, it is ”crucial to settle the interpretation of  $E_F$  as a resource quantity. The typical kind of tensor products appearing in the theory are pairs created by (maybe different) sources of entangled states, and kept for later use.” [19]

### 1.2.10 Entanglement of distillation

Entanglement of distillation describes the reverse of entanglement dilution (this is also known as entanglement concentration, or entanglement purification). If one starts with  $m$  copies of the pure or mixed state  $\hat{\rho}$  and, using LOCC only, one produces  $n$  Bell pairs from them, the distillable entanglement of  $\hat{\rho}$  is the fraction  $n/m$  as  $n \rightarrow \infty$ . This fraction is also known as the *efficiency* of the distillation process. If  $\hat{\rho}$  is a pure quantum state, then the distillable entanglement can be shown to equal the von Neumann entropy, and thus the entanglement of formation [21].

For mixed states, the entanglement of distillation is bounded from above by the entanglement of formation:

$$D \leq E_F. \quad (1.93)$$

Thus for mixed states, distillation is an *irreversible* process - if you distill a certain number of Bell pairs from a mixed state, you will require extra Bell pairs in order to reconstruct that mixed state using dilution. There are thus two types of entanglement, ‘free’ entanglement which is distillable, and ‘bound’ entanglement which is not. Indeed there are some states, the ‘bound entangled’ states, which contain only bound entanglement and from which no useful entanglement can be distilled [22, 23]. For certain classes of mixed states, the inequality in equation (1.93) can be shown to be strict [24].

## 1.3 What can entanglement do?

Why are people interested in entanglement? Here are a few reasons:

- It reveals quantum non-locality.
- It can be used to achieve secure communications.
- It plays a role in allowing quantum mechanical techniques to be used to process information.

The following sections describe more fully these motivating applications of entanglement.

### 1.3.1 Bell's theorem

#### Preamble

Einstein, Podolsky, and Rosen's famous paper [25] argued that quantum mechanics could not be a complete, realistic theory without the addition of 'hidden variables'. These were supposed to be additional parameters that completely specified the state of a quantum system and in doing so restored locality to the theory.

In 1964, Bell showed [26] that such a theory, however formulated, will not produce results consistent with experimental observation.

The validity of Bell's theorem is a pre-requisite for the validity of much of quantum information theory. If it is not valid, it is possible that quantum mechanics is a local theory, and QIT protocols such as quantum teleportation cannot possibly work. This is because, for example, the states of the spins in a singlet pair would be determined when the pair was produced, and there would be no possibility of using their states to transmit information.

#### Nomenclature

Consider a pair of spin-half particles in a singlet state, which have been spatially separated. Their spins are denoted  $\sigma_1$  and  $\sigma_2$ . We can use Stern-Gerlach apparatuses to measure their spins along arbitrary axes: say those specified by the unit vectors  $\hat{\mathbf{a}}$  and  $\hat{\mathbf{b}}$ . For a singlet state, if  $\sigma_1 \cdot \hat{\mathbf{a}} = +1$  then a subsequent measurement along the same axis on  $\sigma_2$  must give  $\sigma_2 \cdot \hat{\mathbf{a}} = -1$ .

Suppose that, as Einstein and his coworkers would have preferred, there is no action-at-a-distance. In that case, it must be that the results of our measurements were set at the time the singlet pair was formed. So from the point of view of the local realist camp, there's nothing mysterious about the

fact that measurements on the two spins always give opposite results even when the spins are spacelike-separated: this only seems ‘weird’ because we do not understand the extra physical parameters or ‘hidden variables’ which govern the spin values assigned to the spins at the time they interacted.

### Introduce a hidden variable

Let’s denote the hidden variable or hidden variables by  $\lambda$ . This (these) variable(s) can be discrete or continuous - we’ll treat  $\lambda$  as the latter. If  $A$  is the result of measuring  $\sigma_1 \cdot \hat{\mathbf{a}}$  and  $B$  is the result of measuring  $\sigma_2 \cdot \hat{\mathbf{b}}$  then now we have

$$\begin{aligned} A(\hat{\mathbf{a}}, \lambda) &= \pm 1 \\ B(\hat{\mathbf{b}}, \lambda) &= \pm 1 \end{aligned} \tag{1.94}$$

where under the Einsteinian definition of ‘locality’ we insist that  $A \neq A(\hat{\mathbf{b}})$ , and  $B \neq B(\hat{\mathbf{a}})$ . In other words, the only way in which the measurement results depend on each other is in the original preparation of the state, and not in the way in which the measurements are subsequently performed.

Denote the probability distribution of  $\lambda$  when a large number of systems are prepared in an apparently identical fashion by us by

$$\int \rho(\lambda) d\lambda = 1 \tag{1.95}$$

I say ‘apparently’ because of course we have no understanding or control of the hidden variable(s). By integrating over this probability distribution, we can obtain a classical expectation value for the product of  $\sigma_1 \cdot \hat{\mathbf{a}}$  and  $\sigma_2 \cdot \hat{\mathbf{b}}$ :

$$P(\hat{\mathbf{a}}, \hat{\mathbf{b}}) = \int d\lambda \rho(\lambda) A(\hat{\mathbf{a}}, \lambda) B(\hat{\mathbf{b}}, \lambda) \tag{1.96}$$

The expectation value which is predicted by quantum mechanics (and which has been experimentally observed) is given by

$$E(\hat{\mathbf{a}}, \hat{\mathbf{b}}) = \langle \sigma_1 \cdot \hat{\mathbf{a}} \times \sigma_2 \cdot \hat{\mathbf{b}} \rangle = -\hat{\mathbf{a}} \cdot \hat{\mathbf{b}}. \tag{1.97}$$

In this discussion, the symbols  $E$  and  $P$  are used to denote quantum mechanical and classical expectation values respectively. The following sections describe how Bell shows that hidden variable theories lead to an inequality between expectation values which experimental observation shows to be incorrect.

### Hidden variables are consistent with the results of measurements on a single spin

Although the real issue here is whether a hidden variable theory can accurately describe the results of measurements on a pair of spins, it is first worth checking whether such a theory can work for the results of measurements on a single spin. Clearly, that is a prerequisite. Consider a spin-half particle in a pure spin state with polarization  $\hat{\mathbf{p}}$ . In this case it will be convenient to represent the hidden variable(s) by a unit vector  $\hat{\lambda}$  which has a uniform probability distribution over the hemisphere  $\hat{\lambda} \cdot \hat{\mathbf{p}} > 0$ .

Let the result of measuring  $\hat{\sigma} \cdot \hat{\mathbf{a}}$  be

$$\text{sign } \hat{\lambda} \cdot \hat{\mathbf{a}}' \quad (1.98)$$

where  $\hat{\mathbf{a}}'$  is related to  $\hat{\mathbf{a}}$  and  $\hat{\mathbf{p}}$  in an arbitrary way. However for this exercise, we shall set the angle between  $\hat{\mathbf{a}}'$  and  $\hat{\mathbf{p}}$  to be  $\theta'$ . Thus if  $\alpha$  is the polar angle (see Figure 1.1 ) then

$$\begin{aligned} 0 < \alpha < \pi - \theta' & : \hat{\lambda} \cdot \hat{\mathbf{a}}' > 1 \\ \alpha > \pi - \theta' & : \hat{\lambda} \cdot \hat{\mathbf{a}}' < 1 \end{aligned} \quad (1.99)$$

and averaging over  $\hat{\lambda}$  gives this expectation value:

$$\begin{aligned} \langle \hat{\sigma} \cdot \hat{\mathbf{a}} \rangle &= \int_{\hat{\lambda}} \text{sign } \hat{\lambda} \cdot \hat{\mathbf{a}}' d\hat{\lambda} \\ &= \frac{1}{2\pi} \int_{\phi=0}^{2\pi} d\phi \frac{1}{\pi} \int_{\alpha=0}^{\pi} (\text{sign } \hat{\lambda} \cdot \hat{\mathbf{a}}') d\alpha \\ &= \frac{1}{\pi} \left( \alpha \Big|_0^{\pi-\theta'} - \alpha \Big|_{\pi-\theta'}^{\pi} \right) \\ &= \frac{1}{\pi} \left( \pi - \theta' - (\pi - (\pi - \theta')) \right) \\ &= 1 - \frac{2\theta'}{\pi} \end{aligned} \quad (1.100)$$

where  $r$  and  $\phi$  are the redundant radial and azimuthal spherical coordinates.

Now we specify the exact relationship between  $\hat{\mathbf{a}}'$ ,  $\hat{\mathbf{a}}$ , and  $\hat{\mathbf{p}}$ . It is this: we obtain  $\hat{\mathbf{a}}'$  by rotating  $\hat{\mathbf{a}}$  towards  $\hat{\mathbf{p}}$  until

$$1 - \frac{2\theta'}{\pi} = \cos \theta \quad (1.101)$$

So we get

$$\langle \hat{\sigma} \cdot \hat{\mathbf{a}} \rangle = \cos \theta \quad (1.102)$$

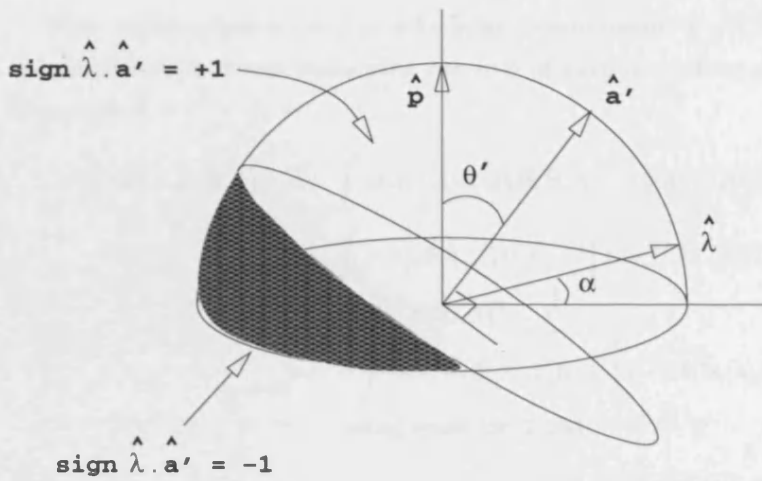


Figure 1.1: Geometry for a spin-half particle in a pure spin state with polarization  $\hat{\mathbf{p}}$ , and one or more hidden variable(s) represented by  $\hat{\lambda}$ , which has a uniform probability distribution over the hemisphere  $\hat{\lambda} \cdot \hat{\mathbf{p}} > 0$ .

which is the correct quantum mechanical result since by the definition of spin polarization,  $\hat{\mathbf{p}} = \langle \hat{\sigma} \rangle$ , and  $\theta$  is the angle between  $\hat{\mathbf{p}}$  and  $\hat{\mathbf{a}}$ .

### Hidden variables are not consistent with the results of separate measurements on two spins in a singlet state

So, hidden variable theories are capable of satisfying the prerequisite condition of correctly describing the results of measurements on a single spin. Now, one now needs to consider whether they are capable of performing the task their proponents claim they are able to perform, ie. correctly describing the results of 2-spin measurements. First, note that:

- The probability distribution  $\rho$  is normalized:

$$\int d\lambda \rho(\lambda) = 1 \quad (1.103)$$

- Since the two spins are in a singlet state, measuring them along the same axis always gives opposite results:

$$A(\hat{\mathbf{a}}, \lambda) = -B(\hat{\mathbf{a}}, \lambda) \quad (1.104)$$

Now we introduce a third axis for spin measurement:  $\hat{\mathbf{c}}$ . What's the difference in  $P(\hat{\mathbf{a}}, \hat{\mathbf{x}})$  between measuring the spin of particle 2 along axis  $\hat{\mathbf{x}} = \hat{\mathbf{b}}$  and along axis  $\hat{\mathbf{x}} = \hat{\mathbf{c}}$ ?

$$\begin{aligned}
P(\hat{\mathbf{a}}, \hat{\mathbf{b}}) - P(\hat{\mathbf{a}}, \hat{\mathbf{c}}) &= \int \rho(\lambda) \left[ A(\hat{\mathbf{a}}, \lambda) B(\hat{\mathbf{b}}, \lambda) - A(\hat{\mathbf{a}}, \lambda) B(\hat{\mathbf{c}}, \lambda) \right] d\lambda \\
&= \int \rho(\lambda) A(\hat{\mathbf{a}}, \lambda) B(\hat{\mathbf{b}}, \lambda) \left[ 1 - B(\hat{\mathbf{b}}, \lambda) B(\hat{\mathbf{c}}, \lambda) \right] d\lambda \\
&\quad \text{since } B(\hat{\mathbf{b}}, \lambda)^2 = 1 \\
&= - \int \rho(\lambda) A(\hat{\mathbf{a}}, \lambda) A(\hat{\mathbf{b}}, \lambda) \left[ 1 + A(\hat{\mathbf{b}}, \lambda) B(\hat{\mathbf{c}}, \lambda) \right] d\lambda \\
&\quad \text{using equation 1.104.} \tag{1.105}
\end{aligned}$$

Now,

$$\begin{aligned}
A &= \pm 1, \\
\rho(\lambda) &\geq 0, \tag{1.106}
\end{aligned}$$

and thus the maximum value of the integrand occurs for  $A(a, \lambda) = A(b, \lambda) = +1$  for all  $\lambda$ . Thus one gets the inequality

$$|P(\hat{\mathbf{a}}, \hat{\mathbf{b}}) - P(\hat{\mathbf{a}}, \hat{\mathbf{c}})| \leq \int \rho(\lambda) \left[ 1 + A(\hat{\mathbf{b}}, \lambda) B(\hat{\mathbf{c}}, \lambda) \right] d\lambda \tag{1.107}$$

ie.

$$|P(\hat{\mathbf{a}}, \hat{\mathbf{b}}) - P(\hat{\mathbf{a}}, \hat{\mathbf{c}})| \leq 1 + P(\hat{\mathbf{b}}, \hat{\mathbf{c}}). \tag{1.108}$$

Any hidden variable theory, regardless of how physically reasonable it is in other respects, must produce expectation values that satisfy this inequality for all  $\hat{\mathbf{a}}, \hat{\mathbf{b}}, \hat{\mathbf{c}}$ .

If this condition is not satisfied, we must conclude that hidden variable theories cannot accurately describe the results of spin measurements along arbitrary axes on two spins that are in a singlet state. We arrived at this conclusion in a very general way - by assuming:

- Measurements made along the same axis on spins 1 and 2 must always give opposite results.
- There are one or more hidden variables, each of which has a definite initial value for a given singlet pair. The value of each variable may evolve up



until the time of the measurements in a way we are indifferent to. The addition of these hidden variables absolutely determines our measurement results on the individual spins.

- The hidden variables are distributed according to a probability distribution  $\rho(\lambda)$  for a large number of systems which we believe we have prepared identically.

In fact, it is easy to find a choice of the directions  $\hat{\mathbf{a}}, \hat{\mathbf{b}}, \hat{\mathbf{c}}$  that violates this inequality, as is shown in the next section.

### A choice of measurement axes which violates Bell's inequality

Choose  $\hat{\mathbf{a}}, \hat{\mathbf{b}}, \hat{\mathbf{c}}$  such that they all lie in the same plane and the angle between  $\hat{\mathbf{a}}, \hat{\mathbf{b}}$  is  $\pi/4$ , and the angle between  $\hat{\mathbf{b}}, \hat{\mathbf{c}}$  is also  $\pi/4$ . The angle between  $\hat{\mathbf{a}}, \hat{\mathbf{c}}$  is thus  $\pi/2$ .

Using the quantum mechanical result in equation (1.97) for the expectation value of the product of  $\sigma_1 \cdot \hat{\mathbf{a}}$  and  $\sigma_2 \cdot \hat{\mathbf{b}}$ , one obtains

$$|E(\hat{\mathbf{a}}, \hat{\mathbf{b}}) - E(\hat{\mathbf{a}}, \hat{\mathbf{c}})| = |-\cos \frac{\pi}{4} + \cos \frac{\pi}{2}| = |-\frac{1}{\sqrt{2}} + 0| = 0.707 \quad (1.109)$$

and

$$1 + E(\hat{\mathbf{b}}, \hat{\mathbf{c}}) = 1 - \cos \frac{\pi}{2} = 1 - \frac{1}{\sqrt{2}} = 0.293 \quad (1.110)$$

and hence Bell's inequality is violated:

$$|E(\hat{\mathbf{a}}, \hat{\mathbf{b}}) - E(\hat{\mathbf{a}}, \hat{\mathbf{c}})| > 1 + E(\hat{\mathbf{b}}, \hat{\mathbf{c}}) \quad (1.111)$$

### Bell's theorem and entanglement

Bell's theorem is inherently relevant to entanglement theory because, as shown above, it is an *entangled* state of two quantum systems (ie. the singlet state) which violates Bell's inequalities. Testing for a violation of Bell's inequalities has thus become the standard method for demonstrating the existence of entanglement in a system [27].

However, it is now known that although all states which violate Bell inequalities must be entangled, the converse is not true. In fact, all pure entangled states violate Bell inequalities, but, as shown by Werner, some mixed entangled states do not [28, 29].

### 1.3.2 Quantum teleportation

Until 1993, physicists believed there was a very good reason why one could not transmit unknown quantum states from one location to another. That reason was the collapse of the wavefunction. How could one transmit a quantum state, it was reasoned, when attempting to measure that state inevitably destroys most of the information carried by that state?

In 1993, Bennett et al [1], developed a method of transmitting quantum states that circumvents this objection. At no point is a measurement made that will destroy the information in the quantum state that is being transmitted. They called this method ‘quantum teleportation’, an inspired choice of name as the inevitable association with ‘Star Trek’ guaranteed widespread media coverage of their new paper.

#### Summary of the teleportation protocol

The protocol is summarized graphically in Figure 1.2.

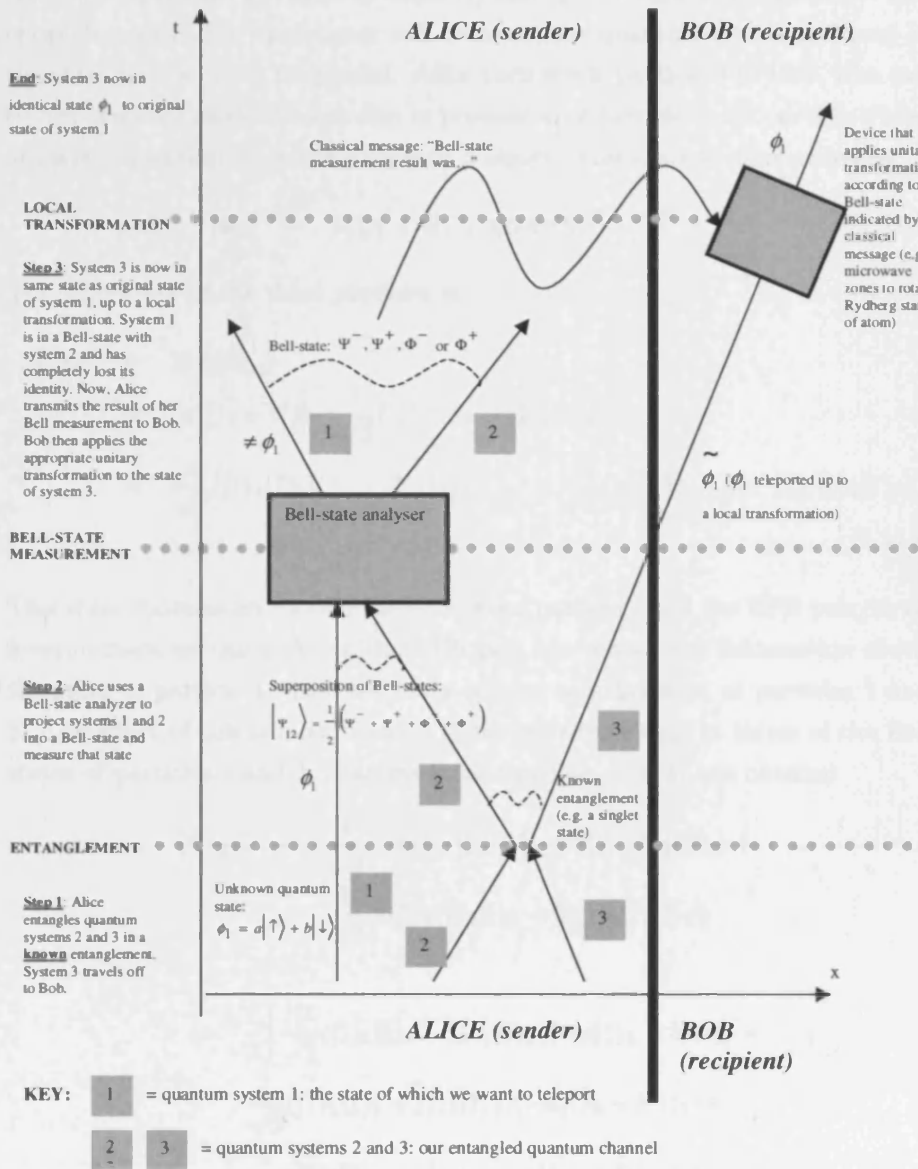
Let Alice be the sender, Bob the recipient. Alice prepares two quantum systems in a maximally entangled state: the ‘carrier pair’. Alice sends one of the two entangled systems to Bob: call this the ‘target system’. Now Alice performs a Bell-state measurement on the joint system composed of the quantum system whose state she wishes to teleport (the ‘source system’) and the local half of the carrier pair: call this the ‘local pair’.

Alice’s Bell-state measurement projects the target system into a quantum state related to the original state of the source system by a simple unitary transformation. Which transformation depends on which Bell-state the local pair was projected into by the measurement. Alice sends by classical means the result of the Bell-state measurement to Bob, who can then apply the appropriate transformation to bring the target system into a state identical to the original state of the source system.

#### Description of the teleportation protocol

Bennet et al described the protocol in terms of spin-1/2 particles, but it is equally applicable to teleporting the state of any 2-state or N-state quantum system. First, Alice prepares two spin-1/2 particles (particles 2 and 3) in an

Figure 1.2: Outline of the Bennett et al. teleportation protocol [1].



EPR singlet state:

$$|\Psi_{23}^-\rangle = \frac{1}{\sqrt{2}}(|\uparrow\rangle_2|\downarrow\rangle_3 - |\downarrow\rangle_2|\uparrow\rangle_3) \quad (1.112)$$

Here,  $|\uparrow\rangle$  represents the spin-up state  $|\uparrow\rangle$  and  $|\downarrow\rangle$  the spin-down state  $|\downarrow\rangle$ . The entanglement in the singlet pair will transmit the quantum-mechanical part of the state that is to be teleported. Alice then sends particle 3 to Bob, who can be any distance away. Alice is also in possession of particle 1, the particle whose unknown quantum state she wishes to teleport. This state is represented by

$$|\phi_1\rangle = a|\uparrow\rangle_1 + b|\downarrow\rangle_1 \text{ where } |a|^2 + |b|^2 = 1 \quad (1.113)$$

The joint state of the three particles is

$$\begin{aligned} |\Psi_{123}\rangle &= |\phi_1\rangle|\Psi_{23}^-\rangle \\ &= (a|\uparrow\rangle_1 + b|\downarrow\rangle_1)\frac{1}{\sqrt{2}}(|\uparrow\rangle_2|\downarrow\rangle_3 - |\downarrow\rangle_2|\uparrow\rangle_3) \\ &= \frac{a}{\sqrt{2}}(|\uparrow\rangle_1|\uparrow\rangle_2|\downarrow\rangle_3 - |\uparrow\rangle_1|\downarrow\rangle_2|\uparrow\rangle_3) + \frac{b}{\sqrt{2}}(|\downarrow\rangle_1|\uparrow\rangle_2|\downarrow\rangle_3 - |\downarrow\rangle_1|\downarrow\rangle_2|\uparrow\rangle_3) \end{aligned} \quad (1.114)$$

This state contains no entanglement between particle 1 and the EPR pair, so no measurement we can make on the EPR pair can obtain any information about the state of particle 1. Instead, make a joint measurement of particles 1 and 2. The effect of this is most obvious if one rewrites  $|\Psi_{123}\rangle$  in terms of the Bell states of particles 1 and 2: Starting from equation (1.114) one obtains:

$$\begin{aligned} |\Psi_{123}\rangle &= \frac{1}{\sqrt{2}}(-a|\uparrow\rangle_1|\downarrow\rangle_2|\uparrow\rangle_3 + b|\downarrow\rangle_1|\uparrow\rangle_2|\downarrow\rangle_3) + \\ &\quad \frac{1}{\sqrt{2}}(a|\uparrow\rangle_1|\uparrow\rangle_2|\downarrow\rangle_3 - b|\downarrow\rangle_1|\downarrow\rangle_2|\uparrow\rangle_3) \\ &= \frac{1}{2}\left[\frac{1}{\sqrt{2}}(|\uparrow\rangle_1|\downarrow\rangle_2 - |\downarrow\rangle_1|\uparrow\rangle_2)(-a|\uparrow\rangle_3 - b|\downarrow\rangle_3) + \right. \\ &\quad \frac{1}{\sqrt{2}}(|\uparrow\rangle_1|\downarrow\rangle_2 + |\downarrow\rangle_1|\uparrow\rangle_2)(-a|\uparrow\rangle_3 + b|\downarrow\rangle_3) + \\ &\quad \frac{1}{\sqrt{2}}(|\uparrow\rangle_1|\uparrow\rangle_2 - |\downarrow\rangle_1|\downarrow\rangle_2)(a|\downarrow\rangle_3 + b|\uparrow\rangle_3) + \\ &\quad \left. \frac{1}{\sqrt{2}}(|\uparrow\rangle_1|\uparrow\rangle_2 + |\downarrow\rangle_1|\downarrow\rangle_2)(a|\downarrow\rangle_3 - b|\uparrow\rangle_3)\right] \end{aligned}$$

Table 1.1: Relationship between Alice's Bell state measurement result, the state of Bob's particle after her measurement, and the correction Bob needs to apply to it

Bell state measured by Alice	State particle 3 is projected into by Alice's measurement	Transformation Bob needs to apply to particle 3 to reproduce $ \phi_1\rangle$
$ \Psi_{12}^-\rangle$	$- \phi_1\rangle$	None
$ \Psi_{12}^+\rangle$	$\begin{pmatrix} -1 & 0 \\ 0 & 1 \end{pmatrix}  \phi_1\rangle$	180° rotation about z axis
$ \Phi_{12}^-\rangle$	$\begin{pmatrix} 0 & 1 \\ 1 & 0 \end{pmatrix}  \phi_1\rangle$	180° rotation about x axis
$ \Phi_{12}^+\rangle$	$\begin{pmatrix} 0 & -1 \\ 1 & 0 \end{pmatrix}  \phi_1\rangle$	180° rotation about y axis

$$\begin{aligned}
&= \frac{1}{2} \left[ |\Psi_{12}^-\rangle (-a|\uparrow\rangle_3 - b|\downarrow\rangle_3) + |\Psi_{12}^+\rangle (-a|\uparrow\rangle_3 + b|\downarrow\rangle_3) + \right. \\
&\quad \left. |\Phi_{12}^-\rangle (a|\downarrow\rangle_3 + b|\uparrow\rangle_3) + |\Phi_{12}^+\rangle (a|\downarrow\rangle_3 - b|\uparrow\rangle_3) \right] \\
&= \frac{1}{2} \left[ |\Psi_{12}^-\rangle \left( -\begin{pmatrix} a \\ b \end{pmatrix} \right) + |\Psi_{12}^+\rangle \begin{pmatrix} -1 & 0 \\ 0 & 1 \end{pmatrix} \begin{pmatrix} a \\ b \end{pmatrix} + |\Phi_{12}^-\rangle \begin{pmatrix} 0 & 1 \\ 1 & 0 \end{pmatrix} \begin{pmatrix} a \\ b \end{pmatrix} + \right. \\
&\quad \left. |\Phi_{12}^+\rangle \begin{pmatrix} 0 & -1 \\ 1 & 0 \end{pmatrix} \begin{pmatrix} a \\ b \end{pmatrix} \right] \tag{1.115}
\end{aligned}$$

So if Alice performs a Bell-state measurement on particles 1 and 2, particle 3 will be projected into one of four states, each of which is related to the original state of particle 1 by a simple unitary transformation (a sign change, or a 180 degree rotation around the  $x$ ,  $y$  or  $z$ -axes), as summarized in table 1.1.

To ensure that Bob has the correct teleported quantum state, all Alice now has to do is transmit via classical means the result of her Bell-state measurement

to Bob. In other words, Alice uses a classical signal to tell Bob which Bell state the joint system comprising particles 1 and 2 was projected into by her measurement. Bob then applies the appropriate transformation to particle 3, and brings it into a state identical to the state of particle 1 prior to teleportation.

Particle 1 has been completely disrupted by the teleportation protocol. Alice is left with particles 1 and 2 in one of the four Bell states. These are maximally entangled states that yield maximally random results for measurements on either particle 1 or 2 separately. This is consistent with the no-cloning theorem [30]: quantum information cannot be copied from one system to another, it can only be moved.

### **Significance of the teleportation protocol**

By using entanglement as a channel to move a qubit from one quantum system to another, quantum teleportation makes explicit the role of entanglement as a resource for QIT. It also provides a fundamental test for the existence of useful entanglement: if a system is claimed to contain entanglement, can one devise a variant of the teleportation protocol to exploit it?

### **1.3.3 Quantum key distribution**

The term ‘quantum cryptography’, although widely used, is somewhat misleading. The cryptographic use of quantum information theoretic techniques does not occur during the transmission of the encoded data itself. Rather, quantum techniques are used during the distribution of the one-time key which ensures the security of the data. For this reason, I prefer the more precise term ‘quantum key distribution’ (QKD).

QKD actually revives the oldest form of classical cryptography, private key cryptography. Before the invention of public key cryptography, this was the only form of cryptography. Its great virtue is that it is provably secure. Its great drawback is that there is no provably secure method of transmitting the one-time key it uses over a public telecommunications channel. QKD exploits the peculiarities of quantum mechanics to provide just such a method.

In private key cryptography, before sending the encrypted data to Bob, Alice sends him (via some physically secure means such as a carrier pigeon, etc) a random bit string of equal length to the data string. Alice then adds (modulo

2) the key bit string to the data bit string, and transmits the result to Bob. Bob simply performs the reverse of this procedure to recover the original data bit string.

Private key cryptography can thus be performed using completely non-electronic techniques, such as a book of one-time keys sent via a trusted courier, and encoded messages printed in a newspaper advert. QKD provides the best of both worlds - far more convenient key distribution over a public fibre optic network. But these keys may still be used to decode messages sent through the post!

Below I describe the original QKD distribution protocol, known as BB84 after its inventors and year of publication.

### The BB84 QKD protocol

Bennett and Brassard [31] describe the following protocol:

1. Alice and Bob communicate using one of two non-orthogonal bases:

‘The rectilinear basis’:

$$|r_1\rangle := (1, 0)$$

$$|r_2\rangle := (0, 1)$$

‘The diagonal basis’:

$$|d_1\rangle := \left(\frac{1}{\sqrt{2}}, \frac{1}{\sqrt{2}}\right) = \frac{1}{\sqrt{2}}(|r_1\rangle + |r_2\rangle)$$

$$|d_2\rangle := \left(\frac{1}{\sqrt{2}}, -\frac{1}{\sqrt{2}}\right) = \frac{1}{\sqrt{2}}(|r_1\rangle - |r_2\rangle) \quad (1.116)$$

It is the non-orthogonality of these bases that provides QKD with its security.

2. Alice chooses

- **The key** - a random bit string that will act as the one-time key that she wishes to transmit.
- **The base string** - a string of equal length that will provide security for the transmission of the key.

3. Alice encodes each bit from the key as either  $0 = |r_1\rangle, 1 = |r_2\rangle$  or  $0 = |d_1\rangle, 1 = |d_2\rangle$  depending on the value of the entry in the base string at the same position, and transmits the qubit to Bob.

4. As Bob receives each qubit, he randomly decides whether to measure it in the rectilinear or diagonal basis. The corresponding bit of his measured key is set according to his measurement result. Since Bob only measures in the correct basis half the time, only approximately half the bits in his received key are correct. This fraction is further reduced by imperfections such as attenuation of the signal or detector inefficiencies.

The remainder of the protocol can be performed over a classical communications channel that is assumed to be subject to eavesdropping. However this channel should be immune to an eavesdropper - who we shall cunningly call Eve - inserting her own messages or modifying existing ones:

5. Alice and Bob exchange messages to determine which qubits Bob successfully received, and which of those was measured in the correct basis. This necessarily involves transmission of the base string, but by now it doesn't matter as it is too late for an eavesdropper to use the base string to eavesdrop on transmission of the key. At the end of this step, Bob knows which bits in his key string should be correct.
6. Suppose Eve makes a measurement on a qubit as it passes from Alice to Bob. One can show that:
  - Any such measurement made by Eve, followed by her **subsequently** learning the correct basis in which she should have measured the qubit, will yield no more than  $\frac{1}{2}$  a bit of information about the key bit encoded by the qubit. This is intuitively obvious, as Eve will only measure in the correct basis half of the time.
  - If Eve then retransmits that qubit to Bob, in the hope of concealing her eavesdropping from him, if she obtained  $b \leq \frac{1}{2}$  bits of information about the key bit then with probability  $b/2$  Bob's measurement of the qubit will disagree with the state originally chosen by Alice.
  - Therefore, in the optimal case, Eve intercepts and measures all qubits in the rectilinear basis, obtaining a correct result for half of them, and causing Bob's measurement of the retransmitted qubit to disagree for a quarter of them.
7. Therefore, Alice and Bob can detect eavesdropping by publically comparing a certain fraction of their key bits. By doing this, they of course make



these unsafe to use. The positions of the bits should be randomly chosen so that any eavesdropping will be detected.

8. If all of the sample key bits agree, then Alice and Bob can conclude that there has been no eavesdropping, and it is safe to use the remaining, undisclosed, key bits as a one-time pad for private key cryptography over a public channel.

9. Although Alice and Bob now know there has been no eavesdropping, transmission errors may have led to disagreements between the remaining keybits. Therefore they perform two procedures on these keybits: i) information reconciliation, and ii) privacy amplification, in order to generate a subset of bits for use as a private key. There is not the scope to describe these protocols in detail here. But information reconciliation is essentially error correction performed over a public channel. Eve can inevitably obtain some information about the key bits from the information reconciliation protocol. Thus, privacy amplification is then performed, which reduces Eve's information about the key bits to below an acceptable threshold.

### The EPR QKD protocol

The BB84 protocol does not exploit the properties of entanglement in any way, although one could certainly use entangled qubits in it. In 1991 Ekert [32] showed how entangled states could be used to generate the key bits. His scheme relies on the strange properties of entanglement for its security. Here it is:

- A source located between Alice and Bob creates singlet pairs.
- Alice and Bob measure their respective halves of each singlet pair along unit vectors which, for simplicity, lie in the  $(x, y)$  plane. They are expressed below in spherical polar coordinates  $(r, \theta, \phi)$ .
- Alice's vectors are:

$$\begin{aligned}
 \hat{\mathbf{a}}_1 &= \left(1, \frac{\pi}{2}, 0\right) \\
 \hat{\mathbf{a}}_2 &= \left(1, \frac{\pi}{2}, \frac{\pi}{4}\right) \\
 \hat{\mathbf{a}}_3 &= \left(1, \frac{\pi}{2}, \frac{\pi}{2}\right)
 \end{aligned} \tag{1.117}$$

- Bob's vectors are:

$$\begin{aligned}
\hat{\mathbf{b}}_1 &= \left(1, \frac{\pi}{2}, \frac{\pi}{4}\right) \\
\hat{\mathbf{b}}_2 &= \left(1, \frac{\pi}{2}, \frac{\pi}{2}\right) \\
\hat{\mathbf{b}}_3 &= \left(1, \frac{\pi}{2}, \frac{3\pi}{4}\right)
\end{aligned} \tag{1.118}$$

- For each measurement, Alice and Bob choose randomly from one of the above vectors.
- Each measurement result is  $\pm \frac{\hbar}{2}$ , and potentially reveals one bit of information.
- Let us denote the probability that Alice's measurement along  $\hat{\mathbf{a}}_i$  gives  $\pm 1$  and Bob's measurement along  $\hat{\mathbf{b}}_j$  gives  $\pm 1$  by

$$P_{\pm\pm}(\hat{\mathbf{a}}_i, \hat{\mathbf{b}}_j) \tag{1.119}$$

- Then the correlation coefficient of Alice's and Bob's possible measurement results is:

$$E(\hat{\mathbf{a}}_i, \hat{\mathbf{b}}_j) = P_{++}(\hat{\mathbf{a}}_i, \hat{\mathbf{b}}_j) + P_{--}(\hat{\mathbf{a}}_i, \hat{\mathbf{b}}_j) - P_{+-}(\hat{\mathbf{a}}_i, \hat{\mathbf{b}}_j) - P_{-+}(\hat{\mathbf{a}}_i, \hat{\mathbf{b}}_j) \tag{1.120}$$

But quantum mechanics tells us that

$$\begin{aligned}
E(\hat{\mathbf{a}}_i, \hat{\mathbf{b}}_j) &= \langle \sigma_1 \cdot \hat{\mathbf{a}}_i \sigma_2 \cdot \hat{\mathbf{b}}_j \rangle \\
&= -\hat{\mathbf{a}}_i \cdot \hat{\mathbf{b}}_j
\end{aligned} \tag{1.121}$$

- If Alice and Bob measure along the same axes, their results are perfectly anticorrelated. Hence

$$E(\hat{\mathbf{a}}_2, \hat{\mathbf{b}}_1) = E(\hat{\mathbf{a}}_3, \hat{\mathbf{b}}_2) = -1 \tag{1.122}$$

- Clauser, Horne, Shimony, and Holt [33] define this quantity:

$$S = E(\hat{\mathbf{a}}_1, \hat{\mathbf{b}}_1) - E(\hat{\mathbf{a}}_1, \hat{\mathbf{b}}_3) + E(\hat{\mathbf{a}}_3, \hat{\mathbf{b}}_1) + E(\hat{\mathbf{a}}_3, \hat{\mathbf{b}}_3) \tag{1.123}$$

As you'll see shortly, evaluating this quantity will enable Alice and Bob to detect any tampering with the singlet pairs that are used to generate the key bits. Evaluating  $S$  quantum mechanically we obtain:

$$\begin{aligned}
S &= -\hat{\mathbf{a}}_1 \cdot \hat{\mathbf{b}}_1 + \hat{\mathbf{a}}_1 \cdot \hat{\mathbf{b}}_3 - \hat{\mathbf{a}}_3 \cdot \hat{\mathbf{b}}_1 - \hat{\mathbf{a}}_3 \cdot \hat{\mathbf{b}}_3 \\
&= -\cos(\phi_1^b - \phi_1^a) + \cos(\phi_3^b - \phi_1^a) - \cos(\phi_1^b - \phi_3^a) - \cos(\phi_3^b - \phi_3^a) \\
&= -\cos\left(\frac{\pi}{4} - 0\right) + \cos\left(\frac{3\pi}{4} - 0\right) - \cos\left(\frac{\pi}{4} - \frac{\pi}{2}\right) - \cos\left(\frac{3\pi}{4} - \frac{\pi}{2}\right) \\
&= -\frac{1}{\sqrt{2}} - \frac{1}{\sqrt{2}} - \frac{1}{\sqrt{2}} - \frac{1}{\sqrt{2}} \\
&= -\frac{4}{\sqrt{2}} = -2\sqrt{2} \tag{1.124}
\end{aligned}$$

- After the pre-agreed number of qubits have been measured by Alice and Bob, they inform each other over a public channel of the directions they used for each measurement. From this discussion, they divide their measurement results into three categories:
  1. Measurements for which Alice and/or Bob failed to measure any particle at all. These results are discarded.
  2. Pairs of measurements made along the same direction: This group of results is a source of correlated classical random bits, which will be used as the key for encrypted messages.
  3. Pairs of measurements made along different directions: This group of results are uncorrelated classical random bits, so are not suitable for use in the key. But instead, and ingeniously, Alice and Bob can use them to verify that no substitution of the genuine singlet pairs with qubits prepared with known spins by an eavesdropper has occurred.

First we need to consider the question of straightforward eavesdropping. This is impossible, as the information which constitutes the key does not come into being until Alice and Bob make their measurements. The flying qubits of the singlet pairs do not carry any information about the key. They just carry the ability to make the key when Alice and Bob make their measurements. It is a curious feature of this QKD technique that, although superluminal transmission of a predetermined classical message over a quantum channel is provably impossible, Alice and Bob can create a string of classical data which is a useful

resource (ie. the key) simultaneously, even though they may be separated by a spacelike interval.

Although eavesdropping is doomed to failure, measuring the qubits en route could aid an eavesdropper in that the resulting projection onto a definite spin direction would enable the eavesdropper Eve to forge her own key. Subsequent use of the forged key by Alice and Bob would of course be insecure. We deal with this attack next.

Alice and Bob can use the measurements in category 3 to detect forgery as follows. They simply calculate  $S$  as given above in equation (1.123). If no tampering has taken place, it should yield the value given in equation (1.124). If Eve has measured the qubits of the singlet pairs, or substituted them with her own specially prepared qubits, one can show that  $S$  will have a value incompatible with equation (1.124).

Suppose that Eve measures the qubits destined for Alice and Bob along her own axes  $\hat{\mathbf{n}}_a$  and  $\hat{\mathbf{n}}_b$ , where  $\hat{\mathbf{n}}_a$  and  $\hat{\mathbf{n}}_b$  also lie in the  $x - y$  plane and have azimuthal angles  $\alpha, \beta$  respectively, and  $\rho(\hat{\mathbf{n}}_a, \hat{\mathbf{n}}_b)$  is the normalized probability distribution for the axes that Eve measures along for a given pair of spins. Then the  $S$  calculated jointly by Alice and Bob becomes

$$\begin{aligned}
S &= \int \rho(\hat{\mathbf{n}}_a, \hat{\mathbf{n}}_b) d\hat{\mathbf{n}}_a d\hat{\mathbf{n}}_b \left[ (\hat{\mathbf{a}}_1 \cdot \hat{\mathbf{n}}_a)(\hat{\mathbf{b}}_1 \cdot \hat{\mathbf{n}}_b) - (\hat{\mathbf{a}}_1 \cdot \hat{\mathbf{n}}_a)(\hat{\mathbf{b}}_3 \cdot \hat{\mathbf{n}}_b) \right. \\
&\quad \left. + (\hat{\mathbf{a}}_3 \cdot \hat{\mathbf{n}}_a)(\hat{\mathbf{b}}_1 \cdot \hat{\mathbf{n}}_b) + (\hat{\mathbf{a}}_3 \cdot \hat{\mathbf{n}}_a)(\hat{\mathbf{b}}_3 \cdot \hat{\mathbf{n}}_b) \right] \\
&= \int \rho(\hat{\mathbf{n}}_a, \hat{\mathbf{n}}_b) d\hat{\mathbf{n}}_a d\hat{\mathbf{n}}_b \left[ \cos(\alpha - 0) \cos(\beta - \frac{\pi}{4}) - \cos(\alpha - 0) \cos(\beta - \frac{3\pi}{4}) \right. \\
&\quad \left. + \cos(\alpha - \frac{\pi}{2}) \cos(\beta - \frac{\pi}{4}) + \cos(\alpha - \frac{\pi}{2}) \cos(\beta - \frac{3\pi}{4}) \right] \\
&= \int \rho(\hat{\mathbf{n}}_a, \hat{\mathbf{n}}_b) d\hat{\mathbf{n}}_a d\hat{\mathbf{n}}_b \left[ \cos(\alpha) \frac{1}{\sqrt{2}} (\cos \beta + \sin \beta) - \cos(\alpha) \frac{1}{\sqrt{2}} (\sin \beta - \cos \beta) \right. \\
&\quad \left. + \sin(\alpha) \frac{1}{\sqrt{2}} (\cos \beta + \sin \beta) + \sin(\alpha) \frac{1}{\sqrt{2}} (\sin \beta - \cos \beta) \right] \\
&= \int \rho(\hat{\mathbf{n}}_a, \hat{\mathbf{n}}_b) d\hat{\mathbf{n}}_a d\hat{\mathbf{n}}_b \frac{1}{\sqrt{2}} \left[ \cos \alpha \cos \beta + \cos \alpha \sin \beta - \cos \alpha \sin \beta + \cos \alpha \cos \beta \right. \\
&\quad \left. + \sin \alpha \cos \beta + \sin \alpha \sin \beta + \sin \alpha \sin \beta - \sin \alpha \cos \beta \right]
\end{aligned}$$

$$\begin{aligned}
&= \int \rho(\hat{\mathbf{n}}_a, \hat{\mathbf{n}}_b) d\hat{\mathbf{n}}_a d\hat{\mathbf{n}}_b \frac{2}{\sqrt{2}} \left[ \cos \alpha \cos \beta + \sin \alpha \sin \beta \right] \\
&= \int \rho(\hat{\mathbf{n}}_a, \hat{\mathbf{n}}_b) d\hat{\mathbf{n}}_a d\hat{\mathbf{n}}_b \sqrt{2} \cos(\beta - \alpha) \\
&= \int \rho(\hat{\mathbf{n}}_a, \hat{\mathbf{n}}_b) d\hat{\mathbf{n}}_a d\hat{\mathbf{n}}_b [\sqrt{2} \hat{\mathbf{n}}_a \cdot \hat{\mathbf{n}}_b] \\
\rightarrow & -\sqrt{2} \leq S \leq \sqrt{2}. \tag{1.125}
\end{aligned}$$

Thus, you can see that regardless of the axes Eve measures along, the value of  $S$  subsequently determined by Alice and Bob in their discussion cannot possibly equal the value of  $-2\sqrt{2}$  they would obtain if no tampering had taken place. Ekert's QKD protocol is provably secure against this, the simplest type of attack.

A more sophisticated attack would be for Eve to forge entangled states of three spins, keeping one of the spins as an auxiliary. The idea is that she measures its spin state after Alice and Bob have made their measurements, by which point her spin will have already been projected into a definite spin state which will tell her the result of Alice and Bob's measurement. Ekert points out that using such a state will mean that Alice and Bob's two particle state will be mixed, rather than pure as it would be if it were the genuine singlet state. He makes the conjecture that whatever 3-spin state is chosen, Alice and Bob will be able to detect the tampering via their measurement of  $S$ .

Aschauer and Briegel have now shown that, with a few minor modifications, the standard two-way entanglement purification protocols are sufficient to make Ekert's protocol perfectly private. They show that the final state of the protocol factorizes into a product state of Eve on one side, and Alice and Bob on the other side - Eve has been 'factored out' [34].

### 1.3.4 Quantum computing

#### Overview of quantum computing

**The qubit** There are certain computing problems that are intractable using conventional computers. Quantum computing exploits some of the distinctive features of quantum mechanics to provide a big enough speed-up to make these problems computable.

The speed-up is provided by using *qubits* rather than bits. The qubit is a parallelised equivalent of the bit, which makes use of the fact that a quantum system may be prepared in a superposition of its possible states. A qubit is

defined thus:

$$|\Psi\rangle = a|0\rangle + b|1\rangle, \quad |a|^2 + |b|^2 = 1. \quad (1.126)$$

An input register made up of  $n$  qubits may thus be prepared in a superposition of all  $2^n$  possible values of an  $n$ -digit binary number. With sufficient care, it is possible to preserve this superposition whilst applying a quantum algorithm to the input values. The output register will also be in a superposition of states. Measuring the state of the output register will of course collapse this superposition to just one of the possible output values. However, this does not make the exercise pointless, as the type of problem for which a quantum computer is suited is one where it is easy to check whether the answer given is the correct one. Factoring a large number is an example of such a problem. If the answer is wrong, one runs the algorithm again. The speed-up provided by the quantum parallelism outweighs the overhead of having to run the algorithm many times before obtaining the correct answer.

**Quantum gates** A classical gate takes one or more input bits, performs an operation on their values, and produces one or more output bits. A quantum gate performs the same function with the superposition of values carried by its input qubits. An example of a quantum gate is the CNOT. It has two input qubits,  $A$  and  $B$ .  $A$  is the control line,  $B$  is the data line. For each state in the superposition of states of the complete system  $AB$ , it flips the state of qubit  $B$  if and only if the state of qubit  $A$  in that superposition equals one. An important feature of a quantum gate is that it must be *reversible*, that is to say, it must be possible to reconstruct the input data to the gate from its outputs. As a consequence, a quantum gate must have an equal number of inputs and outputs.

**Quantum computation requires a universal unitary transformation** Any function  $f$  can be regarded as a transformation taking  $n$  bits to  $m$  bits, ie.

$$f : \{0, 1\}^n \longrightarrow \{0, 1\}^m \quad (1.127)$$

To achieve this on a classical computer requires a set of classical gates which are *universal*. The equivalent statement in quantum computing is that any quantum computation can be regarded as a unitary transformation taking a state of  $n$

qubits to a state of  $m$  qubits. A *universal* set of quantum gates are a set that may be used to construct a completely arbitrary unitary transformation.

### A universal set of quantum gates must have at least one entangling gate

Bremner et al [35] show that any entangling two qubit gate is universal for quantum computation, when it is assisted by one qubit gates. A similar exercise [36] shows that the same result holds for an entangling two qudit gate assisted by one qudit gates. Here, only the simpler two-qubit case is considered.

**Lemma: A two-qubit gate  $U$  is universal iff its action generates entanglement.**

### Outline of proof

- Bremner et al define a gate  $U$  as *primitive* if it is a product of one-qubit gates or if it is equivalent to the SWAP gate. Otherwise, it's *imprimitive*.
- They show that any imprimitive gate  $U$  together with one-qubit gates can be used to implement  $W = \exp(i\phi Z \otimes Z)$  where  $0 < |\phi| < \frac{\pi}{2}$ .
- Then they show that one can produce the CNOT gate by combining  $W$  with one-qubit gates.
- $\therefore$  since CNOT is universal,  $W$  and  $\therefore U$  must be universal.
- Since any universal gate is entangling and any entangling gate is imprimitive, the class of entangling gates is the same as the class of imprimitive gates.

**Details of proof** In the following, the symbol  $\stackrel{\text{equiv } U}{\equiv}$  is used to denote equivalence between two unitary transformations. If, by applying one qubit gates to the two-qubit unitary gate  $U$ , one can reach the two-qubit unitary gate  $V$ , then  $U$  and  $V$  are said to be equivalent.

1. Define

$$V := \exp[i(\theta_x X \otimes X + \theta_y Y \otimes Y + \theta_z Z \otimes Z)] \stackrel{\text{equiv } U}{\equiv} U. \quad (1.128)$$

2. For an imprimitive gate, at least one of the  $\theta_\alpha$  is non-zero.
3. First consider the two special cases where one or two of the  $\theta_\alpha$  is  $\frac{\pi}{4}$  and the others are zero:

(a) Special case 1:  $\theta_z = \frac{\pi}{4}, \theta_x = \theta_y = 0$ . Then  $V = \exp[i\frac{\pi}{4}Z \otimes Z]$  and so the desired  $W$  has been obtained.

(b) Special case 2:  $\theta_x = \theta_z = \frac{\pi}{4}, \theta_y = 0$ . Then:

$$V e^{i\frac{\pi}{4}X \otimes I} V^\dagger = e^{i\frac{\pi}{4}V X \otimes I V^\dagger} = e^{i\frac{\pi}{4}Y \otimes Z} \equiv e^{i\frac{\pi}{4}Z \otimes Z} \quad (1.129)$$

and again the desired  $W$  has been obtained.

4. Now consider the more general case,  $\theta_z \neq \frac{\pi}{4}$ . Now

$$\begin{aligned} (I \otimes Z)(X \otimes X)(I \otimes Z) &= -(X \otimes X) \\ (I \otimes Z)(Y \otimes Y)(I \otimes Z) &= -(Y \otimes Y) \\ (I \otimes Z)(Z \otimes Z)(I \otimes Z) &= +(Z \otimes Z) \end{aligned} \quad (1.130)$$

thus:

$$\begin{aligned} (I \otimes Z)V(I \otimes Z)V &= e^{(I \otimes Z)i(\theta_x X \otimes X + \theta_y Y \otimes Y + \theta_z Z \otimes Z)(I \otimes Z)} V \\ &= e^{i(-\theta_x X \otimes X - \theta_y Y \otimes Y + \theta_z Z \otimes Z)} V \\ &= e^{2i\theta_z Z \otimes Z} = e^{i\phi Z \otimes Z} = W \end{aligned} \quad (1.131)$$

**The aim now is to get from  $W$  to a CNOT. First, one expresses  $W$  in a more convenient form**

5. A rotation of a qubit about the z-axis is given by (cf. eg. Nielsen and Chuang page 174):

$$\begin{aligned} R_z(\theta) &:= e^{-i\theta Z/2} \\ &= \cos(\theta/2)I - i \sin(\theta/2)Z \\ &= \begin{pmatrix} e^{-i\theta/2} & 0 \\ 0 & e^{i\theta/2} \end{pmatrix} \end{aligned} \quad (1.132)$$



So with a little manipulation, you can see that  $W$  is equivalent to a controlled rotation about the z-axis:

$$\begin{aligned}
e^{i\phi Z_A \otimes Z_B} &= e^{Z_A \otimes i\phi Z_B} \\
&= \sum_n \frac{(Z_A \otimes i\phi Z_B)^n}{n!} \\
&= \sum_{n \text{ odd}} \frac{(i\phi)^n}{n!} (Z_A \otimes Z_B) + \sum_{n \text{ even}} \frac{(i\phi)^n}{n!} \\
&= \cos \phi + i \sin \phi (Z_A \otimes Z_B)
\end{aligned} \tag{1.133}$$

Then

$$\begin{aligned}
{}_A\langle 0 | e^{Z_A \otimes (i\phi Z_B)} | 0 \rangle_A &= {}_A\langle 0 | \cos \phi + i \sin \phi (Z_A \otimes Z_B) | 0 \rangle_A \\
&= \cos \phi + i \sin \phi ({}_A\langle 0 | Z_A | 0 \rangle_A \otimes Z_B) \\
&= \cos \phi + i \sin \phi (1 \otimes Z_B) \\
&= e^{i\phi Z_B}
\end{aligned} \tag{1.134}$$

and similarly

$${}_A\langle 1 | e^{Z_A \otimes (i\phi Z_B)} | 1 \rangle_A = \cos \phi - i \sin \phi Z_B = e^{-i\phi Z_B} \tag{1.135}$$

Thus

$$\begin{aligned}
e^{i\phi Z_A \otimes Z_B} &= |0\rangle_{AA}\langle 0| \otimes e^{i\phi Z_B} + |1\rangle_{AA}\langle 1| \otimes e^{-i\phi Z_B} \\
&\equiv |0\rangle_{AA}\langle 0| \otimes I + |1\rangle_{AA}\langle 1| \otimes e^{2i\phi Z_B}
\end{aligned} \tag{1.136}$$

6. Introduce the following notation for a controlled rotation about an arbitrary axis  $\mathbf{n}$ :

$$U_{\mathbf{n}} \stackrel{\text{equiv } U}{\equiv} |0\rangle\langle 0| \otimes I + |1\rangle\langle 1| \otimes e^{i\mathbf{n} \cdot (X, Y, Z)}. \tag{1.137}$$

So  $U_{(0,0,2|\phi)}$  is the symbol for the controlled rotation in (1.133).

7. One can apply one-qubit gates to the second qubit to change the *axis* of rotation but not the *angle* of rotation. So one can always find a one-qubit gate  $A$  to go from  $\mathbf{n}$  to  $\mathbf{n}'$ :

$$(I \otimes A) U_{\mathbf{n}} (I \otimes A^\dagger) = U_{\mathbf{n}'}. \tag{1.138}$$

**Now, apply one-qubit gates to turn  $W$  into a CNOT:**

8. The target gate is CNOT, defined by

$$U_{(0,0,\pi/2)} \stackrel{\text{equiv U}}{\equiv} \text{CNOT}. \quad (1.139)$$

You can see that CNOT is reachable from this as follows:

$$\begin{aligned} U_{(0,0,\pi/2)} &= |0\rangle\langle 0| \otimes I + |1\rangle\langle 1| \otimes e^{i(\pi/2)Z} \\ &= |0\rangle\langle 0| \otimes I + |1\rangle\langle 1| \otimes \begin{pmatrix} e^{i\pi/2} & 0 \\ 0 & e^{-i\pi/2} \end{pmatrix} \\ &= \begin{pmatrix} 1 & 0 & 0 & 0 \\ 0 & 1 & 0 & 0 \\ 0 & 0 & 0 & 0 \\ 0 & 0 & 0 & 0 \end{pmatrix} + \begin{pmatrix} 0 & 0 & 0 & 0 \\ 0 & 0 & 0 & 0 \\ 0 & 0 & e^{i\pi/2} & 0 \\ 0 & 0 & 0 & e^{-i\pi/2} \end{pmatrix} \\ &= \begin{pmatrix} 1 & 0 & 0 & 0 \\ 0 & 1 & 0 & 0 \\ 0 & 0 & i & 0 \\ 0 & 0 & 0 & -i \end{pmatrix} \end{aligned} \quad (1.140)$$

where equation (1.132) has been used.

It is easy to reach CNOT from this: one simply applies the identity  $HZH = X$  to qubit B, where  $H$  is the Hadamard gate:

$$\begin{aligned} &(I_A \otimes H_B)U_{(0,0,\pi/2)}(I_A \otimes H_B) \\ &= \frac{1}{\sqrt{2}} \begin{pmatrix} 1 & 1 & 0 & 0 \\ 1 & -1 & 0 & 0 \\ 0 & 0 & 1 & 1 \\ 0 & 0 & 1 & -1 \end{pmatrix} \begin{pmatrix} 1 & 0 & 0 & 0 \\ 0 & 1 & 0 & 0 \\ 0 & 0 & i & 0 \\ 0 & 0 & 0 & -i \end{pmatrix} \frac{1}{\sqrt{2}} \begin{pmatrix} 1 & 1 & 0 & 0 \\ 1 & -1 & 0 & 0 \\ 0 & 0 & 1 & 1 \\ 0 & 0 & 1 & -1 \end{pmatrix} \\ &= \begin{pmatrix} 1 & 0 & 0 & 0 \\ 0 & 1 & 0 & 0 \\ 0 & 0 & 0 & i \\ 0 & 0 & i & 0 \end{pmatrix}. \end{aligned} \quad (1.141)$$

All that is needed to reach CNOT now is to apply the phase gate

$$S := \begin{pmatrix} 1 & 0 \\ 0 & i \end{pmatrix} \quad (1.142)$$

to qubit B:

$$(I_A \otimes S_B)(I_A \otimes H_B)U_{(0,0,\pi/2)}(I_A \otimes H_B) = \begin{pmatrix} 1 & 0 & 0 & 0 \\ 0 & 1 & 0 & 0 \\ 0 & 0 & -i & 0 \\ 0 & 0 & 0 & -i \end{pmatrix} \begin{pmatrix} 1 & 0 & 0 & 0 \\ 0 & 1 & 0 & 0 \\ 0 & 0 & 0 & i \\ 0 & 0 & i & 0 \end{pmatrix} = \begin{pmatrix} 1 & 0 & 0 & 0 \\ 0 & 1 & 0 & 0 \\ 0 & 0 & 0 & 1 \\ 0 & 0 & 1 & 0 \end{pmatrix} = U_{\text{CNOT}}. \quad (1.143)$$

9. So in fact, the goal is to reach  $U_{(0,0,\pi/2)}$ :

- First, use  $U_{(0,0,2|\phi|)}$  a number of times  $q = \frac{\pi/2}{2|\phi|}$ .
- If  $2|\phi|$  doesn't exactly go into  $\pi/2$ , an extra gate is needed for the remainder:

$$U_{\mathbf{m}} \text{ where } 0 < |\mathbf{m}| = \frac{\pi}{2} - 2q|\phi| < 2|\phi|. \quad (1.144)$$

- To obtain  $U_{\mathbf{m}}$  the following controlled rotations are useful:

$$\begin{aligned} U_{(0,0,0)} &= U_{(0,0,2|\phi|)}U_{(0,0,-2|\phi|)} \\ U_{(0,0,4|\phi|)} &= U_{(0,0,2|\phi|)}U_{(0,0,2|\phi|)} \end{aligned}$$

- If  $\mathbf{n}$  is chosen such that  $|\mathbf{n}| = 2|\phi|$  then

$$U_{\mathbf{n}} \equiv U_{(0,0,2|\phi|)} \quad (1.146)$$

and thus one obtains another  $U_{\mathbf{m}}$  from

$$U_{\mathbf{m}} = U_{(0,0,2|\phi|)}U_{\mathbf{n}}. \quad (1.147)$$

In this  $U_{\mathbf{m}}$ ,  $|\mathbf{m}|$  varies continuously as a function of  $\mathbf{n}$ , so by the Intermediate Value Theorem it must pass through all the angles between 0 and  $4|\phi|$ . So a suitable choice of  $\mathbf{n}$  gives  $|\mathbf{m}| = \frac{\pi}{2} - 2q|\phi|$ .

- So, since  $U_{(0,0,|\mathbf{m}|)} \equiv U_{\mathbf{m}}$ , one gets

$$U_{(0,0,\pi/2)} = U_{(0,0,2|\phi|)}^q (I \otimes A)U_{\mathbf{m}}(I \otimes A^\dagger) \quad (1.148)$$

where  $A$  is an appropriate one-qubit gate.

10. Hence, CNOT can be implemented using a combination of any entangling  $U$  and one-qubit gates.

## Quantum logic gate model of the teleportation protocol

It is possible to model the teleportation protocol, which was described in section 1.3.2, as a quantum logic gate circuit. This has the advantage that Alice does not have to perform a Bell state measurement. Under this model, Alice performs a CNOT on qubit 1 (the qubit whose state is to be teleported) and her half of the Bell pair (qubit 2), using qubit 1 as the control line. This has the following effect on the state of all three qubits from equation (1.114):

$$\begin{aligned}
 |\Psi_{123}\rangle' &:= U_{\text{CNOT}}^{12} |\Psi_{123}\rangle \\
 &= \frac{a}{\sqrt{2}} (|\uparrow\rangle_1 |\downarrow\rangle_2 |\downarrow\rangle_3 - |\uparrow\rangle_1 |\uparrow\rangle_2 |\uparrow\rangle_3) + \frac{b}{\sqrt{2}} (|\downarrow\rangle_1 |\uparrow\rangle_2 |\downarrow\rangle_3 - |\downarrow\rangle_1 |\downarrow\rangle_2 |\uparrow\rangle_3)
 \end{aligned} \tag{1.149}$$

She then performs a Hadamard transform on qubit 1:

$$\begin{aligned}
 |\uparrow\rangle_1 &\rightarrow \frac{1}{\sqrt{2}} (|\uparrow\rangle_1 + |\downarrow\rangle_1) \\
 |\downarrow\rangle_1 &\rightarrow \frac{1}{\sqrt{2}} (|\uparrow\rangle_1 - |\downarrow\rangle_1)
 \end{aligned} \tag{1.150}$$

hence

$$\begin{aligned}
 |\Psi_{123}\rangle'' &:= H_1 |\Psi_{123}\rangle' = \frac{a}{2} (|\uparrow\rangle_1 + |\downarrow\rangle_1) (|\downarrow\rangle_2 |\downarrow\rangle_3 - |\uparrow\rangle_2 |\uparrow\rangle_3) \\
 &\quad + \frac{b}{2} (|\uparrow\rangle_1 - |\downarrow\rangle_1) (|\uparrow\rangle_2 |\downarrow\rangle_3 - |\downarrow\rangle_2 |\uparrow\rangle_3) \\
 &= \frac{1}{2} \left( |\uparrow\rangle_1 |\uparrow\rangle_2 (-a|\uparrow\rangle_3 + b|\downarrow\rangle_3) + |\uparrow\rangle_1 |\downarrow\rangle_2 (a|\downarrow\rangle_3 - b|\uparrow\rangle_3) + \right. \\
 &\quad \left. |\downarrow\rangle_1 |\uparrow\rangle_2 (-a|\uparrow\rangle_3 - b|\downarrow\rangle_3) + |\downarrow\rangle_1 |\downarrow\rangle_2 (a|\downarrow\rangle_3 + b|\uparrow\rangle_3) \right)
 \end{aligned} \tag{1.151}$$

One can see that this is the same as equation (1.115), except that Alice's qubits are in a pure product state rather in Bell states. These are considerably easier for Alice to measure. Thus, Alice measures which pure product state her qubits are in, and she and Bob complete the protocol as described previously.

## 1.4 Conclusion

This chapter has outlined some of the necessary tools and concepts in quantum information theory, and some of its most common applications. The following

chapters consider how these methods can be applied to describe quantum states of indistinguishable particles.

## Chapter 2

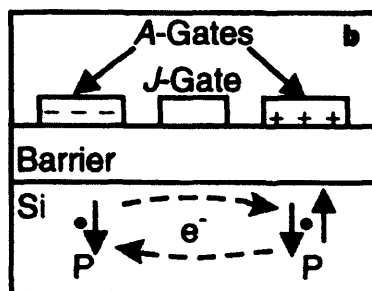
# Entanglement of indistinguishable particles

### 2.1 Introduction

As shown in chapter 1, the peculiarly non-local correlations exhibited by the states of quantum systems are key to the implementation of quantum information processing technologies, such as quantum computation and quantum teleportation. However, it is easily shown that the correlations due to the (anti)symmetrization of the states of indistinguishable bosons (fermions) are not themselves a physically useful resource for quantum information technologies (QIT): for example, there is no measurement one can make locally on a fermion in a localized state which is affected by the existence of identical fermions in other parts of the universe [37]. However, it is possible to produce entanglement that is a resource for QIT by suitable preparation: for example, by producing a  $|\Psi\rangle^-$  Bell state of the spins of two fermions. Indeed, in practice, all potential implementations of QIT involve identical particles (such as photons, electrons, or protons) as ‘carriers’ of entanglement.

For example, any proposal for a solid state implementation of quantum computing will almost certainly use states of indistinguishable particles to carry the qubits. Examples of such proposed implementations are the Kane computer [2], and Loss and di Vincenzo’s proposal [38]. It is therefore important to be able to quantify the degree of ‘useful’ entanglement in a system of identical particles.

Figure 2.1: Positioning of ‘A’- and ‘J’-gates relative to donor nuclei in the Kane quantum computer (reproduced from [2]).



### 2.1.1 Why the focus on fermions?

There is a particular focus on one particular class of indistinguishable particles in this chapter - fermions. Why is this?

Fermions are *the* matter particles of our universe - protons, neutrons, and electrons (which are of special relevance to QIT) are all fermions. Also, approximately half of all atomic nuclei are fermions. We thus need to understand entanglement between fermions to understand entanglement in metals, liquid <sup>3</sup>He, and cold, degenerate gases.

Plus, entanglement in bosons is better understood, as photons are bosons and their entanglement has been well studied by the quantum optics community. Also, the canonical two-state system used to study entanglement is the spin-half, which due to the spin statistics theorem, must be a fermion.

### 2.1.2 The Kane proposal

Kane proposes a solid-state quantum computer in which the qubits are carried by spins of <sup>31</sup>P donor nuclei (spin  $\frac{1}{2}$ ) in a <sup>28</sup>Si (nuclear spin 0) substrate. The hyperfine interaction couples the spin of a <sup>31</sup>P nucleus to its excess electron (which is localized because the system is kept cool). The nuclei and associated gates are arranged as in Figure 2.1.

Single-qubit operations (such as the Hadamard transform) are performed by ‘A’-gates positioned above the <sup>31</sup>P nuclei: these perform single-qubit operations on them by manipulating the associated electron. The coupling is thus

electron  $\overset{\text{hyperfine}}{\longleftrightarrow}$  nucleus

Two qubit operations (such as the CNOT gate) are performed by ‘J’-gates positioned above the midpoint between pairs of  $^{31}\text{P}$  nuclei. These control the strength of the exchange coupling between their associated electrons, and thus the strength of the coupling between the nuclei. The coupling is thus

nucleus  $\overset{\text{hyperfine}}{\longleftrightarrow}$  electron  $\overset{\text{exchange}}{\longleftrightarrow}$  electron  $\overset{\text{hyperfine}}{\longleftrightarrow}$  nucleus

$\hat{U}_{\text{swap}}$  is achieved by exploiting the energy difference between two different entangled nuclear spin states:  $|10 + 01\rangle$  can be (controllably) raised with respect to  $|10 - 01\rangle$  by  $h\nu_j$ . Hence

$$|10(t)\rangle = e^{-i\omega_0 t} [(e^{-2\pi i\nu_j t} + 1)|10\rangle + (e^{-2\pi i\nu_j t} - 1)|01\rangle] \quad (2.1)$$

so by allowing evolution for  $t = \frac{1}{2\nu_j}$  we swap  $|10\rangle$  to  $|01\rangle$ . So the implementation of the swap gate (and hence of the CNOT gate) in the Kane computer explicitly depends on being able to entangle the spin states of nuclei.

To read qubit values, one transfers the nuclear spin polarization to the electron and determines the nuclear spin state by its effect on the orbital wavefunction, via capacitance measurements.

### 2.1.3 Why is quantifying entanglement between indistinguishable particles a problem?

Discussion of the entanglement between pure states of indistinguishable particles has previously been dealt with almost as a separate topic from that of distinguishable particles. It is the aim of sections 2.3 through to 2.7 to show that the entanglement of pure states of either type of particle can be described within the same theoretical framework. This framework involves the von Neumann entropy of the reduced density matrix for the subsystem whose entanglement with the rest of the system we wish to find, expressed in an occupation number basis [39]. This also allows us to understand better the division between spin and spatial entanglement in systems where both may exist, and the manner in which entanglement may be transferred between spin and space. It is important to emphasize that in sections 2.3 to 2.7 only pure states of the full system are considered. It is already known that for such states the von Neumann entropy provides the correct measure of entanglement between two distinguishable subsystems [40]. The case of an overall mixed state, for which (as discussed in



section 1.2.9) the definition of an entanglement measure is more subtle [41], is not addressed.

In section 2.3 the partitioning of Hilbert space that is implicit to any meaningful definition of entanglement is discussed. In section 2.4 some requirements for a successful entanglement measure are reviewed, and in sections 2.5, 2.6, 2.7 the extent to which three potential definitions meet these requirements is considered. In section 2.7 it is demonstrated that one of these definitions, the site entropy measure due to Zanardi, passes all the tests, and can be related to the conventional definition of entanglement in the limit where the exchange symmetry of the particles is irrelevant.

Finally, the entanglement predicted by Zanardi for one particular system, the doubly-occupied bonding molecular orbital, is justified in section 2.9, which presents a teleportation protocol capable of teleporting two qubits. This is consistent with the entanglement value of two ebits predicted by Zanardi.

## 2.2 There is no entanglement due to the overall symmetry of the wavefunction

This section shows that the (anti)symmetrization of the wavefunction of two indistinguishable particles, which may be in remote locations from one another, does not lead to any measurable entanglement. What does ‘remote’ mean in this context? Broadly speaking, the length scale of the measuring apparatus required to perform a given quantum measurement defines what is ‘remote’ *for that particular* measurement. For example, if  $\hat{A}$  represents a measurement that cannot be performed with equipment bigger than one metre, then a state  $|\phi_X\rangle$  localized more than one metre away is ‘remote’.

### 2.2.1 Definition of a ‘remote’ state for any measurement

More generally, the state  $|\phi_X\rangle$  located at site  $X$  is ‘remote’ with respect to site  $A$  if  $\|\hat{A}|\phi_X\rangle\|$  is vanishingly small for *any* operator  $\hat{A}$ , where  $\hat{A}$  represents a quantum test performed at a location near to site  $A$ . Using Schwarz’s inequality, one has

$$\begin{aligned} |\langle\phi_Y|\hat{A}\phi_X\rangle|^2 &\leq \langle\phi_Y|\phi_Y\rangle\langle\hat{A}\phi_X|\hat{A}\phi_X\rangle \\ &= \langle\phi_Y|\phi_Y\rangle\|\hat{A}\phi_X\|^2. \end{aligned} \quad (2.2)$$

Thus since  $\|\hat{A}\phi_X\|$  is vanishingly small, any matrix element of the inner product of  $\hat{A}|\phi_X\rangle$  with some other state  $|\phi_Y\rangle$ , which may not be remote, is also vanishingly small.

### 2.2.2 Entanglement and overall symmetry

The overall (anti)symmetrization of the wavefunction for two bosons (fermions) applies to *any* two such particles in the universe. However, it's easy to show that this has no effect at all on any measurements one makes on just one of those particles [37]. Suppose that Alice and Bob each possess a particle of the same type (fermion or boson). Alice prepares her particle in the state  $\phi_A$  and Bob prepares his in the state  $\phi_B$ . Then, the overall state of the two **particles**, which are labelled '1' and '2' will be

$$\Psi_{12} = \frac{1}{\sqrt{2}}[\phi_A \otimes \phi_B \pm \phi_B \otimes \phi_A] \quad (2.3)$$

where the first state in each tensor product is that of particle 1, and the second state is that of particle 2.

Now suppose that Alice can perform a measurement of an observable  $\hat{A}$ . In order that this operator is agnostic as to whether it is particle 1 or 2 in Alice's possession, it must be written

$$\hat{A} \otimes I + I \otimes \hat{A} \quad (2.4)$$

where the same ordering convention as above has been used for each tensor product. Nielsen and Chuang [42] give the following identity for linear operators  $\hat{A}$  and  $\hat{B}$  acting respectively on  $|v\rangle$  and  $|w\rangle$ :

$$(\hat{A} \otimes \hat{B})(|v\rangle \otimes |w\rangle) = \hat{A}|v\rangle \otimes \hat{B}|w\rangle. \quad (2.5)$$

Thus the expectation value of this operator in the state  $\Psi_{12}$  is

$$\begin{aligned} \langle \Psi_{12} | \hat{A} \otimes I + I \otimes \hat{A} | \Psi_{12} \rangle &= \\ \frac{1}{\sqrt{2}} \langle \Psi_{12} | \hat{A} \phi_A \otimes \phi_B \pm \phi_B \otimes \hat{A} \phi_A \rangle &= \\ = \frac{1}{\sqrt{2}} \langle \frac{1}{\sqrt{2}} [\phi_A \otimes \phi_B \pm \phi_B \otimes \phi_A] | \hat{A} \phi_A \otimes \phi_B \pm \phi_B \otimes \hat{A} \phi_A \rangle &= \\ = \frac{1}{2} \left( \langle \phi_A | \hat{A} | \phi_A \rangle \otimes \langle \phi_B | \phi_B \rangle + \langle \phi_B | \phi_B \rangle \otimes \langle \phi_A | \hat{A} | \phi_A \rangle \right) &= \\ = \langle \phi_A | \hat{A} | \phi_A \rangle. & \quad (2.6) \end{aligned}$$

So the expectation value of Alice's observable  $\hat{A}$  has not been affected in any way by the fact that the joint state of her and Bob's bosons (fermions) is (anti)symmetrized. The entanglement of an indistinguishable particle with any other indistinguishable particle in another, possibly remote, location has no measurable consequences.

## 2.3 Methods of partitioning Hilbert space of two entangled spinful particles

Implicit to any measure which attempts to describe the entanglement of two subsystems is an assumption about the correct manner in which to partition the total Hilbert space. This section considers the requirements for a correct partitioning, and looks at how this is actually performed by existing entanglement measures. It will frequently be necessary to talk about the states of internal degrees of freedom of particles. Therefore, for brevity any states of such internal degrees of freedom will henceforth be referred to simply as 'spin states'.

### 2.3.1 Requirements for partitioning

#### Tensor product structure

In order to express entanglement between two components of an entangled system, some kind of partitioning of their Hilbert space is necessary to identify the 'components'. The aim is to quantify the entanglement resource shared between parts  $A$  and  $B$  of a composite quantum system. These parts may be identified with particles (in the case of a state of the system where the particles are localized), with sites (in the case of a state of the system where the particles are delocalized over sites), or with some arbitrary subdivision of an experimental apparatus (as will be examined in section 3.4.4). For the purposes of the greater part of this thesis, subsystems of a system will be considered to be synonymous with sites. But it is important to emphasize that the conclusions made here are more general: they apply to any division of a system into subsystems.

For entangled states of distinguishable particles (or particles which are effectively distinguishable because of their localization) one would normally use a tensor product structure  $\mathcal{H} = \mathcal{H}_A \otimes \mathcal{H}_B$  where  $\mathcal{H}_A$  and  $\mathcal{H}_B$  are Hilbert spaces for states of particles in parts  $A$  and  $B$ . It is important that we correctly par-

tition the Hilbert space because this ensures that basic operations such as the partial trace  $\hat{\rho}_B := \text{tr}_B \rho$  (defined in section 1.1.7) are valid. The partial trace is the correct and only way to describe the properties of one part of a composite quantum system when nothing is known about the other parts, as it gives the correct measurement statistics for observations on that subsystem [6].

But if one attempts to use the tensor product structure partitioning for entangled states of indistinguishable particles, two problems are encountered:

- The Hilbert space of two indistinguishable particles is a symmetric or antisymmetric product, not a direct product.
- There is no correspondence between the particles and the subsystems used in the partitioning.

### Delocalization

For spin-only entangled states of distinguishable particles—i.e. states where we have unambiguously given one particle to Alice, and the other to Bob—the phrase ‘the states of Alice’s spin’ is completely equivalent to the phrase ‘the states of Alice’s particle’. There is no ambiguity about which particle Alice has in her possession at any time, and therefore there is no logical difference between a one-site (local) unitary transformation, and a one-particle (possibly non-local) unitary transformation. Thus when deciding on a basis in which to describe the spin-only entanglement of a system of distinguishable particles it may seem a matter of taste whether spin states should be assigned to particles, or to sites.

However, it is perfectly possible to write down states in which each particle is shared between Alice and Bob. An example of such a ‘spin-space entangled state’ is obtained if particle 1 is put into  $\frac{1}{\sqrt{2}}(A \uparrow + B \uparrow)$  and particle 2 into  $\frac{1}{\sqrt{2}}(A \downarrow + B \downarrow)$ , where  $A, B$  are site labels, ie.

$$\begin{aligned}
 |\Psi\rangle_{12} &= \frac{1}{2} \left( |A \uparrow\rangle(1) + |B \uparrow\rangle(1) + |A \downarrow\rangle(2) + |B \downarrow\rangle(2) \right) \\
 &\quad \pm \frac{1}{2} \left( |A \uparrow\rangle(2) + |B \uparrow\rangle(2) + |A \downarrow\rangle(1) + |B \downarrow\rangle(1) \right) \quad (2.7)
 \end{aligned}$$

### Indistinguishability

When the entangled particles are indistinguishable, one can no longer be sure which particle Alice has in her possession. The distinction between one-particle

unitary transformations, and one-site unitary transformations becomes relevant. Entanglement should be invariant under one-site unitary transformations, but not necessarily under one-particle unitary transformations, which may generate entanglement if they involve both subsystems. An entanglement measure which works successfully for indistinguishable particles must respect this distinction.

The natural way to achieve this distinction is to use a basis which assigns spin states to **sites** rather than **particles**.

### 2.3.2 Partitioning used by existing entanglement measures

When partitioning the total Hilbert space of two entangled quantum systems, we need to ask ourselves:

- For indistinguishable subsystems: to what extent can my system be regarded as a symmetric/antisymmetric product of the single-subsystem states?
- For distinguishable subsystems: to what extent can my system be regarded as a direct product of the single-subsystem states?

In most descriptions of entanglement, the tensor product structure is used, for example in the entanglement measure introduced by Wootters [9]. This measure is suitable for spin-only entanglement of localized distinguishable particles. However, it does not describe which site a particle occupies, so is not suited to describing either entangled indistinguishable particles, or entangled states of distinguishable particles where the ‘particle’ and ‘subsystem’ divisions do not coincide.

One example where indistinguishable particles have been treated is by Schliemann *et al.* [43] [44], who explicitly consider the antisymmetric product space belonging to two fermions, each of which inhabits a four-dimensional one-particle space. They write a general state in the six-dimensional two-particle Hilbert space as

$$|w\rangle = \sum_{a,b \in \{1,2,3,4\}} w_{ab} c_a^\dagger c_b^\dagger |0\rangle \quad (2.8)$$

where  $a, b$  run over the orthonormalized single particle states, and Pauli exclusion requires that the  $4 \times 4$  coefficient matrix  $w$  is antisymmetric:  $w_{ab} = -w_{ba}$ .

It may seem that Schliemann's partitioning is indeed in terms of sites rather than particles, since the single particle states are labelled by sites. But, as we shall see later, Schliemann's measure is derived by considering the number of elemental Slater determinants needed to expand the entangled state. It is therefore actually a particle-based, rather than a site-based, description of entanglement. As a consequence, as will be shown later in this document, it suffers from a number of serious flaws; in particular, it is possible to devise one-site (i.e. local) transformations which generate 'entanglement' according to the Schliemann measure.

## **2.4 Desirable properties of any entanglement measure**

What are the desirable properties of an entanglement measure?

### **2.4.1 Invariance under local unitary transformations**

If a measure is correct, it should not be possible to generate 'entanglement' using only unitary transformations local to a particular site (as expressed by equation 1.56).

### **2.4.2 Non-invariance under some non-local unitary transformations is not an undesirable property**

Conversely, it should be possible to find non-local (i.e. multisite) unitary transformations which change the entanglement.

### **2.4.3 Correct behaviour as distinguishability of subsystems A and B is lost**

A correct measure should also reflect the fact that entanglement is affected when the distinguishability of the subsystems involved is lost. A simple example of this is as follows. For two fermions whose spin degrees of freedom are maximally entangled, we require that as the overlap of the single-particle spatial wavefunctions approaches unity the entanglement should asymptotically approach zero.

This is easily seen by considering the full expression for the Bell basis states in terms of Slater determinants.

### Behaviour of $|\Psi\rangle^\pm$ Bell states

If the two fermions are localized, one in site  $A$  and one in site  $B$ , then the  $|\Psi\rangle^\pm$  Bell state can be written

$$|\Psi\rangle^\pm \equiv \frac{1}{\sqrt{2}}(|\uparrow\downarrow\rangle \pm |\downarrow\uparrow\rangle) \quad (2.9)$$

where the full expression for  $|\uparrow\downarrow\rangle$  is

$$|\uparrow\downarrow\rangle = \frac{1}{\sqrt{2}} \begin{vmatrix} \phi_A(1) \uparrow(1) & \phi_B(1) \downarrow(1) \\ \phi_A(2) \uparrow(2) & \phi_B(2) \downarrow(2) \end{vmatrix}. \quad (2.10)$$

Here,  $\phi_A$  and  $\phi_B$  are the spatial states corresponding to sites  $A$  and  $B$ , and 1 and 2 are the particle labels. When the two fermions are brought together to occupy the same site, the spatial parts of the two single-particle states coincide, i.e.  $\phi_A \rightarrow \phi_B$ , and we have

$$\begin{aligned} |\uparrow\downarrow\rangle &\rightarrow \frac{1}{\sqrt{2}} \begin{vmatrix} \phi(1) \uparrow(1) & \phi(1) \downarrow(1) \\ \phi(2) \uparrow(2) & \phi(2) \downarrow(2) \end{vmatrix} \\ &= \frac{\phi(1)\phi(2)}{\sqrt{2}} \begin{vmatrix} \uparrow(1) & \downarrow(1) \\ \uparrow(2) & \downarrow(2) \end{vmatrix} \end{aligned} \quad (2.11)$$

where  $\phi$  is the **same** spatial state for sites  $A$  and  $B$ .

A similar result is obtained for  $|\downarrow\uparrow\rangle$ , but with an exchange of columns and therefore the same result applies for it as for  $|\uparrow\downarrow\rangle$  but with an overall minus sign. Hence  $|\uparrow\downarrow\rangle$  and  $|\downarrow\uparrow\rangle$  are now linearly dependent, and the behaviour of the entangled Bell state is:

$$\begin{aligned} |\Psi\rangle^\pm &\xrightarrow{\phi_A \rightarrow \phi_B} \frac{1}{\sqrt{2}} \frac{\phi(1)\phi(2)}{\sqrt{2}} \\ &\quad \left( \begin{vmatrix} \uparrow(1) & \downarrow(1) \\ \uparrow(2) & \downarrow(2) \end{vmatrix} \pm \begin{vmatrix} \downarrow(1) & \uparrow(1) \\ \downarrow(2) & \uparrow(2) \end{vmatrix} \right) \\ &= \frac{1}{2} \phi(1)\phi(2) \left( \uparrow(1)\downarrow(2) - \downarrow(1)\uparrow(2) \right. \\ &\quad \left. \pm (\downarrow(1)\uparrow(2) - \uparrow(1)\downarrow(2)) \right) \end{aligned} \quad (2.12)$$

and hence

$$|\Psi\rangle^- \rightarrow \phi(1)\phi(2) \begin{vmatrix} \uparrow(1) & \downarrow(1) \\ \uparrow(2) & \downarrow(2) \end{vmatrix} \quad (2.13)$$

up to a normalization factor, whereas  $|\Psi\rangle^+ \rightarrow 0$ .

Thus the one ebit of entanglement present in a  $|\Psi\rangle^\pm$  state should be destroyed as the spatial overlap of the two fermions' wavefunctions asymptotically approaches unity—in the case of  $|\Psi\rangle^+$  because the state itself is destroyed, and in the case of  $|\Psi\rangle^-$  because the entangled Bell state becomes a non-entangled product state. (At least, this is the case if neither Alice nor Bob can measure with spatial resolution sufficient to determine the substructure of the spatial state  $\phi$ .) A correct entanglement measure should reflect this fact.

For a pair of bosons in the  $|\Psi\rangle^\pm$  state, exactly the same loss of entanglement would occur, although the behaviours of  $|\Psi\rangle^+$  and  $|\Psi\rangle^-$  are exchanged, due to the change of sign introduced by the use of permanents rather than determinants.

### Behaviour of $|\Phi\rangle^\pm$ Bell states

Both the  $|\Phi\rangle^+$  and  $|\Phi\rangle^-$  Bell states are destroyed as the spatial overlap of the two fermions' wavefunctions asymptotically approaches unity. This is readily seen by considering the behaviour of the determinants for the individual kets:

$$\begin{aligned} |\uparrow\uparrow\rangle &= \frac{1}{\sqrt{2}} \begin{vmatrix} \phi_A(1) \uparrow(1) & \phi_B(1) \uparrow(1) \\ \phi_A(2) \uparrow(2) & \phi_B(2) \uparrow(2) \end{vmatrix} \\ &\xrightarrow{\phi_A \rightarrow \phi_B} \begin{vmatrix} \phi(1) \uparrow(1) & \phi(1) \uparrow(1) \\ \phi(2) \uparrow(2) & \phi(2) \uparrow(2) \end{vmatrix} \\ &= 0 \end{aligned} \quad (2.14)$$

and similarly for  $|\downarrow\downarrow\rangle$ . It is therefore easy to see that the  $|\Phi\rangle^\pm$  Bell states are both destroyed as the spatial overlap increases:

$$\begin{aligned} |\Phi\rangle^\pm &:= \frac{1}{\sqrt{2}} (|\uparrow\uparrow\rangle \pm |\downarrow\downarrow\rangle) \\ &\xrightarrow{\phi_A \rightarrow \phi_B} 0. \end{aligned} \quad (2.15)$$



## 2.5 Wootters measure for distinguishable particles (tangle)

In his definition of entanglement, described in section 1.2.5, Wootters considers a general spin-state of two distinguishable particles where it is implicit that the particles are effectively made distinguishable by occupying definite and orthogonal spatial states. Since the tensor product decomposition of  $H$  allows us to define a reduced density matrix  $\hat{\rho}_B$  describing the mixed state of system  $B$ , the von Neumann entropy of  $\hat{\rho}_B$  is a natural measure of entanglement. The Wootters entanglement is simply a reexpression of this.

Since  $E_{\text{Wootters}}$  expresses the entropy of a single site, there is no single-site operation which can affect it.

The Wootters measure applies only when the particles are totally distinguishable by virtue of occupying distinct sites. But our aim is to describe more general states in which each particle occupies a superposition of sites—what happens if we simply go ahead and use the Wootters measure regardless? Since the Wootters measure does not depend on the nature of the spatial states, there is no way its value can change. So for example, there is no way that the Wootters entanglement of a  $|\Psi\rangle^\pm$  Bell state will ever be affected by the spatial overlap of the single-particle wavefunctions of the constituent particles.

## 2.6 Schliemann measure for fermions

Schliemann *et al.* [44] define the entanglement of spin states of a pair of fermions by

$$\eta(w) := |\langle \tilde{w} | w \rangle|, \quad (2.16)$$

where the dual  $\tilde{w}$  of  $w$  is defined by

$$\tilde{w}_{ab} = \frac{1}{2} \epsilon^{abcd} \bar{w}_{cd} \quad (2.17)$$

and the coefficients  $\tilde{w}_{ab}$  are as defined in equation 2.8. The inner product is expressed as

$$\begin{aligned}\langle \tilde{w}|w\rangle &= \sum_{abcd} \tilde{w}_{ab}^* w_{cd} \langle 0|c_b c_a c_c^\dagger c_d^\dagger|0\rangle \\ &= \sum_{abcd} \epsilon^{abcd} w_{ab} w_{cd} \\ &= 8(w_{12}w_{34} + w_{13}w_{42} + w_{14}w_{23}).\end{aligned}\quad (2.18)$$

A similar definition was introduced for a pair of bosons by Paškauskas and You [45]. However, their equivalent of Schliemann's w-matrix is symmetric, rather than antisymmetric as Schliemann's is. This permits non-zero entries on the diagonals - these correspond to the doubly-filled states which are of course forbidden by the exclusion principle in a system of two fermions.

A comparison with Hill and Wootters's pure state concurrence, in equation (1.48), shows that Schliemann's measure is motivated by the desire to find an analogous measure for fermions, with the dual  $\tilde{w}$  as the 'spin-flipped' state.

### 2.6.1 Slater decomposition form

It is possible to relate the Schliemann measure  $\eta$  to the number of elementary Slater determinants that are required to construct the entangled state. The Hilbert space for a two-fermion,  $K$ -site system is the antisymmetric space  $\mathcal{A}(\mathcal{C}^{2K} \otimes \mathcal{C}^{2K})$ . Any vector in this space can be represented in terms of single particle functions  $f_{a(i)}^\dagger$ , which are members of the single-particle space  $\mathcal{C}^{2K}$ , by the Slater decomposition

$$|\Psi\rangle = \frac{1}{\sqrt{\sum_{i=1}^K |z_i|^2}} \sum_{i=1}^K z_i f_{a1(i)}^\dagger f_{a2(i)}^\dagger |0\rangle \quad (2.19)$$

This is reached from equation 2.8 via a suitably chosen unitary transformation

$$c_a^\dagger = \sum_b U_{ba} (f_b')^\dagger \quad (2.20)$$

which implies that in the new basis

$$w' = U w U^T. \quad (2.21)$$

The number of non-zero coefficients  $z_i$  required to construct  $|\Psi\rangle$ , i.e. the number of elementary Slater determinants, is known as the Slater rank of the entangled

state. Then for a two-fermion two-site system,  $|\Psi\rangle$  has Slater rank 1 (consists of a single Slater determinant) iff  $\eta(|\Psi\rangle) = 0$ .

### 2.6.2 Behaviour as overlap of single particle wavefunctions is increased

This entanglement measure behaves in the following way as the overlap is increased between the single-particle wavefunctions of the particles, as is shown in Figure 2.2. As the fermions are brought together, the basis states  $\{|\uparrow\uparrow\rangle, |\uparrow\downarrow\rangle, |\downarrow\uparrow\rangle, |\downarrow\downarrow\rangle\}$  are no longer orthogonal. Thus, orthogonalization was necessary, and this was achieved using Löwdin's method [46, 47]. The orthogonalized version of  $w$  is given by

$$w_{\text{orth}} = MwM^\dagger \quad (2.22)$$

where the  $M$  matrix

$$M := (1 - S^2)^{\frac{1}{4}} \begin{pmatrix} \cosh(\theta/2) & 0 & \sinh(\theta/2) & 0 \\ 0 & \cosh(\theta/2) & 0 & \sinh(\theta/2) \\ \sinh(\theta/2) & 0 & \cosh(\theta/2) & 0 \\ 0 & \sinh(\theta/2) & 0 & \cosh(\theta/2) \end{pmatrix} \quad (2.23)$$

in the Schliemann basis

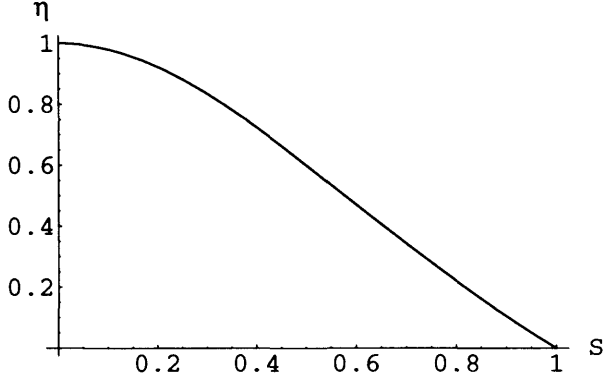
$$A \uparrow, A \downarrow, B \uparrow, B \downarrow \quad (2.24)$$

and

$$\begin{aligned} S &:= |\langle \phi_a | \phi_b \rangle| \\ \sinh(\theta) &:= \frac{S}{\sqrt{1 - S^2}}, \\ \cosh(\theta) &:= \frac{1}{\sqrt{1 - S^2}}. \end{aligned} \quad (2.25)$$

You can see that the  $M$  matrix mixes together the spatial but not spin parts of the wave function, e.g. it connects  $A \uparrow$  with  $B \uparrow$ , but not with  $A \downarrow$  or  $B \downarrow$ .

Figure 2.2: Schliemann entanglement  $\eta$  of all Bell states vs overlap  $S = |\langle\phi_a|\phi_b\rangle|$  of single particle states.



### 2.6.3 Relation to Wootters measure

Let us consider how the Schliemann measure works for the class of states considered by Wootters:

$$\begin{aligned} |\phi\rangle &= a|\uparrow\uparrow\rangle + b|\uparrow\downarrow\rangle + c|\downarrow\uparrow\rangle + d|\downarrow\downarrow\rangle, \\ |a|^2 + |b|^2 + |c|^2 + |d|^2 &= 1 \end{aligned} \quad (2.26)$$

In the representation used by Schliemann, we can write the  $w$ -matrices for the two-particle basis states in the  $A \uparrow, A \downarrow, B \uparrow, B \downarrow$  basis as

$$\begin{aligned} w_{\uparrow\uparrow} &= \begin{pmatrix} 0 & 0 & \frac{1}{2} & 0 \\ 0 & 0 & 0 & 0 \\ -\frac{1}{2} & 0 & 0 & 0 \\ 0 & 0 & 0 & 0 \end{pmatrix}, w_{\downarrow\downarrow} = \begin{pmatrix} 0 & 0 & 0 & 0 \\ 0 & 0 & 0 & \frac{1}{2} \\ 0 & 0 & 0 & 0 \\ 0 & -\frac{1}{2} & 0 & 0 \end{pmatrix}, \\ w_{\uparrow\downarrow} &= \begin{pmatrix} 0 & 0 & 0 & \frac{1}{2} \\ 0 & 0 & 0 & 0 \\ 0 & 0 & 0 & 0 \\ -\frac{1}{2} & 0 & 0 & 0 \end{pmatrix}, w_{\downarrow\uparrow} = \begin{pmatrix} 0 & 0 & 0 & 0 \\ 0 & 0 & \frac{1}{2} & 0 \\ 0 & -\frac{1}{2} & 0 & 0 \\ 0 & 0 & 0 & 0 \end{pmatrix}. \end{aligned} \quad (2.27)$$

Therefore the state considered by Wootters,  
 $|\phi\rangle = a|\uparrow\uparrow\rangle + b|\uparrow\downarrow\rangle + c|\downarrow\uparrow\rangle + d|\downarrow\downarrow\rangle,$

$|a|^2 + |b|^2 + |c|^2 + |d|^2 = 1$ , has the coefficient matrix

$$w = \frac{1}{2} \begin{pmatrix} 0 & 0 & a & b \\ 0 & 0 & c & d \\ -a & -c & 0 & 0 \\ -b & -d & 0 & 0 \end{pmatrix} \quad (2.28)$$

and thus we obtain the relation

$$\begin{aligned} |\langle \tilde{w} | w \rangle| &= |\epsilon^{abcd} w_{ab} w_{cd}| \\ &= |8(w_{12}w_{34} + w_{13}w_{42} + w_{14}w_{23})| \\ &= 2|ad - bc| = \sqrt{\tau}. \end{aligned} \quad (2.29)$$

Hence for the state of two distinguishable particles considered by Wootters, the Schliemann measure  $\eta$  is related to the Wootters ‘tangle’  $\tau$  by

$$\eta = \sqrt{\tau}. \quad (2.30)$$

#### 2.6.4 Non-invariance under local unitary transformations

We can however easily show that there are local (one-site) unitary transformations that generate ‘entanglement’ by the Schliemann measure. Consider this two particle state:

$$|\psi\rangle = \frac{1}{\sqrt{2}}(c_{A\uparrow}^\dagger + c_{B\uparrow}^\dagger) \frac{1}{\sqrt{2}}(c_{A\downarrow}^\dagger + c_{B\downarrow}^\dagger)|0\rangle. \quad (2.31)$$

The physical interpretation of this state is that it describes a doubly filled ‘molecular orbital’

$$\frac{|A\rangle + |B\rangle}{\sqrt{2}} \quad (2.32)$$

where  $|A\rangle, |B\rangle$  are the spatial states for sites  $A, B$  respectively.

Its antisymmetric coefficient matrix is

$$w = \frac{1}{2} \frac{1}{\sqrt{2}} \frac{1}{\sqrt{2}} \begin{pmatrix} . & 1 & . & 1 \\ -1 & . & -1 & . \\ . & 1 & . & 1 \\ -1 & . & -1 & . \end{pmatrix} \quad (2.33)$$

giving a Schliemann entanglement of  $\eta = 0$  (no entanglement, since it is a single Slater determinant).

Now consider applying the infinitesimal one-site two-particle unitary transformation  $(1 - i\epsilon H)$  with  $H = Un_{A\uparrow}n_{A\downarrow}$ . This purely local operation transforms the  $w$ -matrix to

$$w \rightarrow \frac{1}{4} \begin{pmatrix} . & 1 - i\epsilon U & . & 1 \\ -1 + i\epsilon U & . & -1 & . \\ . & 1 & . & 1 \\ -1 & . & -1 & . \end{pmatrix} \quad (2.34)$$

which gives a Schliemann entanglement of  $\eta = 8|\frac{-i\epsilon U}{4}| = 2\epsilon U$  which is non-zero to first order in  $\epsilon$ . We have succeeded in generating Schliemann ‘entanglement’ via a purely local unitary operation, something that it should not be possible to achieve.

### 2.6.5 Invariance under non-local unitary transformations

Although the conclusion does not necessarily indicate a problem with the Schliemann measure, for the sake of completeness we now consider whether an infinitesimal two-site one-particle unitary transformation has any effect on Schliemann entanglement. This example is generated by a Hamiltonian describing intersite hopping accompanied by a spin-flip:

$$H = t(c_{A\uparrow}^\dagger c_{B\downarrow} + c_{B\downarrow}^\dagger c_{A\uparrow}). \quad (2.35)$$

(The spin-flip is introduced so that our state is not an eigenvector of  $H$ ). The Hamiltonian’s action on our example state is

$$H|\psi\rangle = -\frac{t}{2}c_{A\uparrow}^\dagger c_{B\uparrow}^\dagger|0\rangle + \frac{t}{2}c_{B\downarrow}^\dagger c_{A\downarrow}^\dagger|0\rangle. \quad (2.36)$$

Hence applying the infinitesimal unitary transformation  $(1 - i\epsilon H)$  with this operator to our example state  $|\psi\rangle = \frac{1}{\sqrt{2}}(c_{A\uparrow}^\dagger + c_{B\uparrow}^\dagger)\frac{1}{\sqrt{2}}(c_{A\downarrow}^\dagger + c_{B\downarrow}^\dagger)|0\rangle$ , we obtain a  $w$  matrix with extra terms  $\pm i\epsilon t$  in the  $A\uparrow B\uparrow$  and  $B\downarrow A\downarrow$  locations:

$$w \rightarrow \frac{1}{4} \begin{pmatrix} 0 & 1 & -i\epsilon t & 1 \\ -1 & 0 & -1 & -i\epsilon t \\ +i\epsilon t & 1 & 0 & 1 \\ -1 & +i\epsilon t & -1 & 0 \end{pmatrix} \quad (2.37)$$

which has a Schliemann entanglement

$$\eta = \frac{1}{2}\epsilon^2 t^2 = O(\epsilon^2). \quad (2.38)$$

Thus, to first order in  $\epsilon$ , the Schliemann entanglement of our example state is unaffected.

### 2.6.6 Understanding the anomalous behaviour of the Schliemann measure in terms of the Slater decomposition

The Slater decomposition representation of an entangled two-fermion, two-site state described earlier provides a particularly simple way of understanding why the Schliemann measure does not behave correctly under either two-site one-particle or one-site two-particle unitary transformations.

According to Schliemann *et al.*, a two-fermion two-site state is entangled iff it has a Slater rank greater than one. It is well-known that a one-particle unitary transformation applied to a Slater determinant will produce another Slater determinant, whereas a two-particle transformation will produce a superposition of Slater determinants. Therefore any one-particle two-site unitary transformation will not affect the Slater rank of a state and so will not change the Schliemann entanglement, despite being a non-local transformation. Similarly, all two-particle one-site unitary transformations will modify the Slater rank of a two-fermion two-site state, and therefore will change the Schliemann entanglement, even though they are local. Schliemann's measure therefore fails to behave as we expect. The entanglement measures introduced in [45] and [48] suffer from analogous problems, since both are based on the rank of the state.

## 2.7 Zanardi measure

Zanardi [39] considers the Fock space of  $N$  spinless fermions in a lattice with  $L$  sites. The state space  $H_L(N)$  for this system is given by

$$H_L(N) := \text{span}\{|A\rangle/A \in \mathcal{P}_L^N\} \quad (2.39)$$

where the antisymmetrized state vector  $|A\rangle$  is given by the Slater determinant

$$|A\rangle := \frac{1}{\sqrt{N!}} \sum_{P \in S_N} (-1)^{|P|} \otimes_{i=1}^N |\psi_{j_{P(i)}}\rangle \quad (2.40)$$

and where  $P$  is a permutation chosen from the symmetric group  $S_N$  which contains  $|P|$  transpositions and thus has parity  $(-1)^{|P|}$ ,  $\mathcal{P}_L^N$  denotes the family

of  $N$ -site subsets of the site labels, and  $|\psi_{j_{P(L)}}\rangle$  is the single particle state for the  $j^{\text{th}}$  site where  $j$  is a member of the subset  $\mathcal{P}_L^N$ .

For some  $|\Psi\rangle \in H_L(N)$ , the local density matrix for the  $j^{\text{th}}$  site is given by

$$\rho_j := \text{tr}_j |\Psi\rangle\langle\Psi| \quad (2.41)$$

where  $\text{tr}_j$  denotes the trace over all but the  $j^{\text{th}}$  site, and therefore the von Neumann entropy of  $\rho_j$  is a measure of the entanglement of the  $j^{\text{th}}$  site with the remaining  $N-1$  sites. We will now show that, unlike the other candidates, Zanardi's measure possesses all the desirable features of an entanglement measure that we have listed above. This is due to the fact that Fock space (to which this representation maps the Hilbert space of a set of indistinguishable particles) has a natural product structure.

### 2.7.1 Behaviour as overlap of single particle wavefunctions is increased

Section 2.6.2 considered how the Schliemann entanglement of a  $|\Psi-\rangle$  Bell state of two fermions is destroyed as the overlap is increased between the single-particle wavefunctions of the fermions. What happens to the Zanardi entanglement of this state when the same process is performed?

To evaluate this, the same Löwdin orthogonalization code was used as in section 2.6.2, and the orthogonalized  $w$ -matrix was then converted to the occupation number representation.

To perform the conversion, one runs over the elements that lie above the diagonal, and for each one calculates the corresponding location in the Fock space vector. For example, the  $A \uparrow A \downarrow$  element in the  $w$ -matrix,  $w_{12}$ , is the coefficient in the term

$$w_{12} c_{A\uparrow}^\dagger c_{A\downarrow}^\dagger |0\rangle \quad (2.42)$$

in the summation in equation 2.8, and thus is the  $|1100\rangle$  element in the Fock vector. This element is set to twice the value in the  $w$ -matrix, due to the commutativity of single particle operators for fermions.



This process yields the following ket:

$$|\Psi-\rangle_{\text{orth}} = \begin{pmatrix} 0 \\ 0 \\ 0 \\ -\frac{S}{\sqrt{2(1+S^2)}} \\ 0 \\ 0 \\ \frac{1}{\sqrt{2(1+S^2)}} \\ 0 \\ 0 \\ -\frac{1}{\sqrt{2(1+S^2)}} \\ 0 \\ 0 \\ \frac{S}{\sqrt{2(1+S^2)}} \\ 0 \\ 0 \\ 0 \end{pmatrix} \quad (2.43)$$

in the usual occupation number basis

$$\{|n_{A\uparrow}n_{A\downarrow}n_{B\uparrow}n_{B\downarrow}\rangle\} = \{|0000\rangle, |0001\rangle, \dots, |1111\rangle\}. \quad (2.44)$$

The results are shown in Figure 2.3. As  $S \rightarrow 1$ , the Zanardi entanglement actually *increases* to 2 ebits. The cause of this can be readily understood by referring to the orthogonalization  $M$  matrix given in equation 2.23. The orthogonalization procedure produces these two *single particle* spatial basis states:

$$\cosh(\theta/2)|A\rangle + \sinh(\theta/2)|B\rangle \quad (2.45)$$

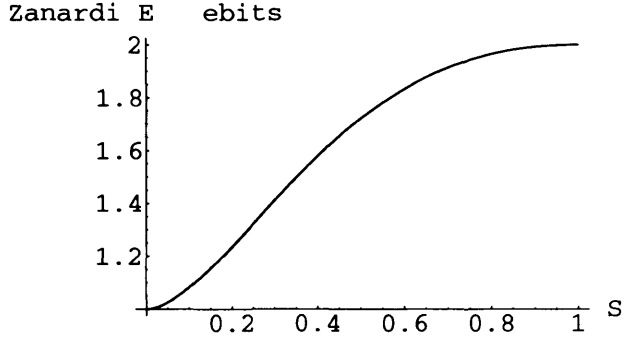
$$\sinh(\theta/2)|A\rangle + \cosh(\theta/2)|B\rangle \quad (2.46)$$

You can see from equation (2.25) that  $S$ , the overlap between the single particle states, and  $\theta$  are related as follows:

$$S \rightarrow 1 \quad \therefore \quad \theta \rightarrow \infty. \quad (2.47)$$

Thus as  $S \rightarrow 1$  these states will tend to an equal mixture of  $|A\rangle$  and  $|B\rangle$ . It therefore becomes equally likely that one will find either no particles, a single

Figure 2.3: Zanardi entanglement  $E$  of a  $|\Psi-\rangle$  Bell state of two fermions vs overlap  $S = |\langle\phi_a|\phi_b\rangle|$  of single particle states.



spin-up particle, a single spin-down particle, or two particles on a given site. This situation corresponds to two ebits of Zanardi entanglement, as has been seen previously.

### 2.7.2 Application to an example state

This section investigates further the properties of Zanardi's 'site entropy' entanglement measure. For example, for the (fermionic or bosonic) state considered in a previous section

$$|\psi\rangle = \frac{1}{\sqrt{2}}(c_{A\uparrow}^\dagger + c_{B\uparrow}^\dagger) \frac{1}{\sqrt{2}}(c_{A\downarrow}^\dagger + c_{B\downarrow}^\dagger)|0\rangle \quad (2.48)$$

the density operator for the full system is

$$\hat{\rho} = \frac{1}{4}(c_{A\uparrow}^\dagger + c_{B\uparrow}^\dagger)(c_{A\downarrow}^\dagger + c_{B\downarrow}^\dagger)|0\rangle\langle 0|(c_{A\downarrow} + c_{B\downarrow})(c_{A\uparrow} + c_{B\uparrow}). \quad (2.49)$$

One can now express this density operator as a density matrix in the binary  $\{n_{A\uparrow}, n_{A\downarrow}, n_{B\uparrow}, n_{B\downarrow}\}$  occupation number basis, ordered in binary number order:

$$\hat{\rho} = \frac{1}{4}(|1100\rangle + |1001\rangle - |0110\rangle + |0011\rangle)(\langle 1100| - \langle 0110| + \langle 1001| + \langle 0011|)$$

$$= \frac{1}{4} \begin{pmatrix} 0 & 0 & 0 & 0 & 0 & 0 & 0 & 0 & 0 & 0 & 0 & 0 & 0 & 0 & 0 \\ 0 & 0 & 0 & 0 & 0 & 0 & 0 & 0 & 0 & 0 & 0 & 0 & 0 & 0 & 0 \\ 0 & 0 & 0 & 0 & 0 & 0 & 0 & 0 & 0 & 0 & 0 & 0 & 0 & 0 & 0 \\ 0 & 0 & 0 & 1 & 0 & 0 & -1 & 0 & 0 & 1 & 0 & 0 & 1 & 0 & 0 & 0 \\ 0 & 0 & 0 & 0 & 0 & 0 & 0 & 0 & 0 & 0 & 0 & 0 & 0 & 0 & 0 & 0 \\ 0 & 0 & 0 & 0 & 0 & 0 & 0 & 0 & 0 & 0 & 0 & 0 & 0 & 0 & 0 & 0 \\ 0 & 0 & 0 & -1 & 0 & 0 & 1 & 0 & 0 & -1 & 0 & 0 & -1 & 0 & 0 & 0 \\ 0 & 0 & 0 & 0 & 0 & 0 & 0 & 0 & 0 & 0 & 0 & 0 & 0 & 0 & 0 & 0 \\ 0 & 0 & 0 & 0 & 0 & 0 & 0 & 0 & 0 & 0 & 0 & 0 & 0 & 0 & 0 & 0 \\ 0 & 0 & 0 & 1 & 0 & 0 & -1 & 0 & 0 & 1 & 0 & 0 & 1 & 0 & 0 & 0 \\ 0 & 0 & 0 & 0 & 0 & 0 & 0 & 0 & 0 & 0 & 0 & 0 & 0 & 0 & 0 & 0 \\ 0 & 0 & 0 & 0 & 0 & 0 & 0 & 0 & 0 & 0 & 0 & 0 & 0 & 0 & 0 & 0 \\ 0 & 0 & 0 & 1 & 0 & 0 & -1 & 0 & 0 & 1 & 0 & 0 & 1 & 0 & 0 & 0 \\ 0 & 0 & 0 & 0 & 0 & 0 & 0 & 0 & 0 & 0 & 0 & 0 & 0 & 0 & 0 & 0 \\ 0 & 0 & 0 & 0 & 0 & 0 & 0 & 0 & 0 & 0 & 0 & 0 & 0 & 0 & 0 & 0 \\ 0 & 0 & 0 & 0 & 0 & 0 & 0 & 0 & 0 & 0 & 0 & 0 & 0 & 0 & 0 & 0 \end{pmatrix} \quad (2.50)$$

in the basis

$$\begin{aligned} \{|n_{A\uparrow}n_{A\downarrow}n_{B\uparrow}n_{B\downarrow}\rangle\} &= \{|n_{A\uparrow}n_{A\downarrow}\rangle\} \otimes \{|n_{B\uparrow}n_{B\downarrow}\rangle\} \\ &= \{|00\rangle, |01\rangle, |10\rangle, |11\rangle\}^{\otimes 2} \\ &= \{|0000\rangle, |0001\rangle, |0010\rangle, |0011\rangle, \\ &\quad |0100\rangle, |0101\rangle, |0110\rangle, |0111\rangle, \\ &\quad |1000\rangle, |1001\rangle, |1010\rangle, |1011\rangle, \\ &\quad |1100\rangle, |1101\rangle, |1110\rangle, |1111\rangle\}. \end{aligned} \quad (2.51)$$

Note that this basis is a tensor product of the occupation number bases for site A and site B, and is thus suited to expressing the entanglement between those two sites. As will be seen later, in section 6.4.4, if instead one were to take the

tensor product of two single-spin, two-site bases

$$\{|n_{A\uparrow}n_{B\uparrow}n_{A\downarrow}n_{B\downarrow}\rangle\} = \{|n_{A\uparrow}n_{B\uparrow}\rangle\} \otimes \{|n_{A\downarrow}n_{B\downarrow}\rangle\}, \quad (2.52)$$

the density matrix obtained would contain sign changes from the above density matrix. These sign changes correspond to the action of the (anti)-commutation relations for fermions (bosons). However, using the above density matrix expressed in equation 2.51, one can reduce the matrix to site  $B$  by tracing out states of side  $A$  using combinations of  $n_{A\uparrow} = 0, 1$  and  $n_{A\downarrow} = 0, 1$  since the number of particles on site  $A$  is  $0, 1 \uparrow, 1 \downarrow$ , or  $2$ . Thus one performs

$$\hat{\rho}_B = \sum_{n_{A\uparrow}=0,1, n_{A\downarrow}=0,1} \langle n_{A\uparrow}, n_{A\downarrow} | \langle n_{B\uparrow}, n_{B\downarrow} | \rho | n'_{B\uparrow}, n'_{B\downarrow} \rangle | n_{A\uparrow}, n_{A\downarrow} \rangle, \quad (2.53)$$

giving

$$\hat{\rho}_B = \frac{1}{4} \begin{pmatrix} 1 & 0 & 0 & 0 \\ 0 & 1 & 0 & 0 \\ 0 & 0 & 1 & 0 \\ 0 & 0 & 0 & 1 \end{pmatrix} \quad (2.54)$$

in the  $\{n_{B\uparrow}, n_{B\downarrow}\} = \{0,0\}, \{1,0\}, \{0,1\}, \{1,1\}$  basis. The von Neumann entropy of this is

$$S(\hat{\rho}_B) = -\text{tr}(\hat{\rho}_B \log_2 \hat{\rho}_B) = -4\left(\frac{1}{4} \log_2 \frac{1}{4}\right) = 2. \quad (2.55)$$

Therefore, according to Zanardi's site entropy entanglement measure this example state contains two ebits of entanglement. By contrast, as has been seen above, the Schliemann measure gives zero entanglement for this state. Section 2.9 gives an explicit construction showing that two qubits may be teleported using this state, further supporting the entanglement value given by the Zanardi measure.

### 2.7.3 Behaviour under unitary transformations

#### One-site two-particle (local) unitary transformations

As before, one applies the infinitesimal one-site, two-particle unitary transformation  $(1 - i\epsilon H)$  with  $H = U n_{A\uparrow} n_{A\downarrow}$ . The result is

$$\hat{\rho}_B = \frac{1}{4} \begin{pmatrix} 1 + \epsilon^2 U^2 & \cdot & \cdot & \cdot \\ \cdot & 1 & \cdot & \cdot \\ \cdot & \cdot & 1 & \cdot \\ \cdot & \cdot & \cdot & 1 \end{pmatrix}. \quad (2.56)$$

Hence, unlike the Schliemann measure, to first order in  $\epsilon$  the site entropy measure is invariant under one-site two-particle unitary transformations. This is the correct behaviour for an entanglement measure: one cannot generate or destroy entanglement through a purely local unitary transformation.

#### Two-site one-particle (non-local) unitary transformations

Let us apply the transformation generated by

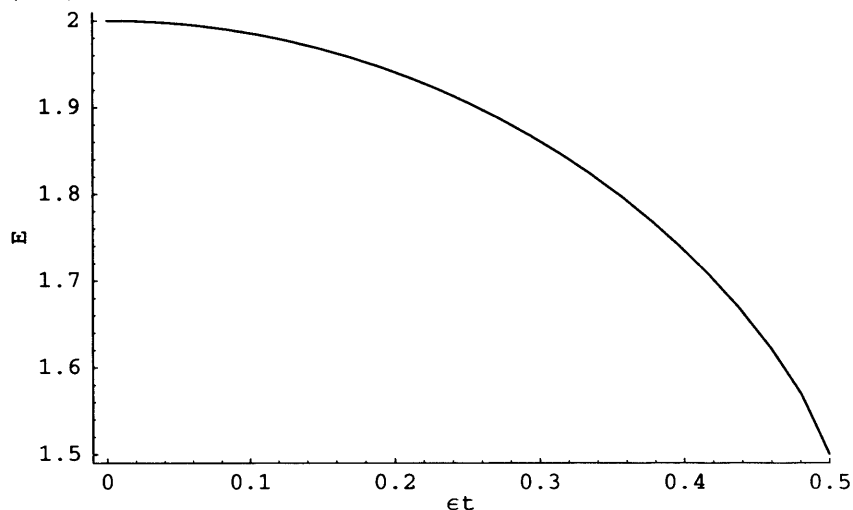
$$H = t(c_{A\uparrow}^\dagger c_{B\downarrow} + c_{B\downarrow}^\dagger c_{A\uparrow}) \quad (2.57)$$

to the doubly-filled molecular orbital  $|\psi\rangle = \frac{1}{\sqrt{2}}(c_{A\uparrow}^\dagger + c_{B\uparrow}^\dagger)\frac{1}{\sqrt{2}}(c_{A\downarrow}^\dagger + c_{B\downarrow}^\dagger)|0\rangle$ . Tracing out site  $A$ , we obtain the reduced density matrix for site  $B$ ,

$$\hat{\rho}_B = \frac{1}{4} \begin{pmatrix} 1 & \cdot & \cdot & \cdot \\ \cdot & 1 & -2i\epsilon t & \cdot \\ \cdot & +2i\epsilon t & 1 & \cdot \\ \cdot & \cdot & \cdot & 1 \end{pmatrix} \quad (2.58)$$

in the  $\{n_{B\uparrow}, n_{B\downarrow}\} = \{0, 0\}, \{1, 0\}, \{0, 1\}, \{1, 1\}$  basis. To first order in  $\epsilon$  this is not equal to the untransformed  $\hat{\rho}_B$ . Therefore, two-site unitary transformations can modify entanglement in the site entropy picture, even if they only operate on one (delocalized) particle. This conclusion is as we would expect. The reduction in Zanardi entanglement caused by this non-local  $\hat{U}$  is plotted in Figure 2.4, for the allowed values of  $\epsilon t$ .

Figure 2.4: Zanardi entanglement  $E$  of the doubly-filled molecular orbital after the application of the non-local unitary transformation generated by equation (2.57).



## 2.7.4 Site entropy measure applied to a completely general state

### Bosonic particles.

Let us now apply the site entropy description of entanglement to completely general two-particle, two-site states. Since the case of bosonic particles does not have the additional complication of the exclusion principle, we consider it first. The state can now be written in terms of the  $w$ -matrix as

$$|w\rangle = \sum_{a,b \in \{1,2,3,4\}} w_{ab} b_a^\dagger b_b^\dagger |0\rangle \quad (2.59)$$

where  $1, 2, 3, 4 = A \uparrow, A \downarrow, B \uparrow, B \downarrow$  label any set of internal degrees of freedom, and  $w$  is now a symmetric coefficient matrix.

Transforming this to the site-spin occupation number basis  $\{n_{A\uparrow}, n_{A\downarrow}, n_{B\uparrow}, n_{B\downarrow}\}$  and tracing out the states of site  $A$ , we obtain a reduced density matrix for site  $B$  of block diagonal form, where each block corresponds to a particular occupancy

(0,1, or 2 bosons) of that site.

$$\hat{\rho}_B^{bosonic} = \begin{pmatrix} \hat{\rho}_{B,0} & \cdot & \cdot \\ \cdot & \hat{\rho}_{B,1} & \cdot \\ \cdot & \cdot & \hat{\rho}_{B,2} \end{pmatrix} \quad (2.60)$$

This is a  $6 \times 6$  matrix, rather than the  $4 \times 4$   $\hat{\rho}_B$  we previously obtained for the two-fermion state, because Bose-Einstein spin statistics permit the extra site- $B$  double-occupancy states  $B \uparrow B \uparrow$  and  $B \downarrow B \downarrow$ .

The ‘zero particles on site  $B$ ’ component is

$$\hat{\rho}_{B,0} = |w_{11}|^2 + |w_{22}|^2 + 4|w_{12}|^2 \quad (2.61)$$

The ‘one particle on site  $B$ ’ component in the  $B \uparrow, B \downarrow$  basis is

$$\hat{\rho}_{B,1} = \begin{pmatrix} 4|w_{13}|^2 + 4|w_{23}|^2 & 4w_{13}w_{14}^* + 4w_{23}w_{24}^* \\ 4w_{13}^*w_{14} + 4w_{23}^*w_{24} & 4|w_{14}|^2 + 4|w_{24}|^2 \end{pmatrix} \quad (2.62)$$

Finally, the ‘two particles on site  $B$ ’ component in the  $\{B \uparrow B \downarrow, B \uparrow B \uparrow, B \downarrow B \downarrow\}$  basis is

$$\hat{\rho}_{B,2} = \begin{pmatrix} 4|w_{34}|^2 & 2w_{34}w_{33}^* & 2w_{34}w_{44}^* \\ 2w_{34}^*w_{33} & |w_{33}|^2 & w_{33}w_{44}^* \\ 2w_{34}^*w_{44} & w_{33}^*w_{44} & |w_{44}|^2 \end{pmatrix} \quad (2.63)$$

### Fermionic particles

Obtaining an expression for  $\hat{\rho}_B$  for a completely general fermionic state is simply a matter of applying the Pauli exclusion principle to  $\hat{\rho}_B^{bosonic}$ . Under Fermi-Dirac statistics, the only possible two-particle state on site  $B$  is  $B \uparrow B \downarrow$ , meaning that the two-particle part of  $\hat{\rho}_B$  is reduced to the  $1 \times 1$  submatrix

$$(\hat{\rho}_{2,B})_{fermionic} = (4|w_{34}|^2) \quad (2.64)$$

Similarly, the only possible two-particle state on site  $A$  is  $A \uparrow A \downarrow$ , meaning that the probability of zero particles on site  $B$  is given by  $4|w_{12}|^2$ . Hence the zero-particle part of  $\hat{\rho}_B^{bosonic}$  is

$$(\hat{\rho}_{0,B})_{fermionic} = (4|w_{12}|^2) \quad (2.65)$$

The one-particle part of  $\hat{\rho}_B^{bosonic}$  is by definition not affected by Pauli exclusion, and therefore  $(\hat{\rho}_{1,B})_{fermionic}$  has the same form as  $(\hat{\rho}_{1,B})_{bosonic}$ , as given in equation 2.62, although the actual values of the  $\{w_{nm}\}$  are not necessarily equal.

### 2.7.5 Relationship to Wootters tangle

The origin of the Wootters entanglement measure is now readily understood. It is simply the von Neumann entropy of the one-particle part  $\rho_1^B$  of the reduced density matrix in the occupation number representation for site  $B$ . Wootters's 'general state'

$$\begin{aligned} |\phi\rangle &= a|\uparrow\uparrow\rangle + b|\uparrow\downarrow\rangle + c|\downarrow\uparrow\rangle + d|\downarrow\downarrow\rangle, \\ |a|^2 + |b|^2 + |c|^2 + |d|^2 &= 1 \end{aligned} \quad (2.66)$$

where the kets represent  $|\sigma_A \sigma_B\rangle$ , can be rewritten in the occupation number basis  $|n_A \uparrow n_A \downarrow n_B \uparrow n_B \downarrow\rangle$  as

$$a|1010\rangle + b|1001\rangle + c|0110\rangle + d|0101\rangle. \quad (2.67)$$

Tracing out site  $A$  yields the following reduced, correctly normalized, density matrix for site  $B$  in the  $B \uparrow, B \downarrow$  basis:

$$\hat{\rho}_B = \begin{pmatrix} |a|^2 + |c|^2 & ab^* + cd^* \\ a^*b + c^*d & |b|^2 + |d|^2 \end{pmatrix} \quad (2.68)$$

with eigenvalues

$$\frac{1}{2}(1 - \sqrt{1 - 4|ad - bc|^2}), \frac{1}{2}(1 + \sqrt{1 - 4|ad - bc|^2}). \quad (2.69)$$

Applying the simplifications  $\tau = 4|ad - bc|^2$  and  $x = \frac{1}{2}(1 + \sqrt{1 - \tau})$  these reduce to  $1 - x, x$ . Thus the entropy of  $\hat{\rho}_B$  is

$$S(\hat{\rho}_B) = -(x \log_2 x + (1 - x) \log_2 (1 - x)) \quad (2.70)$$

which is identical to the Wootters result for entanglement given by

$$E = h\left[\frac{1}{2}(1 + \sqrt{1 - \tau})\right]. \quad (2.71)$$

### 2.7.6 Relationship to 'mode' picture of entanglement

The Zanardi measure is consistent with the 'mode' picture of entanglement developed by van Enk [49]. According to him,

"In the quantum theory of light, which is a second-quantized theory, it is not the 'particle', the photons, that form systems, but



rather the EM field modes... the amount of entanglement depends on the definition of the modes... Entanglement between two particular modes and the very definitions of the modes are only useful if one can perform measurements on those modes”.

He describes how unitary transformations may be made between different ‘definitions’ of modes. Then he shows that for two photons occupying a system of four modes, the minimum entanglement is  $E_{\min} = 1$ , and the maximum is  $E_{\max} = 2$ . Clearly, this value of  $E_{\max}$  is consistent with the value found in section 2.7.2 for the Zanardi entanglement in the doubly-occupied molecular bonding orbital.

It is also completely consistent with the study in section 2.7.1 of the behaviour of the Zanardi entanglement of a  $|\Psi-\rangle$  Bell state as the overlap between the single-particle wavefunctions of the fermions is increased. It was found that the entanglement actually *increases* from one ebit at zero overlap to two ebits at maximum overlap. Thus, the orthogonalization of the basis states used in that exercise is equivalent to van Enk’s method of performing unitary transformations between different modes.

Hines *et al.*[50] have used van Enk’s mode entanglement picture to study the entanglement between two tunnel-coupled Bose-Einstein condensates, and between the two chemically distinct components of the atom-molecule Bose-Einstein condensate. According to them, ”the entanglement is only meaningful if the system is viewed as a bipartite system, where the subsystems are the two modes”.

## 2.8 Vaccaro’s accessible entanglement, $E_P$

Vaccaro and co-workers have investigated the question of how much Zanardi or mode entanglement is actually *available* for use.

Vaccaro and Wiseman [51] point out that in order to make full use of the mode entanglement, it is necessary to change the number of particles at sites  $A$  and  $B$ . In other words, fully exploiting Zanardi entanglement will violate local particle number conservation.

Consequently, they propose a new measure called *available entanglement*,  $E_P$ , which quantifies the entanglement available to Alice and Bob if they can only perform operations which respect local particle number conservation.  $E_P$

thus gives the mode entanglement under an SSR for local particle number conservation. SSRs are discussed in chapter 4, and section 4.3 finds that the value obtained for the Zanardi entanglement of the doubly-occupied bonding orbital under the SSR for local particle number conservation is the same as the value of  $E_P$ .

As the next section points out, in the case of bosons, one can circumvent the objections of Vaccaro *et al.* by using a coherent state as a source/sink of particles. Local particle number conservation is therefore not violated, as the complete state of site  $A$  is a product of the coherent state plus Alice's half of the system that contains mode entanglement between sites  $A$  and  $B$ .

A subsequent paper by Vaccaro and Anselmi considers what role the phase plays when using this coherent state technique [52]. They argue that the lack of a shared reference phase between Alice and Bob results in the entanglement being reduced to the value  $E_P$ ; we shall return to this point in section 2.9.4 below.

## 2.9 Teleporting two qubits using an example delocalized state

### 2.9.1 Protocol design.

Consider again the delocalized state

$$|\psi\rangle = \frac{1}{\sqrt{2}}(c_{A\uparrow}^\dagger + c_{B\uparrow}^\dagger) \frac{1}{\sqrt{2}}(c_{A\downarrow}^\dagger + c_{B\downarrow}^\dagger)|0\rangle. \quad (2.72)$$

Since the Zanardi measure says it contains two ebits of entanglement, we should be able to teleport two qubits of quantum information using it. The standard teleportation protocol was described in section 1.3.2. Clearly, since the two ebits are spread across spin and spatial degrees of freedom, we shall need to modify the original protocol somewhat. How can this be done?

The key to teleporting via the delocalized state (2.72) lies in recognizing that the two ebits in the delocalized state are equivalent to two pairs of qubits, each of which is maximally spin-entangled ('channel pairs'), and making the

following isomorphism:

$$\begin{aligned} \{\sigma_\alpha \sigma_\beta\} &= \{|\uparrow\uparrow\rangle, |\uparrow\downarrow\rangle, |\downarrow\uparrow\rangle, |\downarrow\downarrow\rangle\} \\ \rightarrow \\ \{n_{A\uparrow} n_{A\downarrow}\} &= \{|00\rangle, |11\rangle, |10\rangle, |01\rangle\}. \end{aligned} \quad (2.73)$$

This connects the occupation numbers of the single particle states of Alice's site to the states of Alice's channel-pair qubits  $\alpha$  and  $\beta$  in the spin-only representation.

Recall that a CNOT performs

$$|\uparrow\uparrow\rangle \rightarrow |\uparrow\downarrow\rangle, |\uparrow\downarrow\rangle \rightarrow |\uparrow\uparrow\rangle, |\downarrow\uparrow\rangle \rightarrow |\downarrow\uparrow\rangle, |\downarrow\downarrow\rangle \rightarrow |\downarrow\downarrow\rangle \quad (2.74)$$

i.e. we flip the second qubit in a basis state iff the state of the first (control) qubit in that basis state is 'up'. What does a CNOT on **one** of Alice's two channel-pair qubits look like after applying the above isomorphism? Using this basis for the states of one of the source qubits ( $C$ ) and Alice's site ( $A$ ):

$$\begin{aligned} \{|n_{C\uparrow} n_{C\downarrow} n_{A\uparrow} n_{A\downarrow}\rangle\} &= \{|1000\rangle, |1010\rangle, |1001\rangle, |1011\rangle, \\ &\quad |0100\rangle, |0110\rangle, |0101\rangle, |0111\rangle\} \end{aligned} \quad (2.75)$$

we obtain the following unitary transformation for the first 'virtual' qubit, which we call  $\alpha$ :

$$\hat{U}_\alpha = \begin{pmatrix} 0 & 1 & 0 & 0 & 0 & 0 & 0 & 0 \\ 1 & 0 & 0 & 0 & 0 & 0 & 0 & 0 \\ 0 & 0 & 0 & 1 & 0 & 0 & 0 & 0 \\ 0 & 0 & 1 & 0 & 0 & 0 & 0 & 0 \\ 0 & 0 & 0 & 0 & 1 & 0 & 0 & 0 \\ 0 & 0 & 0 & 0 & 0 & 1 & 0 & 0 \\ 0 & 0 & 0 & 0 & 0 & 0 & 1 & 0 \\ 0 & 0 & 0 & 0 & 0 & 0 & 0 & 1 \end{pmatrix}. \quad (2.76)$$

The action of this is thus:

$$\begin{aligned} |1000\rangle &\leftrightarrow |1010\rangle, |1001\rangle \leftrightarrow |1011\rangle, \\ |01n_{A\uparrow} n_{A\downarrow}\rangle &\text{ unchanged.} \end{aligned} \quad (2.77)$$

Referring to the isomorphism in (2.73) we see that this  $\hat{U}$  flips the first ‘virtual’ qubit  $\alpha$  in Alice’s half of the delocalized state iff the control qubit  $C$  is spin-up. Similar considerations lead to a similar unitary transformation for the second ‘virtual’ qubit  $\beta$ . We also note that since we are teleporting two qubits, we need to send four classical bits to complete the protocol.

### 2.9.2 Protocol implementation.

The two CNOTs described above will clearly allow us to exploit the two ebits of entanglement present in the delocalized state. However some consideration needs to be paid to how we can implement these CNOTs. Considering again the first ‘virtual’ qubit, the Hamiltonian we can use to generate equation (2.76) is

$$\begin{aligned}
\hat{H}_\alpha &= |10\rangle_{CC}\langle 10| \left( |00\rangle_{AA}\langle 10| + \right. \\
&\quad \left. |10\rangle_{AA}\langle 00| + |11\rangle_{AA}\langle 01| + |01\rangle_{AA}\langle 11| \right) \\
&= \frac{1}{2}(\sigma_{z,C} + 1) \left( c_{A\uparrow}^\dagger + c_{A\uparrow} \right) \\
&= \frac{1}{2} \left[ \begin{pmatrix} 1 & 0 \\ 0 & -1 \end{pmatrix} + \begin{pmatrix} 1 & 0 \\ 0 & 1 \end{pmatrix} \right] \otimes \left[ \begin{pmatrix} 0 & 0 & 0 & 0 \\ 1 & 0 & 0 & 0 \\ 0 & 0 & 0 & 0 \\ 0 & 0 & 1 & 0 \end{pmatrix} + \begin{pmatrix} 0 & 1 & 0 & 0 \\ 0 & 0 & 0 & 0 \\ 0 & 0 & 0 & 1 \\ 0 & 0 & 0 & 0 \end{pmatrix} \right] \\
&= \begin{pmatrix} 1 & 0 \\ 0 & 0 \end{pmatrix} \otimes \begin{pmatrix} 0 & 1 & 0 & 0 \\ 1 & 0 & 0 & 0 \\ 0 & 0 & 0 & 1 \\ 0 & 0 & 1 & 0 \end{pmatrix} = \begin{pmatrix} 0 & 1 & 0 & 0 & 0 & 0 & 0 & 0 \\ 1 & 0 & 0 & 0 & 0 & 0 & 0 & 0 \\ 0 & 0 & 0 & 1 & 0 & 0 & 0 & 0 \\ 0 & 0 & 1 & 0 & 0 & 0 & 0 & 0 \\ 0 & 0 & 0 & 0 & 0 & 0 & 0 & 0 \\ 0 & 0 & 0 & 0 & 0 & 0 & 0 & 0 \\ 0 & 0 & 0 & 0 & 0 & 0 & 0 & 0 \\ 0 & 0 & 0 & 0 & 0 & 0 & 0 & 0 \end{pmatrix} \quad (2.78)
\end{aligned}$$

in the usual occupation number bases for the single spin matrices, and double-spin matrices respectively.  $\hat{U}_\alpha$  can then be obtained through a straightforward

exponentiation:

$$\hat{U}_\alpha = -i \exp\left(i\hat{H}_\alpha \frac{\pi}{2}\right) = \begin{pmatrix} 0 & 1 & 0 & 0 & 0 & 0 & 0 & 0 \\ 1 & 0 & 0 & 0 & 0 & 0 & 0 & 0 \\ 0 & 0 & 0 & 1 & 0 & 0 & 0 & 0 \\ 0 & 0 & 1 & 0 & 0 & 0 & 0 & 0 \\ 0 & 0 & 0 & 0 & 1 & 0 & 0 & 0 \\ 0 & 0 & 0 & 0 & 0 & 1 & 0 & 0 \\ 0 & 0 & 0 & 0 & 0 & 0 & 1 & 0 \\ 0 & 0 & 0 & 0 & 0 & 0 & 0 & 1 \end{pmatrix}. \quad (2.79)$$

The first expression given above for  $\hat{H}_\alpha$  used the bases

$$|n_{C\uparrow}n_{C\downarrow}\rangle \text{ and } |n_{A\uparrow}n_{A\downarrow}\rangle. \quad (2.80)$$

In the second expression for  $\hat{H}_\alpha$ , the projectors for the occupation number state of site  $A$  were reexpressed in second-quantized notation. Similarly, the Hamiltonian generating a CNOT on the second ‘virtual’ qubit is

$$\hat{H}_\beta = \frac{1}{2}(\sigma_{z,C} + 1) \left( c_{A\uparrow}^\dagger c_{A\downarrow}^\dagger + c_{A\downarrow} c_{A\uparrow} \right). \quad (2.81)$$

Neither of these Hamiltonians conserves particle number, thus we need to introduce a coherent source/sink of particles to the system. We shall see in a moment that we can easily do this for bosons. Introducing a system  $D$  which acts as a particle source/sink,  $\hat{H}_\alpha$  becomes

$$\hat{H}_\alpha = |10\rangle_{CC}\langle 10| \left( c_{A\uparrow}^\dagger c_D + c_D^\dagger c_{A\uparrow} \right). \quad (2.82)$$

At this point we face a problem. By changing the number of particles in system  $D$  as a consequence of our CNOT, we are introducing new correlations between the states of subsystems  $A$  and  $D$ . This is thus a type of decoherence affecting the entanglement of the ‘carrier-pair’  $AB$ . This is clearly unavoidable in a real-world system, but we can show that for bosons, by choosing a suitable initial state for subsystem  $D$  we can minimize this decoherence to a negligible level. We seek to put system  $D$  in an approximate eigenstate of the creation and annihilation operators, so that they leave it unchanged and no decoherence of the entanglement in the  $AB$  carrier pair occurs. A suitable choice is the coherent state

$$|\alpha\rangle_D = \exp\left(-\frac{1}{2}|\alpha|^2\right) \sum_n \frac{\alpha^n}{(n!)^{1/2}} |n\rangle_D. \quad (2.83)$$

It is well known that this state is an eigenstate of the annihilation operator, a fact which suits our requirements perfectly, but it is not an eigenstate of the creation operator. However, as the mean number of particles  $|\alpha|^2$  in the coherent state asymptotically approaches  $\infty$ , the state asymptotically approaches an eigenstate of the creation operator.

In a real-world system, how does the decoherence introduced to the system relate to the number of particles in the source/sink system? Ozawa [53] has looked at implementing a Hadamard gate using the standard spin-up, spin-down computational basis, with a control system coupled via a rotationally invariant interaction such as the Heisenberg exchange interaction. He finds that the decoherence caused by the control system due to conservation of total angular momentum is significant. Specifically, if the control system comprises  $n$  spin-half systems, then the gate error probability has this lower bound:

$$P_e \geq \frac{1}{4 + 4n^2}. \quad (2.84)$$

### 2.9.3 Applicability to fermionic systems

It is important to note that this method for coherently producing a non-number-conserving interaction applies to bosons only. For fermions, Pauli exclusion prevents us using such a simple approach and there is no analogue of the coherent state available within the Hilbert space.

However, it *would* be possible to produce  $\hat{H}_\beta$  for fermion pairs, by using an S-wave superconductor. Such a superconductor acts as a reservoir of Cooper pairs with net momentum zero, and is to an excellent approximation an eigenstate of  $c_{D\uparrow}^\dagger c_{D\downarrow}^\dagger$ , and  $c_{D\uparrow} c_{D\downarrow}$ . If one were to construct a tunnel junction between Alice's system and such a superconductor, and allow Cooper pairs to tunnel across it, then one would be able to construct an  $\hat{H}_\beta$  along these lines:

$$\hat{H}_\beta = \frac{1}{2}(\sigma_{z,C} + 1) \left( c_{A\uparrow}^\dagger c_{A\downarrow}^\dagger c_{D\uparrow} c_{D\downarrow} + c_{A\downarrow} c_{A\uparrow} c_{D\uparrow}^\dagger c_{D\downarrow}^\dagger \right). \quad (2.85)$$

### 2.9.4 Phase considerations due to the use of a coherent state

Vaccaro and Anselmi have studied what role the phase plays when using this coherent state technique [52]. They find that the lack of a shared reference phase between Alice and Bob results in the entanglement being reduced to the

value  $E_P$ . The phase difference arises because, using their model of transferring the mode entanglement to quantum registers, both Alice and Bob require coherent states to act as sources/sinks of particles in order to make a full set of transformations and make use of the full entanglement. However, even without the quantum register approach, it can readily be seen that the use of a coherent state introduces the need for a reference phase in the teleportation protocol, by considering the state of the full system consisting of the qubit being teleported, the shared state (doubly-occupied bonding orbital), and the coherent state(s) at the end of the protocol.

Vaccaro and Anselmi argue that a shared reference phase can only be established non-locally, by transporting particles between sites  $A$  and  $B$ , and hence should be regarded as an additional non-local resource needed to make use of the entanglement.

## 2.10 Conclusion

This chapter has examined the use of the Zanardi measure to evaluate the entanglement between two indistinguishable particles. It relies on the fact that when an occupation number basis is used to express the overall state of the particles, their Hilbert space is a direct product of the Hilbert spaces of the two particles. The von Neumann entropy can then be used as a measure of the entanglement between the particles. However, the Zanardi entanglement is an overestimate, due to the need to use non-local resources to establish a shared reference phase. Vaccaro and Anselmi's accessible entanglement quantifies the reduction in the Zanardi entanglement due to this requirement.

Later in this thesis, chapter 4 discusses how entanglement between indistinguishable particles is affected by applying superselection rules, that is constraints on the operations allowed on a quantum system. Clearly, that discussion would not be possible without the Zanardi measure. The concept of an SSR allows one to clarify issues such as the impossibility of constructing a coherent source of fermions, due to Pauli exclusion, as has just been discussed.

Chapter 5 looks at a conjugate gradient algorithm to estimate the entanglement of formation in mixed quantum states. This algorithm is combined with the Zanardi measure in chapter 6 to study entanglement in degenerate quantum gases, specifically a Bose-Einstein condensate, the Fermi sea, and a BCS super-

conductor. These all involve indistinguishable particles (bosons or fermions) and thus the existence of the Zanardi measure was a prerequisite for this study.



## Chapter 3

# Spin-only, space-only, spin-space entanglement

### 3.1 Introduction

We have seen suggestions in the previous chapter that entanglement can exist both within the spatial degrees of freedom of a system, and within its spin degrees of freedom. This chapter attempts to place this concept on a more explicit footing. It asks these questions:

1. Is it meaningful to talk about entanglement *between* the space and spin degrees of freedom of a system?
2. Is it meaningful to divide the total entanglement between two subsystems of a system into the entanglement carried only in the spin degrees of freedom, and that carried only in the spatial degrees of freedom?

Since the previous chapter established that the Zanardi measure correctly evaluates the entanglement present in pure states of indistinguishable particles, it will be used when considering the examples of space-only and spin-only entanglement in this chapter.

In section 3.4.4 Zanardi's measure is used to discuss spin-space entanglement transfer. In section 3.3.1 it is shown that a space-only description of an entangled system may be incomplete: in some sense, spatial and spin degrees

of freedom can be ‘entangled’ in a system. This is made more concrete by considering two examples. In section 3.3.3 spin and spatial degrees of freedom are traced out from a doubly-occupied molecular bonding orbital and the Zanardi measure is used to evaluate the ‘entanglement’ between space and spin in that orbital. In section 3.3.5 the same exercise is performed for the Omar apparatus, a hypothetical experiment that contains entanglement both in its spin and spatial degrees of freedom, and which is described in section 3.2.

Finally, in sections 3.3.12 and 3.3.13 an attempt is made to relate the von Neumann entropy of the reduced space-only and spin-only descriptions of the doubly-occupied molecular orbital to the mutual information between possible measurements. The Holevo bound is also obtained, and it is shown that it is satisfied (but not saturated) by the one-site measurements considered in section 3.3.12.

## 3.2 The Omar thought-experiment

A particularly interesting system that contains entanglement both in its spin and spatial degrees of freedom was introduced by Omar *et al.* [3]. They consider an apparatus which takes as its input two pairs of indistinguishable particles,  $A$  and  $B$ , each pair maximally entangled in some internal degree of freedom (e.g. spin), and transfers some of that entanglement to the spatial degrees of freedom of the particles. This is achieved by passing one particle from each pair through a beam splitter on one side of the apparatus, and doing likewise with the remaining particles from each pair through another beam splitter on the other side of the apparatus (see Figure 3.1). The two sides are labelled 1 and 2.

The state of the particles at the beginning of the thought-experiment (‘the input state’) in second-quantized notation is

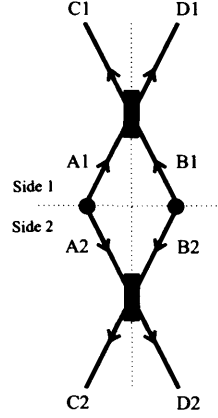
$$\frac{1}{\sqrt{2}}(a_{A1\uparrow}^\dagger a_{A2\downarrow}^\dagger \pm a_{A1\downarrow}^\dagger a_{A2\uparrow}^\dagger) \frac{1}{\sqrt{2}}(a_{B1\uparrow}^\dagger a_{B2\downarrow}^\dagger \pm a_{B1\downarrow}^\dagger a_{B2\uparrow}^\dagger). \quad (3.1)$$

where eg.  $a_{A1\uparrow}^\dagger$  is a creation operator for a spin-up particle in arm  $A1$ , and the ‘ $\pm$ ’ sign for each pair of particles depends on whether that pair is in an  $m_s = 0$  triplet (plus sign) or singlet (minus sign) state.

They draw three main conclusions:

1. By making certain measurements on the output state from the apparatus,

Figure 3.1: The spin-space entanglement apparatus used in the Omar et al. thought experiment (reproduced from [3]).



it is possible to determine whether the particles involved are bosons or fermions.

2. The output state differs depending on whether both input states to the apparatus are  $m_s = 0$  triplets, or if one is an  $m_s = 0$  triplet and the other a singlet.
3. For the case where both pairs of particles in the input state are  $m_s = 0$  triplets, some entanglement (they do not determine exactly how much) is transferred from the spin degrees of freedom to the spatial degrees of freedom. Ie. *spin-space entanglement transfer* is shown to occur.

Conclusion (1) can be achieved by measuring the total spin  $\mathbf{S}$  for the entire apparatus along the x-axis (which from the perspective of Alice and Bob on sides 1 and 2 respectively is a non-local measurement), and then selecting the  $S_x = 0$  results. If the particles are fermions, the wave function is projected onto the state

$$\frac{1}{\sqrt{2}} \left[ \frac{1}{\sqrt{2}} (|L\rangle_1 + |R\rangle_1) \frac{1}{\sqrt{2}} (|L\rangle_2 + |R\rangle_2) - \frac{1}{\sqrt{2}} |A\rangle_1 \frac{1}{\sqrt{2}} |A\rangle_2 \right]. \quad (3.2)$$

where, for example,  $|L\rangle_1$  represents both particles in the left arm on side 1 of the apparatus (bunching), and  $|A\rangle_1$  represents one particle in each arm on side 1 (antibunching). On the other hand, if the particles are bosons, the wave

function is projected onto

$$\frac{1}{\sqrt{2}} \left[ \frac{1}{\sqrt{2}} (|L\rangle_1 + |R\rangle_1) \frac{1}{\sqrt{2}} (|L\rangle_2 + |R\rangle_2) + \frac{1}{\sqrt{2}} |A\rangle_1 \frac{1}{\sqrt{2}} |A\rangle_2 \right]. \quad (3.3)$$

These states are orthogonal, and so can be distinguished between by a suitable measurement. This procedure thus gives a way of determining if the particles are bosons or fermions.

For (2), we consider measuring the total spin on one side of the apparatus only along the z-direction. As there are two spin-half particles involved, the result of measuring  $\hat{S}_z$  can take the values 0 or  $\pm 1$  only. As total spin will have been conserved, the measurement result for the same quantity on the other side of the apparatus must be 0 or  $\mp 1$ . Omar *et al.* show that the ‘++’ case and the ‘+-’ case have different  $|\hat{S}_z| = 0$  components of the output wave function following such a measurement.

For (3), consider the entanglement between the two sides of the apparatus present in the ‘++’ output state for fermions. For the  $|\hat{S}_z| = 1$  component of the output wave function, Pauli exclusion means that the terms must consist entirely of anti-bunching spatial states. There can thus be no spatial entanglement between sides 1 and 2 in this component as the spatial states are identical on both sides for all terms. However, due to conservation of total spin, the spin states on the two sides are perfectly correlated and thus there is one ebit of spin entanglement between sides 1 and 2.

With the  $|\hat{S}_z| = 0$  component, however, Pauli exclusion is not a factor, and the terms in this component are a mixture of bunching and antibunching spatial states. This component thus contains one ebit of entanglement between sides 1 and 2, carried both in the spin and spatial degrees of freedom. Omar *et al.* do not attempt to quantify how much of this entanglement is spatial, and how much is spin.

There has thus been a transfer of entanglement between sides 1 and 2. The input state of two  $m_s = 0$  triplets contains two ebits carried only in the spin degrees of freedom. The output state contains two ebits carried partly in the spin degrees of freedom and partly in the spatial degrees of freedom. Omar *et al.* call this *spin-space entanglement transfer*.

### 3.3 Can space and spin degrees of freedom be ‘entangled’ with one another?

#### 3.3.1 A density operator which gives correct measurement averages for spatial measurements is also parameterized by spin

For systems which contain spatial as well as spin entanglement, it seems natural to try to obtain a reduced description of the system in terms of only spin or spatial degrees of freedom by applying the usual technique of the partial trace. One would expect this to yield a reduced density matrix which contains information about only the spin or spatial degrees of freedom of the system. The justification for using the partial trace is that it gives a description of a given subsystem which is in agreement with statistics for measurements made on that subsystem alone [6].

This section demonstrates that in fact, a density operator which gives the correct statistics for a **spatial** measurement will necessarily contain information about the spin of the system. In other words, it is impossible to obtain a truly space-only density operator. Put another way, tracing out spin from such a system will give a mixed spatial state, indicating that the spatial and spin degrees of freedom are in some sense ‘entangled’ within the system. Converse conclusions would of course apply to a spin-only density operator.

Consider  $N$  fermions occupying  $2M$  single-particle states  $\psi_{i,j} := \phi_i(\mathbf{r})\alpha_j$  where

- $\phi_i(\mathbf{r})$  are spatial states with  $i = 1, \dots, M$
- $\alpha_j$  are spin states with  $j = 1, 2$

This system is described by  $\binom{2M}{N}$  Slater determinants  $\{|\Psi_R\rangle\}$ . The expectation value of some purely **spatial** operator  $\hat{A} := \hat{A}(r_1, \dots, r_N)$  between those Slater determinants is given by  $\langle \Psi_R | \hat{A} | \Psi'_R \rangle =$

- 0 unless the set of spin functions is the same in  $|\Psi_R\rangle, |\Psi'_R\rangle$ .
- $A_{P,P',S}$  where  $P, P'$  denote the set of spatial states in  $|\Psi_R\rangle, |\Psi'_R\rangle$  respectively, and  $S$  is total spin.

Using the  $\{|\Psi_R\rangle\}$  as a basis we can write some general state as

$$|\Psi\rangle := \sum_R c_R |\Psi_R\rangle \quad (3.4)$$

where R labels one of the  $\binom{2M}{N}$  Slater determinants. Then

$$\begin{aligned} \langle\Psi|\hat{A}|\Psi'\rangle &= \sum_{R,R'} c_R^* \langle\Psi_R|\hat{A}|\Psi_{R'}\rangle c_{R'} \\ &= \sum_{P,P',S} A_{PP'}^S \hat{\rho}_{PP'}^S \text{ by using the usual result } \langle\hat{A}\rangle = \text{tr}(\hat{\rho}\hat{A}) \\ &= \sum_S \sum_{P,P'} A_{PP'}^S \hat{\rho}_{PP'}^S \end{aligned} \quad (3.5)$$

We now wish to write this using continuous indices rather than discrete set labels. Equation (1.2.21) in [54] gives  $\langle\hat{A}\rangle = \text{tr}(\hat{A}\hat{\rho})$  in an arbitrary basis

$$|r\rangle = |r_1, \dots, r_N\rangle \quad (3.6)$$

where  $|r\rangle$  is a Slater determinant with particles at  $r_1, \dots, r_N$  as

$$\langle\hat{A}\rangle = \int A(r, r') \hat{\rho}(r', r) d^N r d^N r' \quad (3.7)$$

where the integral symbol denotes an integration over continuous position variables, or for the case of discrete variables, a summation, and where the matrix representations of  $A$  and  $\hat{\rho}$  with respect to  $|r\rangle$  are

$$\begin{aligned} A(r, r') &= \langle r_1, \dots, r_N | \hat{A} | r'_1, \dots, r'_N \rangle \\ \hat{\rho}(r, r') &= \sum_i \Psi_i(r) w_i \Psi_i^*(r') \end{aligned} \quad (3.8)$$

So here, we can write

$$\langle\Psi|\hat{A}|\Psi'\rangle = \sum_S \int dr_1 \dots dr_N dr'_1 \dots dr'_N A^S(r_1 \dots r_N r'_1 \dots r'_N) \times \hat{\rho}^S(r'_1 \dots r'_N r_1 \dots r_N) \quad (3.9)$$

$$= \int dr_1 \dots dr_N dr'_1 \dots dr'_N A(r_1 \dots r_N r'_1 \dots r'_N) \times \hat{\rho}_{\text{spatial}}(r'_1 \dots r'_N r_1 \dots r_N) \quad (3.10)$$

where

$$A = \sum_S A^S \text{ and } \hat{\rho}_{\text{spatial}} = \sum_S \hat{\rho}^S \quad (3.11)$$

and

$$\hat{\rho}^S(r'_1 \dots r'_N r_1 \dots r_N) = \sum_{P, P'} w_{PP'}^S \Psi_P(r'_1 \dots r'_N) \Psi_{P'}^*(r_1 \dots r_N) \quad (3.12)$$

Note that since each  $A^S$  and  $\hat{\rho}^S$  has a different spatial symmetry,

$$\int A^S \hat{\rho}^{S'} \propto \delta_{SS'} \quad (3.13)$$

Thus, the ‘space-only’ density matrix  $\hat{\rho}_{\text{spatial}}$  which gives the correct statistics for measurements made by the spatial operator  $\hat{A}$  is in fact a sum of density matrices  $\{\hat{\rho}^S\}$  which are parameterized by the total spin quantum number  $S$ . In some sense, it is incorrect to say that  $\hat{\rho}_{\text{spatial}}$  is purely spatial, as it includes information about spin.

It is possible to draw an analogy here with the work of Peres et al [55], who show that for a single free spin- $\frac{1}{2}$  the reduced spin-only density matrix is not covariant under a Lorentz transformation, and therefore the von Neumann entropy of the spin-only density matrix is not relativistically invariant. However, Peres’s work applies only to a single spin- $\frac{1}{2}$ , not a system of spins, and therefore some caution should be exercised with this comparison.

### Variable number of particles

If the number of particles  $N$  in the system is variable, then  $\hat{\rho}$  is an incoherent mixture of pure states, and the expectation value of  $\hat{A}$  is

$$\langle \hat{A} \rangle := \sum_{P, P', S, N} \hat{\rho}_{PP'}^{SN} A_{PP'}^{SN}. \quad (3.14)$$

### Example: Side 1 of the Omar apparatus

There are always two particles, i.e.  $N = 2$ . For fermions, there are six two-fermion states:

- 3 spatial  $\times$  1 singlet = 3 states:  $|L\rangle, |R\rangle, |A_{\chi_{0,0}}\rangle$
- 1 spatial  $\times$  3 triplet = 3 states:  $|A_{\chi_{1,-1}}\rangle, |A_{\chi_{1,0}}\rangle, |A_{\chi_{1,1}}\rangle$

using the  $\chi_{S, m_S}$  notation. So the spatial density matrices are

- $\hat{\rho}_{S=0} = 3 \times 3$
- $\hat{\rho}_{S=1} = 1 \times 1$

and the full density matrix is

$$\hat{\rho} = \sum_{S=0}^1 \hat{\rho}^S \quad (3.15)$$

Note that these results are different from those obtained for the entire Omar apparatus in section 3.3.5, because here we are considering only one side of the apparatus.

### 3.3.2 Tracing out space and spin

The results of the previous section would indicate that in a system where entanglement is present both in the spatial and spin degrees of freedom, those degrees of freedom are themselves in some sense ‘entangled’. So in order to evaluate this ‘entanglement’ between spin and space it would seem logical to apply the standard method: trace out one set of degrees of freedom and evaluate the von Neumann entropy for the resulting reduced density matrix. We will now perform this for two systems: the doubly-filled bonding molecular orbital, and the Omar apparatus.

### 3.3.3 Showing that the delocalized state $|\psi\rangle = \frac{1}{\sqrt{2}}(c_{A\uparrow}^\dagger + c_{B\uparrow}^\dagger)\frac{1}{\sqrt{2}}(c_{A\downarrow}^\dagger + c_{B\downarrow}^\dagger)|0\rangle$ is separable into space-only and spin-only pure states

In order to trace out space and spin for this state, we need to write it in a spin-space product basis, choosing spin and spatial states that each form a complete basis for spin and space in the system. These are

- Spin:  $|\chi_{S,m_S}\rangle = \{|\chi_{0,0}\rangle, |\chi_{1,-1}\rangle, |\chi_{1,0}\rangle, |\chi_{1,1}\rangle\}$
- Space:  $|AA\rangle, |BB\rangle, |AB-\rangle, |AB+\rangle$  where

–  $|AA\rangle, |BB\rangle$  denote double-occupancy of sites A,B respectively

–  $|AB\pm\rangle := \frac{1}{\sqrt{2}}\left(A(1)B(2) \pm A(2)B(1)\right)$

In the expansion of this state, it is clear that the double-occupancy terms correspond to products of doubly-occupied spatial states and the spin singlet



state, i.e.

$$\begin{aligned} c_{A\uparrow}^\dagger c_{A\downarrow}^\dagger |0\rangle &= |AA\rangle |\chi_{0,0}\rangle \\ c_{B\uparrow}^\dagger c_{B\downarrow}^\dagger |0\rangle &= |BB\rangle |\chi_{0,0}\rangle \end{aligned} \quad (3.16)$$

The single-occupancy terms require a little rearranging:

$$\begin{aligned} \frac{1}{\sqrt{2}} \left( c_{A\uparrow}^\dagger c_{B\downarrow}^\dagger + c_{B\uparrow}^\dagger c_{A\downarrow}^\dagger \right) |0\rangle &= \frac{1}{\sqrt{2}} \left( \begin{vmatrix} A\uparrow(1) & B\downarrow(1) \\ A\uparrow(2) & B\downarrow(2) \end{vmatrix} + \begin{vmatrix} B\uparrow(1) & A\downarrow(1) \\ B\uparrow(2) & A\downarrow(2) \end{vmatrix} \right) \\ &= \frac{1}{\sqrt{2}} \left( \frac{1}{\sqrt{2}} (A(1)\uparrow(1)B(2)\downarrow(2) \right. \\ &\quad - A(2)\uparrow(2)B(1)\downarrow(1)) \\ &\quad + \frac{1}{\sqrt{2}} (B(1)\uparrow(1)A(2)\downarrow(2) \\ &\quad \left. - B(2)\uparrow(2)A(1)\downarrow(1)) \right) \\ &= \frac{1}{\sqrt{2}} \left( A(1)B(2) + A(2)B(1) \right) \\ &\quad \frac{1}{\sqrt{2}} \left( \uparrow(1)\downarrow(2) - \uparrow(2)\downarrow(1) \right) \\ &= |AB+\rangle |\chi_{0,0}\rangle \end{aligned} \quad (3.17)$$

So

$$\begin{aligned} |\psi\rangle &= \frac{1}{\sqrt{2}} (c_{A\uparrow}^\dagger + c_{B\uparrow}^\dagger) \frac{1}{\sqrt{2}} (c_{A\downarrow}^\dagger + c_{B\downarrow}^\dagger) |0\rangle \\ &= \left( \frac{1}{2} |AA\rangle + \frac{1}{2} |BB\rangle + \frac{1}{\sqrt{2}} |AB+\rangle \right) |\chi_{0,0}\rangle \\ &= |\psi\rangle_{\text{space}} |\psi\rangle_{\text{spin}} \end{aligned} \quad (3.18)$$

$|\psi\rangle$  is thus separable in space and spin - there is no ‘entanglement’ between space and spin degrees of freedom in this state.

### 3.3.4 Space-spin entanglement of a parameterized version of the delocalized state $|\psi\rangle = \frac{1}{\sqrt{2}} (c_{A\uparrow}^\dagger + c_{B\uparrow}^\dagger) \frac{1}{\sqrt{2}} (c_{A\downarrow}^\dagger + c_{B\downarrow}^\dagger) |0\rangle$

What happens to the separability of space and spin components in this state if we introduce a parameter to make the delocalized spin-up and spin-down states

different? For example, if the state is parameterized thus:

$$\begin{aligned}
|\psi\rangle_{\text{param}} &= (\cos\theta c_{A\uparrow}^\dagger + \sin\theta c_{B\uparrow}^\dagger) \frac{1}{\sqrt{2}} (c_{A\downarrow}^\dagger + c_{B\downarrow}^\dagger) |0\rangle \\
&= \frac{1}{\sqrt{2}} |\chi_{0,0}\rangle \left( \cos\theta |AA\rangle + \sin\theta |BB\rangle + \frac{1}{\sqrt{2}} (\cos\theta + \sin\theta) |AB+\rangle \right) \\
&\quad + \frac{1}{2} |\chi_{1,0}\rangle (\cos\theta - \sin\theta) |AB-\rangle. \tag{3.19}
\end{aligned}$$

If this state is written as a density matrix, and then the spin degrees of freedom are traced out, the resulting space-only density matrix is

$$\hat{\rho}_{\text{space}} = \begin{pmatrix} \frac{1}{2} \cos^2\theta & \frac{\cos\theta \sin\theta}{2} & \frac{\cos\theta(\cos\theta + \sin\theta)}{2\sqrt{2}} & 0 \\ \frac{1}{2} \cos\theta \sin\theta & \sin^2\theta & \frac{\sin\theta(\cos\theta + \sin\theta)}{2\sqrt{2}} & 0 \\ \frac{\cos\theta(\cos\theta + \sin\theta)}{2\sqrt{2}} & \frac{\sin\theta(\cos\theta + \sin\theta)}{2\sqrt{2}} & \frac{1}{4}(1 + \sin(2\theta)) & 0 \\ 0 & 0 & 0 & \frac{(1 - 2\cos\theta \sin\theta)}{4} \end{pmatrix} \tag{3.20}$$

in the basis

$$|AA\rangle, |BB\rangle, |AB+\rangle, |AB-\rangle. \tag{3.21}$$

Figure 3.2 shows the von Neumann entropy of this density matrix, plotted against the parameter  $\theta$ . Its minimum value of 0 ebits is at  $\theta = \frac{\pi}{4} \pm n\pi$  where  $n$  is an integer. This is because for  $\theta = \frac{\pi}{4}$ ,

$$\begin{aligned}
\sin \frac{\pi}{4} &= \cos \frac{\pi}{4} = \frac{1}{\sqrt{2}} \\
\therefore |\psi\rangle_{\text{param}} &= \frac{1}{2} |\chi_{0,0}\rangle \left( |AA\rangle + |BB\rangle + \sqrt{2} |AB+\rangle \right) \tag{3.22}
\end{aligned}$$

which clearly contains no entanglement between space and spin. Whereas for  $\theta = \frac{3\pi}{4} \pm n\pi$ ,

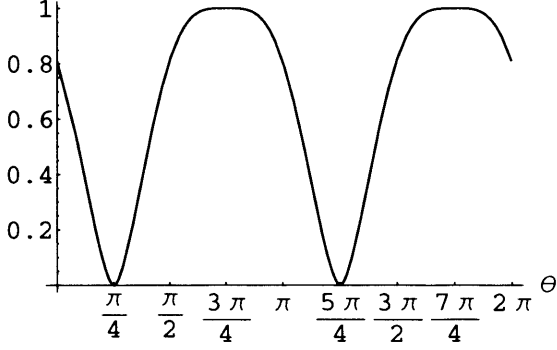
$$\begin{aligned}
\sin \frac{3\pi}{4} &= \frac{1}{\sqrt{2}}, \quad \cos \frac{3\pi}{4} = -\frac{1}{\sqrt{2}}, \\
\therefore |\psi\rangle_{\text{param}} &= \frac{1}{2} |\chi_{0,0}\rangle \left( -|AA\rangle + |BB\rangle \right) - \frac{1}{\sqrt{2}} |\chi_{1,0}\rangle |AB-\rangle. \tag{3.23}
\end{aligned}$$

which is a state containing maximal entanglement between space and spin.

### 3.3.5 Tracing out space and spin from the locally antisymmetrized Omar output state

In this exercise, we will consider only the ++ output state for fermions with 50/50 beamsplitters. As with the doubly-filled bonding molecular orbital, in

Figure 3.2: Von Neumann entropy of  $\rho_{\text{space}}$ , traced out from a parameterized version of the doubly-occupied molecular bonding orbital, versus parameter  $\theta$ .  $S(\rho_{\text{space}})$



order to trace out the space and spin degrees of freedom and obtain spin-only and space-only (respectively) reduced density matrices, we need to write this state as a sum of products of space and spin eigenfunctions. Each set of eigenfunctions should form a complete set. The eigenfunctions are obtained and presented in Appendix A. Using a product basis of these spin and spatial eigenfunctions:

$$\begin{aligned} &\Phi_{0,0}^{0,0}|L\rangle_1|L\rangle_2, \Phi_{0,0}^{0,0}|R\rangle_1|R\rangle_2, \Phi_{0,0}^{0,0}|L\rangle_1|R\rangle_2, \Phi_{0,0}^{0,0}|R\rangle_1|L\rangle_2, \\ &\Phi_{0,0}^{0,0}|A+\rangle_1|A+\rangle_2, \Phi_{1,1}^{0,0}|A-\rangle_1|A-\rangle_2, \Phi_{1,1}^{2,0}|A-\rangle_1|A-\rangle_2 \end{aligned} \quad (3.24)$$

the output state for the entire apparatus can be written

$$\begin{aligned} |\text{out}\rangle_{\text{fermion}}^{++} &= \frac{1}{2}\Phi_{0,0}^{0,0}(|L\rangle_1|L\rangle_2 + |R\rangle_1|R\rangle_2 + |L\rangle_1|R\rangle_2 + |R\rangle_1|L\rangle_2 \\ &\quad - 2|A+\rangle_1|A+\rangle_2 + |A-\rangle_1|A-\rangle_2) \left( \frac{2}{\sqrt{3}}\Phi_{1,1}^{0,0} + \sqrt{\frac{2}{3}}\Phi_{1,1}^{2,0} \right). \end{aligned} \quad (3.25)$$

The corresponding density matrix is, after renormalizing,

$$\hat{\rho} = \frac{1}{4} \begin{pmatrix} \frac{1}{4} & \frac{1}{4} & \frac{1}{4} & \frac{1}{4} & -\frac{1}{2} & \frac{1}{\sqrt{3}} & \frac{1}{\sqrt{6}} \\ \frac{1}{4} & \frac{1}{4} & \frac{1}{4} & \frac{1}{4} & -\frac{1}{2} & \frac{1}{\sqrt{3}} & \frac{1}{\sqrt{6}} \\ \frac{1}{4} & \frac{1}{4} & \frac{1}{4} & \frac{1}{4} & -\frac{1}{2} & \frac{1}{\sqrt{3}} & \frac{1}{\sqrt{6}} \\ \frac{1}{4} & \frac{1}{4} & \frac{1}{4} & \frac{1}{4} & -\frac{1}{2} & \frac{1}{\sqrt{3}} & \frac{1}{\sqrt{6}} \\ -\frac{1}{2} & -\frac{1}{2} & -\frac{1}{2} & -\frac{1}{2} & 1 & -\frac{2}{\sqrt{3}} & -\sqrt{\frac{2}{3}} \\ \frac{1}{\sqrt{3}} & \frac{1}{\sqrt{3}} & \frac{1}{\sqrt{3}} & \frac{1}{\sqrt{3}} & -\frac{2}{\sqrt{3}} & \frac{4}{3} & \frac{2\sqrt{2}}{3} \\ \frac{1}{\sqrt{6}} & \frac{1}{\sqrt{6}} & \frac{1}{\sqrt{6}} & \frac{1}{\sqrt{6}} & -\sqrt{\frac{2}{3}} & \frac{2\sqrt{2}}{3} & \frac{2}{3} \end{pmatrix} \quad (3.26)$$

**Spin-only density matrix** Tracing out space, the reduced spin-only density matrix is

$$\hat{\rho}_{\text{spin}} = \text{tr}_{\text{space}} \hat{\rho} = \begin{pmatrix} \frac{1}{2} & 0 & 0 \\ 0 & \frac{1}{3} & \frac{1}{3\sqrt{2}} \\ 0 & \frac{1}{3\sqrt{2}} & \frac{1}{6} \end{pmatrix} \quad (3.27)$$

in the basis

$$\Phi_{0,0}^{0,0}, \Phi_{1,1}^{0,0}, \Phi_{1,1}^{2,0} \quad (3.28)$$

This has eigenvalues  $0, \frac{1}{2}, \frac{1}{2}$  and thus a von Neumann entropy  $S(\hat{\rho}_{\text{spin}}) = 1$ .

**Space-only density matrix** If we trace out the spin degrees of freedom, the space-only density matrix is

$$\hat{\rho}_{\text{space}} = \text{tr}_{\text{spin}} \hat{\rho} = \begin{pmatrix} \frac{1}{4} & \frac{1}{4} & \frac{1}{4} & \frac{1}{4} & -\frac{1}{2} & 0 \\ \frac{1}{4} & \frac{1}{4} & \frac{1}{4} & \frac{1}{4} & -\frac{1}{2} & 0 \\ \frac{1}{4} & \frac{1}{4} & \frac{1}{4} & \frac{1}{4} & -\frac{1}{2} & 0 \\ \frac{1}{4} & \frac{1}{4} & \frac{1}{4} & \frac{1}{4} & -\frac{1}{2} & 0 \\ -\frac{1}{2} & -\frac{1}{2} & -\frac{1}{2} & -\frac{1}{2} & 1 & 0 \\ 0 & 0 & 0 & 0 & 0 & 2 \end{pmatrix} \quad (3.29)$$

in the basis

$$|L\rangle_1|L\rangle_2, |R\rangle_1|R\rangle_2, |L\rangle_1|R\rangle_2, |R\rangle_1|L\rangle_2, |A+\rangle_1|A+\rangle_2, |A-\rangle_1|A-\rangle_2 \quad (3.30)$$

This has eigenvalues  $0, 0, 0, 0, \frac{1}{2}, \frac{1}{2}$  and thus a von Neumann entropy  $S(\hat{\rho}_{\text{space}}) = 1$ . This equals  $S(\hat{\rho}_{\text{spin}})$  as you would expect. So the space and spin degrees of freedom in the full Omar apparatus share one ebit of ‘entanglement’.

### 3.3.6 Tracing out space and spin from the fully antisymmetrized Omar output state

We saw in section 3.3.5 that attempting to factor the Omar output state into a sum of products of space-only and spin-only eigenfunctions, when performed using basis states which have only been antisymmetrized with respect to exchange of particles on each side of the apparatus individually, leads to a spatial density matrix where the same spatial state is parameterized by different values of the total spin for the system.

The origin of this problem is that we have constructed the density matrix from a state which has only been antisymmetrized with respect to the exchange

of labels of any two particles on a given side, not across the entire apparatus. To obtain a density matrix which lives up to the claim advertised in equation (3.11) we need to antisymmetrize the output state with respect to exchange of any two of the four particles in the apparatus.

Our scheme to do this will be as follows:

- Fully antisymmetrize the Omar output state with respect to exchange of any two of the four particles.
- Take inner products of this antisymmetrized output state with the previously-described four-spin-half eigenfunctions  $\{\Phi_{S_A, S_B}^{S, m, s}\}$ . This yields coefficients of these eigenfunctions which are spatial in nature.
- It turns out that these coefficients are both orthogonal and of defined symmetry. They thus form a basis for spatial states of the entire system.

### 3.3.7 Fully antisymmetrizing the output state

We apply the four-particle antisymmetrizer to the Omar output state as given in equation (A.7). Before we apply the antisymmetrizer to them, the kets representing the combined spin and spatial states of sides 1 and 2 are not taken to be antisymmetrized. Eg. the ket  $|A \uparrow \downarrow\rangle_1$  represents particle  $a$  definitely spin-up in the left arm on side 1, and particle  $b$  definitely spin-down in the right arm on side 1. Similarly,  $|A \uparrow \uparrow\rangle_2$  represents particle  $c$  definitely spin-up in the left arm on side 2, and particle  $d$  definitely spin-up in the right arm on side 2. This state contains 10 terms.

Using Mathematica, we then apply the antisymmetrizer projection operator

$$\frac{1}{\sqrt{N!}} \sum_P (-1)^P \hat{P} \quad (3.31)$$

where the sum is over all permutations  $\{P\}$  of the particle labels, and

$$\begin{aligned} \text{For an even permutation:} & \quad (-1)^P = +1 \\ \text{For an odd permutation:} & \quad (-1)^P = -1 \end{aligned} \quad (3.32)$$

An even (odd) permutation is one where the number of transpositions of particle labels is even (odd). This produces a state in which the exchange of the labels of any two of the particles  $\{a, b, c, d\}$  will produce the same state, but with the

sign flipped. The antisymmetrized state contains  $10 * 4! = 240$  terms, hence the use of Mathematica.

For example, consider the term

$$|A \uparrow \downarrow\rangle_1 |A \downarrow \uparrow\rangle_2 \quad (3.33)$$

We perform

$$\begin{aligned} \frac{1}{\sqrt{N!}} \sum_P (-1)^P \hat{P} |A \uparrow \downarrow\rangle_1 |A \downarrow \uparrow\rangle_2 &= \frac{1}{\sqrt{N!}} \sum_P (-1)^P \hat{P} \left[ L1(a) \uparrow (a) R1(b) \downarrow (b) \right. \\ &\quad \left. L2(c) \downarrow (c) R2(d) \uparrow (d) \right] \end{aligned} \quad (3.34)$$

### 3.3.8 Obtaining the coefficients of the four-spin-half eigenfunctions

The four-spin-half eigenfunctions  $\{\Phi_{S_A, S_B}^{S, m_S}\}$  obtained in section A.1.1 form a basis for the spin-state of four spin halves, and therefore remain a suitable choice for the spin state of the entire apparatus. The complexity of the fully antisymmetrized state means it is not possible to reexpress the state in terms of the  $\{\Phi_{S_A, S_B}^{S, m_S}\}$  by inspection. Instead, the approach taken was to take inner products of the fully antisymmetrized output state with the  $\{\Phi_{S_A, S_B}^{S, m_S}\}$ , again using Mathematica. Ie if.

$$|\text{out}_{\text{fermion}}^{++}\rangle = \sum_{S, m_s} c_{S, m_s} |\Phi^{S, m_s}\rangle \quad (3.35)$$

then

$$c_{S, m_s} = \langle \Phi^{S, m_s} | \text{out}_{\text{fermion}}^{++} \rangle \quad (3.36)$$

The only non-zero coefficients obtained are those for

$$\Phi_{00}^{00}, \Phi_{11}^{00}, \Phi_{11}^{20} \quad (3.37)$$

The coefficients are all orthogonal, so they look like a basis for spatial states. Henceforth, we shall refer to them as ‘putative spatial states’, and denote them by the symbols

$$K_{00}^{00}, K_{11}^{00}, K_{11}^{20} \quad (3.38)$$

respectively.

### 3.3.9 Symmetry projections of the four-way antisymmetrized spatial states

The symmetry of the putative spatial states was checked by applying to them the projection operators for the irreducible representations of the  $\mathcal{S}_4$  symmetric group (the group of all permutations of four objects). Equation 4.51 in Elliott and Dawber [56] gives the general expression for the operator which projects from the vector space  $L$  onto the subspace  $L_\alpha$  as

$$P^{(\alpha)} = \frac{s_\alpha}{g} \sum_a \chi^{(\alpha)*}(G_a) T(G_a) \quad (3.39)$$

where

- $\{G_a\}$  are the elements of the group  $\mathcal{G}$ ,
- $T := \{T(G_a)\}$  are a set of operators which form a representation of  $\mathcal{G}$  in the vector space  $L$ ,
- $T^{(\alpha)}$  is an irreducible representation of  $\mathcal{G}$  with an associated vector space  $L^{(\alpha)}$ , and
- $\chi^{(\alpha)*}(G_a)$  is the character of  $G_a$  in the irrep  $T^{(\alpha)}$ .

Thus, the projection operator for the irreducible representation  $[n_1 n_2 \dots]$  of the symmetric group is

$$\begin{aligned} P^{[n_1 n_2 \dots]} &= \sum_{\text{classes}} \sum_{\substack{\text{class} \\ \text{members}}} \chi^{[n_1 n_2 \dots]*}(\text{class}) T(\text{class member}) \\ &= \sum_{(l_1 l_2 \dots)} \sum_{\substack{\text{class} \\ \text{members}}} \chi^{[n_1 n_2 \dots]*}(l_1 l_2 \dots) T(\text{class member}) \quad (3.40) \end{aligned}$$

The relevant characters are given in Table 17.1 in Elliott and Dawber, which is reproduced here in Table 3.1. So to project a coefficient onto a given  $\mathcal{S}_4$  irrep, the Mathematica code runs through all possible permutations of the particle labels, applying each permutation to the coefficient, weighting the result by the appropriate character, and summing the results. The simplest example is the projector onto the  $\chi^{[1111]}$  irrep (the antisymmetrizer projector), in which the character of each permutation is, as discussed above, its parity.

Table 3.1: Character table for  $S_4$

$S_4$	(1111)	(211)	(22)	(31)	(4)
$\chi^{[4]}$	1	1	1	1	1
$\chi^{[31]}$	3	1	-1	0	-1
$\chi^{[22]}$	2	0	2	-1	0
$\chi^{[211]}$	3	-1	-1	0	1
$\chi^{[1111]}$	1	-1	1	1	-1

We find that the only non-zero projections of the  $\{K_{S_A S_B}^{S m_S}\}$  are:

$$\begin{aligned}
 K_{00}^{00} &\rightarrow [22] \\
 K_{11}^{00} &\rightarrow [22] \\
 K_{11}^{20} &\rightarrow [1111]
 \end{aligned} \tag{3.41}$$

### 3.3.10 Calculating the space-spin entanglement from the fully antisymmetrized output state

The moduli of the non-zero coefficients are

$$\begin{aligned}
 \langle K_{00}^{00} | K_{00}^{00} \rangle &= 5/12 \\
 \langle K_{11}^{00} | K_{11}^{00} \rangle &= 5/12 \\
 \langle K_{11}^{20} | K_{11}^{20} \rangle &= 1/6.
 \end{aligned} \tag{3.42}$$

So we introduce a new set of normalized coefficients, the  $\{M_{S_A S_B}^{S m_S}\}$  and thus write

$$\begin{aligned}
 |K_{00}^{00}\rangle &= \sqrt{\frac{5}{12}} |M_{00}^{00}\rangle \\
 |K_{11}^{00}\rangle &= \sqrt{\frac{5}{12}} |M_{11}^{00}\rangle \\
 |K_{11}^{20}\rangle &= \sqrt{\frac{1}{6}} |M_{11}^{20}\rangle
 \end{aligned} \tag{3.43}$$



and thus

$$|\text{out}_{\text{fermion}}^{++}\rangle = \sqrt{\frac{5}{12}}|M_{00}^{00}\rangle|\Phi_{00}^{00}\rangle + \sqrt{\frac{5}{12}}|M_{11}^{00}\rangle|\Phi_{11}^{00}\rangle + \sqrt{\frac{1}{6}}|M_{11}^{20}\rangle|\Phi_{11}^{20}\rangle. \quad (3.44)$$

The coefficients in this expansion are clearly normalized. Thus we can write the density matrix for the entire apparatus in the  $++$  fermionic output state as

$$\begin{aligned} \hat{\rho} &= |\text{out}_{\text{fermion}}^{++}\rangle\langle\text{out}_{\text{fermion}}^{++}| \\ &= \frac{1}{6} \begin{pmatrix} \frac{5}{2} & \frac{5}{2} & \sqrt{\frac{5}{2}} \\ \frac{5}{2} & \frac{5}{2} & \sqrt{\frac{5}{2}} \\ \sqrt{\frac{5}{2}} & \sqrt{\frac{5}{2}} & 1 \end{pmatrix} \end{aligned} \quad (3.45)$$

using the basis

$$|M_{00}^{00}\rangle|\Phi_{00}^{00}\rangle, |M_{11}^{00}\rangle|\Phi_{11}^{00}\rangle, |M_{11}^{20}\rangle|\Phi_{11}^{20}\rangle. \quad (3.46)$$

Since the four-spin eigenfunctions are an orthogonal set, as are the putative spatial states, the space-only and spin-only density matrices for the entire apparatus are trivial to obtain:

$$\hat{\rho}_{\text{space}} = \hat{\rho}_{\text{spin}} = \frac{1}{6} \begin{pmatrix} \frac{5}{2} & 0 & 0 \\ 0 & \frac{5}{2} & 0 \\ 0 & 0 & 1 \end{pmatrix} \quad (3.47)$$

in the bases, respectively:

$$|M_{00}^{00}\rangle, |M_{11}^{00}\rangle, |M_{11}^{20}\rangle, \quad (3.48)$$

$$|\Phi_{00}^{00}\rangle, |\Phi_{11}^{00}\rangle, |\Phi_{11}^{20}\rangle. \quad (3.49)$$

In this sense, the entanglement between spin and spatial degrees of freedom is

$$S(\hat{\rho}_{\text{space}}) = S(\hat{\rho}_{\text{spin}}) = 1.48336 \text{ ebits}. \quad (3.50)$$

### 3.3.11 Calculating the space-spin entanglement in the fully antisymmetrized *input* state

We can perform a similar exercise for the input state to the Omar interferometer. Recall that this consists of two pairs of particles which are maximally entangled

in some internal degree of freedom: eg. two electron singlet pairs. One finds as before, the non-zero coefficients are

$$K_{00}^{00}, K_{11}^{00}, K_{11}^{20} \quad (3.51)$$

but this time their moduli are

$$\begin{aligned} \langle K_{00}^{00} | K_{00}^{00} \rangle &= \frac{1}{6} \\ \langle K_{11}^{00} | K_{11}^{00} \rangle &= \frac{1}{6} \\ \langle K_{11}^{20} | K_{11}^{20} \rangle &= \frac{2}{3}. \end{aligned} \quad (3.52)$$

Thus, introducing the normal basis of the  $\{M_{S_A S_B}^{S_m S_s}\}$ ,

$$\begin{aligned} |\text{in}_{\text{fermion}}^{++}\rangle &= |K_{00}^{00}\rangle|\Phi_{00}^{00}\rangle + |K_{11}^{00}\rangle|\Phi_{11}^{00}\rangle + |K_{11}^{20}\rangle|\Phi_{11}^{20}\rangle \\ &= \sqrt{\frac{1}{6}}|M_{00}^{00}\rangle|\Phi_{00}^{00}\rangle + \sqrt{\frac{1}{6}}|M_{11}^{00}\rangle|\Phi_{11}^{00}\rangle + \sqrt{\frac{2}{3}}|M_{11}^{20}\rangle|\Phi_{11}^{20}\rangle \end{aligned} \quad (3.53)$$

and thus written in the basis in (3.46)

$$\begin{aligned} \hat{\rho} &= |\text{in}_{\text{fermion}}^{++}\rangle\langle\text{in}_{\text{fermion}}^{++}| \\ &= \begin{pmatrix} \frac{1}{6} & \frac{1}{6} & \sqrt{\frac{2}{18}} \\ \frac{1}{6} & \frac{1}{6} & \sqrt{\frac{2}{18}} \\ \sqrt{\frac{2}{18}} & \sqrt{\frac{2}{18}} & \frac{2}{3} \end{pmatrix}. \end{aligned} \quad (3.54)$$

Tracing out the space or spin degrees of freedom yields

$$\hat{\rho}_{\text{space}} = \hat{\rho}_{\text{spin}} = \begin{pmatrix} \frac{1}{6} & 0 & 0 \\ 0 & \frac{1}{6} & 0 \\ 0 & 0 & \frac{2}{3} \end{pmatrix} \quad (3.55)$$

using the bases in (3.48) and (3.49). Thus the entanglement between space and spin is

$$S(\hat{\rho}_{\text{space}}) = S(\hat{\rho}_{\text{spin}}) = 2. - \frac{1}{6}\log_2 \frac{1}{6} - \frac{2}{3}\log_2 \frac{2}{3} = 1.25 \text{ ebits} \quad (3.56)$$

This result is not as surprising as it may seem. Although in the input state the entanglement between sides 1 and 2 of the apparatus is carried entirely in the spin degrees of freedom, there are correlations between the spin and spatial

states of the particles. For example, measuring  $S_1^2 = 1$  tells us that the spins on side 1 of the apparatus are in a spin triplet state (symmetric) and therefore the spatial state must be antisymmetric to preserve the overall antisymmetry of the state on side 1.

### 3.3.12 Mutual information between measurements on $|\psi\rangle =$

$$\frac{1}{\sqrt{2}}(c_{A\uparrow}^\dagger + c_{B\uparrow}^\dagger)\frac{1}{\sqrt{2}}(c_{A\downarrow}^\dagger + c_{B\downarrow}^\dagger)|0\rangle$$

Consider a two-site two-fermion system in the delocalized state

$$\frac{1}{\sqrt{2}}(c_{A\uparrow}^\dagger + c_{B\uparrow}^\dagger)\frac{1}{\sqrt{2}}(c_{A\downarrow}^\dagger + c_{B\downarrow}^\dagger)|0\rangle. \quad (3.57)$$

#### One-site measurements

Consider the results of an experiment to measure total charge, and total spin-z, at one of the sites  $A$  and  $B$ . The former could be achieved using a single-electron transistor scanning electrometer (SETSE) [57], the latter using a Stern-Gerlach-type experiment. The possible measurement results are

- $x :=$  spin results =  $\{0, -\frac{1}{2}, \frac{1}{2}\}$  (total  $m_s$ )
- $y :=$  charge results =  $\{0, 1, 2\}$  (number of particles)

Let's suppose we perform the  $y$  (charge) measurement first. How much information about the spin states of the fermions will we gain from this spatial measurement? The answer is given by the mutual information  $H(X : Y)$  between the probability distributions  $X$  and  $Y$  of  $x$  and  $y$ , defined by

$$H(X : Y) = H(X) - H(X|Y) \quad (3.58)$$

Let us consider measurements made at site  $A$ . The expansion of the delocalized state is:

$$\begin{aligned} |\psi\rangle &= \left( \frac{1}{2}c_{A\uparrow}^\dagger c_{A\downarrow}^\dagger + \frac{1}{2}c_{A\uparrow}^\dagger c_{B\downarrow}^\dagger + \frac{1}{2}c_{B\uparrow}^\dagger c_{A\downarrow}^\dagger + \frac{1}{2}c_{B\uparrow}^\dagger c_{B\downarrow}^\dagger \right) |0\rangle \\ &= \frac{1}{2}|x_A = 0\rangle + \frac{1}{2}|x_A = \frac{1}{2}\rangle + \frac{1}{2}|x_A = -\frac{1}{2}\rangle + \frac{1}{2}|x_A = 0\rangle \\ &= \frac{1}{2}|y_A = 2\rangle + \frac{1}{2}|y_A = 1\rangle + \frac{1}{2}|y_A = 1\rangle + \frac{1}{2}|y_A = 0\rangle \end{aligned} \quad (3.59)$$

So the probability distributions  $X$  and  $Y$  are

$$\begin{aligned} X := \{p(x)\} & : p(-\frac{1}{2}) = \frac{1}{4}, p(0) = \frac{1}{2}, p(\frac{1}{2}) = \frac{1}{4} \\ Y := \{p(y)\} & : p(0) = \frac{1}{4}, p(1) = \frac{1}{2}, p(2) = \frac{1}{4} \end{aligned} \quad (3.60)$$

and have a Shannon entropy given by

$$\begin{aligned} H(X) & = -\sum_x p_x \log_2 p_x \\ & = -\frac{1}{2} \log_2 \frac{1}{2} - 2 \frac{1}{4} \log_2 \frac{1}{4} \\ & = \frac{3}{2} = H(Y) \end{aligned} \quad (3.61)$$

Note that  $H(Y) = H(X)$  because  $y$  has an identical probability distribution to  $x$ . Using

$$p(x, y) = p(x)p(y|x) \quad (3.62)$$

we obtain the joint probabilities for measurements of  $x$  and  $y$  shown in Table 3.2. We hence obtain a conditional Shannon entropy of

$$\begin{aligned} H(X|Y) & = \langle -\log_2 p(x|y) \rangle = -\sum_{x,y} p(x, y) \log_2 p(x|y) \\ & = (\text{contributions from } y = 0, 2) + (\text{contributions from } y = 1) \\ & = 2 \times \frac{1}{4} \times 0 + \frac{1}{4} \times 2 \times (-\log_2 \frac{1}{2}) \\ & = \frac{1}{2} \end{aligned} \quad (3.63)$$

The mutual information between  $X$  and  $Y$  is now readily calculated:

$$H(X : Y) = H(X) - H(X|Y) = \frac{3}{2} - \frac{1}{2} = 1 \text{ bit} \quad (3.64)$$

so when we make a charge (i.e. spatial) measurement at site  $A$ , we gain one bit of information about the total spin-z projection at site  $A$ . The same conclusions apply to measurements at site  $B$ , of course.

It is worth noting that this discussion is possible only because the  $\hat{S}_z$  and charge operators commute - by rotating the spin axes we can always choose a representation in which  $\hat{\rho}$  is diagonal. The above treatment would not be possible if we e.g. were considering position and momentum measurements.

Table 3.2: One site measurements: joint probabilities

$y$	$x$	$p(y)$	$p(x   y)$	$p(x,y)$
0	0	$\frac{1}{4}$	1	$\frac{1}{4}$
0	$\frac{1}{2}, -\frac{1}{2}$	$\frac{1}{4}$	0	0
1	0	$\frac{1}{2}$	0	0
1	$\frac{1}{2}, -\frac{1}{2}$	$\frac{1}{2}$	$\frac{1}{2}$	$\frac{1}{4}$
2	0	$\frac{1}{4}$	1	$\frac{1}{4}$
2	$\frac{1}{2}, -\frac{1}{2}$	$\frac{1}{4}$	0	0

### Two-site measurements

Now consider making a joint classical (two-site) measurement on the entire system  $A + B$ . One possible (non-optimal) set of spin and spatial measurement results is

- $x = \{(m_{s,A}, m_{s,B})\} = (\frac{1}{2}, -\frac{1}{2}); (-\frac{1}{2}, \frac{1}{2}); (0, 0)$  spin measurement results
- $y = AA, BB, AB$  space measurement results

The probability distributions are

$$\begin{aligned}
 X := \{p(x)\} & : p(\frac{1}{2}, -\frac{1}{2}) = \frac{1}{4}, p(-\frac{1}{2}, \frac{1}{2}) = \frac{1}{4}, p(0, 0) = \frac{1}{2} \\
 Y := \{p(y)\} & : p(AA) = \frac{1}{4}, p(BB) = \frac{1}{4}, p(AB) = \frac{1}{2}
 \end{aligned}
 \tag{3.65}$$

with a Shannon entropy of  $H(X) = H(Y) = \frac{3}{2}$  as calculated in equation (3.61). The joint and conditional probabilities are given in Table 3.3.

Thus the conditional entropy  $H(X|Y)$  is

$$\begin{aligned}
 H(X|Y) & = \langle -\log_2 p(x|y) \rangle = - \sum_{x,y} p(x,y) \log_2 p(x|y) \\
 & = \text{(contributions from } AB \text{ results)} \\
 & \quad + \text{(contributions from } AA \text{ and } BB \text{ results)} \\
 & = -2 \frac{1}{4} \log_2 \frac{1}{2} - 2 \frac{1}{4} \log_2 1 \\
 & = -2 \frac{1}{4} (-1) - 2 \frac{1}{4} (0) \\
 & = \frac{1}{2}
 \end{aligned}
 \tag{3.66}$$

Table 3.3: Two site measurements: joint probabilities

$y$	$x$	$p(y)$	$p(x   y)$	$p(x,y)$
$AA$	$0,0$	$\frac{1}{4}$	$1$	$\frac{1}{4}$
$AA$	$\frac{1}{2}, -\frac{1}{2}$	$\frac{1}{4}$	$0$	$0$
$AA$	$-\frac{1}{2}, \frac{1}{2}$	$\frac{1}{4}$	$0$	$0$
$BB$	$0,0$	$\frac{1}{4}$	$1$	$\frac{1}{4}$
$BB$	$\frac{1}{2}, -\frac{1}{2}$	$\frac{1}{4}$	$0$	$0$
$BB$	$-\frac{1}{2}, \frac{1}{2}$	$\frac{1}{4}$	$0$	$0$
$AB$	$0,0$	$\frac{1}{2}$	$0$	$0$
$AB$	$\frac{1}{2}, -\frac{1}{2}$	$\frac{1}{2}$	$\frac{1}{2}$	$\frac{1}{4}$
$AB$	$-\frac{1}{2}, \frac{1}{2}$	$\frac{1}{2}$	$\frac{1}{2}$	$\frac{1}{4}$

So the mutual information is

$$\begin{aligned}
 H(X : Y) &= H(X) - H(X|Y) \\
 &= \frac{3}{2} - \frac{1}{2} \\
 &= 1 \text{ bit}
 \end{aligned} \tag{3.67}$$

### 3.3.13 Holevo bound on mutual information between measurements on

$$|\psi\rangle = \frac{1}{\sqrt{2}}(c_{A\uparrow}^\dagger + c_{B\uparrow}^\dagger) \frac{1}{\sqrt{2}}(c_{A\downarrow}^\dagger + c_{B\downarrow}^\dagger)|0\rangle$$

#### One-site measurements

Let's try to relate our discussion of the mutual information between one-site spin and charge (i.e. spatial) measurements discussed above, to the Holevo bound.

**Holevo bound:** If Alice prepares  $\hat{\rho}_X$  with probability  $p_X$  where  $X = 0, \dots, n$  and Bob then performs any POVM  $\{E_y\}$  with result  $Y$  then

$$H(X : Y) \leq S(\hat{\rho}) - \sum_x p_x S(\hat{\rho}_x) = \chi \tag{3.68}$$

$$\text{where } \hat{\rho} = \sum_x p_x \hat{\rho}_x$$

**Accessible information:** Bob's accessible information is defined as the maximum of the mutual information  $H(X : Y)$  over all possible measurement schemes, (i.e. it is the optimal mutual information).

Written in the occupation number basis

$$|n_{A\uparrow}n_{A\downarrow}\rangle = |00\rangle, |10\rangle, |01\rangle, |11\rangle \quad (3.69)$$

the reduced density matrix for site  $A$  in the delocalized state we are considering is

$$\begin{aligned} \hat{\rho}_A &= \frac{1}{4} \begin{pmatrix} 1 & . & . & . \\ . & 1 & . & . \\ . & . & 1 & . \\ . & . & . & 1 \end{pmatrix} \\ &= \frac{1}{2} \left( |00\rangle\langle 00| + |10\rangle\langle 10| + |01\rangle\langle 01| + |11\rangle\langle 11| \right) \end{aligned} \quad (3.70)$$

Imagine that Alice performs a spin-z measurement, and then passes the state that the delocalized state is projected into to Bob. We can say that she 'prepares'  $\hat{\rho}_X$  by her spin measurement. The accessible information is the optimal information that Bob can obtain about the result of Alice's spin measurement through any measurement he performs on  $\hat{\rho}_X$ . The mappings between Alice's measurement result and the projected state are given in Table 3.4.

Alice passes the projected state  $\hat{\rho}_X$  to Bob: he receives

$$\begin{aligned} \hat{\rho}'_A &= \sum_{m_s} p_{m_s} \hat{\rho}_{m_s} \\ &= \frac{1}{2} \cdot \frac{1}{2} \begin{pmatrix} 1 & . & . & . \\ . & 0 & . & . \\ . & . & 0 & . \\ . & . & . & 1 \end{pmatrix} + \frac{1}{4} \begin{pmatrix} 0 & . & . & . \\ . & 1 & . & . \\ . & . & 0 & . \\ . & . & . & 0 \end{pmatrix} + \frac{1}{4} \begin{pmatrix} 0 & . & . & . \\ . & 0 & . & . \\ . & . & 1 & . \\ . & . & . & 0 \end{pmatrix} \\ &= \begin{pmatrix} \frac{1}{4} & . & . & . \\ . & \frac{1}{4} & . & . \\ . & . & \frac{1}{4} & . \\ . & . & . & \frac{1}{4} \end{pmatrix} \\ &= \hat{\rho}_A \end{aligned} \quad (3.71)$$

Table 3.4: Projection outcomes corresponding to Alice's measurement results

Alices measures $m_s =$	...with probability $p_{m_s} =:$	...and projects $\hat{\rho}_X =$
0	$\frac{1}{2}$	$\frac{1}{2} \begin{pmatrix} 1 & 0 & 0 & 0 \\ 0 & 0 & 0 & 0 \\ 0 & 0 & 0 & 0 \\ 0 & 0 & 0 & 1 \end{pmatrix}$
$\frac{1}{2}$	$\frac{1}{4}$	$\begin{pmatrix} 0 & 0 & 0 & 0 \\ 0 & 1 & 0 & 0 \\ 0 & 0 & 0 & 0 \\ 0 & 0 & 0 & 0 \end{pmatrix}$
$-\frac{1}{2}$	$\frac{1}{4}$	$\begin{pmatrix} 0 & 0 & 0 & 0 \\ 0 & 0 & 0 & 0 \\ 0 & 0 & 1 & 0 \\ 0 & 0 & 0 & 0 \end{pmatrix}$



Now

$$\chi(\hat{\rho}'_A) = S(\hat{\rho}'_A) - \sum_{m_s} p_{m_s} S(\hat{\rho}_{m_s}) \quad (3.72)$$

where

$$\begin{aligned} S(\hat{\rho}'_A) &= 2 \\ p_{m_s=0} S(\hat{\rho}_{m_s=0}) &= \frac{1}{2} \cdot 2 \cdot -\frac{1}{2} \log_2 \frac{1}{2} = \frac{1}{2} \\ p_{m_s=\frac{1}{2}} S(\hat{\rho}_{m_s=\frac{1}{2}}) &= \frac{1}{4} \cdot -1 \log_2 1 = 0 \\ p_{m_s=-\frac{1}{2}} S(\hat{\rho}_{m_s=-\frac{1}{2}}) &= 0 \end{aligned} \quad (3.73)$$

hence

$$\chi = 2 - \frac{1}{2} = \frac{3}{2} \quad (3.74)$$

In the discussion in section 3.3.12 of one-site spin ( $X$ ) and charge ( $Y$ ) measurements, we obtained a mutual information between them of  $H(X : Y) = 1$  bit. So for this particular example of the mutual information between measurements,  $H(X : Y) \leq \chi$  and thus the Holevo bound is satisfied.

## 3.4 Can space and spin degrees of freedom carry entanglement between two parts, and how do they contribute to the total entanglement?

### 3.4.1 Space-only and spin-only entanglement

Previous sections have shown how to obtain reduced descriptions of a system that contains a mixture of spin and space entanglement in terms of only the spin or space degrees of freedom. So it would seem natural to seek to quantify the entanglement between two physical subsystems of the system that is carried solely in the states of the spin or space degrees of freedom. This entanglement will be called ‘spin-only’ and ‘space-only’ entanglement, respectively. Although such a characterization seems natural and desirable, it is necessary to proceed with caution and define exactly what is meant by the terms.

As will shortly be shown, there are certain systems (such as the Omar apparatus) where ‘spin-only’ entanglement seems an entirely natural and non-problematic quantity. In the case of the Omar apparatus, this is specifically

because it is constrained always to contain two particles on each side of the apparatus. Thus, ‘spin-only’ entanglement between the two sides is an easy and unambiguous quantity. However, imagine that Alice and Bob share a number of spins. The ‘spin-only’ density matrix, obtained by tracing out the spatial degrees of freedom as above, is unaffected by whether Alice has all, some, or none of the spins. Yet Alice and Bob certainly cannot share any ‘spin-only’ entanglement if Alice possesses none of the spins.

**Definition of spin-only entanglement.** This is the amount of entanglement Alice and Bob can make use of when performing a teleportation experiment in which they can only make spin measurements. What is meant here by a ‘spin measurement’? After all, it would be perfectly possible for Alice to make a set of spin measurements which gave information about the spatial state of her subsystem, ie. measurements that had spatial resolution. For example, measuring  $\hat{S}_z = 0$  indicates she has 0 or 2 spins in her possession, but not 1.

So ‘spin measurement’ means that one does not allow magnetic field gradients that are more localized than Alice’s subsystem. In other words, the characteristic length scale of the magnetic field gradients used:

$$\sim \frac{|B|}{d|B|/dx} \tag{3.75}$$

is of the order of the spatial dimension of Alice’s subsystem.

It should be noted that any operation Alice makes that respects the indistinguishability of the particles must commute with  $P_{12}$ , the operator that exchanges the particles. And consequently, that operation must also commute with  $\hat{S}^2$ , since, for a system of two spin-1/2 particles,  $\hat{S}^2$  can be expressed as  $\hat{S}^2 = \hbar^2(\hat{P}_{12} + 1)$ . So, for example, if we restrict Alice to spin-only operations, she can’t transform between the singlet and triplet states, as to do so would require a change in the spatial state. This is of course all a consequence of the fact that the total Hilbert space is not a direct product of the spatial and spin Hilbert spaces.

**Definition of space-only entanglement.** This is somewhat easier to define rigorously than spin-only entanglement. Arbitrarily accurate measurements of position within Alice’s side of the apparatus are allowed, but Alice is not allowed to use any magnetic fields when making her measurements, or performing the

operations necessary for her CNOT. She thus has no access to information about the spin state of her subsystem.

**A spin-only basis from which we can trace out a physical subsystem (site).** Consider the spin-only density matrix with elements

$$\rho_{S_{tot} m_{S_{tot}} \alpha, S'_{tot} m'_{S_{tot}} \alpha'} \quad (3.76)$$

where  $\alpha$  is a label which distinguishes between eg.  $\Phi_{00}^{00}$  and  $\Phi_{11}^{00}$ .

Trivially, this can be rewritten in terms of a basis from which site  $A$  or  $B$  can be traced out, thus:

$$\rho_{S_A m_{S_A} \alpha, S_B m_{S_B} \beta, S'_A m'_{S_A} \alpha'} \quad (3.77)$$

This is  $\rho$  in a basis of eigenfunctions of

$$(\hat{S}^A, \hat{S}_z^A) \otimes (\hat{S}^B, \hat{S}_z^B). \quad (3.78)$$

### 3.4.2 Available entanglement in the doubly-filled bonding MO under spin-only and charge-only measurement restrictions

What happens to the entanglement available in the doubly-filled bonding MO if restrictions are placed on the type of measurements that Alice can make when performing the teleportation protocol? Not surprisingly, the effect is to reduce the available entanglement, as Alice can no longer perform a completely reliable Bell-state measurement. The following sections quantify this reduction.

As is discussed later in section 4.3, a more severe restriction is to limit the types of *operations* that Alice can perform when carrying out the teleportation protocol. Restricting the possible operations corresponds to imposing a *superselection rule*, a concept discussed in chapter 4. This causes an even greater reduction in available entanglement than the measurement restrictions, as Alice is also not able to perform her CNOT correctly, as will be shown in section 4.3.

The isomorphism used for teleportating two qubits using the doubly-filled bonding MO

$$|\psi\rangle = \frac{1}{\sqrt{2}}(c_{A\uparrow}^\dagger + c_{B\uparrow}^\dagger) \frac{1}{\sqrt{2}}(c_{A\downarrow}^\dagger + c_{B\downarrow}^\dagger) |0\rangle \quad (3.79)$$

was given in equation (2.73):

$$\begin{aligned} \{\sigma_\alpha \sigma_\beta\} &= \{|\uparrow\uparrow\rangle, |\uparrow\downarrow\rangle, |\downarrow\uparrow\rangle, |\downarrow\downarrow\rangle\} \\ &\rightarrow \\ \{n_{A\uparrow} n_{A\downarrow}\} &= \{|00\rangle, |11\rangle, |10\rangle, |01\rangle\} \end{aligned} \quad (3.80)$$

This connects the occupation number state of Alice's site  $A$  with the spin state of 'virtual' qubits  $\alpha$  and  $\beta$ . Virtual qubits  $\alpha$  and  $\beta$  thus play the role of Alice's half of the singlet pair in the original description of the teleportation protocol by Bennett et al. The variant of the protocol described in section 2.9 means Alice does not have to perform a measurement in the Bell basis on the qubit whose state she wishes to teleport and her half of the virtual singlet pair. Instead, she only needs to measure their state in the z-basis. Clearly, the measurement of the source qubit's state is straightforward. Now, suppose Alice can only perform spin measurements. More specifically, suppose she can only make the particular spin measurement

$$\hat{S}_z |n_{A\uparrow} n_{A\downarrow}\rangle = m_s^{\text{total}} |n_{A\uparrow} n_{A\downarrow}\rangle, \quad (3.81)$$

ie. she has a magnet that can put a field along the z-axis, allowing her to perform a Stern-Gerlach experiment. What effect does this have on the amount of information she can teleport using the delocalized state? Let us rewrite the states of Alice's 'virtual' qubits in terms of the eigenvalues of Alice's commuting observables that they correspond to. These are the number of particles  $N$ , measurable via a charge measurement, and the total  $\hat{S}_z$  eigenvalue  $m_s^{\text{total}}$ , and this rewriting is shown in Table 3.5.

### Available entanglement in the doubly-filled bonding MO when Alice can only measure spin

If Alice is restricted to measuring  $m_s^{\text{total}}$ , she can still measure the state of each qubit that she is trying to teleport, assuming it was encoded as a spin state. For each of Alice's measurement results on site  $A$ , the possible corresponding states of each virtual qubit are shown in Table 3.6. In the protocol for teleportation using a given virtual qubit, after Alice performs her CNOT and Hadamard gates, she measures the states in the z-basis of the qubit  $\gamma$  whose state she wishes to teleport, and the virtual qubit  $\alpha$  or  $\beta$  which will be used for the teleportation:

$$|\sigma_\gamma \sigma_{\alpha/\beta}\rangle = \{|\uparrow\uparrow\rangle, |\uparrow\downarrow\rangle, |\downarrow\uparrow\rangle, |\downarrow\downarrow\rangle\} \quad (3.82)$$

Table 3.5: The states of Alice's 'virtual' qubits in terms of the eigenvalues of Alice's commuting observables that they correspond to

$n_{A\uparrow}n_{A\downarrow}$	$\sigma_\alpha\sigma_\beta$	$ N; m_s^{\text{total}}\rangle$
$ 00\rangle$	$ \uparrow\uparrow\rangle$	$ 0; 0\rangle$
$ 11\rangle$	$ \uparrow\downarrow\rangle$	$ 2; 0\rangle$
$ 10\rangle$	$ \downarrow\uparrow\rangle$	$ 1; +\frac{1}{2}\rangle$
$ 01\rangle$	$ \downarrow\downarrow\rangle$	$ 1; -\frac{1}{2}\rangle$

Table 3.6: The states of Alice's 'virtual' qubits in terms of Alice's  $m_s^{\text{total}}$  measurement results on site  $A$

$m_s^{\text{total}}$ result	Possible states of qubit $\alpha$	Possible states of qubit $\beta$
0	$ \uparrow\rangle$	$ \uparrow\rangle,  \downarrow\rangle$
+1/2	$ \downarrow\rangle$	$ \uparrow\rangle$
-1/2	$ \downarrow\rangle$	$ \downarrow\rangle$

What effect does the restriction to only measuring  $m_s^{\text{total}}$  have on her use of the teleportation protocol?

- For  $|\sigma_\gamma\sigma_\alpha\rangle$  she can always unambiguously determine the product state.
- For  $|\sigma_\gamma\sigma_\beta\rangle$  she will only correctly identify the state 50 percent of the time, ie. when she measures  $m_s = \pm 1/2$ . When she measures  $m_s = 0$  she has no idea if the ‘spin’ of virtual qubit  $\beta$  is up or down.

Thus

- Alice can teleport a qubit using virtual qubit  $\alpha$  with 100 percent reliability.
- But she can only teleport a qubit using virtual qubit  $\beta$  with 50 percent reliability.

So on average, if Alice is restricted to measuring  $m_s^{\text{total}}$ , she can teleport  $3/2$  qubits using the doubly filled bonding MO. Interestingly, this result is consistent with the Shannon entropy of the probability distribution of spin-only measurements on the doubly-filled bonding MO, calculated in section 3.3.12. But it’s not clear if this connection holds in general.

### **Available entanglement in the doubly-filled bonding MO when Alice can only measure charge**

If Alice is restricted to only measuring particle number (ie. charge) on site  $A$ , and if we suppose that she is still allowed to measure the spin state of qubit  $\gamma$  (the qubit she wishes to teleport), then we obtain the same result of  $3/2$  qubits, as shown in Table 3.7.

### **3.4.3 Available entanglement in the doubly-filled bonding MO under a charge-only measurement restriction, calculated from the reduced density matrix**

In the above section, we considered the effect that restricting the types of measurement Alice is allowed to make has on the amount of information she can teleport to Bob. We did so by explicitly looking at the effect that such a restriction has on her ability to distinguish different states of the virtual qubits used by the teleportation protocol. If we describe this restriction instead in the

Table 3.7: The states of Alice’s ‘virtual’ qubits vs Alice’s charge measurement results

$N$ result	Possible states of qubit $\alpha$	Possible states of qubit $\beta$
0	$ \uparrow\rangle$	$ \uparrow\rangle$
1	$ \downarrow\rangle$	$ \uparrow\rangle,  \downarrow\rangle$
2	$ \uparrow\rangle$	$ \downarrow\rangle$

language of the density matrix and the tracing-out operation, do we get the same answer?

First, we recall the result of equation (3.18) in order to write the overall state as a product of space-only and spin-only functions:

$$\begin{aligned}
 |\psi\rangle &= \left( \frac{1}{2}|AA\rangle + \frac{1}{2}|BB\rangle + \frac{1}{\sqrt{2}}|AB+\rangle \right) |\chi_{0,0}\rangle \\
 &= |\psi\rangle_{\text{space}} |\psi\rangle_{\text{spin}}.
 \end{aligned}
 \tag{3.83}$$

The spatial state looks in some ways like a system of two spinless bosons, shared between sites  $A$  and  $B$ :

$$\frac{(c_A^\dagger + c_B^\dagger)^2}{2} |0\rangle
 \tag{3.84}$$

where the following equivalences apply, using kets  $|n_A n_B\rangle$ :

$$\begin{aligned}
 |AA\rangle &\equiv |20\rangle \\
 |BB\rangle &\equiv |02\rangle \\
 |AB+\rangle &\equiv |11\rangle.
 \end{aligned}
 \tag{3.85}$$

The boson analogy is chosen here because  $|\psi\rangle_{\text{space}}$  explicitly violates Pauli exclusion. The above pure state of two bosons can be written in this basis as the density matrix

$$\hat{\rho}_{\text{space}} = \begin{pmatrix} \frac{1}{4} & \frac{1}{4} & \frac{1}{2\sqrt{2}} \\ \frac{1}{4} & \frac{1}{4} & \frac{1}{2\sqrt{2}} \\ \frac{1}{2\sqrt{2}} & \frac{1}{2\sqrt{2}} & \frac{1}{2} \end{pmatrix}
 \tag{3.86}$$

Site  $B$  can then be traced out as follows:

$$\begin{aligned}
{}_B\langle 0|\hat{\rho}_{\text{space}}|0\rangle_B &= \frac{1}{4}|2\rangle_{AA}\langle 2| \\
{}_B\langle 1|\hat{\rho}_{\text{space}}|1\rangle_B &= \frac{1}{2}|1\rangle_{AA}\langle 1| \\
{}_B\langle 2|\hat{\rho}_{\text{space}}|2\rangle_B &= \frac{1}{4}|0\rangle_{AA}\langle 0|
\end{aligned} \tag{3.87}$$

and thus the charge-only density matrix for site  $A$  is

$$\hat{\rho}_{\text{space}, A} = \begin{pmatrix} \frac{1}{4} & 0 & 0 \\ 0 & \frac{1}{2} & 0 \\ 0 & 0 & \frac{1}{4} \end{pmatrix} \tag{3.88}$$

in the basis

$$|0\rangle_A, |1\rangle_A, |2\rangle_A. \tag{3.89}$$

The entanglement available under a charge-only measurement restriction is thus

$$\begin{aligned}
S(\hat{\rho}_{\text{space}, A}) &= -2 \cdot \frac{1}{4} \log_2 \frac{1}{4} - \frac{1}{2} \log_2 \frac{1}{2} \\
&= -2 \cdot \frac{1}{4}(-2) - \frac{1}{2}(-1) = \frac{3}{2}
\end{aligned} \tag{3.90}$$

which is consistent with the result obtained in section 3.4.2.

### 3.4.4 Spin-space entanglement transfer in the Omar thought experiment

The Omar apparatus was first introduced in section 3.2 as an example of a system which contains entanglement both in its spin and spatial degrees of freedom. But furthermore, the action of this thought experiment is actually to *transfer* some entanglement from the spin degrees of freedom to the spatial degrees of freedom. This section considers that transfer process.

#### Side 1 of the apparatus.

First, let us consider the input state to the apparatus, and its entanglement according to the site entropy measure. This state is

$$\frac{1}{\sqrt{2}}(a_{A1\uparrow}^+ a_{A2\downarrow}^+ \pm a_{A1\downarrow}^+ a_{A2\uparrow}^+) \frac{1}{\sqrt{2}}(a_{B1\uparrow}^+ a_{B2\downarrow}^+ \pm a_{B1\downarrow}^+ a_{B2\uparrow}^+). \tag{3.91}$$



Henceforth we follow Omar *et al.* in arbitrarily choosing the case where all four particles are fermions, and the above product state consists of triplets (described as the ‘++ case for fermions’ in [3]). If we write this in the occupation number representation, and then trace out side 2 of the apparatus, we obtain the following reduced density matrix for the state of side 1 of the apparatus *before* the passage of the particles through the beamsplitters:

$$\hat{\rho}_{1,\text{in}} = \begin{pmatrix} 0 & \cdot & \cdot & \cdot & \cdot & \cdot \\ \cdot & 0 & \cdot & \cdot & \cdot & \cdot \\ \cdot & \cdot & \frac{1}{4} & \cdot & \cdot & \cdot \\ \cdot & \cdot & \cdot & \frac{1}{4} & \cdot & \cdot \\ \cdot & \cdot & \cdot & \cdot & \frac{1}{4} & \cdot \\ \cdot & \cdot & \cdot & \cdot & \cdot & \frac{1}{4} \end{pmatrix} \quad (3.92)$$

using the reduced basis for side 1

$$|n_{L1\uparrow}n_{L1\downarrow}n_{R1\uparrow}n_{R1\downarrow}\rangle = \{|1100\rangle, |0011\rangle, \\ |0110\rangle, |1001\rangle, |1010\rangle, |0101\rangle\}. \quad (3.93)$$

This state has two ebits of entanglement. Examining equation (3.92), we see that this entanglement is carried entirely in the bottom right part of the density matrix, which corresponds to single-occupancy states which differ only by the spin. Therefore, this entanglement is purely spin entanglement.

It is a straightforward exercise to show that the site entropy measure gives the same total entanglement between sides 1 and 2 of the apparatus (two ebits) for the input and output states. This must be so since the operation of each beamsplitter is local to its side of the apparatus. The unnormalized output state for 50/50 beam-splitters for our input state is given in [3] as

$$\begin{aligned} & -\frac{1}{2}|L\rangle_1|L\rangle_2 - \frac{1}{2}|R\rangle_1|R\rangle_2 \\ & -\frac{1}{2}(|L\rangle_1|R\rangle_2 + |R\rangle_1|L\rangle_2) \\ & +\frac{1}{2}(|A\uparrow\downarrow\rangle_1|A\downarrow\uparrow\rangle_2 + |A\downarrow\uparrow\rangle_1|A\uparrow\downarrow\rangle_2) \\ & -\frac{1}{2}(|A\uparrow\downarrow\rangle_1|A\uparrow\downarrow\rangle_2 + |A\downarrow\uparrow\rangle_1|A\downarrow\uparrow\rangle_2) \\ & +(|A\uparrow\uparrow\rangle_1|A\downarrow\downarrow\rangle_2 + |A\downarrow\downarrow\rangle_1|A\uparrow\uparrow\rangle_2) \end{aligned} \quad (3.94)$$

where for example,  $|L\rangle_1$  indicates both fermions on side 1 of the apparatus have passed into the left arm and thus necessarily have opposite spins, and

$|A \uparrow \downarrow\rangle_1$  indicates that each particle on side 1 of the apparatus has passed into a different arm, with the particle occupying the left arm being spin up, the particle occupying the right arm being spin down.

If we rewrite this in the occupation number representation

$$|n_{L1\uparrow}n_{L1\downarrow}n_{R1\uparrow}n_{R1\downarrow}n_{L2\uparrow}n_{L2\downarrow}n_{R2\uparrow}n_{R2\downarrow}\rangle, \quad (3.95)$$

trace out side 2 of the apparatus, and renormalize, we obtain the following reduced density matrix for side 1 of the apparatus:

$$\hat{\rho}_{1,\text{out}} = \begin{pmatrix} \frac{1}{8} & \frac{1}{8} & 0 & 0 & 0 & 0 \\ \frac{1}{8} & \frac{1}{8} & 0 & 0 & 0 & 0 \\ 0 & 0 & \frac{1}{8} & -\frac{1}{8} & 0 & 0 \\ 0 & 0 & -\frac{1}{8} & \frac{1}{8} & 0 & 0 \\ 0 & 0 & 0 & 0 & \frac{1}{4} & 0 \\ 0 & 0 & 0 & 0 & 0 & \frac{1}{4} \end{pmatrix} \quad (3.96)$$

which has entropy  $S(\hat{\rho}_{1,\text{out}}) = 2$ , showing that the total entanglement is unaffected by the operation of the apparatus. However, we can see from the fact that the double-occupancy top-left sector of this matrix is now non-zero that the system now contains spatial entanglement, because this state is now mixed in arm-occupancy number as well as spin.

### Single-occupancy and double-occupancy entanglements are additive.

Since in (3.96) there are no non-zero off-diagonal elements connecting the double-occupancy and single-occupancy sectors of the matrix, we can unambiguously assign each eigenvalue to one sector, and hence divide the total entanglement into double-occupancy and single-occupancy parts. In this case, the double-occupancy sector

$$\hat{\rho}_{1,\text{out}}^{\text{double occup}} = \begin{pmatrix} \frac{1}{8} & \frac{1}{8} \\ \frac{1}{8} & \frac{1}{8} \end{pmatrix} \quad (3.97)$$

in the basis

$$|n_{L1\uparrow}n_{L1\downarrow}n_{R1\uparrow}n_{R1\downarrow}\rangle = \{|1100\rangle, |0011\rangle\} \quad (3.98)$$

has eigenvalues  $\frac{1}{4}, 0$  and hence contributes 0.5 ebits to the entanglement.

The single-occupancy sector

$$\hat{\rho}_{1,\text{out}}^{\text{occup}} = \begin{pmatrix} \frac{1}{8} & -\frac{1}{8} & 0 & 0 \\ -\frac{1}{8} & \frac{1}{8} & 0 & 0 \\ 0 & 0 & \frac{1}{4} & 0 \\ 0 & 0 & 0 & \frac{1}{4} \end{pmatrix} \quad (3.99)$$

in the basis

$$|n_{L1\uparrow}n_{L1\downarrow}n_{R1\uparrow}n_{R1\downarrow}\rangle = \{|0110\rangle, |1001\rangle, |1010\rangle, |0101\rangle\} \quad (3.100)$$

has eigenvalues of  $\frac{1}{4}, 0, \frac{1}{4}, \frac{1}{4}$  and hence contributes 1.5 ebits.

It is clear from these definitions that the single-occupancy and double-occupancy entanglements will always sum to the total entanglement, provided that the off-diagonal elements connecting the two sectors are zero. The single-occupancy entanglement is a form of spin entanglement, since the single-occupancy states do not differ in the spatial distribution of particles between the arms. Likewise, the double-occupancy entanglement is a form of space entanglement, since the double-occupancy states do not differ in their  $m_s$  values. However it is not obvious that these are the most general forms of spin and space entanglement, since for example, the double-occupancy entanglement does not take account of the spatial states in which each arm contains one particle.

The distinction between spatial and double-occupancy entanglement is further clarified by the procedure suggested by Omar *et al.* for their output state. They suggest making a projective measurement of  $S_x$  and they show that with probability  $\frac{1}{2}$  the result  $S_x = 0$  is obtained in which case the spatial state is projected onto

$$\frac{1}{\sqrt{2}} \left[ \frac{1}{\sqrt{2}} (|L\rangle_1 + |R\rangle_1) \frac{1}{\sqrt{2}} (|L\rangle_2 + |R\rangle_2) \mp \frac{1}{\sqrt{2}} |A\rangle_1 \frac{1}{\sqrt{2}} |A\rangle_2 \right] \quad (3.101)$$

where the  $\mp$  sign is negative for fermions, and positive for bosons. This output state involves a superposition of both double- and single-occupancy components, and can easily be seen to contain one ebit of spatial entanglement between sides 1 and 2, since this state was obtained by a projective measurement of the system's spin state.

### Left arm of side 1 of the apparatus.

It is instructive now to reduce further the input and output density matrices to those for just the left arm of side 1 of the apparatus. For the input state, this is

$$\hat{\rho}_{1L,\text{in}} = \begin{pmatrix} 0 & \cdot & \cdot & \cdot \\ \cdot & 0 & \cdot & \cdot \\ \cdot & \cdot & \frac{1}{2} & \cdot \\ \cdot & \cdot & \cdot & \frac{1}{2} \end{pmatrix} \quad (3.102)$$

in the basis

$$|n_{L1\uparrow}n_{L1\downarrow}\rangle = \{|11\rangle, |00\rangle, |01\rangle, |10\rangle\} \quad (3.103)$$

which has entropy  $S(\hat{\rho}_{1L,\text{in}}) = 1$ . In the same basis, the reduced density matrix for the output state is

$$\hat{\rho}_{1L,\text{out}} = \begin{pmatrix} \frac{1}{8} & \cdot & \cdot & \cdot \\ \cdot & \frac{1}{8} & \cdot & \cdot \\ \cdot & \cdot & \frac{3}{8} & \cdot \\ \cdot & \cdot & \cdot & \frac{3}{8} \end{pmatrix} \quad (3.104)$$

which has entropy  $S(\hat{\rho}_{1L,\text{out}}) = 1.81$ , showing that the action of the beamsplitter on side 1 of the apparatus has introduced an additional 0.81 ebits of entanglement between the left arm of side 1 and the rest of the system, in addition to the 1 ebit of entanglement already present between those two subsystems.

### Operator-sum representation for spin-space entanglement transfer.

It is possible to find an operator-sum representation for the spin-space entanglement transfer within the left arm of side 1 of the apparatus that we have discussed above. An easy way to do this is to make the following isomorphism between the spin states of two qubits A and B, and the occupation numbers for the spin-up and spin-down single particle states of the left arm:

$$\begin{aligned} \{\sigma_A\sigma_B\} &= \{|\uparrow\uparrow\rangle, |\uparrow\downarrow\rangle, |\downarrow\uparrow\rangle, |\downarrow\downarrow\rangle\} \\ \rightarrow \\ \{n_{1L\uparrow}n_{1L\downarrow}\} &= \{|00\rangle, |01\rangle, |10\rangle, |11\rangle\}. \end{aligned} \quad (3.105)$$

We then find that the action of the Omar interferometer in transforming  $\hat{\rho}_{1L,\text{in}}$  to  $\hat{\rho}_{1L,\text{out}}$  can be represented by the action of the depolarizing channel [40] on  $\hat{\rho}_{1L,\text{in}}$  with probability  $p = \frac{3}{8}$ .

### 3.4.5 Calculating space-only and spin-only entanglement between sides 1 and 2 of the Omar interferometer

We calculated in sections 3.3.5 and 3.3.10 the entanglement between the space and spin degrees of freedom in the full Omar apparatus. But how much entanglement between the two sides of the apparatus is carried only in the space or spin degrees of freedom? In other words, what is the ‘spatial entanglement’ and what is the ‘spin entanglement’ between the two sides of the Omar apparatus?

#### Spin-only entanglement between the two sides of the Omar apparatus

The spin-only density operator for the entire Omar apparatus is given in equation 3.27. Calculating the spin-only entanglement between the two sides of the Omar apparatus is thus a question of calculating the entanglement of formation of this density operator with respect to a division of the Hilbert space between spin eigenfunctions of sides 1 and 2.

From the block-diagonal form of this density matrix, one obvious pure-state decomposition of  $\hat{\rho}_{\text{spin}}$  is

$$\begin{aligned} |\tilde{\psi}_1\rangle &= \frac{1}{\sqrt{2}}|\Phi_{0,0}^{0,0}\rangle = \frac{1}{\sqrt{2}}|\chi_{0,0}^A\rangle|\chi_{0,0}^B\rangle \\ |\tilde{\psi}_2\rangle &= \frac{1}{\sqrt{3}}|\Phi_{1,1}^{0,0}\rangle + \frac{1}{\sqrt{3}}\frac{1}{\sqrt{2}}|\Phi_{1,1}^{2,0}\rangle = \frac{1}{2}|\chi_{1,-1}^A\rangle|\chi_{1,1}^B\rangle + \frac{1}{2}|\chi_{1,1}^A\rangle|\chi_{1,-1}^B\rangle \end{aligned} \quad (3.106)$$

where the tildes indicate that the pure states are ‘subnormalized’. The average entanglement of this decomposition can be easily seen to be equal to  $\frac{1}{2}$  ebits, since

$$E_{av} = \sum_i p_i E_i = \frac{1}{2} \times 0 + \frac{1}{2} \times 1 = \frac{1}{2} \quad (3.107)$$

ie. the first state in the decomposition is a pure product state with zero entanglement between sides 1 and 2, and the second state in the decomposition has one ebit of entanglement between sides 1 and 2 and occurs with probability half. Application of the code for calculating the entanglement of formation indicates that this decomposition is in fact optimal: ie. the spin-only entanglement between the two sides of the Omar apparatus is  $\frac{1}{2}$  ebits.

### Space-only entanglement between the two sides of the Omar apparatus

The space-only density operator for the entire Omar apparatus is given in equation 3.29. An obvious pure-state decomposition of this is:

$$\begin{aligned} |\tilde{\psi}_1\rangle &= \frac{1}{4}(|L\rangle_1 + |R\rangle_1)(|L\rangle_2 + |R\rangle_2) - \frac{1}{2}|A+\rangle_1|A+\rangle_2 \\ |\tilde{\psi}_2\rangle &= \frac{1}{\sqrt{2}}|A-\rangle_1|A-\rangle_2 \end{aligned} \quad (3.108)$$

Here, the first state contains 1 ebit of entanglement between sides 1 and 2, and occurs with probability half. The second state is a pure product state and contains no entanglement between sides 1 and 2. The average entanglement of this decomposition is thus half an ebit. Again, we find that this decomposition is optimal: the space-only entanglement between the two sides of the Omar apparatus is  $\frac{1}{2}$  ebits.

### An argument for the optimality of the space-only decomposition

This argument is due to V. Vedral. One can see why the pure state decomposition in equation 3.108 is optimal, ie. why the entanglement of formation must equal the average entanglement of that particular decomposition, as follows:

**Lower bound.**  $|\tilde{\psi}_1\rangle$  and  $|\tilde{\psi}_2\rangle$  are distinguishable via local measurements at site  $A$ . So if Alice measures  $|\tilde{\psi}_1\rangle$  (non-destructively) at site  $A$ , she knows she can distill 1 ebit's worth of Bell states from it. If she measures the pure product state  $|\tilde{\psi}_2\rangle$  she knows she can't distill any Bell states from it. Now  $p(|\tilde{\psi}_1\rangle) = p(|\tilde{\psi}_2\rangle) = \frac{1}{2}$ . So on average, Alice can distill at least 0.5 ebits from  $\hat{\rho}_{\text{space}}$ .

**Upper bound.**  $E_F$  can't be any greater than 0.5 ebits because, by definition,  $E_F(\hat{\rho}) \leq E_{av}(\hat{\rho})$ .

**Conclusion.** From these lower and upper bounds, it is clear that  $E_F = 0.5$  ebits for  $\hat{\rho}_{\text{space}}$ .

## Chapter 4

# Entanglement and super-selection rules

### 4.1 Introduction to superselection rules

The superposition principle is a fundamental tenet of quantum mechanics. So it can be a surprise to learn that there are limits to its applicability. For example, no-one has ever prepared a particle such that its mass is a superposition of different values. Neither has anyone prepared a particle such that it is simultaneously a boson and fermion. The reason for this is that both the mass and parity quantum numbers are subject to a *superselection rule* (SSR) - a prohibition on preparing a quantum system so that it is in a superposition of states with different values of these quantum numbers. Because of this, one normally regards mass and parity as being immutable *parameters* of a particle, rather than quantum mechanical operators. The concept of an SSR was invented by Wick [58], who used it to explain the impossibility of preparing a superposition of bosonic and fermionic states.

It seems reasonable to suppose that if Alice and Bob share two parts of an entangled state, restricting the local operations they can carry out on their respective systems will reduce the entanglement that is available to them to use for teleportation. This turns out to be the case, as will be seen later in this chapter.

### 4.1.1 Definition of a superselection rule (SSR)

A review paper by Cisneros et al [59] offers the following definition:

A superselection rule induced by  $\hat{G}$  operates in a quantum system if in that system:

- $\hat{G}$  commutes with every observable  $O$  in the system (eg.  $\hat{p}$ ,  $\hat{q}$ , and possibly spin)
- And  $\hat{G}$  is not a multiple of the identity

Note that  $\hat{G}$  is a constant of the motion, since it commutes with every operator and therefore commutes with  $\hat{H}$ .

### 4.1.2 Showing that a superposition of eigenstates of $\hat{G}$ with different eigenvalues is not possible

- First, suppose one *could* produce such a superposition:

$$|u\rangle = \sum_m u_m |g_m; \alpha_m\rangle \quad (4.1)$$

where  $g_m$  labels an eigenvalue of  $\hat{G}$  and  $\alpha_m$  signifies every other quantum number needed to specify  $|g_m; \alpha_m\rangle$ .

- $\hat{G}$  commutes with every other observable in the system, so  $|u\rangle$  is an eigenstate of every other operator *in a given complete set of commuting observables (CSCO)* :

$$\begin{aligned} \hat{O}_s |u\rangle &= o_s |u\rangle \\ &= o_s \sum_m u_m |g_m; \alpha_m\rangle \end{aligned} \quad (4.2)$$

where

$$\{\hat{O}_s\}, \quad s = 1, \dots, N \quad (4.3)$$

is the CSCO. The definition of a CSCO is the largest set of commuting observables which can be found for a given system.



- But as  $\hat{G}$  commutes with  $\hat{O}_s$ ,  $|g_m; \alpha_m\rangle$  is also an eigenstate of  $\hat{O}_s$ :

$$\begin{aligned}\hat{O}_s|g_m; \alpha_m\rangle &= o_s^m|g_m; \alpha_m\rangle \\ \therefore \hat{O}_s|u\rangle &= \sum_m u_m \hat{O}_s|g_m; \alpha_m\rangle \\ &= \sum_m u_m o_s^m|g_m; \alpha_m\rangle.\end{aligned}\quad (4.4)$$

- The  $\{|g_m; \alpha_m\rangle\}$  are all linearly independent, so comparing equation 4.2 with equation 4.4, one sees it must be that:

$$o_s^m = o_s \quad \forall m. \quad (4.5)$$

If this were not so, there would be more than one possible expansion of  $|u\rangle$  in the same basis. This is only possible with linearly dependent basis vectors.

- Consider

$$|u'\rangle = \sum_m u_m e^{i\delta_m} |g_m; \alpha_m\rangle \quad (4.6)$$

ie.  $|u\rangle$  with the relative phases of its components modified by arbitrary phases. Applying  $\hat{O}_s$  to it gives:

$$\hat{O}_s|u'\rangle = o_s \sum_m u_m e^{i\delta_m} |g_m; \alpha_m\rangle = o_s|u'\rangle \quad (4.7)$$

- The quantum numbers  $\{o_s\}$  for the states  $|u\rangle, |u'\rangle$  are identical  $\therefore$  the relative phases  $\{e^{i\delta_m}\}$  are experimentally inaccessible. There is no measurement one can perform to distinguish  $|u'\rangle$  from  $|u\rangle$ . This inaccessibility of relative phases is precisely what leads us to call a mixed state ‘incoherent’.
- So, the conclusion is that if a superposition of eigenstates of  $\hat{G}$  were possible, then it would be impossible to perform any measurement upon it which would distinguish it from another such superposition with different relative phases.  $|u\rangle$  thus cannot be regarded as a coherent pure state (since in such a state the relative phases must be experimentally accessible) and thus the superposition in equation 4.1 is not possible to realize.

## SSRs and the density matrix

If a particular operator induces an SSR in a system, then certain entries in the density matrix describing the state of that system will necessarily be zero. For example, suppose that Alice has a two-spin system whose state is written in the basis

$$\{|\sigma_1\sigma_2\rangle\} = \{|\uparrow\uparrow\rangle, |\uparrow\downarrow\rangle, |\downarrow\uparrow\rangle, |\downarrow\downarrow\rangle\}. \quad (4.8)$$

Now, suppose that she doesn't have a suitable means for transforming the spin-z state of her system, and thus cannot produce a superposition of total  $\hat{S}_z$  states, and thus an SSR for total  $\hat{S}_z$  is in force. (This view of an SSR as a restriction on operations is key to understanding the effect an SSR has on entanglement, as will be seen shortly). Because of the SSR, the density matrix describing her system, written in the above basis, will have a block diagonal form:

$$\rho_{\text{Alice}} = \begin{pmatrix} \rho_{11} & 0 & 0 & 0 \\ 0 & \rho_{22} & \rho_{23} & 0 \\ 0 & \rho_{32} & \rho_{33} & 0 \\ 0 & 0 & 0 & \rho_{44} \end{pmatrix}. \quad (4.9)$$

To see this, suppose Alice *could* prepare a superposition of states of different total  $\hat{S}_z$ . To achieve this, the elements of the density matrix connecting such states would have to be non-zero. For example, for the  $\rho_{12}$  element at  $|\uparrow\uparrow\rangle$  to be non-zero, Alice would have to be able to prepare a superposition of  $|\uparrow\uparrow\rangle$  and  $|\uparrow\downarrow\rangle$  states:

$$|\psi\rangle = \langle \text{snip} \rangle + c_{\uparrow\uparrow}|\uparrow\uparrow\rangle + c_{\uparrow\downarrow}|\uparrow\downarrow\rangle + \langle \text{snip} \rangle. \quad (4.10)$$

Then a mixed state which contained  $|\psi\rangle$  in its pure state decomposition would contain the contribution

$$|\psi\rangle\langle\psi| = \langle \text{snip} \rangle + c_{\uparrow\uparrow}c_{\uparrow\downarrow}^*|\uparrow\uparrow\rangle\langle\uparrow\downarrow| + c_{\uparrow\downarrow}^*c_{\uparrow\uparrow}|\uparrow\downarrow\rangle\langle\uparrow\uparrow| + \langle \text{snip} \rangle, \quad (4.11)$$

and thus  $\rho_{12}$  might be non-zero (depending on the contributions from other pure states in the decomposition).

### 4.1.3 Example of an SSR: Wick's description of the SSR for parity

The original paper by Wick et al [58] was less general than the above treatment of SSRs. In it, the authors defined SSRs by considering a specific example: the

impossibility of producing a superposition of integer and half-integer angular momentum states. Their proof of the necessity of SSRs differs somewhat from the above treatment by Cisneros et al. Wick demonstrated that unless an SSR exists for parity, a state which should be invariant under a particular operator (double time reversal) will actually be transformed by that operator into another state with different relative phases. In Wick's example,  $\hat{G} = \hat{T}^2$ , ie. the operator that commutes with all observables is the square of the time reversal operator. In the words of Wick et al:

*One must introduce a superselection rule between at least two subspaces of the whole Hilbert space if one wishes to preserve the relativistic invariance of this space. The first of these subspaces,  $A$ , contains the states in which the total angular momentum of the system is an integer multiple of  $\hbar$ , the second subspace  $B$  contains the states with half-integer angular momenta.*

Their proof goes like this:

- Consider the action of the parity operator, denoted by  $\hat{I}$ , on a state vector  $|F\rangle$ :

$$|F'\rangle = \hat{I}|F\rangle. \quad (4.12)$$

- Then for a pseudoscalar field (ie. a field whose field function is odd),  $\hat{I}$  is of the form

$$\hat{I}|F\rangle = \omega \times (-1)^{N_0+N_2+N_4+\dots}|F\rangle, \quad (4.13)$$

where

- $N_l$  is the number of particles with angular momentum  $l$ , and
- $\omega$  is an arbitrary phase factor.

For a single particle, an SSR operates between fermionic and bosonic states. Wick shows that, if this were not the case, a superposition of half-angular momenta and integer angular momenta state vectors would not be invariant under double-time-reversal. Suppose

- $f_A, g_A, \dots$  are the state vectors of the integer angular momentum subspace  $A$ ,

- $f_B, g_B, \dots$  are those of the half angular momentum subspace  $B$ .

Applying time inversion  $t \rightarrow -t$  *twice* to any state vector should give a result indistinguishable from the original state vector. In fact, applying time inversion twice to

$$f_A + f_B \tag{4.14}$$

gives

$$\text{const}(f_A - f_B). \tag{4.15}$$

The only way to avoid a contradiction is to make the relative phases between  $f_A, f_B$  experimentally inaccessible, ie. to introduce an SSR between  $A$  and  $B$ . Then (4.14) and (4.15) are indistinguishable as required.

On the other hand, as seen in section 4.1.2, Cisneros et al show that if it were not the case that an SSR exists for an operator  $\hat{G}$  that commutes with all observables, it would be possible to prepare two different superpositions of eigenstates of that operator with different relative phases which had identical eigenvalues when measured with any operator.

## 4.2 Superselection rules and entanglement

As described above, superselection rules prevent a superposition of particular quantum numbers. This restriction can also be viewed as a restriction on the *operations* that can be performed on a system, ie. an SSR for a particular quantum number on a particular system is equivalent to a prohibition on performing the operations which would enable such a superposition to be prepared.

A straightforward example, which happens to be relevant to the ‘site-entropy’ picture of entanglement, is to consider restricting Alice and Bob to number-conserving local operations. This prevents Alice and Bob from creating or destroying particles at their sites, and thus creates an SSR for *local* particle number.

Thus, Bartlett and Wiseman [60] make the following definition of an SSR: **An SSR is a restriction on the allowed local operations on a system, and is associated with a group of physical transformations.** This is a restatement of the definition of an SSR given in section 4.1.1: the only operations allowed are those that commute with the operator  $\hat{G}$  that defines the SSR.

This allows them to define operations which are allowed under a particular SSR as follows. For a particular local quantum system with Hilbert space  $\mathbb{H}$ , the set of possible operations on the system is given by the semigroup of completely positive trace-preserving maps  $\{\mathcal{E}_{CP}\}$ . If  $G$  is a group of operations acting on  $\mathbb{H}$  through a unitary representation  $T$ , then some operation  $\mathcal{O} \in \{\mathcal{E}_{CP}\}$  is defined to be ‘G-covariant’ if

$$\mathcal{O}[T(g)\hat{\rho}T^\dagger(g)] = T(g)\mathcal{O}[\hat{\rho}]T^\dagger(g) \quad \forall g \in G \text{ and } \forall \hat{\rho}. \quad (4.16)$$

Then, the SSR associated with  $G$ , denoted by  $G$ -SSR, is defined thus.  **$G$ -SSR is a restriction on the allowed operations on the system to those CP maps  $\{\mathcal{O}_{G-SSR}\} \subset \{\mathcal{E}_{CP}\}$  that are G-covariant.** It’s now possible to define the **G-invariant state**, which for finite groups is

$$\mathcal{G}[\hat{\rho}] := (\dim G)^{-1} \sum_{g \in G} T(g) \hat{\rho} T^\dagger(g). \quad (4.17)$$

It’s so-called because it’s invariant under the action of  $G$ : ie.

$$T(g)\mathcal{G}[\hat{\rho}]T^\dagger(g) = \mathcal{G}[\hat{\rho}] \quad \forall g \in G. \quad (4.18)$$

And it turns out (I won’t reproduce the proof here) that the usable entanglement  $E_{G-SSR}(\hat{\rho}^{ab})$  that Alice and Bob can obtain from the state  $\hat{\rho}^{ab}$  by using LOCC when they are restricted by  $G$ -SSR is given by the entanglement  $E(\mathcal{G}[\hat{\rho}^{ab}])$  that they can produce from the state  $\mathcal{G}[\hat{\rho}^{ab}]$  by LOCC when  $G$ -SSR is not in force. Here,  $E$  is what Bartlett and Wiseman describe as ”a standard measure of entanglement”.

### 4.3 Effect of superselection rules on entanglement of the doubly-filled bonding MO in the site entropy picture

Sections 3.4.2 and 3.4.3 discussed how restricting the measurements Alice can make at her site limits the entanglement available from the doubly-filled bonding MO. However, a more severe restriction is to limit the *operations* that Alice can perform, i.e. to apply an SSR to the system. This limits the available entanglement still further, as this section shows.

Table 4.1: CNOT on virtual qubit  $\alpha$

$ n_{C\uparrow}n_{C\downarrow}n_{A\uparrow}n_{A\downarrow}\rangle$	$ n_{C\uparrow}n_{C\downarrow}\sigma_\alpha\sigma_\beta\rangle$
$ 1000\rangle \leftrightarrow  1010\rangle$	$ 10\uparrow\uparrow\rangle \leftrightarrow  10\downarrow\uparrow\rangle$
$ 1001\rangle \leftrightarrow  1011\rangle$	$ 10\downarrow\downarrow\rangle \leftrightarrow  10\uparrow\downarrow\rangle$
$ 01n_{A\uparrow}n_{A\downarrow}\rangle$ unchanged	$ 01\sigma_\alpha\sigma_\beta\rangle$ unchanged

### 4.3.1 By explicit consideration of possible quantum operations

The protocol outlined in section 2.9 for teleporting two qubits using the doubly-filled bonding MO requires local, non-number conserving operations in order to perform the CNOTs involving virtual qubits  $\alpha$  and  $\beta$ . If we restrict Alice to only using local, number-conserving operations on site  $A$  - ie. operations which only involve spin-flips at site  $A$  - what is the effect on the amount of entanglement she can exploit?

If Alice can only perform spin flips at site  $A$ , she is restricted to performing unitary evolutions generated by Hamiltonians of the form

$$\alpha c_{A\uparrow}^\dagger c_{A\uparrow} + \beta c_{A\downarrow}^\dagger c_{A\downarrow} + \gamma c_{A\uparrow}^\dagger c_{A\downarrow} + \gamma^* c_{A\downarrow}^\dagger c_{A\uparrow}. \quad (4.19)$$

Recall from equation (2.73) that the protocol uses this isomorphism between the occupation number states of Alice's site  $A$  and the spin states of two virtual qubits  $\alpha$  and  $\beta$ :

$$\begin{aligned} \{\sigma_\alpha\sigma_\beta\} &= \{|\uparrow\uparrow\rangle, |\uparrow\downarrow\rangle, |\downarrow\uparrow\rangle, |\downarrow\downarrow\rangle\} \\ &\rightarrow \\ \{n_{A\uparrow}n_{A\downarrow}\} &= \{|00\rangle, |11\rangle, |10\rangle, |01\rangle\} \end{aligned} \quad (4.20)$$

**CNOT on virtual qubit  $\alpha$**  The effect of CNOT on virtual qubit  $\alpha$  is to flip  $\alpha$  iff the control qubit  $\gamma$  is spin-up. Its action is thus as shown in Table 4.1 where  $|n_{C\uparrow}, n_{C\downarrow}\rangle$  is the state of the control qubit  $\gamma$  located at site  $C$  in the occupation number basis. Both of the flip operations of virtual qubit  $\alpha$  in this

Table 4.2: CNOT on virtual qubit  $\beta$

$ n_{C\uparrow}n_{C\downarrow}n_{A\uparrow}n_{A\downarrow}\rangle$	$ n_{C\uparrow}n_{C\downarrow}\sigma_\alpha\sigma_\beta\rangle$
i) $ 1000\rangle \leftrightarrow  1011\rangle$	$ 10\uparrow\uparrow\rangle \leftrightarrow  10\uparrow\downarrow\rangle$
ii) $ 1001\rangle \leftrightarrow  1010\rangle$	$ 10\downarrow\downarrow\rangle \leftrightarrow  10\downarrow\uparrow\rangle$
iii) $ 01n_{A\uparrow}n_{A\downarrow}\rangle$ unchanged	$ 01\sigma_\alpha\sigma_\beta\rangle$ unchanged

CNOT thus involve changing the number of particles at site  $A$  - a non-number conserving operation. So this CNOT cannot be performed using only spin-flips. The restriction on the type of operation Alice can perform thus means she cannot use virtual qubit  $\alpha$  for teleportation; we might guess that this would reduce the entanglement available in the state from two ebits to one.

**CNOT on virtual qubit  $\beta$**  The action of the CNOT on virtual qubit  $\beta$  is shown in Table 4.2. Clearly, operation (ii) can be produced using only spin-flips at site  $A$ . On the other hand, operation (i) changes the number of particles at site  $A$  and is thus impossible. Thus, the restricted version of the CNOT on virtual qubit  $\beta$  is simply the unitary matrix that expresses the operation (ii), and is written

$$\hat{U}_{\beta, \text{CNOT}}^{\text{restricted}} = \begin{pmatrix} 1 & 0 & 0 & 0 & 0 & 0 & 0 & 0 & 0 \\ 0 & 0 & 1 & 0 & 0 & 0 & 0 & 0 & 0 \\ 0 & 1 & 0 & 0 & 0 & 0 & 0 & 0 & 0 \\ 0 & 0 & 0 & 1 & 0 & 0 & 0 & 0 & 0 \\ 0 & 0 & 0 & 0 & 1 & 0 & 0 & 0 & 0 \\ 0 & 0 & 0 & 0 & 0 & 1 & 0 & 0 & 0 \\ 0 & 0 & 0 & 0 & 0 & 0 & 1 & 0 & 0 \\ 0 & 0 & 0 & 0 & 0 & 0 & 0 & 1 & 0 \\ 0 & 0 & 0 & 0 & 0 & 0 & 0 & 0 & 1 \end{pmatrix} \quad (4.21)$$

in the basis

$$\{|1000\rangle, |1010\rangle, |1001\rangle, |1011\rangle, |0100\rangle, |0110\rangle, |0101\rangle, |0111\rangle\}. \quad (4.22)$$

**Performing the teleportation protocol using the restricted CNOT on virtual qubit  $\beta$**  Under this restriction, it seems intuitively obvious that if virtual qubit  $\alpha$  is unusable for teleportation, and if only one of the two operations which make up the CNOT for virtual qubit  $\beta$  is possible, then it should only be possible to teleport  $\frac{1}{4} \times 2 = \frac{1}{2}$  qubits using the protocol. Let us write out the teleportation protocol using  $\hat{U}_{\beta, \text{CNOT}}^{\text{restricted}}$  to verify this guess.

First, we write out  $|\psi\rangle_C |\psi\rangle_{AB}$ , and apply  $\hat{U}_{\beta, \text{CNOT}}^{\text{restricted}}$  to the  $CA$  system, then the Hadamard to the  $C$  system. Now

$$\begin{aligned} |\psi\rangle_{AB} &= \frac{1}{\sqrt{2}}(c_{A\uparrow}^\dagger + c_{B\uparrow}^\dagger) \frac{1}{\sqrt{2}}(c_{A\downarrow}^\dagger + c_{B\downarrow}^\dagger) |0\rangle \\ &= \frac{1}{2} \left[ |11\rangle_A |00\rangle_B + |10\rangle_A |01\rangle_B + |01\rangle_A |10\rangle_B + |00\rangle_A |11\rangle_B \right] \end{aligned} \quad (4.23)$$

and the state we wish to teleport is

$$|\psi\rangle_C = a|10\rangle_C + b|01\rangle_C. \quad (4.24)$$

So the action of  $\hat{U}_{\beta, \text{CNOT}}^{\text{restricted}}$  is

$$\begin{aligned} \hat{U}_{\beta, \text{CNOT}}^{\text{restricted}} |\psi\rangle_C |\psi\rangle_{AB} &= \\ ('X') : \frac{1}{2} a |10\rangle_C &\left[ |11\rangle_A |00\rangle_B + |01\rangle_A |01\rangle_B + |10\rangle_A |10\rangle_B + |00\rangle_A |11\rangle_B \right] \\ ('Y') : + \frac{1}{2} b |01\rangle_C &\left[ |11\rangle_A |00\rangle_B + |10\rangle_A |01\rangle_B + |01\rangle_A |10\rangle_B + |00\rangle_A |11\rangle_B \right] \end{aligned} \quad (4.25)$$

Performing the Hadamard on  $|\psi\rangle_C$  has this effect:

$$\begin{aligned} |10\rangle_C &\rightarrow \frac{1}{\sqrt{2}}(|10\rangle_C + |01\rangle_C) \\ |01\rangle_C &\rightarrow \frac{1}{\sqrt{2}}(|10\rangle_C - |01\rangle_C) \end{aligned} \quad (4.26)$$



And the result of this on  $\hat{U}_{\beta, \text{CNOT}}^{\text{restricted}}|\psi\rangle_C|\psi\rangle_{AB}$  is

$$\begin{aligned}
&= \frac{1}{2}a\frac{1}{\sqrt{2}}(|10\rangle_C + |01\rangle_C) \times ('X') + \frac{1}{2}b\frac{1}{\sqrt{2}}(|10\rangle_C - |01\rangle_C) \times ('Y') \\
&= \frac{1}{2}\frac{1}{\sqrt{2}}|10\rangle_C \left[ a(|11\rangle_A|00\rangle_B + |01\rangle_A|01\rangle_B + |10\rangle_A|10\rangle_B + |00\rangle_A|11\rangle_B) \right. \\
&\quad \left. + b(|11\rangle_A|00\rangle_B + |10\rangle_A|01\rangle_B + |01\rangle_A|10\rangle_B + |00\rangle_A|11\rangle_B) \right] \\
&\quad + \frac{1}{2}\frac{1}{\sqrt{2}}|01\rangle_C \left[ a(|11\rangle_A|00\rangle_B + |01\rangle_A|01\rangle_B + |10\rangle_A|10\rangle_B + |00\rangle_A|11\rangle_B) \right. \\
&\quad \left. - b(|11\rangle_A|00\rangle_B + |10\rangle_A|01\rangle_B + |01\rangle_A|10\rangle_B + |00\rangle_A|11\rangle_B) \right] \\
&= \frac{1}{2}\frac{1}{\sqrt{2}} \left[ |10\rangle_C|11\rangle_A(a+b)|00\rangle_B + \right. \\
&\quad |10\rangle_C|01\rangle_A(a|01\rangle_B + b|10\rangle_B) + \\
&\quad |10\rangle_C|10\rangle_A(a|10\rangle_B + b|01\rangle_B) + \\
&\quad |10\rangle_C|00\rangle_A(a+b)|11\rangle_B + \\
&\quad |01\rangle_C|11\rangle_A(a-b)|00\rangle_B + \\
&\quad |01\rangle_C|01\rangle_A(a|01\rangle_B - b|10\rangle_B) + \\
&\quad |01\rangle_C|10\rangle_A(a|10\rangle_B - b|01\rangle_B) + \\
&\quad \left. |01\rangle_C|00\rangle_A(a-b)|11\rangle_B \right]. \tag{4.27}
\end{aligned}$$

It is clear from the last expression that only 50 percent of measurement results on the pure product state of the system  $CA$  will result in the occupation state of site  $B$  being projected into a state which contains a single particle which is in the original state of system  $C$  up to a local unitary transformation. Thus teleportation with the virtual qubit  $\beta$ , when Alice is restricted to number-conserving local operations, can only be achieved with 50 percent efficiency. Therefore our intuition that only half a qubit can be teleported with the doubly-filled bonding MO under such a restriction is correct.

### 4.3.2 By application of Bartlett and Wiseman's approach SSR for local particle number conservation

A simpler way to evaluate the impact of an SSR for local particle number conservation on the entanglement in the doubly-occupied bonding molecular

orbital is to apply Bartlett and Wiseman's result. One simply zeros out those elements of the density matrix that connect states with different occupancies of site  $A$  with each other, and/or of site  $B$  with each other. Doing this to the density matrix given in equation (2.50) yields

$$\hat{\rho}_{\text{local-N-SSR}} = \begin{pmatrix} 0 & 0 & 0 & 0 & 0 & 0 & 0 & 0 & 0 & 0 & 0 & 0 & 0 & 0 & 0 \\ 0 & 0 & 0 & 0 & 0 & 0 & 0 & 0 & 0 & 0 & 0 & 0 & 0 & 0 & 0 \\ 0 & 0 & 0 & 0 & 0 & 0 & 0 & 0 & 0 & 0 & 0 & 0 & 0 & 0 & 0 \\ 0 & 0 & 0 & \frac{1}{4} & 0 & 0 & 0 & 0 & 0 & 0 & 0 & 0 & 0 & 0 & 0 \\ 0 & 0 & 0 & 0 & 0 & 0 & 0 & 0 & 0 & 0 & 0 & 0 & 0 & 0 & 0 \\ 0 & 0 & 0 & 0 & 0 & 0 & 0 & 0 & 0 & 0 & 0 & 0 & 0 & 0 & 0 \\ 0 & 0 & 0 & 0 & 0 & 0 & \frac{1}{4} & 0 & 0 & -\frac{1}{4} & 0 & 0 & 0 & 0 & 0 \\ 0 & 0 & 0 & 0 & 0 & 0 & 0 & 0 & 0 & 0 & 0 & 0 & 0 & 0 & 0 \\ 0 & 0 & 0 & 0 & 0 & 0 & 0 & 0 & 0 & 0 & 0 & 0 & 0 & 0 & 0 \\ 0 & 0 & 0 & 0 & 0 & 0 & -\frac{1}{4} & 0 & 0 & \frac{1}{4} & 0 & 0 & 0 & 0 & 0 \\ 0 & 0 & 0 & 0 & 0 & 0 & 0 & 0 & 0 & 0 & 0 & 0 & 0 & 0 & 0 \\ 0 & 0 & 0 & 0 & 0 & 0 & 0 & 0 & 0 & 0 & 0 & 0 & 0 & 0 & 0 \\ 0 & 0 & 0 & 0 & 0 & 0 & 0 & 0 & 0 & 0 & 0 & 0 & \frac{1}{4} & 0 & 0 \\ 0 & 0 & 0 & 0 & 0 & 0 & 0 & 0 & 0 & 0 & 0 & 0 & 0 & 0 & 0 \\ 0 & 0 & 0 & 0 & 0 & 0 & 0 & 0 & 0 & 0 & 0 & 0 & 0 & 0 & 0 \\ 0 & 0 & 0 & 0 & 0 & 0 & 0 & 0 & 0 & 0 & 0 & 0 & 0 & 0 & 0 \end{pmatrix} \quad (4.28)$$

in the basis

$$\begin{aligned} \{|n_{A\uparrow}n_{A\downarrow}n_{B\uparrow}n_{B\downarrow}\rangle\} &= \{|0000\rangle, |0001\rangle, |0010\rangle, |0011\rangle, \\ &|0100\rangle, |0101\rangle, |0110\rangle, |0111\rangle, \\ &|1000\rangle, |1001\rangle, |1010\rangle, |1011\rangle, \\ &|1100\rangle, |1101\rangle, |1110\rangle, |1111\rangle\}. \end{aligned} \quad (4.29)$$

This state has  $\text{tr}(\hat{\rho}^2) = \frac{3}{8}$  and is thus impure, and has an entanglement of formation of

$$E_F(\hat{\rho}_{\text{local-N-SSR}}) = 0.5 \text{ ebits} \quad (4.30)$$

which is consistent with the result obtained by a more laborious analysis in the previous section.

### SSR for local particle number conservation modulo 2

Performing the same exercise but with an SSR for local particle number conservation modulo 2 (ie. that allows two particles to be created or destroyed at either site), gives the density matrix

$$\hat{\rho}_{\text{local-N-mod-2-SSR}} = \begin{pmatrix} 0 & 0 & 0 & 0 & 0 & 0 & 0 & 0 & 0 & 0 & 0 & 0 & 0 & 0 & 0 \\ 0 & 0 & 0 & 0 & 0 & 0 & 0 & 0 & 0 & 0 & 0 & 0 & 0 & 0 & 0 \\ 0 & 0 & 0 & 0 & 0 & 0 & 0 & 0 & 0 & 0 & 0 & 0 & 0 & 0 & 0 \\ 0 & 0 & 0 & \frac{1}{4} & 0 & 0 & 0 & 0 & 0 & 0 & 0 & \frac{1}{4} & 0 & 0 & 0 \\ 0 & 0 & 0 & 0 & 0 & 0 & 0 & 0 & 0 & 0 & 0 & 0 & 0 & 0 & 0 \\ 0 & 0 & 0 & 0 & 0 & 0 & 0 & 0 & 0 & 0 & 0 & 0 & 0 & 0 & 0 \\ 0 & 0 & 0 & 0 & 0 & 0 & \frac{1}{4} & 0 & 0 & -\frac{1}{4} & 0 & 0 & 0 & 0 & 0 \\ 0 & 0 & 0 & 0 & 0 & 0 & 0 & 0 & 0 & 0 & 0 & 0 & 0 & 0 & 0 \\ 0 & 0 & 0 & 0 & 0 & 0 & 0 & 0 & 0 & 0 & 0 & 0 & 0 & 0 & 0 \\ 0 & 0 & 0 & 0 & 0 & 0 & -\frac{1}{4} & 0 & 0 & \frac{1}{4} & 0 & 0 & 0 & 0 & 0 \\ 0 & 0 & 0 & 0 & 0 & 0 & 0 & 0 & 0 & 0 & 0 & 0 & 0 & 0 & 0 \\ 0 & 0 & 0 & 0 & 0 & 0 & 0 & 0 & 0 & 0 & 0 & 0 & 0 & 0 & 0 \\ 0 & 0 & 0 & \frac{1}{4} & 0 & 0 & 0 & 0 & 0 & 0 & 0 & \frac{1}{4} & 0 & 0 & 0 \\ 0 & 0 & 0 & 0 & 0 & 0 & 0 & 0 & 0 & 0 & 0 & 0 & 0 & 0 & 0 \\ 0 & 0 & 0 & 0 & 0 & 0 & 0 & 0 & 0 & 0 & 0 & 0 & 0 & 0 & 0 \\ 0 & 0 & 0 & 0 & 0 & 0 & 0 & 0 & 0 & 0 & 0 & 0 & 0 & 0 & 0 \end{pmatrix} \quad (4.31)$$

in the same basis as for the previous SSR. This state has  $\text{tr}(\hat{\rho}^2) = \frac{1}{2}$  and is thus impure, and has an entanglement of formation of

$$E_F(\hat{\rho}_{\text{local-N-mod-2-SSR}}) = 1 \text{ ebits.} \quad (4.32)$$

### Applicability to fermionic and bosonic systems

When does an SSR for local particle number conservation apply? As was seen in section 2.9.2, coherent sources of particles are only available for bosons. For fermions, due to the non-availability of coherent sources, any attempt to change the occupancy of a site in the doubly-occupied molecular bonding orbital inevitably decoheres the system.

An attempt to use the fermionic version of this system for teleportation, therefore, will be restricted to using operations that preserve local particle number. On the other hand, with the bosonic system, the availability of coherent sources means that all possible LOCC can be used.

One would thus expect the above value of the entanglement of the doubly occupied molecular bonding orbital under an SSR for local particle number conservation (0.5 ebits) to describe the usable entanglement of the fermionic system, whereas the full value of 2 ebits describes the usable entanglement of the bosonic system.

## Chapter 5

# Numerically estimating the entanglement of formation

### 5.1 Introduction

The entanglement of formation  $E_F$  characterizes the amount of entanglement present in a mixed state  $\hat{\rho}$ . The definition of  $E_F$  is known: it is the average entanglement of the pure states  $\{|\psi_i\rangle\}$  in the decomposition of  $\hat{\rho}$  minimized over all possible decompositions  $\{p_i, |\psi_i\rangle\}$  of  $\hat{\rho}$ . However, except for the special case of two qubits [11], no formula for  $E_F$  has been found, nor a prescription for obtaining the decomposition which realizes the minimum.

This chapter describes the development of a gradient for the average entanglement  $E_{av}$ , and a conjugate gradient algorithm that uses it to calculate  $E_F$  numerically. The algorithm successfully minimizes the average entanglement of random two qutrit ( $3 \times 3$ ) mixed states within a few hours on an ordinary desktop computer. The algorithm has been tested against the known result for general states of two qubits, and against exact results for  $E_F$  for the special class of ‘isotropic’ mixed states of two qutrits. Although the examples discussed in this paper involve a division of the Hilbert space into subspaces of equal dimension, the algorithm works equally well for any division of the Hilbert space. For example, it could be used to study the entanglement between a qutrit and quqit (d=4 system) whose joint state is mixed.

After publishing a preprint on this work, it was brought to our attention

that the algorithm had already been developed, and a paper published on it, by Audenaert *et al.* in 2001 [61].

The code developed by Audenaert *et al.* to implement their algorithm is heavily used in chapter 6, in order to study the entanglement in various degenerate quantum gas systems such as the BCS superconductor. These states are rarely pure and therefore the conjugate gradient algorithm is invaluable for studying the entanglement they contain.

## 5.2 Introduction to the conjugate gradient algorithm.

We seek to minimize a cost function  $f(\mathbf{p})$  in a situation where we can easily compute  $\nabla f(\mathbf{p})$ .

### 5.2.1 What's wrong with steepest descent

This is the simplest method, and at first glance would appear to guarantee success. As we shall see, that is not so. Starting from  $\mathbf{p}_0$ , as many times as we need to, move from  $\mathbf{p}_i$  to  $\mathbf{p}_{i+1}$  by minimizing along the line from  $\mathbf{p}_i$  in the direction of the local downhill gradient  $-\nabla f(\mathbf{p}_i)$ .

The definition of a line minimization is that, starting at point  $P$ , one seeks the scalar  $\mu$  that minimizes

$$f(\mathbf{P} + \mu\mathbf{n}) \tag{5.1}$$

along the straight line  $\mathbf{n}$ .

The problem with the steepest descent method is that the new gradient  $\mathbf{g}_{i+1}$  at  $\mathbf{p}_{i+1}$  is perpendicular to the direction  $\mathbf{h}_i$  that one has just travelled along, ie.

$$\mathbf{h}_i \cdot \mathbf{g}_{i+1} = 0 \tag{5.2}$$

where

$$\begin{aligned} \mathbf{h}_i &:= \mathbf{g}_i = -\nabla f(\mathbf{p}_i) \\ \mathbf{g}_{i+1} &:= -\nabla f(\mathbf{p}_{i+1}) \end{aligned} \tag{5.3}$$

and so the algorithm must make a right-angle turn after each line minimization. In general, this does not lead directly to the minimum. Instead, the method tends to make many small steps going down a long narrow valley.

## 5.2.2 Conjugate gradient minimization

This method uses ‘non-interfering’ or ‘conjugate’ directions to avoid the problems with steepest descent. If  $\mathbf{P}$  is the origin of the coordinate system with coordinates  $\mathbf{x}$  then

$$\begin{aligned} f(\mathbf{x}) &= f(\mathbf{P}) + \sum_i \frac{\partial f}{\partial x_i} x_i + \frac{1}{2} \sum_{ij} \frac{\partial^2 f}{\partial x_i \partial x_j} x_i x_j + \dots \\ &\approx c - \mathbf{b} \cdot \mathbf{x} + \frac{1}{2} \mathbf{x} \cdot \mathbf{A} \cdot \mathbf{x} \end{aligned} \quad (5.4)$$

where

$$c \equiv f(\mathbf{P}), \quad \mathbf{b} \equiv -\nabla f \Big|_{\mathbf{P}}, \quad [A]_{ij} \equiv \frac{\partial^2 f}{\partial x_i \partial x_j} \Big|_{\mathbf{P}} \quad (5.5)$$

$\mathbf{A}$  is known as the ‘Hessian matrix’ of  $f(\mathbf{P})$ , ie.

$$\nabla f = \mathbf{A} \cdot \mathbf{x} - \mathbf{b} \quad (5.6)$$

and thus one can obtain  $\nabla f = 0$  by solving  $\mathbf{A} \cdot \mathbf{x} = \mathbf{b}$ . So as we move along some direction, we have

$$\delta(\nabla f) = \mathbf{A} \cdot (\delta \mathbf{x}) \quad (5.7)$$

If one moves along  $\mathbf{u}$  to some minimum, and then one decides to move along another direction  $\mathbf{v}$ , in order that one doesn’t ‘spoil’ the minimization along  $\mathbf{u}$  it is necessary to choose  $\mathbf{v}$  such that the gradient stays perpendicular to  $\mathbf{u}$ , ie. such that the change in gradient is perpendicular to  $\mathbf{u}$ : ie.

$$0 = \mathbf{u} \cdot \delta(\nabla f) = \mathbf{u} \cdot \mathbf{A} \cdot \mathbf{v} \quad (5.8)$$

This equation defines what it means for directions  $\mathbf{u}$  and  $\mathbf{v}$  to be ‘conjugate’. A **conjugate set** of directions  $\{\mathbf{u}\}$  are a set for which this equation holds for any two members.

### Fletcher-Reeves conjugate gradient algorithm

The Fletcher-Reeves algorithm is an efficient conjugate gradient algorithm. It removes the need to know the Hessian matrix  $\mathbf{A}$ . Each choice of conjugate direction is made solely on the basis of:

- the previous direction  $\mathbf{h}_i$  along which line minimization was performed,

- the gradient  $\mathbf{g}_i = -\nabla f(\mathbf{p}_i)$  at the start of that previous line minimization, and
- the gradient  $\mathbf{g}_{i+1} = \nabla f(\mathbf{p}_{i+1})$  at the beginning of the new line minimization.

Starting at  $\mathbf{p}_0$  one chooses the initial  $\mathbf{g}$ -vector and initial direction as

$$\mathbf{g}_0 = -\nabla f(\mathbf{p}_0) \quad (5.9)$$

$$\mathbf{h}_0 = \mathbf{g}_0 \quad (5.10)$$

and proceeds along the initial direction to the local minimum at  $\mathbf{p}_1$ , where one sets the new  $\mathbf{g}$ -vector to the negated gradient at that point:

$$\mathbf{g}_1 = -\nabla f(\mathbf{p}_1). \quad (5.11)$$

However, the new direction is a linear combination of the current gradient and the previous direction, rather than just the current gradient as in the steepest descent method:

$$\mathbf{h}_1 = \mathbf{g}_1 + \gamma_0 \mathbf{h}_0 \quad (5.12)$$

where

$$\gamma_i = \frac{\mathbf{g}_{i+1} \cdot \mathbf{g}_{i+1}}{\mathbf{g}_i \cdot \mathbf{g}_i}. \quad (5.13)$$

It can be shown that the  $\mathbf{g}$ -vectors and direction vectors thus chosen are both orthogonal and conjugate to each other:

$$\mathbf{g}_i \cdot \mathbf{g}_j = 0 \text{ (orthogonality of successive gradient vectors)}$$

$$\mathbf{g}_i \cdot \mathbf{h}_j = 0 \text{ (orthogonality of current gradient to previous direction)}$$

$$\mathbf{h}_i \cdot \mathbf{A} \cdot \mathbf{h}_j = 0 \text{ (conjugacy of successive directions)} \quad (5.14)$$

for all  $j < i$ .

### Fletcher-Reeves in full

The Fletcher-Reeves algorithm makes use of a clever shortcut. Strictly speaking the  $\mathbf{g}$ -vectors, although suggestively represented by  $\mathbf{g}$ , are not simply the negated



gradient at the start of each line minimization. Instead, one should use this expression for the next choice of  $\mathbf{g}$ -vector:

$$\mathbf{g}_{i+1} = \mathbf{g}_i - \lambda_i \mathbf{A} \cdot \mathbf{h}_i \quad (5.15)$$

with

$$\lambda_i = \frac{\mathbf{g}_i \cdot \mathbf{g}_i}{\mathbf{h}_i \cdot \mathbf{A} \cdot \mathbf{h}_i} = \frac{\mathbf{g}_i \cdot \mathbf{h}_i}{\mathbf{h}_i \cdot \mathbf{A} \cdot \mathbf{h}_i}. \quad (5.16)$$

But this requires the user of the algorithm to know the Hessian matrix  $\mathbf{A}$ . However one can get away with simply setting the  $\mathbf{g}$ -vector to the negated gradient, ie. using

$$\mathbf{g}_{i+1} = -\nabla f(\mathbf{p}_{i+1}). \quad (5.17)$$

This is because:

$$\begin{aligned} \nabla f(\mathbf{x}) &= \mathbf{A} \cdot \mathbf{x} - \mathbf{b} \\ \therefore \mathbf{g}_i &= \nabla f(\mathbf{p}_i) = \mathbf{A} \cdot \mathbf{p}_i + \mathbf{b} \end{aligned} \quad (5.18)$$

and hence if we choose  $\mu$  such that it takes us to the minimum along  $\mathbf{h}_i$ ,

$$\begin{aligned} \mathbf{g}_{i+1} &= -\nabla f(\mathbf{p}_{i+1}) \\ &= -\mathbf{A} \cdot \mathbf{p}_{i+1} + \mathbf{b} \\ &= -\mathbf{A} \cdot (\mathbf{p}_i + \mu \mathbf{h}_i) + \mathbf{b} \\ &= \mathbf{g}_i - \mu \mathbf{A} \cdot \mathbf{h}_i \end{aligned} \quad (5.19)$$

But at the minimum along some direction  $\mathbf{h}_i$ , the gradient is always perpendicular to that direction, ie.

$$\mathbf{h}_i \cdot \nabla f = -\mathbf{h}_i \cdot \mathbf{g}_{i+1} = 0. \quad (5.20)$$

Solve equations (5.19) and (5.20) for  $\mu$ :

$$\begin{aligned} -\mathbf{h}_i \cdot \mathbf{g}_{i+1} &= -\mathbf{h}_i \cdot (\mathbf{g}_i - \mu \mathbf{A} \cdot \mathbf{h}_i) \\ &= -\mathbf{h}_i \cdot \mathbf{g}_i + \mu \mathbf{h}_i \cdot \mathbf{A} \cdot \mathbf{h}_i = 0 \\ \therefore \mu &= \frac{\mathbf{g}_i \cdot \mathbf{h}_i}{\mathbf{h}_i \cdot \mathbf{A} \cdot \mathbf{h}_i} = \lambda_i \end{aligned} \quad (5.21)$$

where  $\lambda_i$  is as given in equation (5.16). So equation (5.19) becomes

$$\begin{aligned} \mathbf{g}_{i+1} &= \mathbf{g}_i - \lambda_i \mathbf{A} \cdot \mathbf{h}_i \\ &\equiv \text{equation (5.15)}. \end{aligned} \quad (5.22)$$

I.e. simply using the negated vector gradient as the  $\mathbf{g}$ -vector at the start of each new line minimization gives the same gradient as if one uses the full expression in equation (5.15), without the need to know or store the Hessian matrix  $\mathbf{A}$ .

### 5.3 A gradient for the average entanglement.

As was explained in section 1.2.9, one can make unitary transformations between different decompositions of the same density matrix: we have *unitary freedom* in the choice of decomposition for a given mixed state. Recall that the average entanglement of a decomposition, in ebits, was defined in equation (1.76) as

$$\begin{aligned} E_{av}(\{|\tilde{\psi}_i\rangle\}) &= \sum_i p_i E_i \\ &= -\sum_i p_i \text{Tr}_A[\hat{\rho}_i^A \log_2 \hat{\rho}_i^A] \end{aligned} \quad (5.23)$$

where  $E_i$  is the entanglement of  $|\psi_i\rangle$ , and that the entanglement of formation of  $\hat{\rho}$  is defined as the minimum of  $E_{av}$  over all possible decompositions of  $\hat{\rho}$ .

For convenience, this derivation works with natural logs. First, write

$$U = \exp(i\epsilon\theta) \quad (5.24)$$

where  $U$  is the unitary transformation between decompositions, as defined in equation (1.78),  $\epsilon$  is a real parameter, and  $\theta$  is a Hermitian matrix. All derivatives are evaluated at  $\epsilon = 0$ . The gradient of  $\hat{\rho}_i^A$  is easily obtained:

$$\frac{d\hat{\rho}_i^A}{d\epsilon} = \frac{1}{p_i} \frac{d}{d\epsilon} \left( \text{Tr}_B(|\tilde{\psi}_i\rangle\langle\tilde{\psi}_i|) \right) - \frac{1}{p_i^2} \frac{dp_i}{d\epsilon} \text{Tr}_B(|\tilde{\psi}_i\rangle\langle\tilde{\psi}_i|) \quad (5.25)$$

The gradient of  $\text{Tr}_A[\hat{\rho}_i^A \ln \hat{\rho}_i^A]$  requires a little more work. If  $\alpha$  labels an eigenvalue  $\lambda_{\alpha i}^A$  of  $\hat{\rho}_i^A$ , and  $|\alpha_i\rangle$  is the corresponding eigenket,

$$\begin{aligned} \frac{d}{d\epsilon} \text{Tr}_A[\hat{\rho}_i^A \ln \hat{\rho}_i^A] &= \frac{d}{d\epsilon} \sum_{\alpha} \lambda_{\alpha i}^A \ln \lambda_{\alpha i}^A \\ &= \text{Tr}_A \left( \ln \hat{\rho}_i^A \frac{d\hat{\rho}_i^A}{d\epsilon} \right) \end{aligned} \quad (5.26)$$

where we have made use of the invariance of  $\text{Tr}(\hat{\rho}_i^A)$  and the Hellman-Feynman theorem [62, 63, 64]. Now we can calculate the promised expression for the

gradient:

$$\begin{aligned}
\frac{dE_{av}}{d\epsilon} &= -\log_2 e \sum_i \left( \frac{dp_i}{d\epsilon} \text{Tr}[\hat{\rho}_i^A \ln \hat{\rho}_i^A] + p_i \text{Tr}[\ln \hat{\rho}_i^A \frac{d\hat{\rho}_i^A}{d\epsilon}] \right) \\
&= -\log_2 e \sum_i \text{Tr}_A \left[ \ln \hat{\rho}_i^A \frac{d}{d\epsilon} \text{Tr}_B |\tilde{\psi}_i\rangle\langle\tilde{\psi}_i| \right]
\end{aligned} \tag{5.27}$$

The result can be further simplified by calculating the gradient of  $p_i \hat{\rho}_i^A = \text{Tr}_B(|\tilde{\psi}_i\rangle\langle\tilde{\psi}_i|)$  and making use of equation (1.78):

$$\begin{aligned}
U &= e^{i\epsilon\theta} \therefore \frac{d}{d\epsilon} U_{ij} \Big|_{\epsilon=0} = i\theta_{ij} \\
\therefore \frac{d}{d\epsilon} (p_i \hat{\rho}_i) \Big|_{\epsilon=0} &= \frac{d}{d\epsilon} \left( \sum_j U_{ij} |\tilde{\psi}_j\rangle \right) \langle\tilde{\psi}_i| + \\
&\quad |\tilde{\psi}_i\rangle \frac{d}{d\epsilon} \left( \sum_j \langle\tilde{\psi}_j| (U^\dagger)_{ji} \right) \\
&= i \sum_j (\theta_{ij} |\tilde{\psi}_j\rangle \langle\tilde{\psi}_i| - \theta_{ji} |\tilde{\psi}_i\rangle \langle\tilde{\psi}_j|)
\end{aligned} \tag{5.28}$$

$$\begin{aligned}
\therefore \frac{dE_{av}}{d\epsilon} &= -\sum_i \text{Tr}_A \left[ \log_2 \hat{\rho}_i^A \left\{ i \sum_j (\theta_{ij} \text{Tr}_B |\tilde{\psi}_j\rangle \langle\tilde{\psi}_i| \right. \right. \\
&\quad \left. \left. - \theta_{ji} \text{Tr}_B |\tilde{\psi}_i\rangle \langle\tilde{\psi}_j|) \right\} \right] \\
&= -i \sum_{i,j} \theta_{ij} \text{Tr}_A \left[ \left( \log_2 \hat{\rho}_i^A - \log_2 \hat{\rho}_j^A \right) \text{Tr}_B |\tilde{\psi}_j\rangle \langle\tilde{\psi}_i| \right] \\
&= \sum_{i,j} \theta_{ij} g_{ji}
\end{aligned} \tag{5.29}$$

where  $\mathbf{g}$  is the matrix of gradient elements with respect to the space of generators  $\{\theta\}$ . Note that:

- $g_{ii} = 0$  so simple changes of phase

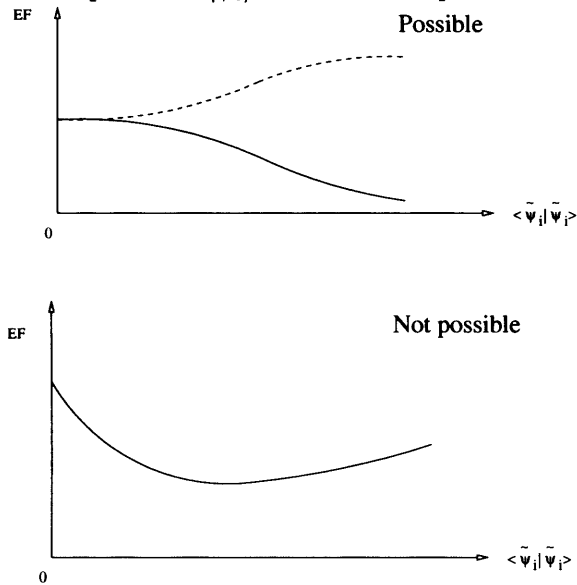
$$|\tilde{\psi}_i\rangle \rightarrow e^{i\theta} |\tilde{\psi}_i\rangle \tag{5.30}$$

in the states in the decomposition have no effect.

- $\mathbf{g}$  is Hermitian.

As shown in Figure 5.1, another consequence of equation (5.29) is that if a new state  $|\tilde{\psi}_i\rangle$  is introduced to the decomposition with initially zero amplitude,

Figure 5.1: Introducing a new state  $|\tilde{\psi}_i\rangle$  to the decomposition doesn't make any difference when its amplitude is small, as the gradient of  $E_{av}$  with respect to the amplitude of  $|\tilde{\psi}_i\rangle$  is zero at that point.



and its amplitude is gradually increased, then at first the new state makes no difference to the average entanglement. This is because if the amplitude of the new state is zero, and therefore the subnormalized state is zero, the trace over system  $B$  in equation (5.29) is also zero.

## 5.4 Existence of local and global minima

In general, a conjugate gradient procedure will converge to a local, rather than a global, minimum. However, Prager [65], has shown that any local minimum of  $E_F$  is also a global minimum. We have encountered points (presumably local maxima or inflexion points) other than the optimal decomposition at which the gradient is zero: when this occurs we find we can restart the conjugate gradient algorithm after a small number of random moves.

## 5.5 Using the gradient to minimize the average entanglement.

The code described here uses the conjugate gradient algorithm to minimize  $E_{av}$  with respect to the space of all possible unitary transformations between some initial decomposition of  $\hat{\rho}$  (the choice of which is entirely arbitrary) and the current decomposition. The initial decomposition is chosen without prejudice to be the ‘eigenstate’ decomposition of  $\hat{\rho}$ , ie. consisting of pure states which are the eigenvectors of  $\hat{\rho}$  and probabilities which are the eigenvalues. We write  $\mathbf{U} = \exp(i\mathbf{H})$  and move through the space of Hermitian matrices  $\{\mathbf{H}\}$  by constructing conjugate gradient moves from the gradient information provided by  $\mathbf{g}$ . The initial unitary transformation is the identity  $\mathbf{I}$ , whose corresponding  $\mathbf{H}$  is the null matrix  $\mathbf{0}$ .

The standard formulation of the conjugate gradient algorithm [66] operates upon vectors. Therefore the point in  $\mathbf{H}$ -space used is the ‘flattened’ vector consisting of the unique elements of  $\mathbf{H}$ . The gradient matrix is flattened in the same way. Conjugate directions are chosen according to the Fletcher-Reeves-Polak-Ribiere algorithm [67]. The gradient information is also made use of by the modified version of Brent’s method [68] that performs the line minimizations. The end result of the algorithm is the unitary transformation which takes us from the ‘eigenstate’ decomposition to the optimal decomposition. An heuristic test for convergence is performed after the algorithm terminates by running a pseudo Monte Carlo algorithm against the final decomposition, using an exponentially wide range of step sizes in random directions through unitary transformation space: we fail to find further steps down to within the target precision. This does not prove that the optimal decomposition has been obtained, but is strongly suggestive of that conclusion. Note that the gradient for  $E_{av}$  is constructed with respect to small unitary transformations of the current decomposition, and therefore the unitarity of  $U$  is preserved to machine precision throughout the execution of the conjugate gradient algorithm.

## 5.6 Performance against two-qubit mixed states

For randomly generated mixed states of two qubits, the algorithm’s estimate of  $E_F$  converges with the Wootters  $E_F$  to 14 decimal places typically in less than

100 iterations. The Wootters  $E_F$  is defined in equation (1.79).

## 5.7 Performance against two-qudit isotropic mixed states

A *qudit* is a quantum system of dimension  $d$ . The  $|\Psi\rangle^+$  state of two qudits is defined as

$$|\Psi\rangle^+ := \frac{1}{\sqrt{d}} \sum_i |ii\rangle. \quad (5.31)$$

For example, a  $|\Psi\rangle^+$  state of two qutrits is

$$|\Psi\rangle^+ = \frac{1}{\sqrt{3}}(|00\rangle + |11\rangle + |22\rangle). \quad (5.32)$$

An isotropic mixed state is a convex mixture of the maximally entangled Bell state  $|\Psi\rangle^+$  and the maximally mixed state  $\rho_I = \mathbf{I}$ :

$$\hat{\rho} := \frac{1-F}{d^2-1}(\mathbf{I} - |\Psi\rangle^+\langle\Psi^+|) + F|\Psi\rangle^+\langle\Psi^+| \quad (5.33)$$

Unlike for more general mixed states, a formula for  $E_F$  exists for isotropic states of two qudits [69]. These states are thus well-suited as a check for the results of the algorithm. In the case of two-qubit isotropic states, a particular difficulty arises which is that  $E_{av}$  generally has a stationary point at the eigenvector decomposition. It is thus necessary to move the initial decomposition away from this stationary point with a few random Monte Carlo moves, after which the conjugate gradient algorithm successfully obtains the correct minimum. For two-qutrit isotropic states we observe perfect correspondence between the results of the algorithm and the value given by the formula.

## 5.8 Performance against two-qutrit random mixed states.

The convergence behaviour when minimizing a sample random general mixed state of two qutrits (ie.  $\dim(\mathcal{H}) = 9$ ) is shown in Figure 5.2. It can be seen that convergence is linear, with approximately 600 iterations required per significant figure. We have found a few examples of states with highly degenerate eigenvalue spectra (e.g. isotropic states) for which convergence may be slower than linear.

## 5.9 Modelling locally depolarized Bell states of two qutrits.

An example of a previously intractable yet conceptually simple problem is local depolarization of one qudit involved in an entangled state. Consider a  $|\Psi\rangle^+$  state of two systems of dimension  $d$  (qudits), as defined in equation (5.31). If one qudit - say qudit  $A$  - decoheres with a certain probability  $p$ , the entanglement of the overall state is reduced in a non-trivial manner. This corresponds to a physical situation in which one party (Bob) prepares two qudits in an entangled state, then passes one qudit to Alice via a noisy channel. How much entanglement do Alice and Bob now share?

In this exercise, three possible types of decoherence are considered: the bitflip channel, the depolarizing channel, and both channels in succession with the same probability. (As the operations commute in this case, the order of bitflip and depolarization operations in the last case is irrelevant.) The results for a  $|\Psi\rangle^+$  state of two qubits can be readily calculated using the Wootters formula. They are shown in Figure 5.3. For the depolarizing channel, the results are consistent with the well-known separability of mixed states in the neighbourhood of the maximally mixed state [70].

How does one perform the same exercise for a  $|\Psi\rangle^+$  state of two qutrits ( $d = 3$ )?

### 5.9.1 Bit flip for qutrits

When one is dealing with 3-state systems, it is not immediately obvious how one 'flips' a qutrit. One solution is to use this operator sum representation:

$$\begin{aligned} & \sqrt{1-p}\mathbf{I}, \\ & \sqrt{\frac{p}{2}}\mathbf{X}_{\text{up}}, \\ & \sqrt{\frac{p}{2}}\mathbf{X}_{\text{down}} \end{aligned} \quad (5.34)$$

where  $p$  represents the probability of a flip.

The operators  $\mathbf{X}_{\text{up}}$  and  $\mathbf{X}_{\text{down}}$  respectively raise and lower a basis state, and

are defined as follows:

$$\begin{aligned}\mathbf{X}_{\text{down}}|i\rangle &= |(i-1) \bmod d\rangle = \begin{pmatrix} 0 & 1 & 0 \\ 0 & 0 & 1 \\ 1 & 0 & 0 \end{pmatrix} \\ \mathbf{X}_{\text{up}}|i\rangle &= |(i+1) \bmod d\rangle = \begin{pmatrix} 0 & 0 & 1 \\ 1 & 0 & 0 \\ 0 & 1 & 0 \end{pmatrix}\end{aligned}\quad (5.35)$$

in the  $|0\rangle, |1\rangle, |2\rangle$  basis. These operators are unitary since eg. for  $\mathbf{X}_{\text{down}}$ :

$$\mathbf{X}_{\text{down}}\mathbf{X}_{\text{down}}^\dagger = \begin{pmatrix} 0 & 1 & 0 \\ 0 & 0 & 1 \\ 1 & 0 & 0 \end{pmatrix} \begin{pmatrix} 0 & 0 & 1 \\ 1 & 0 & 0 \\ 0 & 1 & 0 \end{pmatrix} = \begin{pmatrix} 1 & 0 & 0 \\ 0 & 1 & 0 \\ 0 & 0 & 1 \end{pmatrix}\quad (5.36)$$

### 5.9.2 Depolarizing channel for qutrits

[71] provides an operator-sum representation of the depolarizing channel for qudits, which we can therefore use for qutrits by setting  $d = 3$ :

$$\begin{aligned}\sqrt{1-p}\mathbf{I} \\ \sqrt{pq} - 1\mathbf{E}_{i,j}\end{aligned}\quad (5.37)$$

where

$$\begin{aligned}\mathbf{E}_{i,j} &= \mathbf{X}^i\mathbf{Z}^j, \quad i, j \in \mathbb{F}_d \\ \mathbf{X}|i\rangle &\equiv \mathbf{X}_{\text{down}} = |(i-1) \bmod d\rangle \\ \mathbf{Z}|j\rangle &= \omega^j|j\rangle\end{aligned}\quad (5.38)$$

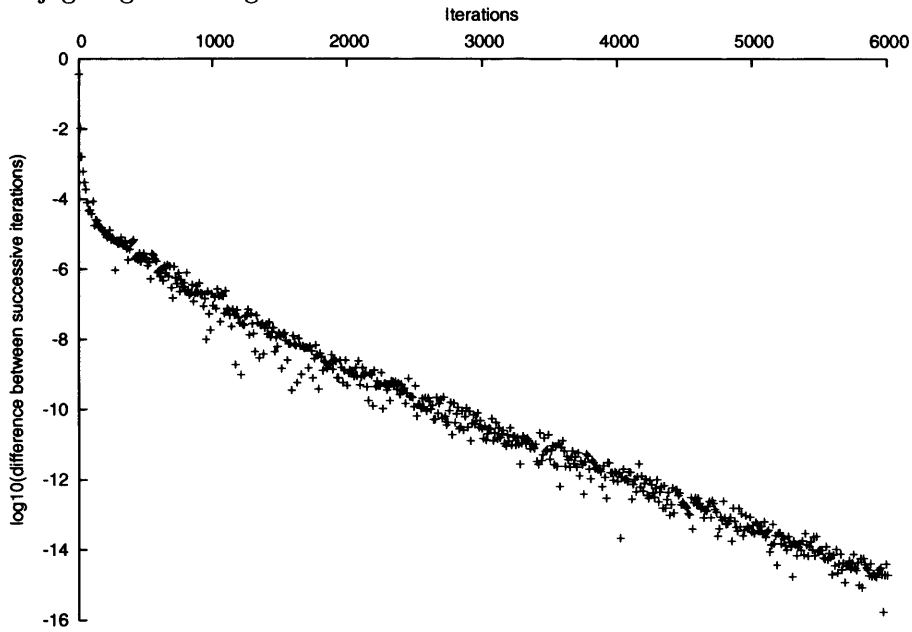
and  $\omega^j$  is a  $d$ 'th root of unity raised to the  $j$ :

$$\omega^j = e^{2\pi ij/d}, \quad j = 0, 1, 2, \dots, d-1\quad (5.39)$$

The results of applying these operations (tensored with the identity on qutrit  $B$ , which does not decohere) are shown in Figure 5.4. The results are plotted in ebits (1 ebit =  $\log_2(3)$  ebits) to facilitate comparison with the results for qubits. (Note that for the depolarization-only case, the results can also be obtained using the formula for  $E_F$  for isotropic states - we have found they are the same). They are similar to those for qubits, however it can be seen that



Figure 5.2: Convergence of  $\min(E_{av})$  for a random two-qutrit mixed state using conjugate gradient algorithm.



for all types of channel, the proportionate reduction in entanglement at a given probability is lower for qutrits. It thus appears that qutrit entanglement is more robust with respect to these types of decoherence than qubit entanglement. This conclusion has potential significance for the design of quantum computers and communication channels.

Figure 5.3: Entanglement of formation (ebits) of  $|\Psi\rangle^+$  of two qubits vs probability of qubit A depolarizing through various channels (calculated using Wootters formula).

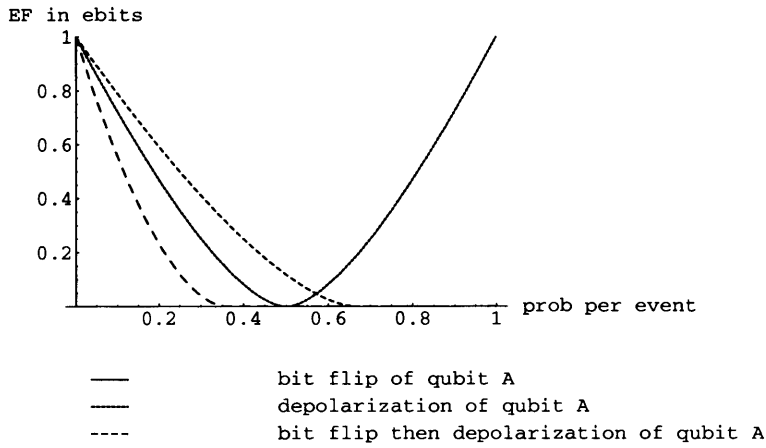
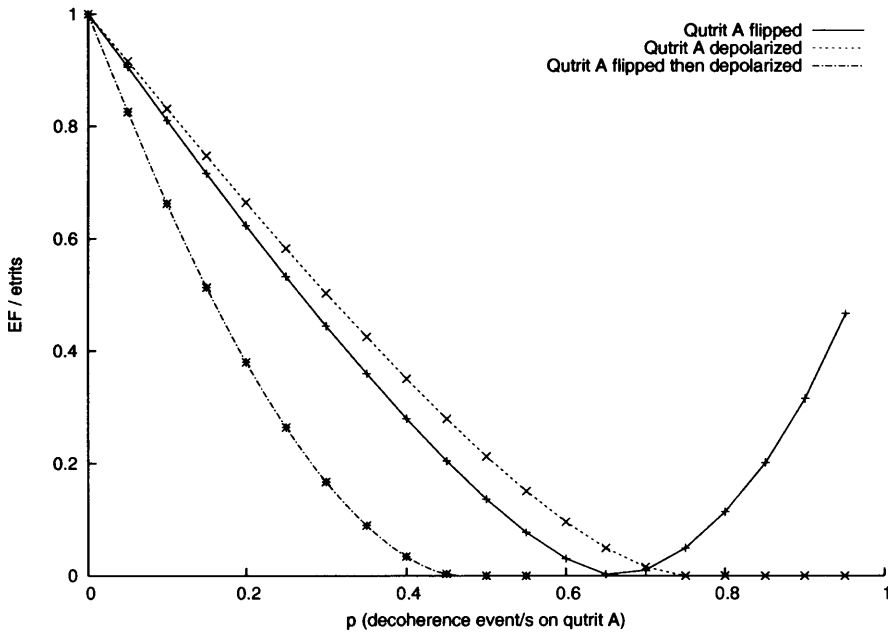


Figure 5.4: Entanglement of formation (etrbits) of  $|\Psi\rangle^+$  of two qutrits vs probability of qutrit A depolarizing through various channels (calculated using conjugate gradient algorithm).



## Chapter 6

# Entanglement in degenerate quantum gases

### 6.1 Introduction

This chapter is concerned with ‘natural’ entanglement in degenerate quantum gases. Natural entanglement is entanglement that is present in naturally occurring states of quantum systems. In other words, this is potentially useful entanglement which occurs in such systems without us having to perform any special preparation on those systems.

‘Degenerate quantum gas’ is a generic term to describe a Fermi sea, a Bose condensate, or a BCS superconductor. A quantum gas becomes ‘degenerate’ when the interatomic distance becomes less than the de Broglie wavelength of the atoms, ie.  $a \ll \lambda_T$ . At this point, the de Broglie waves associated with each atom overlap. Since the de Broglie wavelength increases as the atoms are cooled, cooling a quantum gas will make it degenerate.

Bose condensates and Fermi gases behave differently because of the different particle statistics of the particles involved. When a gas of bosonic atoms is cooled to just above absolute zero, all of the atoms condense into the same ground state. With a gas of fermionic atoms, this is not possible as the Pauli exclusion principle prevents more than one atom occupying a given quantum state. Instead, the atoms sequentially fill the lowest energy states available.

A BCS superconductor is an extension of the Fermi gas concept. In the Fermi

sea, fermions move as independent particles, with no correlations between the spin-up and spin-down particles. Correlations between fermions with the same spin direction do exist of course, because of the Pauli exclusion principle. In a BCS superconductor, a weak attraction between the electrons causes a pair of excited electrons with opposite spins, whose individual kinetic energies are near the Fermi surface, to form a bound pair whose combined energy is *lower* than  $2E_F$ . This is because their combined energy has been lowered by the attractive potential between them.

In 1956 Cooper showed that if an attractive interaction between electrons exists in a Fermi sea, however weak that interaction is, at least one bound pair of electrons will form [72]. What is the origin of the attractive interaction? What happens is that one electron polarizes the superconductor's lattice by attracting positive ions. The other electron is then attracted to this excess of positive ions, and hence an effective interaction between the electrons arises.

Since all three types of degenerate quantum gas involve indistinguishable particles, to calculate the entanglement between sites in any of them requires the use of the Zanardi (site entropy) entanglement measure, and thus requires them to be described using an occupation number representation. Very simple models will be used for all three types: non-interacting bosons and fermions for the bose condensate and fermi sea respectively, and the BCS ground state at  $T = 0$  for the superconductor. Note the entanglement in the Fermi sea is subject to an SSR for local particle number conservation, as discussed in Chapter 2.

## 6.2 Natural entanglement in spin systems

Before considering natural entanglement in degenerate quantum gases, it is useful to review what is already known about natural entanglement in condensed-phase systems. This has been most thoroughly studied for the case of spins, ie. the Ising model, the Heisenberg model, and the XY model.

### 6.2.1 The Ising model

#### 1D Ising model at $T = 0$

Gunlycke et al [73] study the entanglement in a one-dimensional Ising model in an external magnetic field, applied in an arbitrary direction. For a two-spin

system at zero temperature, they find that the entanglement is greatest for  $B$ -vectors which are almost (but not quite) parallel to the Ising direction, and zero for  $B$ -vectors which are perpendicular to the Ising direction.

Thus for the conventional choice  $\hat{z}$  of Ising direction, the 2-qubit entanglement is greatest when  $\mathbf{B}$  is almost parallel to  $\hat{z}$ , and zero when  $\mathbf{B}$  lies along  $\hat{x}$ . However, when  $\mathbf{B}$  is actually parallel to  $\hat{z}$ , the entanglement is zero. Thus there is an extremely thin line of zero entanglement at  $\mathbf{B}_x = 0$ .

### 1D Ising model at $T > 0$

At  $T > 0$ , the degeneracy which gives rise to the zero-entanglement line at  $\mathbf{B}_x = 0$  broadens, and there is a band of zero entanglement around  $\mathbf{B}_x = 0$ .

### 6.2.2 The Heisenberg model

Arnesen et al [74] consider the entanglement between two spins in a one-dimensional,  $N$ -spin, closed Heisenberg chain. The Hamiltonian for the 1D Heisenberg chain in an applied magnetic field  $\mathbf{B}$  is

$$\mathbf{H} = \sum_{i=1}^N (B\sigma_z^i + J\mathbf{s}_i\mathbf{s}_{i+1}) \quad (6.1)$$

where the spin vector for the  $i$ 'th spin is  $\mathbf{s}_i := (\sigma_{i,x}\sigma_{i,y}\sigma_{i,z})$ . The antiferromagnetic case is  $J > 0$ , the ferromagnetic one is  $J < 0$ . They find that there is never any entanglement in the ferromagnetic chain.

This makes sense because the state of the system at  $T = 0$  and  $B = 0$  is an equal mixture of the three triplet states, which is disentangled. This can be seen by rewriting the mixture in the form of an isotropic state:

$$\begin{aligned} \hat{\rho} &= \frac{1}{3} \left[ |00\rangle\langle 00| + \frac{1}{2}(|01\rangle + |10\rangle)(\langle 01| + \langle 10|) + |11\rangle\langle 11| \right] \\ &= \frac{1}{3} \left[ I - \frac{1}{2}(|01\rangle - |10\rangle)(\langle 01| - \langle 10|) \right] \end{aligned} \quad (6.2)$$

Increasing  $B$  increases the proportion of  $|00\rangle$  in the state - doing this cannot make the state entangled. And increasing  $T$  increases the proportion of singlet in the state, which can only decrease entanglement by mixing with the triplet.

The antiferromagnetic chain can contain entanglement, however. The maximum entanglement occurs for applied field  $\mathbf{B} = 0$  and temperature  $T = 0$ .

Generally, increasing  $\mathbf{B}$  or  $T$  decreases the entanglement. However, for values of  $\mathbf{B}$  close to the critical value of  $\mathbf{B}$ ,  $\mathbf{B}_c = 4J$ , it is possible to increase the entanglement by *increasing*  $T$ .

### 6.2.3 The hybrid XY and Ising model

Osterloh et al [75] consider a spin-half ferromagnetic chain with an exchange coupling  $J$  in a transverse magnetic field of strength  $h$ .

They use a special Hamiltonian which combines tunable amounts of the Hamiltonians of the XY and Ising models:

$$H = -\frac{J}{2}(1+\gamma)\sum_{i=1}^N\sigma_i^x\sigma_{i+1}^x - \frac{J}{2}(1-\gamma)\sum_{i=1}^N\sigma_i^y\sigma_{i+1}^y - h\sum_{i=1}^N\sigma_i^z \quad (6.3)$$

where the  $\{\sigma\}$  are the Pauli matrices and  $N$  is the number of sites. For  $\gamma = 1$  the model reduces to the Ising model:

$$H = -J\sum_{i=1}^N\sigma_i^x\sigma_{i+1}^x - h\sum_{i=1}^N\sigma_i^z. \quad (6.4)$$

For  $\gamma = 0$  it gives the XY model:

$$H = -\frac{J}{2}\sum_{i=1}^N\sigma_i^x\sigma_{i+1}^x - \frac{J}{2}\sum_{i=1}^N\sigma_i^y\sigma_{i+1}^y - h\sum_{i=1}^N\sigma_i^z \quad (6.5)$$

For their measure of entanglement, Osterloh et al use the two-site concurrence:

$$C(i, j) = \max\{r_1(i, j) - r_2(i, j) - r_3(i, j) - r_4(i, j), 0\} \quad (6.6)$$

where the  $r_\alpha(i, j)$  are the square roots of the eigenvalues of the product matrix  $R = \rho(i, j)\tilde{\rho}(i, j)$  in descending order, and  $\tilde{\rho}$  is the spin flipped matrix:

$$\tilde{\rho} := \sigma_y \otimes \sigma_y \rho^* \sigma_y \otimes \sigma_y \quad (6.7)$$

Concurrence is an entanglement measure which was described earlier, in sections 1.2.6 for pure states, and section 1.2.9 for mixed states.

Osterloh et al define a dimensionless coupling constant:

$$\lambda := \frac{J}{2h}. \quad (6.8)$$

For  $N = \infty$ , the system has a critical point at  $\lambda_c = 1$ .

They then consider the range of entanglement  $\xi_E$  in this model, defined as the maximum separation between spins for which the concurrence is non-zero.

### $\gamma = 1$ : the Ising model

For the Ising model, the concurrence turns out to be zero unless sites  $i$  and  $j$  are next-nearest neighbours, or closer. Surprisingly, this turns out to be true even at the critical point, where spin-spin correlations have infinite range, and decay only algebraically.

### $\gamma < 1$ : models which are intermediate between Ising and XY

The range of entanglement  $\xi_E$  turns out to be a function of  $\gamma$ . As  $\gamma \rightarrow 0$ , the maximum possible distance between entangled pairs increases, tending to infinity. In fact, Osterloh et al find that  $\xi_E$  goes as  $\gamma^{-1}$ . Consistent with this is their finding that the total concurrence stored in the chain is an increasing function of  $\gamma$ :

$$\text{For } 0 < \gamma \leq 1 \quad , \quad 0 < \sum_n C(n) < 0.2, \quad (6.9)$$

where  $C(1)$  is nearest-neighbour concurrence,  $C(2)$  is next-nearest-neighbour concurrence, and so on. Thus, although the range of entanglement increases as the model tends towards the XY model, (ie. as  $\gamma$  tends towards zero), the total entanglement in the system tends towards zero.

#### 6.2.4 A star network of interacting spins

Hutton and Bose [76] consider the entanglement present in a star network of spins, that is to say, one in which each spin only interacts with a central spin at its hub. If  $N$  is the number of outer spins, they find that for odd  $N$  the concurrence is

$$C = \frac{1}{N} \quad (6.10)$$

whilst for even  $N$  it is

$$C = \frac{1}{N} - \frac{1}{N(N-1)}. \quad (6.11)$$

There are thus oscillations in the entanglement as  $N$  is increased. This is due to mixedness (ie.  $1 - \text{tr}(\hat{\rho}^2)$ ) of the zero temperature density matrix for even  $N$ .

### 6.2.5 A spin chain

Bose [77] studies the transmission of a quantum state through an unmodulated spin chain. That is to say, the state is transmitted along the chain simply by being placed in proximity with one end of the chain. The ability to switch interactions between the spins on and off is not required, nor is the application of external fields required to modulate those interactions.

Bose finds that for direct transmission of a spin along the chain, short chains give excellent results. For example, a chain of length 8 gives fidelity  $F = 0.994$ . In fact, chains as long as 80 exceeds the highest possible fidelity for classical transmission of the state, in the time interval used in the study.

More recently, Stefanatos *et al.* [78] describe the relaxation optimized transfer of spin order in Ising spin chains, using NMR control techniques.

### 6.2.6 A chain of harmonic oscillators

Plenio and Semião [79] have performed similar work for a chain of coupled harmonic oscillators, which they dub a ‘quantum data bus’ because of its ability to transfer quantum information and entanglement from one location to another without having to use active spatial and temporal control.

Specifically, they consider a ring of  $M$  harmonically coupled identical oscillators, coupled with two additional harmonic oscillators  $a$  and  $b$  at arbitrary positions on the ring. System  $a$  is initially entangled with an external oscillator  $c$ , and the aim is to transfer that entanglement so that system  $c$  is entangled with system  $b$ .

They first consider this system for the case of Gaussian continuous variable states. They find that for a quantum data bus containing 20 oscillators, and a nearest-neighbour coupling strength of  $C = 1$ , then for a situation where  $a$  and  $c$  are initially in a pure entangled two-mode squeezed state, the efficiency of entanglement transfer between oscillators  $a$  and  $b$  oscillates as a function of time, with a minimum efficiency of zero, and a maximum efficiency of better than 0.99.

Plenio and Semião then consider the case where states are restricted to the basis of a single excitation, i.e.  $|0\rangle$  and  $|1\rangle$ . They show that, in that case, the system is equivalent to an xy-spin chain. They consider coupling three external oscillators to the chain,  $a$ ,  $b$ , and  $c$ . They show that in the limit of large  $M$ ,



an initial state which has an excitation in only oscillator  $a$  evolves to a  $W$  state of the three external oscillators, which is disentangled from the quantum data bus. This form of the data bus can thus be used to generate multi particle entanglement.

A more extensive study of entanglement in systems of coupled harmonic oscillators is by Plenio, Hartley, and Eisert [80]. They find that for harmonic oscillators coupled by springs (which corresponds to a phonon model) the transfer efficiency is related non-monotonically to the initial amount of entanglement - an intermediate amount of entanglement is transferred with the greatest efficiency. On the other hand, for the rotating wave approximation the relationship is monotonic. They also examine physical configurations of oscillators other than a ring.

### 6.3 Entanglement in a BCS superconductor

To model the formation of Cooper pairs above the Fermi surface, one uses a tight-binding approach. In the tight binding model, the wave functions of the propagating electrons are made up of linear combinations of localized wave functions each of which corresponds to a site on the lattice.

In the superconductor, the lowest energy state of the system should have zero total momentum, so the state of the system is a superposition of fermions in opposite momentum states:

$$\psi_0(\mathbf{r}_1, \mathbf{r}_2) = \sum_{\mathbf{k}} g_{\mathbf{k}} e^{i\mathbf{k} \cdot \mathbf{r}_1} e^{-i\mathbf{k} \cdot \mathbf{r}_2} \quad (6.12)$$

Since the interaction between electrons is attractive, one expects each pair to be in a singlet state, hence the overall state is

$$\psi_0(\mathbf{r}_1 - \mathbf{r}_2) = \left( \sum_{\mathbf{k} > \mathbf{k}_F} g_{\mathbf{k}} \cos(\mathbf{k} \cdot (\mathbf{r}_1 - \mathbf{r}_2)) \right) (\alpha_1 \beta_2 - \beta_1 \alpha_2). \quad (6.13)$$

#### 6.3.1 The BCS ground state

In evaluating the entanglement between two sites in a superconductor, this chapter models the superconductor using the BCS theory [81]. The following is based on Tinkham's treatment [82]. When discussing entanglement generally, 'site' means a region of space where Alice/Bob makes her/his measurements. In

the context of the BCS superconductor, ‘site’ means one atom in the lattice. In the BCS theory, the ground state takes the form

$$|\Psi_{\text{BCS}}\rangle = \prod_{\mathbf{k}} (u_{\mathbf{k}} + v_{\mathbf{k}} c_{\mathbf{k}\uparrow}^{\dagger} c_{-\mathbf{k}\downarrow}^{\dagger}) |0\rangle \quad (6.14)$$

where  $|v_{\mathbf{k}}|^2$  is the probability of the pair of momentum states  $(\mathbf{k} \uparrow, -\mathbf{k} \downarrow)$  being occupied, and  $|u_{\mathbf{k}}|^2$  is the probability of non-occupation. Hence

$$|u_{\mathbf{k}}|^2 + |v_{\mathbf{k}}|^2 = 1. \quad (6.15)$$

In a normal metal,

$$\begin{aligned} v &= 1 \text{ for } k < k_F \\ v &= 0 \text{ for } k > k_F \end{aligned} \quad (6.16)$$

and  $u$  shows the converse behaviour, of course. In a superconductor, there is broadening of  $u, v$  around  $k_F$ .

A key feature to note about this state is that it is not number-conserving, ie. the number of particles  $N$  is not fixed. It can vary between zero and  $2M$  (twice the number of sites). Instead, one has to work with the average number of particles,  $\bar{N}$ , which is fixed.

What are the coefficients  $u_{\mathbf{k}}$  and  $v_{\mathbf{k}}$ ? The strategy to determine this is as follows:

1. Use a ‘reduced’ Hamiltonian, which only contains interactions which scatter a pair of electrons from one momentum Cooper pair state to another.
2. Use the variational method to minimize this Hamiltonian.

### 6.3.2 The reduced Hamiltonian for the BCS ground state

$$\begin{aligned} \hat{H}_{\text{reduced}} &= \sum_{\mathbf{k}} \epsilon_{\mathbf{k}} (\hat{n}_{\mathbf{k}\uparrow} + \hat{n}_{\mathbf{k}\downarrow}) + \sum_{k,l} V_{\mathbf{k}l} c_{\mathbf{k}\uparrow}^{\dagger} c_{-\mathbf{k}\downarrow}^{\dagger} c_{-l\downarrow} c_{l\uparrow} \\ &= KE + PE \end{aligned} \quad (6.17)$$

This number-conserving, ‘reduced’ Hamiltonian excludes all interactions apart from those which will scatter a pair of electrons from one Cooper pair state  $(\mathbf{k} \uparrow, -\mathbf{k} \downarrow)$  to another. Thus,  $V_{\mathbf{k}l}$  is the scattering potential for scattering

a Cooper pair from the momentum state  $(\mathbf{l} \uparrow, -\mathbf{l} \downarrow)$  to the momentum state  $(\mathbf{k} \uparrow, -\mathbf{k} \downarrow)$ .

$V_{\mathbf{k}\mathbf{l}}$  is derived from the most general interaction that preserves total momentum and spin:

$$V_{\mathbf{k}\mathbf{l}m} c_{m+\mathbf{l}-\mathbf{k},\sigma'}^\dagger c_{\mathbf{k},\sigma}^\dagger c_{m,\sigma'} c_{\mathbf{l},\sigma} \quad (6.18)$$

which scatters a pair of electrons from

$$(\mathbf{l}\sigma, m\sigma') \text{ to } (\mathbf{k}\sigma, (m+\mathbf{l}-\mathbf{k})\sigma'). \quad (6.19)$$

As mentioned before, an undesirable feature of  $|\Psi_{\text{BCS}}\rangle$  is that it has no fixed particle number. So one fixes the expectation value of the particle number by using Lagrange's method of undetermined multipliers.

The chemical potential  $\mu$  is used as the undetermined multiplier, and  $\hat{N}$  is the operator whose expectation value gives the function one wishes to fix (ie. the number of particles). One takes  $\hat{H}_{\text{reduced}}$  as the cost function, and  $\mu\hat{N}$  as the constraint function. Thus, one subtracts  $\mu\hat{N}$  from the reduced Hamiltonian, and then seeks to solve

$$\langle \Psi_{\text{BCS}} | \hat{H}_{\text{reduced}} - \mu\hat{N} | \Psi_{\text{BCS}} \rangle = 0. \quad (6.20)$$

The effect of this is to set the kinetic energy 'zero' at the energy of the Fermi sea,  $E_F$ . The single-particle energy of an electron with momentum  $\mathbf{k}$  thus becomes

$$\xi_{\mathbf{k}} = \epsilon_{\mathbf{k}} - \mu \quad (6.21)$$

and equation (6.20) can be rewritten

$$\langle \Psi_{\text{BCS}} | \sum_{\mathbf{k}} \xi_{\mathbf{k}} (\hat{n}_{\mathbf{k}\uparrow} + \hat{n}_{\mathbf{k}\downarrow}) + \sum_{\mathbf{k},\mathbf{l}} V_{\mathbf{k}\mathbf{l}} c_{\mathbf{k}\uparrow}^\dagger c_{-\mathbf{k}\downarrow}^\dagger c_{-\mathbf{l}\downarrow} c_{\mathbf{l}\uparrow} | \Psi_{\text{BCS}} \rangle = 0 \quad (6.22)$$

ie. using  $\hat{H}_{\text{reduced}}$  but with the energy of an electron with momentum  $\mathbf{k}$  set to

$\xi_{\mathbf{k}}$  instead of  $\epsilon_{\mathbf{k}}$ . Now, the first term is

$$\begin{aligned}
\langle \Psi_{\text{BCS}} | \sum_{\mathbf{k}} \xi_{\mathbf{k}} (\hat{n}_{\mathbf{k}\uparrow} + \hat{n}_{\mathbf{k}\downarrow}) | \Psi_{\text{BCS}} \rangle &= 2 \langle \Psi_{\text{BCS}} | \sum_{\mathbf{k}} \xi_{\mathbf{k}} \hat{n}_{\mathbf{k}\uparrow} | \Psi_{\text{BCS}} \rangle \\
&\text{(because the electrons being considered here are all in Cooper pairs} \\
&\text{and therefore the number of up and down spin electrons with} \\
&\text{a particular momentum is the same).} \\
&= 2 \langle \Psi_{\text{BCS}} | \sum_{\mathbf{k}} \xi_{\mathbf{k}} c_{\mathbf{k}\uparrow}^\dagger c_{\mathbf{k}\uparrow} | \Psi_{\text{BCS}} \rangle \\
&= 2 \langle 0 | \prod_{\mathbf{l}} (u_{\mathbf{l}}^* + v_{\mathbf{l}}^* c_{-\mathbf{l}\downarrow} c_{\mathbf{l}\uparrow}) \sum_{\mathbf{k}} \xi_{\mathbf{k}} c_{\mathbf{k}\uparrow}^\dagger c_{\mathbf{k}\uparrow} \prod_{\mathbf{m}} (u_{\mathbf{m}} + v_{\mathbf{m}} c_{\mathbf{m}\uparrow}^\dagger c_{-\mathbf{m}\downarrow}^\dagger) | 0 \rangle \\
&= 2 \sum_{\mathbf{k}} \langle 0 | (u_{\mathbf{k}}^* + v_{\mathbf{k}}^* c_{-\mathbf{k}\downarrow} c_{\mathbf{k}\uparrow}) \xi_{\mathbf{k}} c_{\mathbf{k}\uparrow}^\dagger c_{\mathbf{k}\uparrow} (u_{\mathbf{k}} + v_{\mathbf{k}} c_{\mathbf{k}\uparrow}^\dagger c_{-\mathbf{k}\downarrow}^\dagger) \\
&\quad \times \prod_{\mathbf{l} \neq \mathbf{k}} (u_{\mathbf{l}}^* + v_{\mathbf{l}}^* c_{-\mathbf{l}\downarrow} c_{\mathbf{l}\uparrow}) (u_{\mathbf{l}} + v_{\mathbf{l}} c_{\mathbf{l}\uparrow}^\dagger c_{-\mathbf{l}\downarrow}^\dagger) | 0 \rangle.
\end{aligned} \tag{6.23}$$

Consider the expectation value of the  $\mathbf{l} \neq \mathbf{k}$  product (the second term in equation 6.23) in the vacuum state:

$$\begin{aligned}
&\langle 0 | \prod_{\mathbf{l} \neq \mathbf{k}} (u_{\mathbf{l}}^* + v_{\mathbf{l}}^* c_{-\mathbf{l}\downarrow} c_{\mathbf{l}\uparrow}) (u_{\mathbf{l}} + v_{\mathbf{l}} c_{\mathbf{l}\uparrow}^\dagger c_{-\mathbf{l}\downarrow}^\dagger) | 0 \rangle \\
&= \langle 0 | \prod_{\mathbf{l} \neq \mathbf{k}} (|u_{\mathbf{l}}|^2 + u_{\mathbf{l}}^* v_{\mathbf{l}} c_{\mathbf{l}\uparrow}^\dagger c_{-\mathbf{l}\downarrow}^\dagger + v_{\mathbf{l}}^* u_{\mathbf{l}} c_{-\mathbf{l}\downarrow} c_{\mathbf{l}\uparrow} + |v_{\mathbf{l}}|^2 c_{-\mathbf{l}\downarrow} c_{\mathbf{l}\uparrow} c_{\mathbf{l}\uparrow}^\dagger c_{-\mathbf{l}\downarrow}^\dagger) | 0 \rangle \\
&= |u_{\mathbf{l}}|^2 + 0 + 0 + |v_{\mathbf{l}}|^2 = 1.
\end{aligned} \tag{6.24}$$

And the expectation value of the first term in equation 6.23 in the vacuum state is

$$\begin{aligned}
&\langle 0 | \sum_{\mathbf{k}} (u_{\mathbf{k}}^* + v_{\mathbf{k}}^* c_{-\mathbf{k}\downarrow} c_{\mathbf{k}\uparrow}) \xi_{\mathbf{k}} c_{\mathbf{k}\uparrow}^\dagger c_{\mathbf{k}\uparrow} (u_{\mathbf{k}} + v_{\mathbf{k}} c_{\mathbf{k}\uparrow}^\dagger c_{-\mathbf{k}\downarrow}^\dagger) | 0 \rangle \\
&= \langle 0 | \sum_{\mathbf{k}} \xi_{\mathbf{k}} |u_{\mathbf{k}}|^2 c_{\mathbf{k}\uparrow}^\dagger c_{\mathbf{k}\uparrow} | 0 \rangle + \langle 0 | \sum_{\mathbf{k}} \xi_{\mathbf{k}} u_{\mathbf{k}}^* v_{\mathbf{k}} c_{\mathbf{k}\uparrow}^\dagger c_{\mathbf{k}\uparrow} c_{\mathbf{k}\uparrow}^\dagger c_{-\mathbf{k}\downarrow}^\dagger | 0 \rangle \\
&\quad + \langle 0 | \sum_{\mathbf{k}} \xi_{\mathbf{k}} v_{\mathbf{k}}^* u_{\mathbf{k}} c_{\mathbf{k}\uparrow}^\dagger c_{\mathbf{k}\uparrow} | 0 \rangle + \langle 0 | \sum_{\mathbf{k}} \xi_{\mathbf{k}} |v_{\mathbf{k}}|^2 c_{-\mathbf{k}\downarrow} c_{\mathbf{k}\uparrow} c_{\mathbf{k}\uparrow}^\dagger c_{\mathbf{k}\uparrow} c_{\mathbf{k}\uparrow}^\dagger c_{-\mathbf{k}\downarrow}^\dagger | 0 \rangle \\
&= \langle 0 | \sum_{\mathbf{k}} \xi_{\mathbf{k}} |u_{\mathbf{k}}|^2 \hat{n}_{\mathbf{k}\uparrow} | 0 \rangle + \langle 0 | \sum_{\mathbf{k}} \xi_{\mathbf{k}} u_{\mathbf{k}}^* v_{\mathbf{k}} c_{\mathbf{k}\uparrow}^\dagger (1 - \hat{n}_{\mathbf{k}\uparrow}) c_{-\mathbf{k}\downarrow}^\dagger | 0 \rangle \\
&\quad + \langle 0 | \sum_{\mathbf{k}} \xi_{\mathbf{k}} v_{\mathbf{k}}^* u_{\mathbf{k}} \hat{n}_{\mathbf{k}\uparrow} | 0 \rangle + \langle 0 | \sum_{\mathbf{k}} \xi_{\mathbf{k}} |v_{\mathbf{k}}|^2 c_{-\mathbf{k}\downarrow} (1 - \hat{n}_{\mathbf{k}\uparrow}) (1 - \hat{n}_{\mathbf{k}\uparrow}) c_{-\mathbf{k}\downarrow}^\dagger | 0 \rangle \\
&= 0 + 0 + 0 + \sum_{\mathbf{k}} \xi_{\mathbf{k}} |v_{\mathbf{k}}|^2.
\end{aligned} \tag{6.25}$$

So the expectation value of the kinetic energy term in  $\hat{H}_{\text{reduced}} - \mu\hat{N}$  is, from the first term in equation (6.22),

$$\begin{aligned}\langle KE - \mu\hat{N} \rangle &= \sum_{\mathbf{k}} \xi_{\mathbf{k}} (\hat{n}_{\mathbf{k}\uparrow} + \hat{n}_{\mathbf{k}\downarrow}) \\ &= 2 \sum_{\mathbf{k}} \xi_{\mathbf{k}} |v_{\mathbf{k}}|^2.\end{aligned}\quad (6.26)$$

The expectation value of the potential energy term can be shown to be

$$\langle PE \rangle = \sum_{\mathbf{k}\mathbf{l}} V_{\mathbf{k}\mathbf{l}} u_{\mathbf{k}} v_{\mathbf{k}}^* u_{\mathbf{l}}^* v_{\mathbf{l}}. \quad (6.27)$$

So, if one assumes  $u_{\mathbf{k}}$  and  $v_{\mathbf{k}}$  are real, the expectation value of  $\hat{H}_{\text{reduced}} - \mu\hat{N}$  is

$$\langle \Psi_{\text{BCS}} | \hat{H}_{\text{reduced}} - \mu\hat{N} | \Psi_{\text{BCS}} \rangle = 2 \sum_{\mathbf{k}} \xi_{\mathbf{k}} v_{\mathbf{k}}^2 + \sum_{\mathbf{k}\mathbf{l}} V_{\mathbf{k}\mathbf{l}} u_{\mathbf{k}} v_{\mathbf{k}} u_{\mathbf{l}} v_{\mathbf{l}} = 0. \quad (6.28)$$

If one sets

$$\begin{aligned}u_{\mathbf{k}} &= \sin \theta_{\mathbf{k}}, \\ v_{\mathbf{k}} &= \cos \theta_{\mathbf{k}}\end{aligned}\quad (6.29)$$

then the normalization condition for  $u_{\mathbf{k}}, v_{\mathbf{k}}$  in equation (6.15) is satisfied. One can thus write the first term in equation 6.28 as

$$\begin{aligned}2 \sum_{\mathbf{k}} \xi_{\mathbf{k}} v_{\mathbf{k}}^2 &= 2 \sum_{\mathbf{k}} \xi_{\mathbf{k}} \cos^2 \theta_{\mathbf{k}} \\ &= \sum_{\mathbf{k}} \xi_{\mathbf{k}} (1 + \cos 2\theta_{\mathbf{k}}).\end{aligned}\quad (6.30)$$

And one can write the second term as

$$\sum_{\mathbf{k}\mathbf{l}} V_{\mathbf{k}\mathbf{l}} u_{\mathbf{k}} v_{\mathbf{k}} u_{\mathbf{l}} v_{\mathbf{l}} = \frac{1}{4} \sum_{\mathbf{k}\mathbf{l}} V_{\mathbf{k}\mathbf{l}} \sin 2\theta_{\mathbf{k}} \sin 2\theta_{\mathbf{l}}. \quad (6.31)$$

So

$$\begin{aligned}\frac{\partial}{\partial \theta_{\mathbf{k}}} \langle \Psi_{\text{BCS}} | \hat{H}_{\text{reduced}} - \mu\hat{N} | \Psi_{\text{BCS}} \rangle &= 0 \\ \therefore 2\xi_{\mathbf{k}} \sin 2\theta_{\mathbf{k}} &= \sum_{\mathbf{l}} V_{\mathbf{k}\mathbf{l}} \cos 2\theta_{\mathbf{k}} \sin 2\theta_{\mathbf{l}}, \\ \tan 2\theta_{\mathbf{k}} &= \frac{\sum_{\mathbf{l}} V_{\mathbf{k}\mathbf{l}} \sin 2\theta_{\mathbf{l}}}{2\xi_{\mathbf{k}}}.\end{aligned}\quad (6.32)$$

### The quasi-particle excitation energy and the energy gap

Now *define* two new quantities. The first is the excitation energy for a Bogliubov quasi-particle whose momentum is  $\hbar\mathbf{k}$ :

$$E_{\mathbf{k}} := \sqrt{\Delta_{\mathbf{k}}^2 + \xi_{\mathbf{k}}^2}. \quad (6.33)$$

The second new quantity is the energy gap in the superconductor:

$$\Delta_{\mathbf{k}} := -\sum_{\mathbf{l}} V_{\mathbf{kl}} u_{\mathbf{l}} v_{\mathbf{l}} = -\frac{1}{2} \sum_{\mathbf{l}} V_{\mathbf{kl}} \sin 2\theta_{\mathbf{l}}. \quad (6.34)$$

This is the range in energy over which  $u$  and  $v$  are ‘smeared out’ around  $k_F$  in the superconductor. The reason that  $\Delta_{\mathbf{k}}$  is known as the *energy gap*, or *minimum excitation energy*, is apparent from the definition of  $E_{\mathbf{k}}$ . It is because even at the Fermi surface, where the energy of an electron relative to the surface is zero, the energy of a Bogliubov quasi-particle is non-zero:  $E_{\mathbf{k}} = |\Delta_{\mathbf{k}}| > 0$ . Although it’s not obvious from its definition,  $\Delta_{\mathbf{k}}$  is in fact a function of  $\mathbf{k}$ , as can be seen from equation 6.40 later in this section. However, in an S-wave superconductor, the dependence is only on the magnitude of  $\mathbf{k}$ , and not its direction.

Putting the definition of the gap into the expression for  $\tan 2\theta_{\mathbf{k}}$  one gets

$$\tan 2\theta_{\mathbf{k}} = -\frac{\Delta_{\mathbf{k}}}{\xi_{\mathbf{k}}} \quad (6.35)$$

and thus one gets

$$2u_{\mathbf{k}}v_{\mathbf{k}} = \sin 2\theta_{\mathbf{k}} = \frac{\Delta_{\mathbf{k}}}{E_{\mathbf{k}}}, \quad (6.36)$$

$$v_{\mathbf{k}}^2 - u_{\mathbf{k}}^2 = \cos 2\theta_{\mathbf{k}} = -\frac{\xi_{\mathbf{k}}}{E_{\mathbf{k}}}. \quad (6.37)$$

The choice of signs for the sine and cosine means that one obtains the desired behaviour that the occupation number  $v_{\mathbf{k}}^2 \rightarrow 0$  as  $\xi_{\mathbf{k}} \rightarrow \infty$ .

### The equation for the energy gap and its solutions

With these last expressions, it is possible to finally obtain the equation for the gap:

$$\begin{aligned} \Delta_{\mathbf{k}} &= -\frac{1}{2} \sum_{\mathbf{l}} V_{\mathbf{kl}} \sin 2\theta_{\mathbf{l}} \\ &= -\frac{1}{2} \sum_{\mathbf{l}} V_{\mathbf{kl}} \frac{\Delta_{\mathbf{l}}}{E_{\mathbf{l}}} \\ &= -\frac{1}{2} \sum_{\mathbf{l}} V_{\mathbf{kl}} \frac{\Delta_{\mathbf{l}}}{\sqrt{\Delta_{\mathbf{l}}^2 + \xi_{\mathbf{l}}^2}}. \end{aligned} \quad (6.38)$$

There are two solutions for  $\Delta_{\mathbf{k}}$ : one trivial, one not. The trivial solution describes the situation in a metal - the energy gap is zero at all energies:

$$\Delta_{\mathbf{k}} = 0 \quad \forall \xi_{\mathbf{k}}. \quad (6.39)$$

The non-trivial solution describes the situation in a superconductor - the energy gap is non-zero in a small energy range around the Fermi surface, and zero elsewhere:

$$\Delta_{\mathbf{k}} = \Delta \text{ for } |\xi_{\mathbf{k}}| < \omega_D, \quad (6.40)$$

$$\Delta_{\mathbf{k}} = 0 \text{ for } |\xi_{\mathbf{k}}| > \omega_D. \quad (6.41)$$

Note that this non-trivial solution makes explicit the fact that  $\Delta_{\mathbf{k}}$  is a function of  $\mathbf{k}$ , justifying its subscripted 'k'. However, in an S-wave superconductor, the dependence is only on the magnitude of  $\mathbf{k}$ , and not its direction. The non-trivial solution is obtained from equation (6.38) by using Cooper's approximation for  $V_{\mathbf{k}\mathbf{l}}$ :

$$\begin{aligned} V_{\mathbf{k}\mathbf{l}} &= -V \text{ for } \mathbf{k} \text{ states out to a cutoff energy } \hbar\omega_D \text{ away from } E_F, \\ &\text{ie. for } |\xi_{\mathbf{k}}| \text{ and } |\xi_{\mathbf{l}}| \leq \hbar\omega_D, \end{aligned} \quad (6.42)$$

$$V_{\mathbf{k}\mathbf{l}} = 0 \text{ beyond } \hbar\omega_D \quad (6.43)$$

where  $V$  is a positive constant. Now since  $V_{\mathbf{k}\mathbf{l}}$  is set to  $V_{\mathbf{k}\mathbf{l}} = V$  for the range of interest, one also has  $\Delta_{\mathbf{k}} = \Delta_{\mathbf{l}} = \Delta$  hence the equation for the gap (6.38) becomes

$$1 = \frac{1}{2} \sum_{\mathbf{k}} \frac{V}{E_{\mathbf{k}}}. \quad (6.44)$$

Since  $V$  is only non-zero within a range of  $\hbar\omega_D$  around the Fermi energy, the summation over  $\mathbf{k}$ -states can be replaced by an integration between  $-\hbar\omega_D$  and  $+\hbar\omega_D$ :

$$\begin{aligned} 1 &= N_0 \frac{1}{2} \int_{-\hbar\omega_D}^{\hbar\omega_D} \frac{V}{E(\xi)} d\xi \\ &= N_0 \frac{1}{2} \int_0^{\hbar\omega_D} \frac{V}{\sqrt{\Delta^2 + \xi^2}} d\xi \\ \therefore \frac{1}{N_0 V} &= \int_0^{\hbar\omega_D} \frac{1}{\sqrt{\Delta^2 + \xi^2}} d\xi. \end{aligned} \quad (6.45)$$

Now set  $\xi = \Delta \sinh u$ , and hence

$$\begin{aligned}
\xi^2 &= \Delta^2(\cosh^2 u - 1) \\
\Delta^2 + \xi^2 &= \Delta^2 \cosh^2 u \\
\text{and } d\xi &= \Delta \cosh(u) du \\
\therefore \frac{1}{N_0 V} &= \int_0^{\sinh^{-1}(\frac{\hbar\omega_D}{\Delta})} du = \sinh^{-1} \frac{\hbar\omega_D}{\Delta} \quad (6.46)
\end{aligned}$$

where  $N_0$  is the density of  $\mathbf{k}$ -states at the Fermi energy for electrons of a given spin. Hence the final solution for the gap is

$$\begin{aligned}
\sinh \frac{1}{N_0 V} &= \frac{\hbar\omega_D}{\Delta} \\
\therefore \Delta &= \frac{\hbar\omega_D}{\sinh \frac{1}{N_0 V}} \approx 2\omega_D \exp\left(-\frac{1}{N_0 V}\right). \quad (6.47)
\end{aligned}$$

### 6.3.3 Constructing a two-site density matrix for a BCS superconductor at $T=0$

To evaluate the entanglement between two sites in a BCS superconductor, it is necessary to build a density matrix in the basis of the occupation numbers of those two sites. One can then apply the Zanardi measure to this to obtain the entanglement.

#### Expressing the matrix elements as strings of second-quantized operators

The aim of this section is to construct a two-site density matrix for a superconductor in the BCS ground state at  $T=0$ , expressed in an occupation number basis. Ie. the elements of the matrix are

$$\begin{aligned}
\hat{\rho}_{nn'} &= \langle n_{i\uparrow} n_{i\downarrow} n_{j\uparrow} n_{j\downarrow} | \hat{\rho}_{\text{BCS}} | (n_{i\uparrow} n_{i\downarrow} n_{j\uparrow} n_{j\downarrow})' \rangle \\
&= \langle n_{i\uparrow} n_{i\downarrow} n_{j\uparrow} n_{j\downarrow} | \Psi_{\text{BCS}} \rangle \langle \Psi_{\text{BCS}} | (n_{i\uparrow} n_{i\downarrow} n_{j\uparrow} n_{j\downarrow})' \rangle \quad (6.48)
\end{aligned}$$

This is easily converted to an expectation value of the occupancies in the BCS ground state by switching the order of the brackets (which of course commute):

$$\hat{\rho}_{nn'} = \langle \Psi_{\text{BCS}} | (n_{i\uparrow} n_{i\downarrow} n_{j\uparrow} n_{j\downarrow})' \rangle \langle n_{i\uparrow} n_{i\downarrow} n_{j\uparrow} n_{j\downarrow} | \Psi_{\text{BCS}} \rangle \quad (6.49)$$



To make this concrete, consider the example of the specific occupancies

$$\begin{aligned} n_{i\uparrow}n_{i\downarrow}n_{j\uparrow}n_{j\downarrow} &= 1111, \\ (n_{i\uparrow}n_{i\downarrow}n_{j\uparrow}n_{j\downarrow})' &= 0000. \end{aligned} \quad (6.50)$$

Then

$$\begin{aligned} \hat{\rho}_{1111,0000} &= \langle \Psi_{\text{BCS}} | \text{all } 1 \rangle \langle \text{all } 0 | \Psi_{\text{BCS}} \rangle \\ &= \langle \Psi_{\text{BCS}} | c_{i\uparrow}^\dagger c_{i\downarrow}^\dagger c_{j\uparrow}^\dagger c_{j\downarrow}^\dagger | 0_{ij} \rangle \langle 0_{ij} | \Psi_{\text{BCS}} \rangle \end{aligned} \quad (6.51)$$

$|0_{ij}\rangle\langle 0_{ij}|$  is the projector onto the vacuum state on sites  $i, j$  only. How does one get rid of it from the above expression? First, note that it can be obtained by tracing out all other sites from the set of states

$$\begin{aligned} |0_{ij}\rangle\langle 0_{ij}| &= \text{tr}_{\{n_k\}} |n_{i\uparrow}n_{i\downarrow}n_{j\uparrow}n_{j\downarrow} = 0000, \{n_k\}\rangle \langle n_{i\uparrow}n_{i\downarrow}n_{j\uparrow}n_{j\downarrow} = 0000, \{n_k\}|, \\ &k \neq i, j. \end{aligned} \quad (6.52)$$

But one can reexpress the zero occupancies of sites  $i, j$  by applying the zero-occupancy projection operator for those sites to the state where they are not necessarily empty:

$$\begin{aligned} |0_{ij}\rangle\langle 0_{ij}| &= \text{tr}_{\{n_k\}} |\{n_k\}\rangle (1 - \hat{n}_{i\uparrow})(1 - \hat{n}_{i\downarrow})(1 - \hat{n}_{j\uparrow})(1 - \hat{n}_{j\downarrow}) \langle \{n_k\}|, \\ &k \in \text{all sites}. \end{aligned} \quad (6.53)$$

So one can write

$$\begin{aligned} \langle \Psi_{\text{BCS}} | 0_{ij} \rangle \langle 0_{ij} | \Psi_{\text{BCS}} \rangle &= \text{tr}_{\{n_k\}, k \neq i, j} \langle \Psi_{\text{BCS}} | n_{i\uparrow}n_{i\downarrow}n_{j\uparrow}n_{j\downarrow} = 0000, \{n_k\} \rangle \\ &\quad \langle n_{i\uparrow}n_{i\downarrow}n_{j\uparrow}n_{j\downarrow} = 0000, \{n_k\} | \Psi_{\text{BCS}} \rangle \\ &= \text{tr}_{\{n_k\}, k \in \text{all sites}} \\ &\quad \langle \Psi_{\text{BCS}} | (1 - \hat{n}_{i\uparrow})(1 - \hat{n}_{i\downarrow})(1 - \hat{n}_{j\uparrow})(1 - \hat{n}_{j\downarrow}) | \{n_k\} \rangle \\ &\quad \langle \{n_k\} | (1 - \hat{n}_{i\uparrow})(1 - \hat{n}_{i\downarrow})(1 - \hat{n}_{j\uparrow})(1 - \hat{n}_{j\downarrow}) | \Psi_{\text{BCS}} \rangle \end{aligned} \quad (6.54)$$

But

$$\text{tr}_{\{n_k\}, k \in \text{all sites}} |\{n_k\}\rangle \langle \{n_k\}| = 1. \quad (6.55)$$

Hence

$$\begin{aligned} \langle \Psi_{\text{BCS}} | 0_{ij} \rangle \langle 0_{ij} | \Psi_{\text{BCS}} \rangle &= \langle \Psi_{\text{BCS}} | (1 - \hat{n}_{i\uparrow})(1 - \hat{n}_{i\downarrow})(1 - \hat{n}_{j\uparrow})(1 - \hat{n}_{j\downarrow}) | \Psi_{\text{BCS}} \rangle \\ &\equiv \langle (1 - \hat{n}_{i\uparrow})(1 - \hat{n}_{i\downarrow})(1 - \hat{n}_{j\uparrow})(1 - \hat{n}_{j\downarrow}) \rangle \end{aligned} \quad (6.56)$$

Now, invoke the anticommutativity of fermion creation and annihilation operators:

$$\begin{aligned}\hat{n}_{i\sigma} &:= c_{i\sigma}^\dagger c_{i\sigma} \\ \text{and } \{c_{i\sigma}^\dagger, c_{i\sigma}\} &= 1 \\ \therefore (1 - \hat{n}_{i\sigma}) &= c_{i\sigma} c_{i\sigma}^\dagger\end{aligned}\quad (6.57)$$

Hence

$$\begin{aligned}\langle \Psi_{\text{BCS}} | 0_{ij} \rangle \langle 0_{ij} | \Psi_{\text{BCS}} \rangle &= \langle \Psi_{\text{BCS}} | c_{i\uparrow}^\dagger c_{i\downarrow}^\dagger c_{i\downarrow} c_{i\uparrow} c_{j\uparrow}^\dagger c_{j\downarrow}^\dagger c_{j\downarrow} c_{j\uparrow} | \Psi_{\text{BCS}} \rangle \\ &\equiv \langle c_{i\uparrow}^\dagger c_{i\downarrow}^\dagger c_{i\downarrow} c_{i\uparrow} c_{j\uparrow}^\dagger c_{j\downarrow}^\dagger c_{j\downarrow} c_{j\uparrow} \rangle\end{aligned}\quad (6.58)$$

The example in equation (6.51) is now easily evaluated. It is

$$\begin{aligned}\hat{\rho}_{1111,0000} &= \langle \Psi_{\text{BCS}} | c_{i\uparrow}^\dagger c_{i\downarrow}^\dagger c_{j\uparrow}^\dagger c_{j\downarrow}^\dagger | 0_{ij} \rangle \langle 0_{ij} | \Psi_{\text{BCS}} \rangle \\ &= \langle \Psi_{\text{BCS}} | c_{i\uparrow}^\dagger c_{i\downarrow}^\dagger c_{j\uparrow}^\dagger c_{j\downarrow}^\dagger c_{i\uparrow} c_{i\downarrow} c_{j\uparrow} c_{j\downarrow} | \Psi_{\text{BCS}} \rangle\end{aligned}\quad (6.59)$$

### Evaluating the matrix elements using Wick's theorem

The elements of  $\hat{\rho}_{nn'}$  are now expressed as expectation values of strings of second-quantized single-particle operators. How can these expectation values be evaluated? Wick's theorem is the answer.

*Wick's theorem:* The average value of a product of creation and annihilation operators is equal to the sum of all complete systems of pairings, in which each pairing preserves the original ordering of the operators in the product. Ie.

$$\langle \hat{A}_1 \hat{A}_2 \dots \hat{A}_s \rangle = \sum_{\text{order-preserving permutations}} \langle \hat{A}_1 \hat{A}_2 \rangle \langle \hat{A}_3 \hat{A}_4 \rangle \dots \langle \hat{A}_{s-1} \hat{A}_s \rangle\quad (6.60)$$

where the sum runs over all permutations of the  $s$  indices which preserve the ordering of the indices in the original product. In other words, each pairing  $\langle \hat{A}_i \hat{A}_j \rangle$  should satisfy  $i < j$ .

A problem which now arises is the length of some of the products of creation and annihilation operators to which Wick's theorem should be applied. For example, the matrix element  $\hat{\rho}_{1111,1111}$  is obtained by evaluating

$$\langle \Psi_{\text{BCS}} | c_{i\uparrow}^\dagger c_{i\downarrow}^\dagger c_{j\uparrow}^\dagger c_{j\downarrow}^\dagger c_{i\uparrow} c_{i\downarrow} c_{j\uparrow} c_{j\downarrow} c_{i\downarrow} c_{i\uparrow} c_{j\downarrow} c_{j\uparrow} | \Psi_{\text{BCS}} \rangle,\quad (6.61)$$

a product with 16 terms. There are in fact 40320 permutations of the operators in this product that preserve the original ordering, and in which all the pairings are non-zero. Thus a Mathematica program was written to construct the superconductor density matrix. On an ordinary 800MHz notebook computer it takes about 15 minutes to produce the matrix, in symbolic form. As the result is symbolic the program only ever needs to be run once.

### **Evaluating the pairings using single-particle operators for Bogliubov quasi-particles**

Each matrix element is now in the form of a sum of products of pairings, where a pairing is the expectation values of a pair of single particle operators. How does one evaluate each pairing?

The annihilation operators  $\hat{\alpha}_{\mathbf{k}}$  and  $\hat{\beta}_{-\mathbf{k}}$  for the Bogliubov quasi-particles are defined by

$$\begin{aligned}\hat{\alpha}_{\mathbf{k}} &= u_{\mathbf{k}}c_{\mathbf{k}\uparrow} - v_{\mathbf{k}}c_{-\mathbf{k}\downarrow}^{\dagger} \\ \hat{\beta}_{-\mathbf{k}} &= u_{\mathbf{k}}c_{-\mathbf{k}\downarrow} + v_{\mathbf{k}}c_{\mathbf{k}\uparrow}^{\dagger}\end{aligned}\tag{6.62}$$

In the framework of these quasi-particles, the BCS ground state is the ‘vacuum state’. Hence the BCS ground state is annihilated by the above operators. For

example, the action of  $\hat{\alpha}_{\mathbf{k}}$  on it is:

$$\begin{aligned}
\hat{\alpha}_{\mathbf{k}}|\Psi_{\text{BCS}}\rangle &= (u_{\mathbf{k}}c_{\mathbf{k}\uparrow} - v_{\mathbf{k}}c_{-\mathbf{k}\downarrow}^\dagger)\left(\prod_l (u_l + v_l c_{l\uparrow}^\dagger c_{-l\downarrow}^\dagger)|0\rangle\right) \\
&= (u_{\mathbf{k}}c_{\mathbf{k}\uparrow} - v_{\mathbf{k}}c_{-\mathbf{k}\downarrow}^\dagger)(u_{\mathbf{k}} + v_{\mathbf{k}}c_{\mathbf{k}\uparrow}^\dagger c_{-\mathbf{k}\downarrow}^\dagger)\prod_{l\neq\mathbf{k}}(u_l + v_l c_{l\uparrow}^\dagger c_{-l\downarrow}^\dagger)|0\rangle \\
&= \prod_{l\neq\mathbf{k}}(u_l + v_l c_{l\uparrow}^\dagger c_{-l\downarrow}^\dagger)(u_{\mathbf{k}}c_{\mathbf{k}\uparrow} - v_{\mathbf{k}}c_{-\mathbf{k}\downarrow}^\dagger)(u_{\mathbf{k}} + v_{\mathbf{k}}c_{\mathbf{k}\uparrow}^\dagger c_{-\mathbf{k}\downarrow}^\dagger)|0\rangle \\
&= \prod_{l\neq\mathbf{k}}(u_l + v_l c_{l\uparrow}^\dagger c_{-l\downarrow}^\dagger)(u_{\mathbf{k}}^2 c_{\mathbf{k}\uparrow} + u_{\mathbf{k}}v_{\mathbf{k}}c_{\mathbf{k}\uparrow}c_{\mathbf{k}\uparrow}^\dagger c_{-\mathbf{k}\downarrow}^\dagger \\
&\quad - u_{\mathbf{k}}v_{\mathbf{k}}c_{-\mathbf{k}\downarrow}^\dagger - v_{\mathbf{k}}^2 c_{-\mathbf{k}\downarrow}^\dagger c_{\mathbf{k}\uparrow}^\dagger c_{-\mathbf{k}\downarrow}^\dagger)|0\rangle \\
&= \prod_{l\neq\mathbf{k}}(u_l + v_l c_{l\uparrow}^\dagger c_{-l\downarrow}^\dagger)(\text{lowering operation on the vacuum} \\
&\quad + u_{\mathbf{k}}v_{\mathbf{k}}c_{-\mathbf{k}\downarrow}^\dagger|0\rangle - u_{\mathbf{k}}v_{\mathbf{k}}c_{-\mathbf{k}\downarrow}^\dagger|0\rangle \\
&\quad - \text{the same raising operation on the vacuum twice}) \\
&= \prod_{l\neq\mathbf{k}}(u_l + v_l c_{l\uparrow}^\dagger c_{-l\downarrow}^\dagger)(0 + u_{\mathbf{k}}v_{\mathbf{k}}c_{-\mathbf{k}\downarrow}^\dagger|0\rangle - u_{\mathbf{k}}v_{\mathbf{k}}c_{-\mathbf{k}\downarrow}^\dagger|0\rangle - 0) \\
&= 0. \tag{6.63}
\end{aligned}$$

In a similar way, one can show that  $\hat{\beta}_{-\mathbf{k}}$  also annihilates the BCS ground state.

Now, one can rewrite the  $\mathbf{k}$ -state creation and annihilation operators in terms of the Bogliubov operators as follows:

$$\begin{aligned}
c_{\mathbf{k}\uparrow} &= u_{\mathbf{k}}\hat{\alpha}_{\mathbf{k}} + v_{\mathbf{k}}\hat{\beta}_{-\mathbf{k}}^\dagger, \\
c_{\mathbf{k}\uparrow}^\dagger &= u_{\mathbf{k}}^*\hat{\alpha}_{\mathbf{k}}^\dagger + v_{\mathbf{k}}^*\hat{\beta}_{-\mathbf{k}}. \tag{6.64}
\end{aligned}$$

Doing so will enable the reexpression of the expectation values obtained using Wick's theorem in terms of the non-occupation and occupation amplitudes  $u$  and  $v$ .

**Off-diagonal one particle density matrix element for a single spin direction** Consider the pairing  $\langle c_{i\uparrow}^\dagger c_{j\uparrow} \rangle$  (where  $M$  is the number of sites):

$$\begin{aligned}
\langle c_{i\uparrow}^\dagger c_{j\uparrow} \rangle &= \frac{1}{M} \sum_{kk'} e^{-i\mathbf{k}\cdot\mathbf{R}_i} e^{i\mathbf{k}'\cdot\mathbf{R}_j} \langle c_{\mathbf{k}\uparrow}^\dagger c_{\mathbf{k}'\uparrow} \rangle \\
&= \frac{1}{M} \sum_{kk'} e^{i(\mathbf{k}'\cdot\mathbf{R}_j - \mathbf{k}\cdot\mathbf{R}_i)} \langle (u_{\mathbf{k}}^* \hat{\alpha}_{\mathbf{k}}^\dagger + v_{\mathbf{k}}^* \hat{\beta}_{-\mathbf{k}}) (u_{\mathbf{k}'} \hat{\alpha}_{\mathbf{k}'} + v_{\mathbf{k}'} \hat{\beta}_{-\mathbf{k}'}) \rangle \\
&= \frac{1}{M} \sum_{kk'} e^{i(\mathbf{k}'\cdot\mathbf{R}_j - \mathbf{k}\cdot\mathbf{R}_i)} \left( u_{\mathbf{k}}^* u_{\mathbf{k}'} \langle \Psi_{\text{BCS}} | \hat{\alpha}_{\mathbf{k}}^\dagger \hat{\alpha}_{\mathbf{k}'} | \Psi_{\text{BCS}} \rangle + \right. \\
&\quad u_{\mathbf{k}}^* v_{\mathbf{k}'} \langle \Psi_{\text{BCS}} | \hat{\alpha}_{\mathbf{k}}^\dagger \hat{\beta}_{-\mathbf{k}'}^\dagger | \Psi_{\text{BCS}} \rangle + v_{\mathbf{k}}^* u_{\mathbf{k}'} \langle \Psi_{\text{BCS}} | \hat{\beta}_{-\mathbf{k}} \hat{\alpha}_{\mathbf{k}'} | \Psi_{\text{BCS}} \rangle + \\
&\quad \left. v_{\mathbf{k}}^* v_{\mathbf{k}'} \langle \Psi_{\text{BCS}} | \hat{\beta}_{-\mathbf{k}} \hat{\beta}_{-\mathbf{k}'}^\dagger | \Psi_{\text{BCS}} \rangle \right) \\
&= \frac{1}{M} \sum_{kk'} e^{i(\mathbf{k}'\cdot\mathbf{R}_j - \mathbf{k}\cdot\mathbf{R}_i)} \left( 0 + 0 + 0 + v_{\mathbf{k}}^* v_{\mathbf{k}'} \langle \Psi_{\text{BCS}} | \hat{\beta}_{-\mathbf{k}} \hat{\beta}_{-\mathbf{k}'}^\dagger | \Psi_{\text{BCS}} \rangle \right) \\
&= \frac{1}{M} \sum_{kk'} e^{i(\mathbf{k}'\cdot\mathbf{R}_j - \mathbf{k}\cdot\mathbf{R}_i)} v_{\mathbf{k}}^* v_{\mathbf{k}'} \delta_{kk'} \\
&= \frac{1}{M} \sum_{\mathbf{k}} e^{i\mathbf{k}\cdot(\mathbf{R}_j - \mathbf{R}_i)} |v_{\mathbf{k}}|^2. \\
&:= I. \tag{6.65}
\end{aligned}$$

The above uses the fact that the only non-zero terms are those where a creation operator is acting to the right and an annihilation operator is acting to the left, ie.

$$\begin{aligned}
\hat{\alpha}_{\mathbf{k}} | \Psi_{\text{BCS}} \rangle &= 0 \\
\hat{\beta}_{\mathbf{k}} | \Psi_{\text{BCS}} \rangle &= 0 \\
\langle \Psi_{\text{BCS}} | \hat{\alpha}_{\mathbf{k}}^\dagger &= 0 \\
\langle \Psi_{\text{BCS}} | \hat{\beta}_{\mathbf{k}}^\dagger &= 0. \tag{6.66}
\end{aligned}$$

It also uses the fact that the Bogliubov transformation is canonical and thus preserves the commutation relations between fermionic creation and annihilation operators, ie.

$$\{ \hat{\beta}_{\mathbf{k}}, \hat{\beta}_{\mathbf{k}'}^\dagger \} = \delta_{kk'}. \tag{6.67}$$

**Two particle density matrix element for two spin directions** The pairing  $\langle c_{i\uparrow}^\dagger c_{j\downarrow}^\dagger \rangle$  can be evaluated by a similar method. This gives

$$\begin{aligned}\langle c_{i\uparrow}^\dagger c_{j\downarrow}^\dagger \rangle &= \frac{1}{M} \sum_{\mathbf{k}} e^{i\mathbf{k} \cdot (\mathbf{R}_j - \mathbf{R}_i)} u_{\mathbf{k}} v_{\mathbf{k}} \\ &= \frac{1}{M} \sum_{\mathbf{k}} e^{i\mathbf{k} \cdot (\mathbf{R}_j - \mathbf{R}_i)} \frac{\Delta_{\mathbf{k}}}{2\sqrt{\Delta_{\mathbf{k}}^2 + \epsilon_K^2}} \\ &:= J\end{aligned}\tag{6.68}$$

where the second line is obtained using equations 6.33 and 6.36.

**Number density** Since they are expectation values of the number operator, pairings of the type  $\langle c_{i\sigma}^\dagger c_{i\sigma} \rangle$  can be written in terms of the number density:

$$\langle c_{i\sigma}^\dagger c_{i\sigma} \rangle = \langle \hat{n}_{i\sigma} \rangle = \frac{1}{M} \sum_{\mathbf{k}} |v_{\mathbf{k}}|^2 := f\tag{6.69}$$

and

$$\langle c_{i\sigma} c_{i\sigma}^\dagger \rangle = \langle 1 - \hat{n}_{i\sigma} \rangle = \frac{1}{M} \sum_{\mathbf{k}} |u_{\mathbf{k}}|^2 := (1 - f).\tag{6.70}$$

**Superconducting pair density** Pairings of the type  $\langle c_{i\uparrow}^\dagger c_{i\downarrow}^\dagger \rangle$  can be written in terms of the superconducting pair density:

$$\begin{aligned}\langle c_{i\uparrow}^\dagger c_{i\downarrow}^\dagger \rangle &= \frac{1}{M} \sum_{\mathbf{k}} u_{\mathbf{k}} v_{\mathbf{k}} := g \\ \langle c_{i\uparrow} c_{i\downarrow} \rangle &= -g\end{aligned}\tag{6.71}$$

### 6.3.4 The full two-site density matrix for the BCS superconductor at $T = 0$

This density matrix has no coherences between states in which the total number of particles is odd or even. Thus the density matrix can be written as a direct sum of two density matrices describing such states respectively:

$$\hat{\rho} = \hat{\rho}_{N\text{even}} \oplus \hat{\rho}_{N\text{odd}}.\tag{6.72}$$

A basis for the full  $16 \times 16$  density matrix, expressed as a tensor product of

the bases for sites  $i$  and  $j$ , is

$$\begin{aligned}
 |n_{i\uparrow}n_{i\downarrow}n_{j\uparrow}n_{j\downarrow}\rangle &= \{|00\rangle, |01\rangle, |10\rangle, |11\rangle\}^{\otimes 2} \\
 &= \{|0000\rangle, |0001\rangle, |0010\rangle, |0011\rangle, |0100\rangle, |0101\rangle, |0110\rangle, |0111\rangle, \\
 &\quad |1000\rangle, |1001\rangle, |1010\rangle, |1011\rangle, |1100\rangle, |1101\rangle, |1110\rangle, |1111\rangle\}.
 \end{aligned}
 \tag{6.73}$$

However, it is almost impossible to fit the full  $16 \times 16$  matrix on one page. Therefore, here the even- $N$  and odd- $N$  matrices are given instead. The density matrix for an even total number of particles is  $\hat{\rho}_{N\text{even}} =$

$$\left( \begin{array}{cccc}
\frac{(J^2-2J(-1+H)+(-1+H)^2+}{(g-j)^2}(J^2-2J(-1+H)-(-1+H)^2) & \frac{(g-j)(g+j)}{(-2+j)(j+H^2-j^2)} & \frac{g^3-2(-1+j)Hj+g(1+(-2+j)(j+H^2-j^2))}{(-2+j)(j+H^2-j^2)} & \frac{g^3-2(-1+j)Hj+g(1+(-2+j)(j+H^2-j^2))}{(-2+j)(j+H^2-j^2)} \\
\frac{g^3-2(-1+j)Hj+g(1+(-2+j)(j+H^2-j^2))}{(-2+j)(j+H^2-j^2)} & \frac{g^3-2(-1+j)Hj+g(1+(-2+j)(j+H^2-j^2))}{(-2+j)(j+H^2-j^2)} & \frac{g^3-2(-1+j)Hj+g(1+(-2+j)(j+H^2-j^2))}{(-2+j)(j+H^2-j^2)} & \frac{g^3-2(-1+j)Hj+g(1+(-2+j)(j+H^2-j^2))}{(-2+j)(j+H^2-j^2)} \\
\frac{g^3-2(-1+j)Hj+g(1+(-2+j)(j+H^2-j^2))}{(-2+j)(j+H^2-j^2)} & \frac{g^3-2(-1+j)Hj+g(1+(-2+j)(j+H^2-j^2))}{(-2+j)(j+H^2-j^2)} & \frac{g^3-2(-1+j)Hj+g(1+(-2+j)(j+H^2-j^2))}{(-2+j)(j+H^2-j^2)} & \frac{g^3-2(-1+j)Hj+g(1+(-2+j)(j+H^2-j^2))}{(-2+j)(j+H^2-j^2)} \\
\frac{g^3-2(-1+j)Hj+g(1+(-2+j)(j+H^2-j^2))}{(-2+j)(j+H^2-j^2)} & \frac{g^3-2(-1+j)Hj+g(1+(-2+j)(j+H^2-j^2))}{(-2+j)(j+H^2-j^2)} & \frac{g^3-2(-1+j)Hj+g(1+(-2+j)(j+H^2-j^2))}{(-2+j)(j+H^2-j^2)} & \frac{g^3-2(-1+j)Hj+g(1+(-2+j)(j+H^2-j^2))}{(-2+j)(j+H^2-j^2)}
\end{array} \right)$$

(6.74)



in the basis

$$|n_{i\uparrow}n_{i\downarrow}n_{j\uparrow}n_{j\downarrow}\rangle = \{|0000\rangle, |0011\rangle, |0101\rangle, |0110\rangle, |1001\rangle, |1010\rangle, |1100\rangle, |1111\rangle\},$$

(6.75)

and where the symbol  $H$  has been used in place of  $I$ . The density matrix for an odd total number of particles is  $\hat{\rho}_{N\text{odd}} =$



in the basis

$$|n_{i\uparrow}n_{i\downarrow}n_{j\uparrow}n_{j\downarrow}\rangle = \{|0001\rangle, |0010\rangle, |0100\rangle, |0111\rangle, |1000\rangle, |1011\rangle, |1101\rangle, |1110\rangle\}. \quad (6.77)$$

As before, the symbol  $H$  has been used in place of  $I$ .

### 6.3.5 Calculating the two-site entanglement in the BCS ground state - results

The Audenaert conjugate gradient code for calculating the entanglement of formation [61] was used to calculate the two-site entanglement of the BCS ground state, from the density matrix obtained in section 6.3.3. A copy of the code was kindly supplied by Konrad Audenaert. This exercise was performed for a range of values of  $f, g, I$ , and  $J$ .

Some combinations of  $f, g, I$ , and  $J$  give a density matrix with one or more negative eigenvalues. Therefore for each combination of parameters, the validity of the density matrix was checked, and only 'legal' density matrices submitted to the conjugate gradient code.

For given values of  $f, g$ , the entanglement of formation was calculated across a fixed grid of values of  $I$  and  $J$ . The results are shown in Figure 6.1, rearranged to show EF surfaces of  $f$  and  $I$  for all possible values of  $g$  and  $J$ .

In Figures 6.2 and 6.3, the exercise is repeated for the BCS ground state density matrix subject, respectively, to an SSR for local particle number conservation, and an SSR for local particle number conservation modulo two. It can be seen that, as expected, the reduction in entanglement is greatest for the local particle number SSR.

### 6.3.6 Martín-Delgado's work on entanglement in the BCS ground state

Martín-Delgado has devised an analytical, concurrence-based entanglement measure for the BCS ground state [83]. He calls it *macrocanonical entanglement of pairing* (MEP), and defines it as

$$E(\text{BCS}) := \langle \text{FS} | \widetilde{\text{FS}} \rangle - \langle \text{BCS} | \widetilde{\text{BCS}} \rangle \quad (6.78)$$

Figure 6.1: Surfaces for the entanglement of formation in the BCS ground state plotted against  $f, I$ , and calculated for all possible values of  $g$  and  $J$ . The maximum is  $E_F = 2.0$  at  $f = I = 0.5, g = J = 0$ .

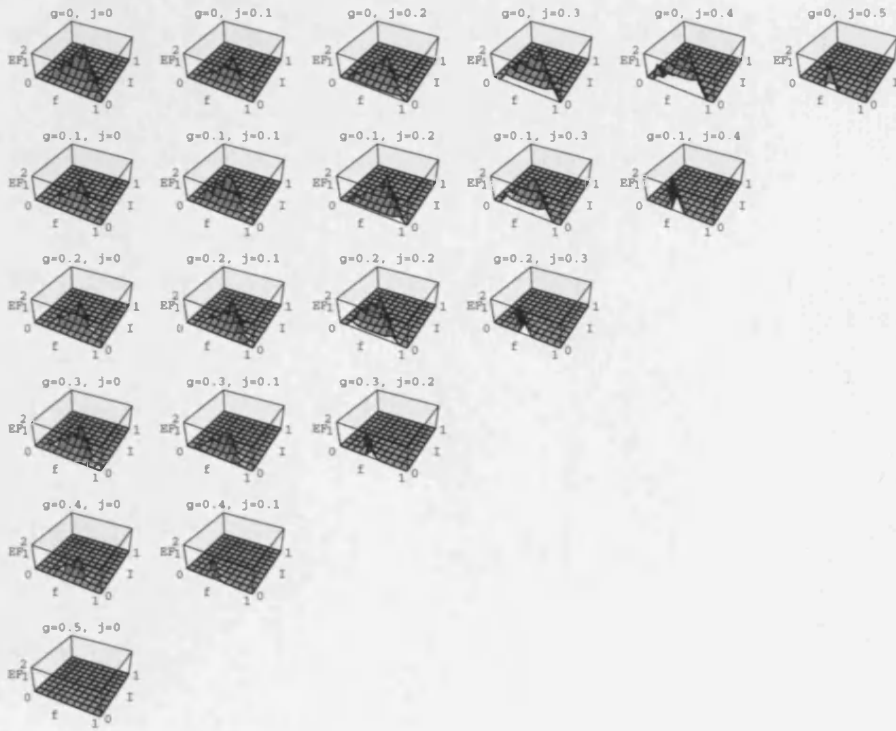


Figure 6.2: The same exercise as in Figure 6.1, performed subject to an SSR for local particle number. The maximum is  $E_F = 0.5$  at  $f = I = 0.5, g = J = 0$ .

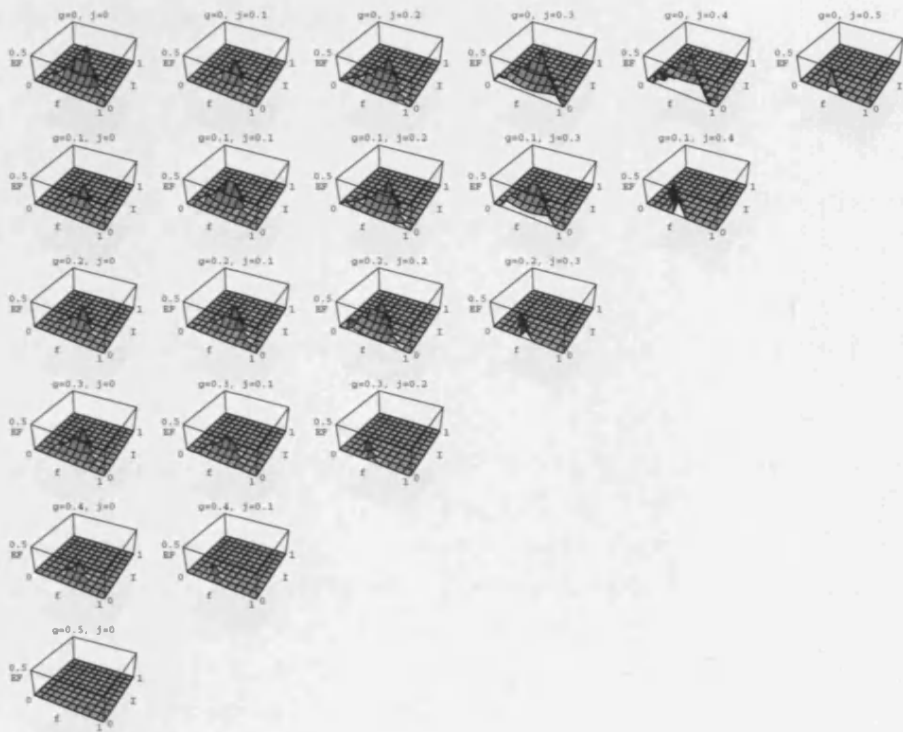
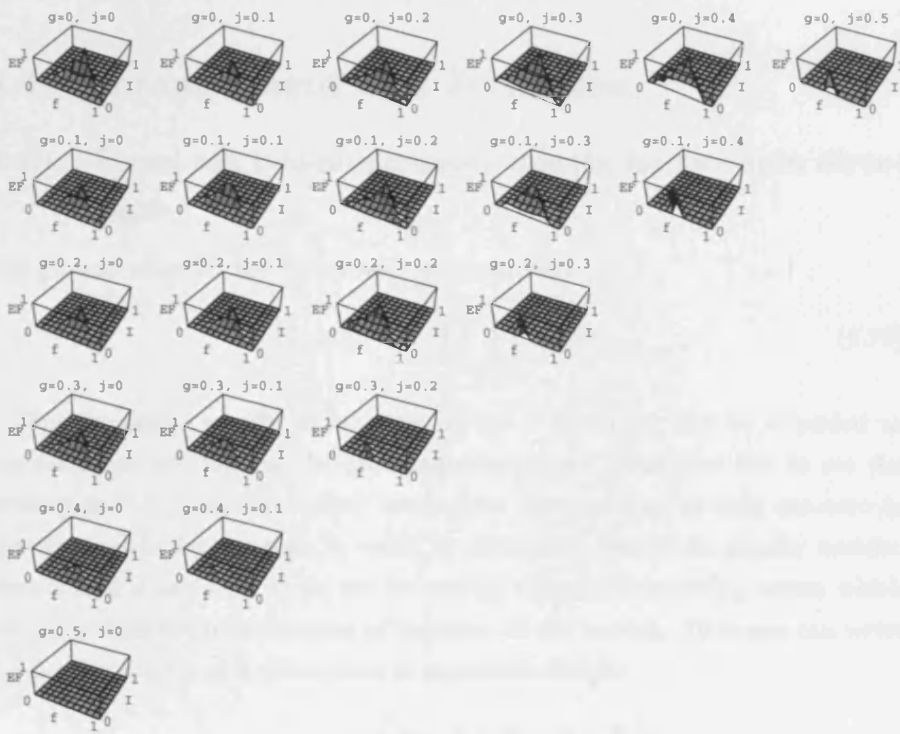


Figure 6.3: The same exercise as in Figure 6.1, performed subject to an SSR for local particle number modulo two. The reduction in entanglement is less than that caused by the SSR for local particle number in Figure 6.2. The maximum is  $E_F = 1.0$  at  $f = I = 0.5, g = J = 0$ .



where  $|BCS\rangle$  is the BCS ground state,  $|\widetilde{BCS}\rangle$  is the time-reversed BCS ground state, and  $|FS\rangle$  and  $|\widetilde{FS}\rangle$  are the Fermi sea state and the time-reversed Fermi sea state respectively. Therefore this definition defines the Fermi sea state as having zero entanglement. The MEP measure suffers from being based on concurrence, as there is no established relationship between concurrence and entanglement of formation for systems of higher dimensionality than two qubits. MEP therefore cannot be used to quantify in ebits the entanglement of the BCS ground state as a resource (to be used for example in teleportation), unlike the procedure given above. Furthermore, it cannot be used to calculate the entanglement between two *sites*, unlike the above method. On the other hand, it has the advantage of being analytical and thus much easier to compute.

## 6.4 Entanglement in a Fermi sea

### 6.4.1 Fermi sea two-site density matrix for two spin directions

The ground state for the Fermi sea can be written

$$|\Psi_{\text{fermi}}\rangle = \prod_{\sigma} \prod_{k \leq k_F} c_{k\sigma}^{\dagger} |0\rangle. \quad (6.79)$$

The two-spin two-site density matrix for a Fermi sea can be regarded as a special case of that for the BCS superconductor. One just has to set the terms  $g$  and  $J$  (which are called ‘anomalous’ because they’re only non-zero in the superconductor) to zero in order to obtain the Fermi sea density matrix. Since  $g$  and  $J$  are zero, there are no matrix elements connecting states which contain a different total number of particles in the system. Thus one can write the density matrix as a direct sum of  $n$ -particle blocks:

$$\hat{\rho}_{\text{FS},ij} = \begin{pmatrix} \hat{\rho}_0 & 0 & 0 & 0 & 0 \\ 0 & \hat{\rho}_1 & 0 & 0 & 0 \\ 0 & 0 & \hat{\rho}_2 & 0 & 0 \\ 0 & 0 & 0 & \hat{\rho}_3 & 0 \\ 0 & 0 & 0 & 0 & \hat{\rho}_4 \end{pmatrix} \quad (6.80)$$

where each block  $\hat{\rho}_N$  is the density matrix for a system containing a total of exactly  $N$  particles. By setting  $g$  and  $J$  to zero in the superconductor density

matrix, the  $\{\hat{\rho}_N\}$  are found to be:

$$\hat{\rho}_0 = \left( ((-1+f)^2 - H^2)^2 \right) \quad (6.81)$$

in the basis

$$|n_{i\uparrow}n_{i\downarrow}n_{j\uparrow}n_{j\downarrow}\rangle = |0000\rangle. \quad (6.82)$$

$$\hat{\rho}_1 = \begin{pmatrix} (1-f+H)(-1+f+ & 0 & (-1+f-H)H(-1+ & 0 \\ H)((-1+f)f-H^2) & -((-1+f-H)(-1+ & f+H) & 0 \\ 0 & f+H)((-1+f)f- & 0 & (-1+f-H)H(-1+ \\ & H^2)) & & f+H) \\ (-1+f-H)H(-1+ & 0 & f+H)((-1+f)f- & 0 \\ f+H) & & H^2)) & \\ 0 & (-1+f-H)H(-1+ & 0 & -((-1+f-H)(-1+ \\ & f+H) & & f+H)((-1+f)f- \\ & & & H^2)) \end{pmatrix} \quad (6.83)$$

in the basis

$$|n_{i\uparrow}n_{i\downarrow}n_{j\uparrow}n_{j\downarrow}\rangle = \{|0001\rangle, |0010\rangle, |0100\rangle, |1000\rangle\}. \quad (6.84)$$

The two-particle density matrix is  $\hat{\rho}_2 =$

$$\begin{pmatrix} (f-f^2+H^2)^2 & 0 & (-1+f)fH-H^3 & H(f-f^2+H^2) & 0 & H^2 \\ & (-1+f-H)(f- & & & & \\ 0 & H)(-1+f+ & 0 & 0 & 0 & 0 \\ & H)(f+H) & & & & \\ (-1+f)fH-H^3 & 0 & (f-f^2+H^2)^2 & -H^2 & 0 & (-1+f)fH-H^3 \\ H(f-f^2+H^2) & 0 & -H^2 & (f-f^2+H^2)^2 & 0 & H(f-f^2+H^2) \\ & & & & (-1+f-H)(f- & \\ 0 & 0 & 0 & 0 & H)(-1+f+ & 0 \\ & & & & H)(f+H) & \\ H^2 & 0 & (-1+f)fH-H^3 & H(f-f^2+H^2) & 0 & (f-f^2+H^2)^2 \end{pmatrix} \quad (6.85)$$

in the basis

$$|n_{i\uparrow}n_{i\downarrow}n_{j\uparrow}n_{j\downarrow}\rangle = \{|0011\rangle, |0101\rangle, |0110\rangle, |1001\rangle, |1010\rangle, |1100\rangle\}. \quad (6.86)$$



The three-particle density matrix is  $\hat{\rho}_3 =$

$$\left( \begin{array}{cccc} -((f-H)(f+H)((-1+ & 0 & -(f^2H)+H^3 & 0 \\ f)f-H^2)) & -((f-H)(f+H)((-1+ & 0 & -(f^2H)+H^3 \\ 0 & f)f-H^2)) & -((f-H)(f+H)((-1+ & 0 \\ -(f^2H)+H^3 & 0 & f)f-H^2)) & -((f-H)(f+H)((-1+ \\ 0 & -(f^2H)+H^3 & 0 & f)f-H^2)) \end{array} \right) \quad (6.87)$$

in the basis

$$|n_{i\uparrow}n_{i\downarrow}n_{j\uparrow}n_{j\downarrow}\rangle = \{|0111\rangle, |1011\rangle, |1101\rangle, |1110\rangle\}. \quad (6.88)$$

The four-particle density matrix (which has only one element) is  $\hat{\rho}_4 =$

$$\left( \begin{array}{c} (f^2-H^2)^2 \end{array} \right) \quad (6.89)$$

in the basis

$$|n_{i\uparrow}n_{i\downarrow}n_{j\uparrow}n_{j\downarrow}\rangle = |1111\rangle. \quad (6.90)$$

The basis for the full density matrix, expressed as a tensor product of the bases for sites  $i$  and  $j$ , is

$$\begin{aligned} |n_{i\uparrow}n_{i\downarrow}n_{j\uparrow}n_{j\downarrow}\rangle &= \{|00\rangle, |01\rangle, |10\rangle, |11\rangle\}^{\otimes 2} \\ &= \{|0000\rangle, |0001\rangle, |0010\rangle, |0011\rangle, |0100\rangle, |0101\rangle, |0110\rangle, |0111\rangle, \\ &\quad |1000\rangle, |1001\rangle, |1010\rangle, |1011\rangle, |1100\rangle, |1101\rangle, |1110\rangle, |1111\rangle\}. \end{aligned} \quad (6.91)$$

## 6.4.2 Fermi sea two-site density matrix for a single spin direction

If one uses a similar procedure to that used in section 6.3.3 to build the two-site density matrix for the BCS ground state, the following density matrix is obtained.

$$\hat{\rho}_\sigma = \left( \begin{array}{cccc} (1-f)^2 - I^2 & 0 & 0 & 0 \\ 0 & f(1-f) + I^2 & I & 0 \\ 0 & I & f(1-f) + I^2 & 0 \\ 0 & 0 & 0 & f^2 - I^2 \end{array} \right) \quad (6.92)$$

in the basis

$$|n_{i\sigma}n_{j\sigma}\rangle = \{|00\rangle, |01\rangle, |10\rangle, |11\rangle\}. \quad (6.93)$$

### Off-diagonal one-particle density matrix element in a Fermi sea

For a spherical Fermi surface, the off-diagonal one-particle density matrix element  $I$  becomes

$$\begin{aligned} I &= \frac{\Omega}{(2\pi)^3} \int_0^{k_F} k^2 dk (2\pi) \int_{-1}^1 d(\cos\theta) \exp(ikR \cos\theta) \\ &= \frac{\Omega}{(2\pi)^3} \int_0^{k_F} k^2 dk (2\pi) \left[ \frac{1}{ikR} \exp(ikR \cos\theta) \right]_{-1}^1 \\ &= \frac{\Omega}{(2\pi)^3} \int_0^{k_F} k^2 dk (2\pi) \frac{2 \exp(ikR)}{ikR} \\ &= \frac{\Omega}{(2\pi)^3} \frac{4\pi}{iR} \int_0^{k_F} k \exp(ikR) dk \\ &= \frac{\Omega}{2\pi^2} \frac{1}{iR} \left[ k \frac{1}{iR} \exp(ikR) - \int_0^{k_F} \frac{1}{iR} \exp(ikR) \cdot 1 \, dk \right]_0^{k_F} \\ &= \frac{\Omega}{2\pi^2} \frac{1}{iR} \left[ k \frac{1}{iR} \exp(ikR) - \left( \frac{1}{iR} \right)^2 \exp(ikR) \right]_0^{k_F} \\ &= \frac{\Omega}{2\pi^2} \left( \frac{1}{iR} \right)^2 \left[ k \exp(ikR) + \frac{i}{R} \exp(ikR) \right]_0^{k_F} \\ &= \frac{\Omega}{2\pi^2} \left( \frac{1}{iR} \right)^2 \left[ \left( k_F \cos(k_F R) - \frac{1}{R} \sin(k_F R) \right) - \left( 0 \cos 0 - \frac{1}{R} \sin 0 \right) \right] \\ &= \frac{\Omega}{2\pi^2 R^2} \left[ \frac{\sin(k_F R)}{R} - k_F \cos(k_F R) \right]. \quad (6.94) \end{aligned}$$

Now

$$\begin{aligned} f &= \text{DOS per unit volume in k-space for a single spin} \\ &\quad \times \text{volume of Fermi sphere in k-space} \\ &= \frac{\Omega}{8\pi^3} \times \frac{4}{3} \pi k_F^3 = \frac{\Omega}{6\pi^2} k_F^3 \\ \therefore \Omega &= \frac{6\pi^2 f}{k_F^3}. \quad (6.95) \end{aligned}$$

Thus

$$I = \frac{3f}{(k_F R)^3} \left[ \sin(k_F R) - (k_F R) \cos(k_F R) \right] \quad (6.96)$$

where  $k_F$  is the Fermi wavevector. In a one-dimensional system

$$\begin{aligned}
I &= \frac{a}{2\pi} \int_{-k_F}^{k_F} \exp(ikR) dk \\
&= \frac{a}{2\pi} \frac{1}{iR} \left[ \cos(k_F R) + i \sin(k_F R) - (\cos(k_F R) - i \sin(k_F R)) \right] \\
&= \frac{a}{\pi R} \sin(k_F R) \\
&= \frac{a}{\pi R} k_F R \frac{\sin(k_F R)}{k_F R} \\
&= f \text{sinc}(k_F R) \tag{6.97}
\end{aligned}$$

where  $a$  is the lattice spacing.

**Infinite separations:**  $R \rightarrow \infty$

Unsurprisingly, the further apart sites  $i$  and  $j$  are, the less correlation exists between them. In other words, as  $R \rightarrow \infty$ ,  $I \rightarrow 0$  and the density matrix tends towards uncorrelated filling of sites  $i$  and  $j$ .

**Finite separations:**  $R < \infty$

For finite separations of sites  $i$  and  $j$ ,  $I \neq 0$ . The presence of  $I$  in the density matrix in equation 6.92 reflects the exclusion principle. It subtracts from the diagonal elements for  $|00\rangle$  and  $|11\rangle$ , making double occupancy of a site less likely. On the other hand, it adds to the diagonal elements for  $|01\rangle$  and  $|10\rangle$ , making single occupancy more likely.

### 6.4.3 Relationship between two spin direction and single spin direction Fermi sea density matrices

The spins in a Fermi sea are non-interacting hence in principle the two-spin-direction two-site density matrix can be constructed from a direct product of spin-up and spin-down density matrices:

$$\hat{\rho}_{\text{FS},\uparrow\downarrow} = \hat{\rho}_{\uparrow} \otimes \hat{\rho}_{\downarrow}, \tag{6.98}$$

i.e.

$$(\hat{\rho}_{\text{FS},\uparrow\downarrow})_{\{n_{i\uparrow} n_{j\uparrow} n_{i\downarrow} n_{j\downarrow}\}, \{n'_{i\uparrow} n'_{j\uparrow} n'_{i\downarrow} n'_{j\downarrow}\}} = (\hat{\rho}_{\uparrow})_{\{n_{i\uparrow} n_{j\uparrow}\}, \{n'_{i\uparrow} n'_{j\uparrow}\}} (\hat{\rho}_{\downarrow})_{\{n_{i\downarrow} n_{j\downarrow}\}, \{n'_{i\downarrow} n'_{j\downarrow}\}}. \tag{6.99}$$

However, on this point some care must be taken. The density matrix  $\hat{\rho}_{\text{FS},ij}$  in equation 6.80 (which was obtained from the superconductor density matrix) is in a tensor product basis of the individual two-spin bases for sites  $i$  and  $j$ . This is suited to calculating the entanglement between sites  $i$  and  $j$ . On the other hand, the density matrix  $\hat{\rho}_{\text{FS},\uparrow\downarrow}$  produced by tensoring up the spin-up and spin-down density matrices is by construction in a tensor product basis of spin-up and spin-down components, and thus not suitable for calculating the entanglement between the two sites.

The basis suitable for calculating entanglement between sites  $i$  and  $j$  is

$$\{|n_{i\uparrow}n_{i\downarrow}n_{j\uparrow}n_{j\downarrow}\rangle\} = \{|n_{i\uparrow}n_{i\downarrow}\rangle\} \otimes \{|n_{j\uparrow}n_{j\downarrow}\rangle\}. \quad (6.100)$$

If the above density matrix  $\hat{\rho}_{\text{FS},\uparrow\downarrow}$  is reexpressed in this basis, it is found to be equal to the superconductor density matrix with  $g = J = 0$ , ie.  $\hat{\rho}_{\text{FS},ij}$  as given in equation 6.80. In order to do this, it is necessary to invoke the commutation relations for creation operators thus:

$$n_{i\downarrow}n_{j\uparrow} = 1, 1 \quad : \quad |n_{i\uparrow}n_{i\downarrow}n_{j\uparrow}n_{j\downarrow}\rangle = -|n_{i\uparrow}n_{j\uparrow}n_{i\downarrow}n_{j\downarrow}\rangle \quad (6.101)$$

$$n_{i\downarrow}n_{j\uparrow} \neq 1, 1 \quad : \quad |n_{i\uparrow}n_{i\downarrow}n_{j\uparrow}n_{j\downarrow}\rangle = |n_{i\uparrow}n_{j\uparrow}n_{i\downarrow}n_{j\downarrow}\rangle \quad (6.102)$$

It is only for the basis kets represented by equation 6.101 that a change of sign is necessary when moving from the  $\{|n_{i\uparrow}n_{j\uparrow}n_{i\downarrow}n_{j\downarrow}\rangle\}$  basis to the  $\{|n_{i\uparrow}n_{i\downarrow}n_{j\uparrow}n_{j\downarrow}\rangle\}$  basis, since it is only for those kets that one has to move one creation operator past another (the  $c_{j\uparrow}^\dagger$  operator past the  $c_{i\downarrow}^\dagger$  operator).

The actual comparison of  $\hat{\rho}_{\text{FS},\uparrow\downarrow}$  and  $\hat{\rho}_{\text{FS},ij}$  was performed using Mathematica. First, the density matrix for  $\hat{\rho}_{\text{FS},\uparrow\downarrow}$  was converted to a symbolic density operator. Then the commutation relations were invoked by declaring the appropriate relations (negation and/or transposition of occupation numbers) between the symbols representing the kets of the respective bases for  $\hat{\rho}_{\text{FS},\uparrow\downarrow}$  and  $\hat{\rho}_{\text{FS},ij}$ . Finally the density operator, now in the basis for  $\hat{\rho}_{\text{FS},ij}$ , was converted back to a density matrix. This was equal to the superconductor density matrix for  $g = J = 0$  as expected.

Since the single-spin-direction two-site density matrix for the Fermi sea was calculated by hand, and the two-spin-direction two-site density matrix for the BCS superconductor was generated by a Mathematica program, this equivalence strongly suggests that both are correct. However, it is not a full check on the validity of the superconductor density matrix as it doesn't include the  $g \neq 0$  and/or  $J \neq 0$  cases.

## Entanglement of formation results

If one chooses as an example  $f = 0.5, I = 0.25$  and of course  $g = J = 0$ , then the following results are obtained for the single spin direction entanglement, and two spin direction entanglement for the Fermi sea.

$$\begin{aligned} \text{EF}(\hat{\rho}_\sigma) &= 0.03670 \text{ ebits,} \\ \text{EF}(\hat{\rho}_{\text{FS},\uparrow\downarrow}) &= 0 \text{ ebits,} \\ \text{EF}(\hat{\rho}_{\text{FS},ij}) &= 0.4019 \text{ ebits.} \end{aligned} \tag{6.103}$$

The single spin direction result was calculated using the Wootters formula, the two spin direction results using the Audenaert conjugate gradient code. The entanglement between the spin-up and spin-down components of the two spin direction state is zero: this is expected as in a Fermi sea there are no correlations between the positions of spin-up and spin-down electrons. I.e. the presence of a spin-up electron at a particular site has no influence on the the probability of occupation of that site by spin-down electrons.

Note that the single spin direction entanglement between sites  $i$  and  $j$  is not additive, as the two spin direction entanglement between sites  $i$  and  $j$  is considerably more than twice the single spin direction entanglement.

## Graphing the entanglement of formation surfaces for a sea of fermions (with or without spin)

Figure 6.4 shows the entanglement of formation for a sea of spinless fermions. Figure 6.5 shows the EF surface for a sea of spinless fermions. And Figure 6.6 shows the excess of entanglement in the spinful Fermi sea compared to the spinless Fermi sea.

### 6.4.4 Physicality of Fermi sea parameters

On one point, some care needs to be taken, concerning the maximum value of  $I$ . The above exercise is only physically meaningful if the two lattice sites under discussion are *distinct*, i.e. are separated by at least one lattice spacing. Therefore  $I$  cannot get arbitrarily close to  $f$  (which is its asymptotic value at zero separation). For the Fermi sea ( $g = J = 0$ ), what is the maximum value of  $I$  for a given  $f$ ?

Figure 6.4: Surface for the entanglement of formation in a sea of spinless fermions. The maximum entanglement is one ebit at  $f = I = 0.5$ .

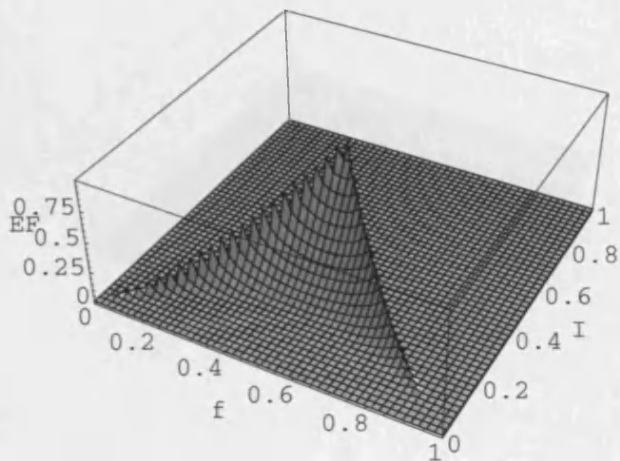


Figure 6.5: Surface for the entanglement of formation in a sea of spinful fermions. The maximum entanglement is two ebits at  $f = I = 0.5$ .

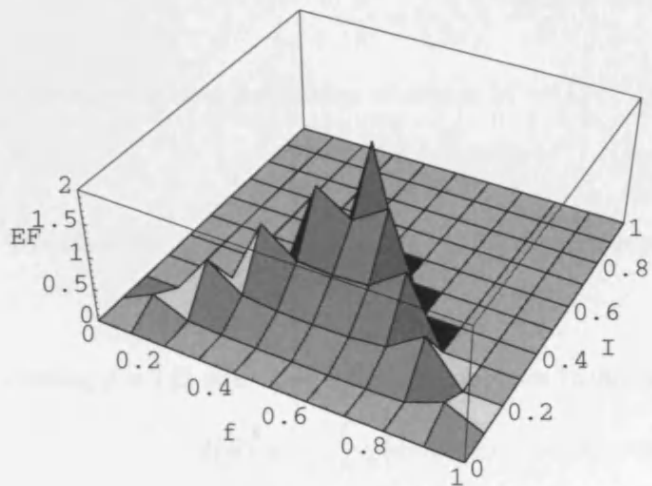
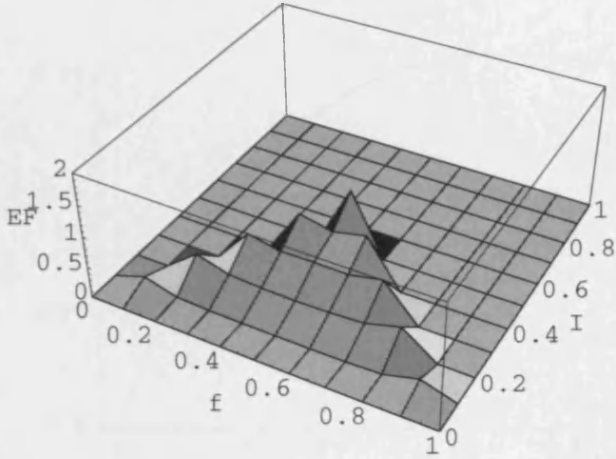


Figure 6.6: Surface for the difference in entanglement of formation between a sea of spinless fermions and a sea of spinful fermions



Consider a simple cubic system with lattice parameter  $a$  and periodic boundary conditions over length  $L$  in all three directions. Let's assume that the interactions are such that the Fermi surface is spherical (see below for the likely limitations of this assumption). The number of carriers per spin is related to the volume of the Fermi sea by

$$\frac{N}{2} = \left(\frac{L}{2\pi}\right)^3 \frac{4\pi k_F^3}{3}. \quad (6.104)$$

Remembering that the number of sites is  $M = (L/a)^3$ , we find the filling factor

$$f = \frac{N}{2M} = \left(\frac{1}{2\pi}\right)^3 \frac{4\pi(k_F a)^3}{3} = \frac{(k_F a)^3}{6\pi^2}. \quad (6.105)$$

Therefore, the lattice spacing  $a$  and the Fermi wavevector  $k_F$  are related by

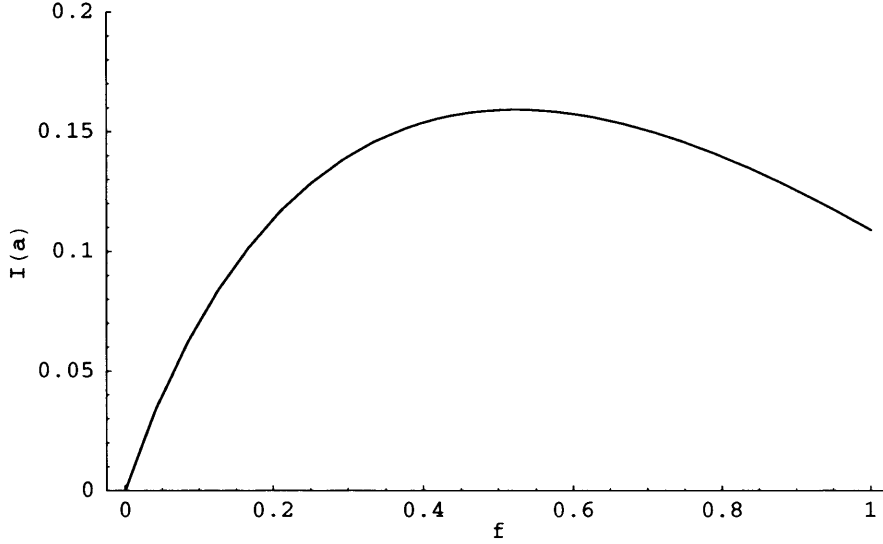
$$k_F a = (6\pi^2 f)^{1/3}. \quad (6.106)$$

Putting  $f = 1/2$  gives  $k_F a = 3.09$ . In equation (6.96), we derived

$$I(R) = \frac{3f}{(k_F R)^3} [\sin(k_F R) - (k_F R) \cos(k_F R)], \quad (6.107)$$

for a spherical Fermi surface, so to find the nearest-neighbour  $I$  all we have to do is evaluate this function with  $R = a$ . The results are plotted in Figure 6.7.

Figure 6.7:  $I_{\max}(f)$  plotted versus  $f$  at  $g = J = 0$ .



Note the likely limitations of the spherical-Fermi-sea approximation; the Fermi surface is likely to get distorted as soon as it approaches the Brillouin zone boundary. This will happen when

$$k_F \approx \frac{\pi}{a} \Rightarrow k_F a \approx \pi \Rightarrow f \approx \frac{\pi}{6} \approx 0.524 \quad (6.108)$$

Figures 6.8, 6.9, and 6.10 are plots of the entanglement in the Fermi sea at the largest physically accessible value of  $I$  for, respectively, no SSR applied, or with either of the two SSRs in force that were previously considered. These entanglement results were calculated using the density matrix for the BCS ground state with  $g$  and  $J$  both set to zero.

### Relationship between single-spin and two-spin entanglements

The results obtained for the entanglement of formation are particularly interesting since they show that, when working in an occupation number basis for fermions, the two-site two-spin entanglement is not equal to twice the two-site single-spin entanglement.

It was found in equation (6.103) that

$$\text{EF}(\hat{\rho}_{\text{FS},ij}) > 2 \times \text{EF}(\hat{\rho}_\sigma). \quad (6.109)$$



Figure 6.8: Entanglement of formation in the Fermi sea plotted against  $f, I_{\max}(f)$ .

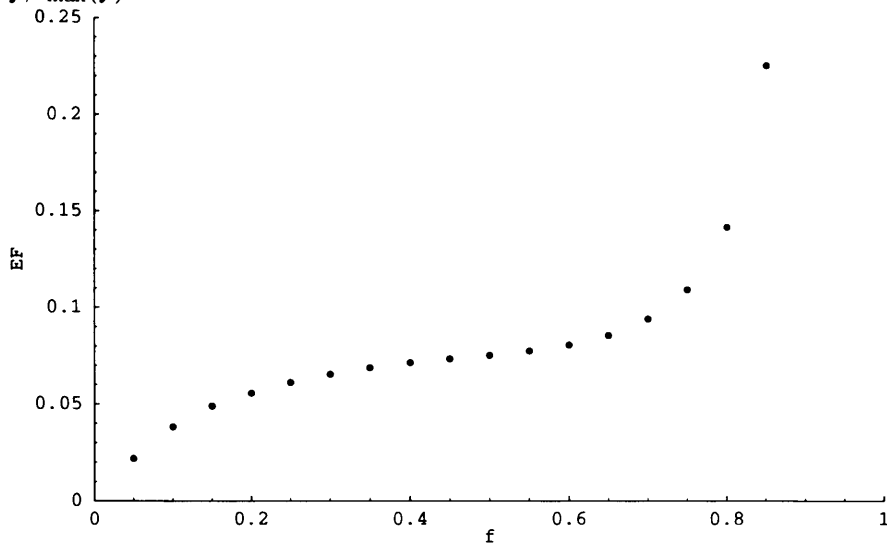


Figure 6.9: Entanglement of formation in the Fermi sea plotted against  $f, I_{\max}(f)$ , with the SSR for local particle number conservation in force.

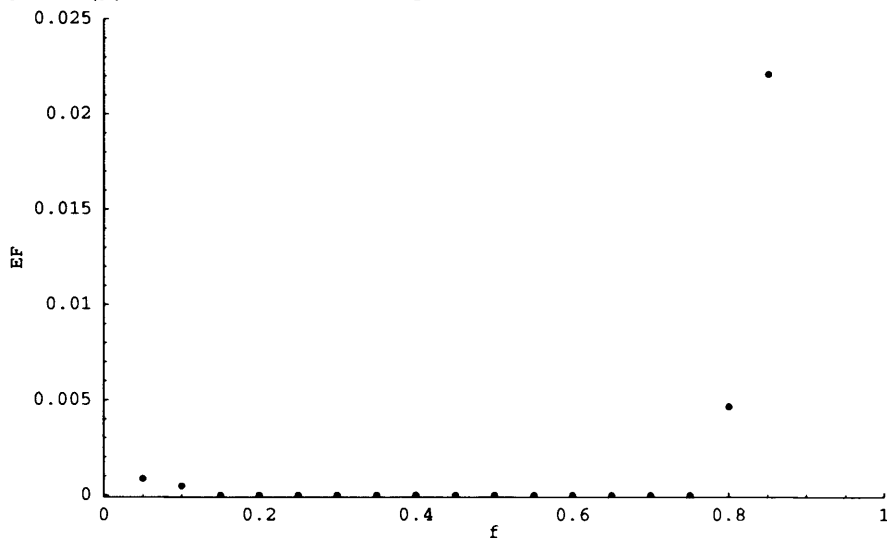
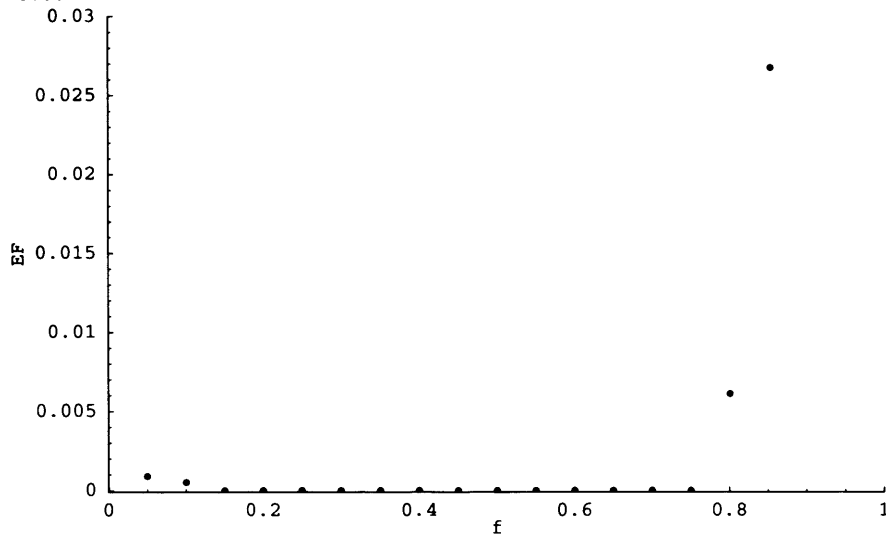


Figure 6.10: Entanglement of formation in the Fermi sea plotted against  $f, I_{\max}(f)$ , with the SSR for local particle number modulo 2 conservation in force.



So not only does equality not apply, but the two-site two-spin entanglement is actually *greater* than the two-site single-spin entanglement. This is because the assumptions required for the additivity of EF are not satisfied, because of the commutation relations expressed by equation 6.101. This is because the overall Hilbert space is not a direct product of Alice's (spin up) and Bob's (spin down) Hilbert spaces.

If the rearrangement is made without the use of minus signs, then one finds that the entanglement of formation is still additive. So for the numerical example in equation (6.103), one finds that

$$\begin{aligned} \text{EF}(\hat{\rho}_{\text{FS},ij}^+) &= 0.07399 \text{ ebits} \\ &= 2 \times \text{EF}(\hat{\rho}_\sigma). \end{aligned} \quad (6.110)$$

Thus, entanglement of formation is in general not additive for fermionic systems, because rearranging the tensor product of bases for bipartite systems 1 and 2 into a joint bipartite tensor product basis of system 12 will involve moving one fermion creation operator past another for certain basis elements, introducing minus signs. However, it is important to emphasize that this conclusion represents a special case, and has absolutely no wider significance for the open

question concerning the additivity of the entanglement of formation for systems of distinguishable particles.

## 6.5 Entanglement in a Bose condensate

Another type of degenerate quantum gas is the Bose-Einstein condensate (BEC). This section constructs a two-site density matrix for this system, then considers the entanglement between the two sites. Simon [84] has also obtained results for bipartite entanglement in BECs. His results are consistent with this study, and are described in section 6.5.5.

What are the elements of the two-site density matrix for sites  $i$  and  $j$  in a Bose condensate at  $T = 0$ , written in an occupation number basis? If there are  $N$  bosons in the condensate, and the system contains  $M$  sites, then by definition each element is

$$\hat{\rho}(n_i, n_j; n'_i, n'_j) = \sum_{n_1 \dots n_M}^{\text{not } n_i, n_j} \langle n_1 \dots n_i \dots n_j \dots n_M | \Psi_B \rangle \langle \Psi_B | n_1 \dots n'_i \dots n'_j \dots n_M \rangle \quad (6.111)$$

where  $|\Psi_B\rangle$  is the ground state of  $N$  bosons at  $T = 0$ . What is  $|\Psi_B\rangle$ ? The unique feature of a Bose condensate is that all  $N$  particles are in their lowest energy state. It will be convenient to express  $|\Psi_B\rangle$  in terms of the occupancies  $n_1 \dots n_i \dots n_j \dots n_M$ . This is achieved as follows. The  $M$ -site lowest energy state can be written

$$\frac{1}{\sqrt{M}} (a_1^\dagger + \dots + a_M^\dagger) |0\rangle. \quad (6.112)$$

So  $N$  particles inserted into this state is written

$$|\Psi_B\rangle = \frac{1}{\sqrt{N!}} \left( \frac{1}{\sqrt{M}} (a_1^\dagger + \dots + a_M^\dagger) \right)^N |0\rangle. \quad (6.113)$$

To reexpress this in terms of occupation numbers, one can use the multinomial expansion:

$$(a_1 + \dots + a_k)^P = \sum_{\{q\}} \frac{P!}{q_1! \dots q_k!} (a_1)^{q_1} \dots (a_k)^{q_k},$$

$$\{q\} := \text{a set of positive integers } q_1 \dots q_k \text{ satisfying } \sum_{i=1}^k q_i = P. \quad (6.114)$$

It's easy to normalize this: one just sets all the  $\{a_i\}$  equal to 1, giving

$$\sum_{\{q\}} \frac{P!}{q_1! \dots q_k!} = k^P. \quad (6.115)$$

Applying the multinomial expansion to equation 6.113 gives

$$|\Psi_B\rangle = \frac{1}{\sqrt{N!}} \left(\frac{1}{\sqrt{M}}\right)^N \sum_{\{n\}} \frac{N!}{n_1! \dots n_M!} (a_1^\dagger)^{n_1} \dots (a_M^\dagger)^{n_M} |0\rangle. \quad (6.116)$$

Then, applying the result

$$(a^\dagger)^n |0\rangle = \sqrt{n!} |n\rangle \quad (6.117)$$

gives

$$|\Psi_B\rangle = \frac{1}{\sqrt{N!}} \left(\frac{1}{\sqrt{M}}\right)^N \sum_{\{n\}} \frac{N!}{\sqrt{n_1! \dots n_M!}} |n_1 \dots n_M\rangle. \quad (6.118)$$

One can now substitute this into the previous expression for the two-site density matrix element:

$$\begin{aligned} \hat{\rho}(n_i, n_j; n'_i, n'_j) &= \sum_{n_1 \dots n_M}^{\text{not } n_i, n_j} \langle n_1 \dots n_i \dots n_j \dots n_M | \Psi_B \rangle \langle \Psi_B | n_1 \dots n'_i \dots n'_j \dots n_M \rangle \\ &= \frac{1}{N!} \frac{1}{M^N} (N!)^2 \sum_{n_1 \dots n_M}^{\text{not } n_i, n_j} \frac{1}{\sqrt{n_1! \dots n_i! \dots n_j! \dots n_M!}} \\ &\quad \frac{1}{\sqrt{n_1! \dots n'_i! \dots n'_j! \dots n_M!}} \delta_{n_i + n_j, n'_i + n'_j} \\ &= \frac{N!}{M^N} \frac{1}{\sqrt{n_i! n_j! n'_i! n'_j!}} \\ &\quad \sum_{n_1 \dots n_M}^{\text{not } n_i, n_j} \frac{1}{n_1! \dots n_{i-1}! n_{i+1}! \dots n_{j-1}! n_{j+1}! \dots n_M!} \delta_{n_i + n_j, n'_i + n'_j} \end{aligned} \quad (6.119)$$

The summation can be eliminated by using the result in equation 6.115 for the normalization of the multinomial expansion:

$$(1 + \dots + 1)^P = \sum_{\{q\}} \frac{P!}{q_1! \dots q_k!} (1)^{q_1} \dots (1)^{q_k}$$

$$\begin{aligned} \therefore \sum_{\{q\}} \frac{P!}{q_1! \dots q_k!} &= k^P \quad \therefore \sum_{\{q\}} \frac{1}{q_1! \dots q_k!} = \frac{k^P}{P!} \\ \therefore \sum_{\substack{\text{not } n_i, n_j \\ n_1 \dots n_M}} \frac{1}{n_1! \dots n_{i-1}! n_{i+1}! \dots n_{j-1}! n_{j+1}! \dots n_M!} &= \frac{(M-2)^{(N-(n_i+n_j))}}{(N-(n_i+n_j))!} \end{aligned} \quad (6.120)$$

since the use of the expansion here involves all  $M$  sites except sites  $i$  and  $j$ , and all  $N$  particles except the  $n_i + n_j$  particles on those sites. Hence

$$\hat{\rho}(n_i, n_j; n'_i, n'_j) = \frac{N!}{M^N} \frac{(M-2)^{(N-(n_i+n_j))}}{(N-(n_i+n_j))!} \frac{1}{\sqrt{n_i! n_j! n'_i! n'_j!}} \delta_{n_i+n_j, n'_i+n'_j}. \quad (6.121)$$

If a superselection rule for local particle number conservation is in force, then clearly this is modified by the addition of further delta function terms:

$$\begin{aligned} \hat{\rho}(n_i, n_j; n'_i, n'_j)_{\text{SSR}} &= \frac{N!}{M^N} \frac{(M-2)^{(N-(n_i+n_j))}}{(N-(n_i+n_j))!} \frac{1}{\sqrt{n_i! n_j! n'_i! n'_j!}} \\ &\quad \times \delta_{n_i+n_j, n'_i+n'_j} \delta_{n_i, n'_i} \delta_{n_j, n'_j}, \end{aligned} \quad (6.122)$$

and in the case of an SSR for local particle number conservation modulo two,

$$\begin{aligned} \hat{\rho}(n_i, n_j; n'_i, n'_j)_{\text{SSR}\%2} &= \frac{N!}{M^N} \frac{(M-2)^{(N-(n_i+n_j))}}{(N-(n_i+n_j))!} \frac{1}{\sqrt{n_i! n_j! n'_i! n'_j!}} \\ &\quad \times \delta_{n_i+n_j, n'_i+n'_j} \delta_{\%(n_i,2), \%(n'_i,2)} \delta_{\%(n_j,2), \%(n'_j,2)}. \end{aligned} \quad (6.123)$$

### 6.5.1 Binomial probability form of the Bose condensate density matrix

It's possible to reexpress the elements of the density matrix in terms of the binomial probability  $P_n$  of finding a total of  $n$  particles on sites  $i$  and  $j$ . When conducting a total of  $t$  trials, if the probability of success is  $p$  and that of failure is  $(1-p)$  then the probability of obtaining exactly  $x$  successes is

$$\begin{aligned} P_x &= C(t, x) p^x (1-p)^{t-x} \\ &= \frac{t!}{x!(t-x)!} p^x (1-p)^{t-x}. \end{aligned} \quad (6.124)$$

Thus the probability of finding exactly  $n$  particles on sites  $i$  and  $j$  is equal to the probability of testing whether the site that a given particle is on is either site  $i$  or  $j$  for all  $N$  particles, and succeeding  $n$  times. The probability of success for each test is  $2/M$  hence

$$P_n = \frac{N!}{n!(N-n)!} \left(\frac{2}{M}\right)^n \left(1 - \frac{2}{M}\right)^{N-n} \quad (6.125)$$

Now if the total number of particles on sites  $i$  and  $j$  is exactly  $n = n_i + n_j$  then this probability can be written

$$\begin{aligned} P_n &= \frac{N!}{(n_i + n_j)!(N - (n_i + n_j))!} \left(\frac{2}{M}\right)^{n_i + n_j} \left(\frac{M-2}{M}\right)^{N - (n_i + n_j)} \\ &= \frac{2^{n_i + n_j}}{(n_i + n_j)!} \frac{N!}{M^N} \frac{(M-2)^{N - (n_i + n_j)}}{(N - (n_i + n_j))!} \end{aligned} \quad (6.126)$$

and thus the elements of the density matrix can be written

$$\hat{\rho}(n_i, n_j; n'_i, n'_j) = \frac{(n_i + n_j)!}{2^{n_i + n_j}} P_n \frac{1}{\sqrt{n_i! n_j! n'_i! n'_j!}} \delta_{n_i + n_j, n'_i + n'_j}. \quad (6.127)$$

One can write  $\hat{\rho}$  as a sum of density matrices  $\{\hat{\rho}_{n_{ij}}\}$  weighted by their respective binomial probabilities, where  $\hat{\rho}_{n_{ij}}$  is the density matrix for exactly  $n_i + n_j = n_{ij}$  particles on sites  $i$  and  $j$ :

$$\hat{\rho} = \sum_{n_{ij}=0}^N P_{n_{ij}} \hat{\rho}_{n_{ij}}. \quad (6.128)$$

From the above result for  $\hat{\rho}(n_i, n_j; n'_i, n'_j)$  one can see that  $\hat{\rho}_{n_{ij}}$  has elements

$$\hat{\rho}_{n_{ij}}(n_i, n_j; n'_i, n'_j) := \frac{(n_i + n_j)!}{2^{n_i + n_j}} \frac{1}{\sqrt{n_i! n_j! n'_i! n'_j!}} \delta_{n_i + n_j, n_i} \delta_{n'_i + n'_j, n_{ij}}. \quad (6.129)$$

### 6.5.2 $\hat{\rho}_{n_{ij}}(n_i, n_j; n'_i, n'_j)$ is the density matrix for $n$ particles in the bonding ground state

In fact,  $\hat{\rho}_{n_{ij}}(n_i, n_j; n'_i, n'_j)$  is exactly the same as the density matrix you get for  $n = n_i + n_j$  particles placed in the bonding ground state of the two sites, as

given by equation 6.113:

$$\begin{aligned} |\Psi_B\rangle &= \frac{1}{\sqrt{N!}} \left( \frac{1}{\sqrt{M}} (a_1^\dagger + \dots + a_M^\dagger) \right)^N |0\rangle \\ &= \frac{1}{\sqrt{(n_i + n_j)!}} \left( \frac{1}{\sqrt{2}} (a_i^\dagger + a_j^\dagger) \right)^{n_i + n_j} |0\rangle. \end{aligned} \quad (6.130)$$

This can easily be seen since you can get  $\hat{\rho}_{n_i, n_j; n'_i, n'_j}$  by setting  $N = n_i + n_j$  and  $M = 2$  and putting them into equation 6.121, which is the expression for the density matrix for  $N$  particles in an  $M$  site ground state.

### 6.5.3 Limit for large systems

For the binomial probability  $P_x$ , if the expected number of successes is  $\nu := tp$  then as the number of trials  $t$  becomes large,  $P_x$  tends towards the Poisson distribution:

$$P_x \rightarrow \frac{\nu^x e^{-\nu}}{x!}. \quad (6.131)$$

Here,  $t = N$  and  $p = 2/M$  hence  $\nu = 2N/M = 2f$  where  $f$  is the filling factor. In a Bose condensate, the filling factor is  $f = N/M$ . Thus for a fixed, finite  $f$ , as the number of particles  $N$  and number of sites  $M$  become large,

$$P_n \rightarrow \frac{(2f)^n e^{-2f}}{n!}. \quad (6.132)$$

And thus

$$\begin{aligned} \hat{\rho}(n_i, n_j; n'_i, n'_j) &\rightarrow \sum_{n_{i,j}=0}^N \frac{(2f)^{n_i + n_j} e^{-2f}}{(n_i + n_j)!} \hat{\rho}_{n_{i,j}} \\ &= \sum_{n_{i,j}=0}^N \frac{(n_i + n_j)! (2f)^{n_i + n_j} e^{-2f}}{2^{n_i + n_j} (n_i + n_j)!} \\ &\quad \frac{1}{\sqrt{n_i! n_j! n'_i! n'_j!}} \delta_{n_i + n_j, n_{i,j}} \delta_{n'_i + n'_j, n_{i,j}} \\ &= \sum_{n_{i,j}=0}^N f^{n_i + n_j} e^{-2f} \frac{1}{\sqrt{n_i! n_j! n'_i! n'_j!}} \delta_{n_i + n_j, n_{i,j}} \delta_{n'_i + n'_j, n_{i,j}} \\ &= f^{n_i + n_j + n'_i + n'_j / 2} e^{-2f} \frac{1}{\sqrt{n_i! n_j! n'_i! n'_j!}} \delta_{n_i + n_j, n'_i + n'_j} \end{aligned} \quad (6.133)$$

Note that the distance between sites  $i$  and  $j$  does not appear anywhere in this result. The density matrix is completely independent of the distance between

the sites. The physical rationale for this is that the system contains no length scale intermediate between the lattice spacing and the system size. Therefore, the interaction must have either zero range or infinite range.

#### 6.5.4 Bose condensate density matrix in the limit of small $f$

If the filling factor  $f$  is very small, the probability of occupancies higher than 1 will be negligible. Thus the density matrix can be accurately approximated using the basis:

$$|n_i n_j\rangle = \{|00\rangle, |01\rangle, |10\rangle, |11\rangle\}. \quad (6.134)$$

##### To first order in $f$

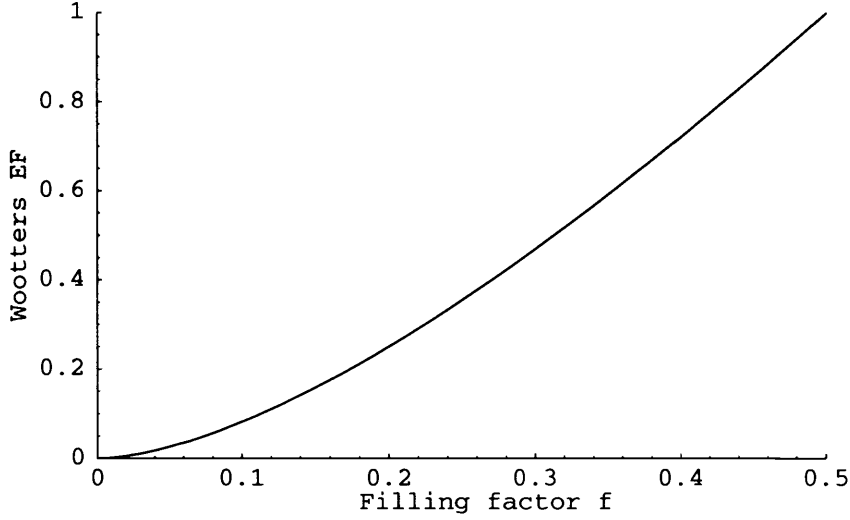
The density matrix in this basis can be calculated to first order in  $f$  from equation 6.133 (assuming that both  $N$  and  $M$  are large):

$$\begin{aligned} \hat{\rho}(n_i, n_j; n'_i, n'_j) &= f^{n_i+n_j+n'_i+n'_j/2} e^{-2f} \frac{1}{\sqrt{n_i! n_j! n'_i! n'_j!}} \delta_{n_i+n_j, n'_i+n'_j} \\ &= f^{n_i+n_j+n'_i+n'_j/2} (1 - 2f + \dots) \frac{1}{\sqrt{1 \times 1 \times 1 \times 1}} \delta_{n_i+n_j, n'_i+n'_j} \\ \therefore \hat{\rho} &= (1 - 2f) \begin{pmatrix} 1 & 0 & 0 & 0 \\ 0 & f & f & 0 \\ 0 & f & f & 0 \\ 0 & 0 & 0 & f^2 \end{pmatrix} = \begin{pmatrix} 1 - 2f & 0 & 0 & 0 \\ 0 & f & f & 0 \\ 0 & f & f & 0 \\ 0 & 0 & 0 & 0 \end{pmatrix} \\ &\text{to first order in } f. \end{aligned} \quad (6.135)$$

The entanglement between sites  $i$  and  $j$  was calculated using the Wootters formula (since the two sites form a two-by-two system). It is non-zero, and is plotted as a function of  $f$  in Figure 6.11. On the basis of this exercise, one would conclude that the Bose condensate does contain entanglement. However the higher order terms in  $f$  which were neglected, above, are in fact important.



Figure 6.11: Entanglement between two sites in a Bose condensate for small filling factors  $f$ , calculated from the density matrix expressed to first order in  $f$ , using the Wootters formula.



### To second order in $f$

Repeating the above exercise with the second order terms included gives

$$\begin{aligned}
 \hat{\rho}_{O2} &= f^{n_i+n_j+n'_i+n'_j/2} \left( 1 - 2f + \frac{(-2f)^2}{2!} + \dots \right) \frac{1}{\sqrt{n_i!n_j!n'_i!n'_j!}} \delta_{n_i+n_j, n'_i+n'_j} \\
 &= \left( 1 - 2f + \frac{(-2f)^2}{2!} + \dots \right) \\
 &\quad \begin{pmatrix} 1 & 0 & 0 & 0 & 0 & 0 & 0 & 0 & 0 \\ 0 & f & 0 & f & 0 & 0 & 0 & 0 & 0 \\ 0 & 0 & f^2/2 & 0 & f^2/\sqrt{2} & 0 & 0 & 0 & 0 \\ 0 & f & 0 & f & 0 & 0 & 0 & 0 & 0 \\ 0 & 0 & f^2/\sqrt{2} & 0 & f^2 & 0 & f^2/\sqrt{2} & 0 & 0 \\ 0 & 0 & 0 & 0 & 0 & f^3/2 & 0 & f^3/2 & 0 \\ 0 & 0 & 0 & 0 & f^2/\sqrt{2} & 0 & f^2/2 & 0 & 0 \\ 0 & 0 & 0 & 0 & 0 & f^3/2 & 0 & f^3/2 & 0 \\ 0 & 0 & 0 & 0 & 0 & 0 & 0 & 0 & f^4/4 \end{pmatrix}
 \end{aligned} \tag{6.136}$$

in the basis

$$|00\rangle, |01\rangle, |02\rangle, |10\rangle, |11\rangle, |12\rangle, |20\rangle, |21\rangle, |22\rangle. \quad (6.137)$$

We can now truncate this to the basis given in equation 6.134, and renormalize, giving the  $4 \times 4$  density matrix:

$$\hat{\rho}_{O1'} = \frac{1}{(1+f)^2} \begin{pmatrix} 1 & 0 & 0 & 0 \\ 0 & f & f & 0 \\ 0 & f & f & 0 \\ 0 & 0 & 0 & f^2 \end{pmatrix}. \quad (6.138)$$

The entanglement of this as calculated using the Woottter's formula is zero for all  $f$ . So for small  $f$ , the Bose condensate does not contain any entanglement between sites.

The above truncation method is rather arbitrary, and therefore a more convincing proof of the lack of entanglement is Peres's test [85] as to whether all the eigenvalues of the partial transpose of a two-system density matrix are positive. The partial transpose is defined by

$$\hat{\sigma}_{m\mu, n\nu} := \hat{\rho}_{n\mu, m\nu} \quad (6.139)$$

where the indices  $m, n$  run over system  $A$ ,  $\mu, \nu$  run over system  $B$ , and the non-partially transposed density matrix is  $\hat{\rho}_{m\mu, n\nu}$ . The partial transpose of  $\hat{\rho}_{O2}$  is

$$\hat{\rho}_{O2}^{PT} := \left( 1 - 2f + \frac{(-2f)^2}{2!} + \dots \right) \begin{pmatrix} 1 & 0 & 0 & 0 & f & 0 & 0 & 0 & \frac{f^2}{2} \\ 0 & f & 0 & 0 & 0 & \frac{f^2}{\sqrt{2}} & 0 & 0 & 0 \\ 0 & 0 & \frac{f^2}{2} & 0 & 0 & 0 & 0 & 0 & 0 \\ 0 & 0 & 0 & f & 0 & 0 & 0 & \frac{f^2}{\sqrt{2}} & 0 \\ f & 0 & 0 & 0 & f^2 & 0 & 0 & 0 & \frac{f^3}{2} \\ 0 & \frac{f^2}{\sqrt{2}} & 0 & 0 & 0 & \frac{f^3}{2} & 0 & 0 & 0 \\ 0 & 0 & 0 & 0 & 0 & 0 & \frac{f^2}{2} & 0 & 0 \\ 0 & 0 & 0 & \frac{f^2}{\sqrt{2}} & 0 & 0 & 0 & \frac{f^3}{2} & 0 \\ \frac{f^2}{2} & 0 & 0 & 0 & \frac{f^3}{2} & 0 & 0 & 0 & \frac{f^4}{4} \end{pmatrix} \quad (6.140)$$

This has only positive eigenvalues for all  $f$ , indicating that  $\hat{\rho}_{O2}$  is separable and supporting the above conclusion that the Bose condensate does not contain any entanglement for small  $f$ .

### **6.5.5 Work of Simon on entanglement in Bose-Einstein condensates**

Simon [84] has obtained results for bipartite entanglement in BECs that are consistent with this study. He finds that any two regions in the BEC are entangled, irrespective of the distance between the regions. This is true even for two subsystems which together comprise just part of a BEC, and thus for which the total particle number is not fixed.

Entanglement only disappears when the BEC contains an infinitely large number of particles, ie. when the occupation probability tends towards a Poisson distribution. This is consistent with the findings above.

## Chapter 7

# Conclusions

With more and more designs being proposed for quantum computers, especially involving the use of solid state architectures, the need for an effective method for quantifying the entanglement between the particles which carry the qubits in such an architecture, ie. electrons, has become increasingly pressing.

**Chapter 2** looked at a number of possible approaches for quantifying bipartite entanglement between indistinguishable particles and found that only the Zanardi ‘site-entropy’ measure is a rational measure, according to the standard tests for a ‘good’ entanglement measure. Vaccaro and co-workers have proposed that one should measure the Zanardi entanglement after an SSR for local particle number conservation has been applied.

With a workable entanglement measure for indistinguishable particles identified, a natural next step was to look at entanglement in systems of such particles. A very simple example of such a system is the doubly-occupied molecular bonding orbital. The Zanardi measure predicts that this contains two ebits of entanglement shared between sites  $A$  and  $B$ . However, these two ebits are spread across spin and space degrees of freedom. To demonstrate that the Zanardi measure indeed gives the correct answer, a teleportation protocol was devised that enables Alice (site  $A$ ) to teleport two qubits to Bob (site  $B$ ) using the doubly-occupied molecular bonding orbital.

**Chapter 3** looked at systems which carry entanglement in both their space and spin degrees of freedom. It considered two questions - i) to what extent are the spin and spatial degrees of freedom ‘entangled’ with each other, and ii) to

what extent can entanglement be carried between two physical subsystems only in the spin degrees of freedom, or only in the spatial degrees of freedom.

First, it was found that for a system of  $N$  fermions occupying  $2M$  single-particle states, the ‘space-only’ density matrix  $\hat{\rho}_{\text{spatial}}$  which gives the correct measurement statistics for measurements made by a spatial operator on that system is a sum of density matrices  $\{\hat{\rho}^S\}$  each of which is parameterized by the total spin quantum number  $S$ .

As regards question i), it is found that the doubly-occupied molecular bonding orbital is separable into space-only and spin-only states. There is thus no ‘space-spin’ entanglement in this system. However, a parameterized version does exhibit space-spin entanglement as a function of the parameter. The space-spin entanglement is calculated twice for the apparatus proposed by Omar *et al.* [3], once for a version where each pair of fermions is only locally antisymmetrized on their respective side of the apparatus, and once for the fully antisymmetrized state.

As regards question ii), space-only and spin-only entanglements are formally defined as entanglement which can be exploited by parties who can only perform spatial or spin (respectively) operations, within the regions of space to which each party has access.

The effect of limiting only the *measurements* that Alice and Bob can perform, but not the operations, is considered for the doubly-filled bonding MO. It was found that such a restriction means that only  $3/2$  qubits can be teleported. The same result was also obtained by drawing an analogy with a system of two spinless bosons occupying two sites. This enables the spatial state to be expressed as a density matrix, and thus enables the von Neumann entropy of the reduced space-only density matrix for site  $A$  to be evaluated.

The spin-only and space-only entanglements between sides 1 and 2 of the Omar apparatus are also evaluated using the locally anti-symmetrized version of the state.

**Chapter 4** looked at the effect that applying a superselection rule for charge to the doubly-occupied bonding MO has on the amount of useful entanglement it contains between its two sites. The teleportation protocol developed for this state requires the use of non-local, non-number conserving operations in order to perform the CNOTs involving the ‘virtual’ qubits that are used by Alice to perform the teleportation of two unknown qubits. If Alice is restricted to using

only local, number-conserving operations at site  $A$ , she can only perform spin-flips at site  $A$ . This prevents her producing a superposition of charge states at site  $A$ , and is thus equivalent to imposing a superselection rule for charge. It was found that the effect of this is to reduce the available entanglement in the state to  $1/2$  ebit. This is the value that Vaccaro's available entanglement  $E_P$  gives for this state.

**Chapter 5** developed a conjugate gradient method to numerically estimate the entanglement of formation. After a description of the generic conjugate gradient algorithm, a gradient for the average entanglement was developed. A brief description was given of how the algorithm and gradient were implemented. Then the results of testing the code against various types of mixed state were described. These were two qubit mixed states, two qudit isotropic mixed states, and two qutrit random mixed states. Finally, the code was used to evaluate the entanglement of locally decohered (ie. decohered only at one site) Bell states of two qutrits. The types of decoherence examined were the bit flip and the depolarizing channel.

Finally, **chapter 6** examined bipartite entanglement between two sites in a degenerate quantum gas. First, the existing literature on entanglement between two sites in a spin system such as the XY and Ising models was described. Then a two-site density matrix for a BCS superconductor in its ground state was developed. A version of this describes the Fermi metal. Separately, a two-site density matrix for a Bose condensate was developed. The entanglement results from these density matrices were described. A direction for future research would be an experiment for detecting the entanglement of formation in degenerate quantum gases, in order to verify the results predicted by this chapter. Other areas for future work include studies at non-zero temperature, and with a larger number of data points.

# Appendix A

## Omar 2 x 2 eigenfunctions

### A.1 Locally antisymmetrized spin and spatial eigenfunctions for the Omar apparatus

#### A.1.1 Locally antisymmetrized spin eigenfunctions

What are the simultaneous eigenfunctions of  $\hat{S}_z$  and  $\hat{S}^2$  for a system of 4 spin- $\frac{1}{2}$ 's? One easy approach is to consider the system as two pairs of spin- $\frac{1}{2}$ 's, and combine them using Clebsch-Gordan coefficients. Our basis states are the eigenstates for a system of 2 spin- $\frac{1}{2}$ 's, i.e.

$$\begin{aligned}\chi_{0,0} &= \frac{1}{\sqrt{2}}[\alpha(1)\beta(2) - \beta(1)\alpha(2)] \\ \chi_{1,1} &= \alpha(1)\alpha(2) \\ \chi_{1,0} &= \frac{1}{\sqrt{2}}[\alpha(1)\beta(2) + \beta(1)\alpha(2)] \\ \chi_{1,-1} &= \beta(1)\beta(2)\end{aligned}\tag{A.1}$$

where  $\alpha, \beta$  are the spin-up, spin-down eigenstates for a single spin- $\frac{1}{2}$ .

The Omar interferometer consists of two beamsplitters, arranged vertically. The top beamsplitter is on 'side 1' of the apparatus, the bottom beamsplitter on 'side 2'. Two pairs of maximally spin-entangled fermions are produced halfway between the beamsplitters (at the interface between sides 1 and 2), and one half of each pair is combined with one half of the other pair at one of the beamsplitters.

We divide the 4 fermions into pairs  $A$  and  $B$ , where pair  $A$  is on side 1 of the apparatus and pair  $B$  is on side 2. Then using the nomenclature  $\Phi_{S_A, S_B}^{S, m_S}$ , where  $S_A$  ( $S_B$ ) denotes the total spin of pair  $A$  ( $B$ ), and  $S, m_S$  denote the total spin and spin-z projection of the 4 fermion system, and using the decomposition

$$\Phi_{S_A, S_B}^{S, m_S} = \sum_{m_{S_A} m_{S_B}} \langle S_A S_B m_{S_A} m_{S_B} | S m_S \rangle \chi_{S_A m_{S_A}} \chi_{S_B m_{S_B}} \quad (\text{A.2})$$

where the  $\{\langle S_A S_B m_{S_A} m_{S_B} | S m_S \rangle\}$  are the Clebsch-Gordon coefficients, we obtain:

**S=0**

$$\begin{aligned} \Phi_{0,0}^{0,0} &= \chi_{0,0}^A \chi_{0,0}^B \\ \Phi_{1,1}^{0,0} &= \frac{1}{\sqrt{3}} [\chi_{1,-1}^A \chi_{1,1}^B + \chi_{1,1}^A \chi_{1,-1}^B - \chi_{1,0}^A \chi_{1,0}^B] \end{aligned} \quad (\text{A.3})$$

**S=1**

$$\begin{aligned} \Phi_{1,0}^{1,-1} &= \chi_{1,-1}^A \chi_{0,0}^B \\ \Phi_{1,0}^{1,0} &= \chi_{1,0}^A \chi_{0,0}^B \\ \Phi_{1,0}^{1,1} &= \chi_{1,1}^A \chi_{0,0}^B \end{aligned}$$


---

$$\begin{aligned} \Phi_{0,1}^{1,-1} &= \chi_{0,0}^A \chi_{1,-1}^B \\ \Phi_{0,1}^{1,0} &= \chi_{0,0}^A \chi_{1,0}^B \\ \Phi_{0,1}^{1,1} &= \chi_{0,0}^A \chi_{1,1}^B \end{aligned}$$


---

$$\begin{aligned} \Phi_{1,1}^{1,-1} &= \frac{1}{\sqrt{2}} [\chi_{1,0}^A \chi_{1,-1}^B - \chi_{1,-1}^A \chi_{1,0}^B] \\ \Phi_{1,1}^{1,0} &= \frac{1}{\sqrt{2}} [\chi_{1,1}^A \chi_{1,-1}^B - \chi_{1,-1}^A \chi_{1,1}^B] \\ \Phi_{1,1}^{1,1} &= \frac{1}{\sqrt{2}} [\chi_{1,1}^A \chi_{1,0}^B - \chi_{1,0}^A \chi_{1,1}^B] \end{aligned}$$


---

(A.4)



**S=2**

$$\begin{aligned}
\Phi_{1,1}^{2,-2} &= \chi_{1,-1}^A \chi_{1,-1}^B \\
\Phi_{1,1}^{2,-1} &= \frac{1}{\sqrt{2}} [\chi_{1,-1}^A \chi_{1,0}^B + \chi_{1,0}^A \chi_{1,-1}^B] \\
\Phi_{1,1}^{2,0} &= \frac{1}{\sqrt{6}} [\chi_{1,1}^A \chi_{1,-1}^B + 2\chi_{1,0}^A \chi_{1,0}^B + \chi_{1,-1}^A \chi_{1,1}^B] \\
\Phi_{1,1}^{2,1} &= \frac{1}{\sqrt{2}} [\chi_{1,1}^A \chi_{1,0}^B + \chi_{1,0}^A \chi_{1,1}^B] \\
\Phi_{x,x}^{x,x} &= \chi_{1,1}^A \chi_{1,1}^B
\end{aligned} \tag{A.5}$$

### A.1.2 Locally antisymmetrized spatial states

These are products of the following states for each side:

$$\begin{aligned}
|LL\rangle &= L(1)L(2) \\
|RR\rangle &= R(1)R(2) \\
|LR+\rangle &= \frac{1}{\sqrt{2}} [L(1)R(2) + L(2)R(1)] \\
|LR-\rangle &= \frac{1}{\sqrt{2}} [L(1)R(2) - L(2)R(1)]
\end{aligned} \tag{A.6}$$

where 1, 2 are particle labels.

### A.1.3 Rewriting the 50/50 ++ output state for fermions as a sum of products of space and spin eigenfns

The unnormalized output state for 50/50 beamsplitters for fermions (++ case) is (as given in equation 53 in quant-ph/0202051):

$$\begin{aligned}
&-\frac{1}{2}|L\downarrow\rangle_1|L\uparrow\rangle_2 - \frac{1}{2}|R\downarrow\rangle_1|R\uparrow\rangle_2 - \frac{1}{2}(|L\downarrow\rangle_1|R\uparrow\rangle_2 + |R\downarrow\rangle_1|L\uparrow\rangle_2) \\
&+\frac{1}{2}(|A\uparrow\rangle_1|A\downarrow\rangle_2 + |A\downarrow\rangle_1|A\uparrow\rangle_2) - \frac{1}{2}(|A\uparrow\rangle_1|A\uparrow\rangle_2 + |A\downarrow\rangle_1|A\downarrow\rangle_2) \\
&+(|A\uparrow\rangle_1|A\downarrow\rangle_2 + |A\downarrow\rangle_1|A\uparrow\rangle_2)
\end{aligned} \tag{A.7}$$

For the doubly-occupied  $H_2^+$  state we used

$$\frac{1}{\sqrt{2}} \left( c_{A\uparrow}^\dagger c_{B\downarrow}^\dagger + c_{B\uparrow}^\dagger c_{A\downarrow}^\dagger \right) |0\rangle = |AB+\rangle | \chi_{0,0} \rangle \tag{A.8}$$

Let's try a similar trick here, taking pairs of "A" spatial state terms, expanding the states as Slater determinants, and rearranging the terms such that we have a sum of products of spin-only and space-only states (a,b,c,d are particle labels):

$$\begin{aligned}
& \frac{1}{2}(|A \uparrow \downarrow\rangle_1 |A \downarrow \uparrow\rangle_2 + |A \downarrow \uparrow\rangle_1 |A \uparrow \downarrow\rangle_2) \\
&= \frac{1}{2} \left( \frac{1}{\sqrt{2}} (L1(a) \uparrow (a) R1(b) \downarrow (b) - L1(b) \uparrow (b) R1(a) \downarrow (a)) \right. \\
& \quad \frac{1}{\sqrt{2}} (L2(c) \downarrow (c) R2(d) \uparrow (d) - L2(d) \downarrow (d) R2(c) \uparrow (c)) \\
& \quad + \frac{1}{\sqrt{2}} (L1(a) \downarrow (a) R1(b) \uparrow (b) - L1(b) \downarrow (b) R1(a) \uparrow (a)) \\
& \quad \left. \frac{1}{\sqrt{2}} (L2(c) \uparrow (c) R2(d) \downarrow (d) - L2(d) \uparrow (d) R2(c) \downarrow (c)) \right) \\
&= \frac{1}{4} \left( L1(a) R1(b) L2(c) R2(d) \right. \\
& \quad \underline{(\uparrow (a) \downarrow (b) \downarrow (c) \uparrow (d) + \downarrow (a) \uparrow (b) \uparrow (c) \downarrow (d))} \\
& \quad - L1(a) R1(b) L2(d) R2(c) \\
& \quad (\uparrow (a) \downarrow (b) \downarrow (d) \uparrow (c) + \downarrow (a) \uparrow (b) \uparrow (d) \downarrow (c)) \\
& \quad - L1(b) R1(a) L2(c) R2(d) \\
& \quad (\uparrow (b) \downarrow (a) \downarrow (c) \uparrow (d) + \downarrow (b) \uparrow (a) \uparrow (c) \downarrow (d)) \\
& \quad + L1(b) R1(a) L2(d) R2(c) \\
& \quad \left. (\uparrow (b) \downarrow (a) \downarrow (d) \uparrow (c) + \downarrow (b) \uparrow (a) \uparrow (d) \downarrow (c)) \right)
\end{aligned} \tag{A.9}$$

Now

$$\chi_{0,0}^1 = \frac{1}{\sqrt{2}} (\uparrow (a) \downarrow (b) - \downarrow (a) \uparrow (b)) \tag{A.10}$$

hence

$$\begin{aligned}
\chi_{0,0}^1 \chi_{0,0}^2 &= \frac{1}{2} (\uparrow (a) \downarrow (b) \uparrow (c) \downarrow (d) - \uparrow (a) \downarrow (b) \downarrow (c) \uparrow (d) \\
& \quad - \downarrow (a) \uparrow (b) \uparrow (c) \downarrow (d) + \downarrow (a) \uparrow (b) \downarrow (c) \uparrow (d))
\end{aligned} \tag{A.11}$$

and  $\chi_{1,0}^1 \chi_{1,0}^2$  is the same but with exclusively '+' signs. Hence we can rewrite the underlined part of equation A.9 as

$$\uparrow (a) \downarrow (b) \downarrow (c) \uparrow (d) + \downarrow (a) \uparrow (b) \uparrow (c) \downarrow (d) = \chi_{1,0}^1 \chi_{1,0}^2 - \chi_{0,0}^1 \chi_{0,0}^2 \tag{A.12}$$

A similar exercise for the other bracketed groups of spin terms in equation A.9 gives

$$\begin{aligned}
& \frac{1}{2}(|A \uparrow \downarrow\rangle_1 |A \downarrow \uparrow\rangle_2 + |A \downarrow \uparrow\rangle_1 |A \uparrow \downarrow\rangle_2) \\
&= \frac{1}{4} \left( L1(a)R1(b)L2(c)R2(d)(\chi_{1,0}^1 \chi_{1,0}^2 - \chi_{0,0}^1 \chi_{0,0}^2) \right. \\
&\quad - L1(a)R1(b)L2(d)R2(c)(\chi_{1,0}^1 \chi_{1,0}^2 + \chi_{0,0}^1 \chi_{0,0}^2) \\
&\quad - L1(b)R1(a)L2(c)R2(d)(\chi_{1,0}^1 \chi_{1,0}^2 + \chi_{0,0}^1 \chi_{0,0}^2) \\
&\quad \left. + L1(b)R1(a)L2(d)R2(c)(\chi_{1,0}^1 \chi_{1,0}^2 - \chi_{0,0}^1 \chi_{0,0}^2) \right) \\
&= \frac{1}{4} \left( L1(a)R1(b)\sqrt{2}|A-\rangle_2 \chi_{1,0}^1 \chi_{1,0}^2 \right. \\
&\quad - L1(a)R1(b)\sqrt{2}|A+\rangle_2 \chi_{0,0}^1 \chi_{0,0}^2 \\
&\quad - L1(b)R1(a)\sqrt{2}|A-\rangle_2 \chi_{1,0}^1 \chi_{1,0}^2 \\
&\quad \left. - L1(b)R1(a)\sqrt{2}|A+\rangle_2 \chi_{0,0}^1 \chi_{0,0}^2 \right) \\
&= \frac{1}{4} \left( \sqrt{2}|A-\rangle_1 \sqrt{2}|A-\rangle_2 \chi_{1,0}^1 \chi_{1,0}^2 - \sqrt{2}|A+\rangle_1 \sqrt{2}|A+\rangle_2 \chi_{0,0}^1 \chi_{0,0}^2 \right) \\
&= \frac{1}{2} \left( |A-\rangle_1 |A-\rangle_2 \chi_{1,0}^1 \chi_{1,0}^2 - |A+\rangle_1 |A+\rangle_2 \chi_{0,0}^1 \chi_{0,0}^2 \right)
\end{aligned} \tag{A.13}$$

A similar exercise yields

$$\begin{aligned}
& \frac{1}{2}(|A \uparrow \downarrow\rangle_1 |A \uparrow \downarrow\rangle_2 + |A \downarrow \uparrow\rangle_1 |A \downarrow \uparrow\rangle_2) \\
&= \frac{1}{2}(|A-\rangle_1 |A-\rangle_2 \chi_{1,0}^1 \chi_{1,0}^2 + |A+\rangle_1 |A+\rangle_2 \chi_{0,0}^1 \chi_{0,0}^2)
\end{aligned} \tag{A.14}$$

So

$$\begin{aligned}
& \frac{1}{2}(|A \uparrow \downarrow\rangle_1 |A \downarrow \uparrow\rangle_2 + |A \downarrow \uparrow\rangle_1 |A \uparrow \downarrow\rangle_2) - \frac{1}{2}(|A \uparrow \downarrow\rangle_1 |A \uparrow \downarrow\rangle_2 + |A \downarrow \uparrow\rangle_1 |A \downarrow \uparrow\rangle_2) \\
&= -|A+\rangle_1 |A+\rangle_2 \chi_{0,0}^1 \chi_{0,0}^2
\end{aligned} \tag{A.15}$$

Thus the output state becomes

$$\begin{aligned}
|\text{out}\rangle_{\text{fermion}}^{++} &= \frac{1}{2}|L\rangle_1|L\rangle_2\chi_{0,0}^1\chi_{0,0}^2 + \frac{1}{2}|R\rangle_1|R\rangle_2\chi_{0,0}^1\chi_{0,0}^2 \\
&\quad + \frac{1}{2}|L\rangle_1|R\rangle_2\chi_{0,0}^1\chi_{0,0}^2 + \frac{1}{2}|R\rangle_1|L\rangle_2\chi_{0,0}^1\chi_{0,0}^2 \\
&\quad - |A+\rangle_1|A+\rangle_2\chi_{0,0}^1\chi_{0,0}^2 + |A-\rangle_1|A-\rangle_2(\chi_{1,1}^1\chi_{1,-1}^2 + \chi_{1,-1}^1\chi_{1,1}^2) \\
&= \frac{1}{2}\Phi_{0,0}^{0,0}(|L\rangle_1|L\rangle_2 + |R\rangle_1|R\rangle_2 + |L\rangle_1|R\rangle_2 + |R\rangle_1|L\rangle_2 - |A+\rangle_1|A+\rangle_2) \\
&\quad + |A-\rangle_1|A-\rangle_2(\chi_{1,1}^1\chi_{1,-1}^2 + \chi_{1,-1}^1\chi_{1,1}^2) \tag{A.16}
\end{aligned}$$

Now

$$\chi_{1,1}^1\chi_{1,-1}^2 + \chi_{1,-1}^1\chi_{1,1}^2 = \frac{2}{\sqrt{3}}\Phi_{1,1}^{0,0} + \sqrt{\frac{2}{3}}\Phi_{1,1}^{2,0} \tag{A.17}$$

So

$$\begin{aligned}
|\text{out}\rangle_{\text{fermion}}^{++} &= \frac{1}{2}\Phi_{0,0}^{0,0}(|L\rangle_1|L\rangle_2 + |R\rangle_1|R\rangle_2 + |L\rangle_1|R\rangle_2 + |R\rangle_1|L\rangle_2 - 2|A+\rangle_1|A+\rangle_2) \\
&\quad + |A-\rangle_1|A-\rangle_2\left(\frac{2}{\sqrt{3}}\Phi_{1,1}^{0,0} + \sqrt{\frac{2}{3}}\Phi_{1,1}^{2,0}\right) \tag{A.18}
\end{aligned}$$

# Bibliography

- [1] C. H. Bennett, G. Brassard, C. Crepeau, R. Jozsa, A. Peres, and W. Wootters. Teleporting an unknown quantum state via dual classical and EPR channels. *Phys. Rev. Lett.*, 70:1895–1899, 1993.
- [2] B. E. Kane. A silicon-based nuclear spin quantum computer. *Nature*, 393:133–137, 1998.
- [3] Y. Omar, N. Paunkovic, S. Bose, and V. Vedral. Spin-space entanglement transfer and quantum statistics. *Phys. Rev. A*, 65:062305, 2002.
- [4] L. Landau. Das dampfungsproblem in der wellenmechanik. *Z. Phys.*, 45:430–441, 1927.
- [5] J. von Neumann. *Gottinger Nachrichten*, page 245, 1927.
- [6] M. A. Nielsen and I. L. Chuang. *Quantum computation and quantum information*, page 107. Cambridge University Press, 1st edition, 2000.
- [7] A. Wehrl. *Rev. Mod. Phys.*, 50:221, 1978.
- [8] M. Ohya and D. Petz. *Quantum entropy and its use*. Springer-Verlag, Berlin, 1993.
- [9] W. K. Wootters. Quantum entanglement as a quantifiable resource. *Phil. Trans. R. Soc. Lond. A*, 356:1717–1731, 1998.
- [10] S. Hill and W. K. Wootters. Entanglement of a pair of quantum bits. *Phys. Rev. Lett.*, 78:5022–5025, 1997.
- [11] W. K. Wootters. Entanglement of formation of an arbitrary state of two qubits. *Phys. Rev. Lett.*, 80:2245–2248, 1998.

- [12] J. J. Sakurai. *Modern Quantum Mechanics*, page 277. Addison Wesley, 2nd edition, 1994.
- [13] G. Vidal. Entanglement monotones. *J. Mod. Opt.*, 47:355, 2000.
- [14] A. Uhlmann. Relative entropy and the Wigner-Yanase-Dyson-Lieb concavity in an interpolation theory. *Commun. Math. Phys.*, 54:21–32, 1977.
- [15] D. Petz. Monotonicity of quantum relative entropy revisited. *Rev. Math. Phys.*, 15:79–91, 2003.
- [16] M. A. Nielsen and I. L. Chuang. *Quantum computation and quantum information*, page 578. Cambridge University Press, 1st edition, 2000.
- [17] R. Jozsa, M. Horodecki, P. Horodecki, and R. Horodecki. Universal quantum information compression. *Phys. Rev. Lett.*, 81:1714–1717, 1998.
- [18] M. A. Nielsen and I. L. Chuang. *Quantum computation and quantum information*, page 103. Cambridge University Press, 1st edition, 2000.
- [19] K. G. H. Vollbrecht. QI Open Problems Project - Problem 7 - Additivity of entanglement of formation. <http://www.imaph.tu-bs.de/qi/problems/>.
- [20] G. Vidal, W. Dür, and J. I. Cirac. Entanglement cost of mixed states. *Phys. Rev. Lett.*, 89:027901, 2002.
- [21] C. H. Bennett, H. J. Bernstein, S. Popescu, and B. Schumacher. Concentrating partial entanglement by local operations. *Phys. Rev. A*, 53:2046–2052, 1996.
- [22] M. Horodecki, P. Horodecki, and R. Horodecki. Mixed-state entanglement and distillation: is there a ‘bound’ entanglement in nature? *Phys. Rev. Lett.*, 80:5239–5242, 1998.
- [23] G. Vidal and J. I. Cirac. Irreversibility in asymptotic manipulations of entanglement. *Phys. Rev. Lett.*, 86:5803–5806, 2001.
- [24] K. G. H. Vollbrecht, R. F. Werner, and M. M. Wolf. On the irreversibility of entanglement distillation. *Phys. Rev. A*, 69:062304, 2004.
- [25] A. Einstein, B. Podolsky, and N. Rosen. Can quantum-mechanical description of physical reality be considered complete? *Phys. Rev.*, 47:777–780, 1935.

- [26] J. S. Bell. On the Einstein - Podolsky - Rosen paradox. *Physics*, 1:195–200, 1964.
- [27] D. G. Angelakis, A. Beige, P. L. Knight, W. J. Munro, and B. Tregenna. Verifying atom entanglement schemes by testing Bell’s inequality. *Z. Naturforsch.*, 56a:27, 2001.
- [28] R. F. Werner. *Phys. Rev. A*, 40:4277, 1989.
- [29] L. Derkacz and L. Jakobczyk. Bell inequalities versus entanglement and mixedness for a class of two-qubit states. *Phys. Lett. A*, 328:26–35, 2004.
- [30] W. K. Wootters and W. H. Zurek. A single quantum cannot be cloned. *Nature*, 299:802–803, 1982.
- [31] C. H. Bennett and G. Brassard. Quantum cryptography: Public key distribution and coin tossing. *Proceedings of IEEE international conference on computers, systems, and signal processing*, pages 175–179, 1984.
- [32] A. K. Ekert. Quantum cryptography based on Bell’s theorem. *Phys. Rev. Lett.*, 67:661–663, 1991.
- [33] J. F. Clauser, M. A. Horne, A. Shimony, and R. A. Holt. *Phys. Rev. Lett.*, 23:880, 1969.
- [34] H. Aschauer and H. J. Briegel. Private entanglement over arbitrary distances, even using noisy apparatus. *Phys. Rev. Lett.*, 88:047902, 2002.
- [35] M. J. Bremner, C. M. Dawson, J. L. Dodd, A. Gilchrist, A. W. Harrow, D. Mortimer, M. A. Nielsen, and T. J. Osborne. A practical scheme for quantum computation with any two-qubit entangling gate. *Phys. Rev. Lett.*, 89:247902, 2002.
- [36] M. A. Nielsen, M. J. Bremner, J. L. Dodd, A. M. Childs, and C. M. Dawson. Universal simulation of Hamiltonian dynamics for quantum systems with finite-dimensional state spaces. *Phys. Rev. A*, 66:022317, 2002.
- [37] A. Peres. *Quantum theory: concepts and methods*. Kluwer Academic, 1995.
- [38] D. Loss and D. P. Di Vincenzo. Quantum computation with quantum dots. *Phys. Rev. A*, 57:120–126, 1998.

- [39] P. Zanardi. Quantum entanglement in fermionic lattices. *Phys. Rev. A*, 65:042101, 2002.
- [40] J. Preskill. PH229 course notes. <http://www.theory.caltech.edu/preskill/ph229>.
- [41] L. Henderson and V. Vedral. Information, relative entropy of entanglement, and irreversibility. *Phys. Rev. Lett.*, 84:2263–2266, 2000.
- [42] M. A. Nielsen and I. L. Chuang. *Quantum computation and quantum information*, page 73. Cambridge University Press, 1st edition, 2000.
- [43] J. Schliemann, J. Ignacio Cirac, M. Kus, M. Lewenstein, and D. Loss. Quantum correlations in two-fermion systems. *Phys. Rev. A*, 64:022303, 2001.
- [44] J. Schliemann, D. Loss, and A. H. MacDonald. Double-occupancy errors, adiabaticity, and entanglement of spin-qubits in quantum dots. *Phys. Rev. B*, 63:085311, 2001.
- [45] R. Paškauskas and L. You. Quantum correlations in two-boson wavefunctions. *Phys. Rev. A*, 64:042310, 2001.
- [46] E. G. Lewars and E. Lewers. *Computational Chemistry*, page 144. Springer, 2003.
- [47] I. Mayer. *Simple Theorems, Proofs, and Derivations in Quantum Chemistry*, page 52. Springer, 2003.
- [48] Y.S. Li, B. Zeng, X.S. Liu, and G.L. Long. Entanglement in a two-identical-particle system. *Phys. Rev. A*, 64:054302, 2001.
- [49] S. J. van Enk. Entanglement of photons. *Phys. Rev. A*, 67:022303, 2003.
- [50] A. P. Hines, R. H. McKenzie, and G. J. Milburn. Entanglement of two-mode Bose-Einstein condensates. *Phys. Rev. A*, 67:013609, 2003.
- [51] H. M. Wiseman and J. A. Vaccaro. The entanglement of indistinguishable particles shared between two parties. *Phys. Rev. Lett.*, 91:097902, 2003.
- [52] J. A. Vaccaro and F. Anselmi. Entanglement of identical particles and reference phase uncertainty. *International Journal of Quantum Information*, 1:427–441, 2003.



- [53] M. Ozawa. Universal uncertainty principle and quantum state control under conservation laws. *Proc. 7th Int. Conf. on Quantum Communication, Measurement and Computing, AIP Conference Proceedings*, 734:95–98, 2004.
- [54] D. Zubarev, V. Morozov, and G. Ropke. *Statistical mechanics of non-equilibrium processes*. Berlin. Akademie Verlag., 1996-1997.
- [55] A. Peres, P. Scudo, and D. Terno. Quantum entropy and special relativity. *Phys. Rev. Lett.*, 88:230402, 2002.
- [56] J. P. Elliott and P. G. Dawber. *Symmetry in physics*. Macmillan, 1979.
- [57] M. J. Yoo, T. A. Fulton, H. F. Hess, R. L. Willett, L. N. Dunkleberger, R. J. Chichester, L. N. Pfeiffer, and K. W. West. Scanning single-electron transistor microscopy: imaging individual charges. *Science*, 276:579–582, 1997.
- [58] G. C. Wick, A. S. Wightman, and E. P. Wigner. *Phys. Rev.*, 88:101, 1952.
- [59] C. Cisneros, R. P. Martinez y Romero, H. N. Nunez-Yepez, and A. L. Salas-Brito. Limitations on the superposition principle: superselection rules in non-relativistic quantum mechanics. *Eur. J. Phys.*, 19:237–243, 1998.
- [60] S. D. Bartlett and H. M. Wiseman. Entanglement constrained by superselection rules. *Phys. Rev. Lett.*, 91:097903, 2003.
- [61] K. Audenaert, F. Verstraete, and B. De Moor. Variational characterizations of separability and entanglement of formation. *Phys. Rev. A*, 64:052304, 2001.
- [62] P. Ehrenfest. *Z. Phys.*, 45:455, 1927.
- [63] H. Hellmann. *Einführung in die Quantenchemie*. Deuticke, Leipzig, 1937.
- [64] R. P. Feynman. *Phys. Rev.*, 56:340, 1939.
- [65] T. Prager. A necessary and sufficient condition for optimal decompositions, 2001. quant-ph/0106030 (unpublished).
- [66] W. H. Press et al. *Numerical recipes in C++, the art of scientific computing*, pages 424–428. Cambridge University Press, 1st edition, 2002.

- [67] E. Polak. *Computational methods in optimization*. New York: Academic Press, 1971.
- [68] R. P. Brent. *Algorithms for minimization without derivatives*. Prentice-Hall, 1973.
- [69] B. M. Terhal and K. G. H. Vollbrecht. The entanglement of formation for isotropic states. *Phys. Rev. Lett.*, 85:2625–2628, 2000.
- [70] S. L. Braunstein et al. Separability of very noisy mixed states and implications for NMR quantum computing. *Phys. Rev. Lett.*, 83:1054–1057, 1999.
- [71] A. Barg. A low-rate bound on the reliability of a quantum discrete memoryless channel. *IEEE Trans. Inform. Theory*, 48, 2002.
- [72] L. N. Cooper. *Phys. Rev.*, 104:1189, 1956.
- [73] D. Gunlycke, S. Bose, V. M. Kendon, and V. Vedral. Thermal concurrence mixing in a 1D Ising model. *Phys. Rev. A*, 64:042302, 2001.
- [74] M. C. Arnesen, S. Bose, and V. Vedral. Natural thermal and magnetic entanglement in 1D Heisenberg model. *Phys. Rev. Lett.*, 87:017901, 2001.
- [75] A. Osterloh, L. Amico, G. Falci, and R. Fazio. Scaling of entanglement close to a quantum phase transition. *Nature*, 416:608–610, 2002.
- [76] A. Hutton and S. Bose. Mediated entanglement and correlations in a star network of interacting spins. *Phys. Rev. A*, 69:042312, 2004.
- [77] S. Bose. Quantum communication through an unmodulated spin chain. *Phys. Rev. Lett.*, 91:207901, 2003.
- [78] D. Stefanatos, S. J. Glaser, and N. Khaneja. Relaxation optimized transfer of spin order in Ising spin chains. *Phys. Rev. A*, 72:062320, 2005.
- [79] M. Plenio and F. L. Semião. High efficiency transfer of quantum information and multi-particle entanglement generation in translation invariant quantum chains. *New J. Phys.*, 7:73, 2005.
- [80] M. B. Plenio, J. Hartley, and J. Eisert. Dynamics and manipulation of entanglement in coupled harmonic systems with many degrees of freedom. *New J. Phys.*, 6:36, 2004.

- [81] J. Bardeen, L. N. Cooper, and J. R. Schrieffer. *Phys. Rev.*, 108:1175, 1957.
- [82] M. Tinkham. *Introduction to superconductivity*, page 43. McGraw-Hill, 2nd edition, 1996.
- [83] M. A. Martín-Delgado. Entanglement and concurrence in the BCS state, 2002. quant-ph/0207026 (unpublished).
- [84] C. Simon. Natural entanglement in Bose-Einstein condensates. *Phys. Rev. A*, 66:052323, 2002.
- [85] A. Peres. Separability criterion for density matrices. *Phys. Rev. Lett.*, 77:1413, 1996.